

**Sedimentology, Sequence Stratigraphy and  
Reservoir Quality of the Early Cretaceous  
Murta Formation, Eromanga Basin,  
Central Australia**

Homoud Al-Anzi, BSc.

This thesis is submitted in partial fulfilment of the requirements for the degree of  
Master of Science (Petroleum Geology & Geophysics)

Australian School of Petroleum,  
The University of Adelaide

April 2008

## **Statement of Authenticity**

The work contained in this thesis has not been previously submitted for a degree or diploma at any other higher education institution. To the best of my knowledge, this thesis contains no material previously published or written by another person except where due reference is made in the text.

I give consent to this copy of my thesis, when deposited in the University Library, being available for loan and photocopying, subject to the provisions of the Copyright Act 1968.

.....  
Homoud Al-Anzi  
10/4/2008

To my parents and my family (*Zarefah, Deema and Basel*)

## **Abstract**

The Eromanga Basin hosts the Early Cretaceous reservoir sediments of the Murta Formation and its basal McKinlay Member of prograding fluvio-lacustrine and deltaic origin that are characterized by low oil production and recovery factors which are heavily controlled by depositional facies. The integration of the concepts of facies associations, sequence stratigraphy and petrography enabled this study to map the continuity of the Murta Formation and to point out the effect of the diagenetic features on the reservoir quality. The diagenetic effects and spatial distribution of the depositional facies in the basin are essential in nominating locations of good quality reservoirs.

The aims of this study were: to characterize the chronostratigraphic depositional facies and distribution, to examine the affect of diagenesis on reservoir quality and to define those parts of the basin where potential reservoir sands are likely to be found.

A detailed analysis of depositional facies in the Murta Formation and its basal McKinlay Member was based on drill core analysis and regional wireline log correlations. The application of non-marine sequence stratigraphic concepts to the wireline logs and core description data have led to the identification of 7 chronostratigraphic units. This data was used in constructing a series of schematic palaeogeographic and isopach maps of the study area to predict the changes in depositional styles with time and space. Six depositional facies were identified in the study area with overall fine-grained sandstones, siltstones and mudstones. These depositional facies include; distributary channels, shoreline, protected shoreline, deltaic mouth bars, tempestites and turbidites deposits.

One particular unit, the transgressive systems tracts of the McKinlay Member, (Unit 7) is the best target for reservoir development because of relatively high proportion of pay sands, medium to coarse-grained sand sizes and good reservoir quality with low diagenetic affects. High stand systems tract units 2, 3 and 5 are considered to be secondary reservoir targets because of diagenetic affects and their fine-grained character. Units 1, 4 and 6 are not considered of economic value for oil production because of their extremely low reservoir quality and muddy lithologies.



The main diagenetic affects on sandstones (quartzarenites) in the study area are quartz overgrowths, formation of authigenic clay (kaolinite), carbonate cement (calcite and siderite), formation of microstylolites (pressure solution) and dissolution of the framework grains to form secondary pores.

The McKinlay Member of the Murta Formation in South Australia consists mainly of medium to coarse-grained sandstones of distributary channel origin (facies association 1). It has the highest recorded porosity and permeability (9.5% and 36.8mD respectively). Shoreline, protected shoreline, deltaic mouth bars and tempestites deposits, mainly from Jackson-Naccowlah Trend wells in Queensland, are of fine-grained sandstones (facies associations 2, 3, 4 and 5 respectively). They have adequate average porosity (7%), but the formation of microstylolites and associated mica parallel to the bedding planes inhibited vertical permeability and has been recorded to be as low as 3.1mD. Turbidites in the central basin are characterized by extremely low reservoir quality (2.6% and 0.25 mD) and muddy lithologies of facies association 6 that are severely degraded by diagenetic effects.

## **Acknowledgements**

I would like to thank the following people and companies for their help, support and guidance during this study. Their support was of considerable value in helping me completing this study.

First of all, I am very grateful to Saudi Aramco for granting me the scholarship to pursue my Master degree at the Australian School of Petroleum (ASP) and for unlimited financial support and encouragement.

Very special thanks must be given to Dr. Nicholas Lemon (Santos Ltd.) for organizing this project and providing me with his precious ideas and helpful comments. Discussions with Dr. Lemon contributed significantly to the progress of this project. This study would not see the light without you. Full cooperation and data support was given by Santos Ltd. by granting unrestricted access to their database and core store.

My further special thanks extended to my supervisor Dr. Tobias Payenberg for his patience, continuous support and outstanding supervision. I wanted to say that I am truly grateful to you and without your support I would not have been able to complete this study.

Thanks go to Alan Sansome and Les Tucker of Primary Industries and Resources of South Australia (PIRSA) for their helpful cooperation during this study and for access to the South Australian cores.

I would like to thank all the staff at (ASP), particularly Dr. Peter Tingate and Dr. Ric Daniel for their guidance and valuable conversations. Thanks to all of my colleagues at (ASP) for their friendship and help during this two year study.

Last, but most of all, I want to thank my parents and my family for their prayers, love and support.

## TABLE OF CONTENTS

<b>Abstract</b>	<b>I</b>
<b>Acknowledgments</b>	<b>III</b>
<b>Table of contents</b>	<b>IV</b>
<b>List of figures</b>	<b>VIII</b>
<b>List of tables</b>	<b>XII</b>
<b>List of abbreviations</b>	<b>XII</b>
<b>Chapter 1</b>	<b>1</b>
<b>1.1 Introduction</b>	<b>1</b>
1.1.1 Rationale	1
1.1.2 Aims and significance	3
1.1.3 Objectives	3
1.1.4 Study area	4
1.1.5 Data support	5
1.1.6 Methodologies	6
1.1.7 Basin setting and tectonics	16
1.2 Literature review of Murta Formation	20
1.2.1 Definition of the Murta Formation	20
1.2.2 Murta Formation units	22
1.2.3 Sequence stratigraphy	24
1.2.4 Facies and reservoirs	26
1.2.5 Isopach maps and depositional models	28
1.2.6 Palaeoclimate and palaeogeography	31
<b>Chapter 2</b>	<b>34</b>
<b>2.1 Review on lake sedimentation</b>	<b>34</b>
<b>2.2 Facies associations of the Murta Formation</b>	<b>37</b>
2.2.1 Facies association 1	38
2.2.2 Facies association 2	42
2.2.3 Facies association 3	45
2.2.4 Facies association 4	47
2.2.5 Facies association 5	50
2.2.6 Facies association 6	54
2.3 Facies associations & depositional environments	57
2.4 Lake Murta sedimentation patterns & modern analogues	60

<b>Chapter 3</b>	<b>Sequence Stratigraphy</b>	<b>67</b>
<b>3.1</b>	<b>Introduction</b>	<b>67</b>
<b>3.2</b>	<b>Lacustrine sequence stratigraphy</b>	<b>69</b>
<b>3.3</b>	<b>Murta Formation sequence stratigraphy</b>	<b>74</b>
<b>3.4</b>	<b>Description of chronostratigraphic intervals</b>	<b>78</b>
<b>3.4.1</b>	<b>Unit 7 (DC60-DC70)</b>	<b>78</b>
<b>3.4.2</b>	<b>Unit 6 (DC50-DC60)</b>	<b>84</b>
<b>3.4.3</b>	<b>Unit 5 (DC40-DC50)</b>	<b>88</b>
<b>3.4.4</b>	<b>Unit 4 (DC30-DC40)</b>	<b>94</b>
<b>3.4.5</b>	<b>Unit 3 (DC20-DC30)</b>	<b>100</b>
<b>3.4.6</b>	<b>Unit 2 (DC10-DC20)</b>	<b>107</b>
<b>3.4.7</b>	<b>Unit 1 (DC00-DC10)</b>	<b>112</b>
<b>Chapter 4</b>	<b>Petrographic Analysis</b>	<b>116</b>
<b>4.1</b>	<b>Introduction</b>	<b>116</b>
<b>4.2</b>	<b>Texture</b>	<b>117</b>
<b>4.2.1</b>	<b>Grain size</b>	<b>117</b>
<b>4.2.2</b>	<b>Sorting</b>	<b>118</b>
<b>4.2.3</b>	<b>Porosity, permeability and textural relationships</b>	<b>121</b>
<b>4.3</b>	<b>Composition</b>	<b>122</b>
<b>4.3.1</b>	<b>Quartz</b>	<b>125</b>
<b>4.3.2</b>	<b>Feldspar</b>	<b>127</b>
<b>4.3.3</b>	<b>Rock fragments (lithic)</b>	<b>129</b>
<b>4.3.4</b>	<b>Mica</b>	<b>129</b>
<b>4.3.5</b>	<b>Clay mineralogy</b>	<b>130</b>
<b>4.3.6</b>	<b>Carbonate and associated pyrite</b>	<b>132</b>
<b>4.3.7</b>	<b>Heavy minerals and opaques</b>	<b>134</b>
<b>4.4</b>	<b>Diagenetic features</b>	<b>135</b>
<b>4.4.1</b>	<b>Cementation</b>	<b>135</b>
<b>4.4.2</b>	<b>Formation of authigenic clays</b>	<b>137</b>
<b>4.4.3</b>	<b>Dissolution</b>	<b>141</b>
<b>4.5</b>	<b>Provenance Discussion and Interpretation</b>	<b>143</b>
<b>4.5.1</b>	<b>Discussion</b>	<b>143</b>
<b>4.5.2</b>	<b>Interpretation</b>	<b>145</b>

<b>Chapter 5</b>	<b>Reservoir Quality and Distribution</b>	<b>148</b>
<b>5.1</b>	<b>Introduction</b>	<b>148</b>
<b>5.2</b>	<b>Variations in reservoir quality</b>	<b>150</b>
<b>5.2.1</b>	<b>Non-reservoir sandstones</b>	<b>150</b>
<b>5.2.2</b>	<b>Secondary reservoir sandstones</b>	<b>151</b>
<b>5.2.3</b>	<b>Primary reservoir sandstones</b>	<b>152</b>
<b>5.3</b>	<b>Stratigraphic position of key reservoirs</b>	<b>155</b>
<b>5.3.1</b>	<b>Non-reservoir sandstones</b>	<b>155</b>
<b>5.3.2</b>	<b>Secondary reservoir sandstones</b>	<b>155</b>
<b>5.3.3</b>	<b>Primary reservoir sandstones</b>	<b>155</b>
<b>5.4</b>	<b>Variations in reservoir with geographic location</b>	<b>156</b>
<b>5.4.1</b>	<b>Non-reservoir sandstones</b>	<b>156</b>
<b>5.4.2</b>	<b>Secondary reservoir sandstones</b>	<b>156</b>
<b>5.4.3</b>	<b>Primary reservoir sandstones</b>	<b>157</b>
<b>Chapter 6</b>	<b>Discussion and Conclusions</b>	<b>158</b>
<b>References</b>		<b>161</b>

## Appendices

All the appendices are contained on the included CD-ROM. The CD-ROM files are in Microsoft word, document imaging, PowerPoint and Excel format.

**Appendix 2.1:** A detailed core description for all cored wells.

**Appendix 2.2:** Logging scheme.

**Appendix 3.1:** Definition of selected sequence stratigraphic terms.

**Appendix 3.2:** A-A' regional cross section from Harkaway Fault area in Queensland (N-NE) to Murteree Ridge in South Australia (S-SW).

**Appendix 3.3:** B-B' cross section through Tenaperra Trough, Murteree Ridge, Nappamerri Trough and Patchawarra Trough in South Australia.

**Appendix 3.4:** C-C' cross section through Patchawarra Trough, GMI Ridge and Tenaperra Trough in South Australia and part of SW Queensland.

**Appendix 3.5:** D-D' cross section of Jackson-Naccowlah Trend in Queensland.

**Appendix 3.6:** E-E' cross section of group of northeastern wells representing the thickest sand columns (sand input) in the study area close to Harkaway fault area in Queensland.

**Appendix 4.1:** Summary table of grainsize analysis showing grainsize in Phi and mm, degree of sorting and facies association of each sample.

**Appendix 4.2:** Standard grainsize chart, showing relationship between Phi ( $\phi$ ) and mm grain sizes.

**Appendix 4.3:** Facies associations probe permeability readings.

**Appendix 4.4:** Examples of silt content and permeability indirectly proportional relationship from all facies associations.

**Appendix 4.5:** A detailed thin section description/mineralogical results.

**Appendix 4.6:** Summary table of XRD analysis methods used in all facies associations.

**Appendix 4.7:** Clay mineralogy profile throughout the Cretaceous succession of Pelican 3 showing variations with depth.

## LIST OF FIGURES

<b>Figure 1.1:</b> Geological summary of the Eromanga Basin.	2
<b>Figure 1.2:</b> Eromanga Basin location map.	4
<b>Figure 1.3:</b> Five regional cross sections across the Eromanga Basin showing the Murta Formation cored wells in South Australia and Queensland.	7
<b>Figure 1.4:</b> Regional log correlation between Gamay-1 in South Australia and Talgeberry-2 in Queensland showing Murta Formation key surfaces and units.	8
<b>Figure 1.5:</b> McKinlay-1 well (4086-4120') as an example of core to log correlation.	10
<b>Figure 1.6:</b> Example of Murta DC60-70 unit (McKinlay Mbr. of Murta Formation).	11
<b>Figure 1.7:</b> Schematic palaeogeographic map of Murta DC40-50 unit showing two sand inputs in Lake Murta.	13
<b>Figure 1.8:</b> Structural elements of the Cooper/Eromanga Basins.	16
<b>Figure 1.9:</b> Cross section through the Eromanga Basin.	18
<b>Figure 1.10:</b> Location of the Eromanga Basin hydrocarbon discoveries in the Cooper region.	19
<b>Figure 1.11:</b> Stratigraphic subdivision and lithologic features from Strzelecki-4 drill-log interpretation, McKinlay Member and Namur Sandstone type section.	21
<b>Figure 1.12:</b> West to east cross section from Nockatunga-5 to Thungo-4 showing Murta Member M1 to M6 units and Namur Sandstone Member N1 and N2 units.	22
<b>Figure 1.13:</b> Murta Formation units from: (A) Dullingari North-1 well, (B) Dullingari-9 well, (C) Nockatunga-3 well, and (D) Dullingari-40 well.	25
<b>Figure 1.14:</b> Murta Member lithofacies, Dullingari 9 and Jackson 1 (Ambrose <i>et al.</i> , 1986).	27
<b>Figure 1.15:</b> Generalised regional lithofacies interpretation, Murta Member, southern Eromanga Basin.	28
<b>Figure 1.16:</b> Isopach map of the Murta Member, southern Eromanga Basin.	29
<b>Figure 1.17:</b> Generalised depositional model, Murta Member, southern Eromanga Basin.	29
<b>Figure 1.18:</b> Murta Formation depositional model in southeastern Eromanga Basin.	31
<b>Figure 1.19:</b> Australia's position in the Early Cretaceous.	32
<b>Figure 1.20:</b> Palaeogeographic change through the Jurassic to Cretaceous.	33
<b>Figure 2.1:</b> Lake response to various forms of physical input.	36
<b>Figure 2.2:</b> Depositional elements in a hydrologically-open, freshwater lake.	36
<b>Figure 2.3:</b> Fluvial-dominated delta and its depositional elements.	40
<b>Figure 2.4:</b> Facies association-1 core photographs.	41

<b>Figure 2.5:</b> Facies association-2 core photograph.	43
<b>Figure 2.6:</b> Offshore profile locating foreshore, shoreface, and offshore.	44
<b>Figure 2.7:</b> Stratal characteristics of an upward-coarsening parasequence. This type of parasequence is interpreted to form in a beach environment on a sandy, fluvial or wave dominated shoreline.	44
<b>Figure 2.8:</b> Bioturbated “wave rippled” laminated sandstone of facies association-3.	46
<b>Figure 2.9:</b> Stratal characteristics of an upward coarsening parasequence. This type of parasequence is interpreted to form in a deltaic environment on a sandy, fluvial or wave dominated shoreline.	48
<b>Figure 2.10:</b> Facies association-4 core photographs.	49
<b>Figure 2.11:</b> Block diagram of hummocky cross stratification.	52
<b>Figure 2.12:</b> Facies association-5 core photographs.	53
<b>Figure 2.13:</b> Facies association-6 core photographs.	56
<b>Figure 2.14:</b> A conceptual diagram for the Murta Formation facies associations including the McKinlay Member.	59
<b>Figure 2.15:</b> Distribution mechanism and resulting sediment types proposed for clastic sedimentation in lacustrine environment.	62
<b>Figure 2.16:</b> Depositional patterns associated with friction-dominated river-mouth outflow.	62
<b>Figure 2.17:</b> Schematic diagram highlights major features of overfilled lake basins.	63
<b>Figure 2.18:</b> Fluvial-dominated delta example from Selenga River delta of the southeastern part of Lake Baikal.	65
<b>Figure 2.19:</b> The Kalawereena terminal splay complex in the dry of July 2003 looking SE.	66
<b>Figure 3.1:</b> Sediment accommodation space and its relationship to eustatic sea level and tectonic uplift and subsidence.	67
<b>Figure 3.2:</b> Lithostratigraphic and sequence stratigraphic interpretations of a gamma ray (GR) log.	68
<b>Figure 3.3:</b> Interplay between accommodation space and sediment supply.	70
<b>Figure 3.4:</b> Relationship between sediment+water supply and total subsidence rate and the resulting lake basin type.	72
<b>Figure 3.5:</b> The position of key surfaces in relation to systems tracts and their relationship to the ratio of accommodation to sediment supply.	73
<b>Figure 3.6:</b> Murta Formation sequence stratigraphy elements from Dullingari-40 well.	76
<b>Figure 3.7:</b> A regional cross section from Harkaway Fault area in Queensland (N-NE) to Murteree Ridge in South Australia (S-SW).	77



<b>Figure 3.8:</b> Isopach map overprint of Unit-7 with log profiles.	81
<b>Figure 3.9-A:</b> Schematic palaeogeographic map of Unit-7 representing the deposition of the McKinlay Member of the Murta Formation associated with the first transgression in Lake Murta.	82
<b>Figure 3.9-B:</b> Schematic palaeogeographic map of the upper McKinlay Member of the Murta Formation before the Maximum Flooding Surface (MFS).	83
<b>Figure 3.10:</b> Isopach map of Unit-6 to represent a high degree of accommodation or high rise in lake level.	86
<b>Figure 3.11:</b> Schematic palaeogeographic map of Unit-6 during the first Maximum Flooding Surface (MFS) of Lake Murta.	87
<b>Figure 3.12:</b> Isopach map overprint with log profiles that show a shallowing lake character of Unit-5.	91
<b>Figure 3.13-A:</b> Schematic palaeogeographic map of Unit-5 to illustrate the shallowing in Lake Murta.	92
<b>Figure 3.13-B:</b> Schematic palaeogeographic map of the localized incised valley fill cutting the lower part of Unit 4.	93
<b>Figure 3.14:</b> Lake Murta Isopach map shows a return to a deep lake conditions after flooding.	97
<b>Figure 3.15-A:</b> Schematic palaeogeographic map of the lower part of Unit-4 directly before flooding of the lake.	98
<b>Figure 3.15-B:</b> Schematic palaeogeographic map of the upper part of Unit-4 defining the second 3 <sup>rd</sup> order Maximum Flooding Surface MFS in Lake Murta.	99
<b>Figure 3.16:</b> Idealized sequence produced by regression in siliciclastic-dominated, hydrologically open lake, eastern Karoo Basin.	102
<b>Figure 3.17:</b> Contrast in timing of play-element deposition between lake types.	103
<b>Figure 3.18:</b> Isopach map of Unit-3.	104
<b>Figure 3.19-A:</b> Schematic palaeogeographic map of the lower part of Unit-3 directly after the second 3 <sup>rd</sup> order Maximum Flooding Surface (MFS) in Lake Murta.	105
<b>Figure 3.19-B:</b> Schematic palaeogeographic map of the upper part of Unit-3.	106
<b>Figure 3.20:</b> Isopach map of Unit-2 showing thick sediments deposited in the southwest part of the study area.	109
<b>Figure 3.21-A:</b> Schematic palaeogeographic map to characterize the deposition in early stages of Unit-2.	110
<b>Figure 3.21-B:</b> Schematic palaeogeographic map representing the deposition of sediments during late Unit-2.	111
<b>Figure 3.22:</b> Isopach map of Unit-1 during the maximum rise of the lake base level with little sediment input.	114

<b>Figure 3.23:</b> Schematic palaeogeographic map representing the deposition of muddy sediments during Unit-1.	115
<b>Figure 4.1:</b> Photomicrograph of associations 1 and 6. Carbonate cement with associated pyrite seen under cross polar light from Three Queens-1 @ 4809’.	119
<b>Figure 4.2:</b> Visual comparators for random sections through log-normally distributed sets of spherical grains.	120
<b>Figure 4.3:</b> Summary chart of mineralogy results from each facies association.	123
<b>Figure 4.4:</b> Summary histograms for each constituent identified in every facies association.	124
<b>Figure 4.5:</b> Classification of Murta Formation sandstones.	126
<b>Figure 4.6:</b> Well-developed rhombohedral crystal faces of quartz overgrowths seen under plane polar light from Merrimelia-6 @ 5185’ (facies association 1).	128
<b>Figure 4.7:</b> Petrographic images of feldspars in the Murta Formation.	128
<b>Figure 4.8:</b> Petrographic images of lithic grains in the Murta Formation.	131
<b>Figure 4.9:</b> Petrographic identification of carbonate minerals in the Murta Formation.	133
<b>Figure 4.10:</b> XRD traces show mineralogical abundances and diagenetic effects on a representative sample of each facies association.	136
<b>Figure 4.11:</b> Petrography of facies associations 1 and 2.	138
<b>Figure 4.12:</b> Petrographic identification of pore-lining clays in the Murta Formation.	140
<b>Figure 4.13:</b> Factors influencing porosity and permeability in the Murta Formation.	142
<b>Figure 4.14:</b> Provenance ternary plot of the Murta Formation sandstones.	146
<b>Figure 4.15:</b> Geographic provenance ternary plot.	147
<b>Figure 5.1:</b> Summary histograms of porosity readings from all facies associations.	154
<b>Figure 5.2:</b> Summary histograms of permeability readings from all facies associations.	154
<b>Figure 5.3:</b> Location map of the primary and secondary reservoir sandstones	158

## LIST OF TABLES

<b>Table 2.1:</b> Summary table of facies associations of the Murta Formation with lithology and sedimentary structures interpretation.	37
<b>Table 2.2:</b> Representative attributes of three major lacustrine facies associations.	64
<b>Table 2.3:</b> Characteristics of lake-basin types: strata, source facies, and hydrocarbons.	64
<b>Table 4.1:</b> Grainsize averages for each facies association in the Murta Formation.	118
<b>Table 4.2:</b> Sorting classification, based on the standard deviation of the grain size ( $\phi$ ).	118

## LIST OF ABBREVIATIONS

GR.....	Gamma Ray
DT.....	Sonic log
Sm.....	Massive sandstone
Sb.....	Bioturbated sandstone
Sr.....	Rippled sandstone
Ss.....	Storm sandstone
Sh.....	Laminated sandstone
Sd.....	Deformed sandstone (storm reworking)
St.....	Trough cross bedded sandstone
Stt.....	Thin sand sheets
Fl.....	Laminated mud
Fb.....	Bioturbated mud
F.A.....	Facies Association
LST.....	Low Stand System Tract
TST.....	Transgressive Stand System Tract
HST.....	High Stand System Tract
FS.....	Flooding Surface
TS.....	Transgressive Surface
MFS.....	Maximum Flooding Surface
mMFS.....	minor Maximum Flooding Surface
SB.....	Sequence Boundary
Q.....	Quartz
F.....	Feldspar
M.....	Mica
K.....	Kaolinite
I.....	Illite
S.....	Siderite
C.....	Calcite
D.....	Dolomite
XRD.....	X-Ray Diffraction
SEM.....	Scanning Electron Microscope

## Chapter 1 Introduction and literature review of the Murta Formation

### 1.1 Introduction

#### 1.1.1 Rationale

The Early Cretaceous (Barremian) Murta Formation and its basal McKinlay Member are largely lacustrine units deposited between the Jurassic fluvial and lacustrine units of Namur Sandstone below and Cretaceous marine shales and thin sands of Cadna-owie Formation above (Fig.1.1) (Mount 1981 & 1982; Ambrose *et al*, 1986; Gorter, 1994; and Krieg *et al*, 1995).

The oil flow in Dullingari North 1 (Murta Formation type section defined by Mount, 1981) was the first hydrocarbon discovery from the Early Cretaceous Murta Formation (Robinson & Butler, 1989). The discovery of the Dullingari-Murta field in 1979 and its reservoirs were the youngest hydrocarbon accumulations in the western Eromanga Basin.

In hydrocarbon terms, the Murta Formation contains the stratigraphically highest, relatively continuous sand units beneath the thickest, most continuous seal in the Eromanga Basin. The reservoirs in this position are commonly oil charged but productivity is strongly controlled by depositional facies associations with generally low production rates and recovery factors.

The study of these facies associations in detail will have a great impact in predicting the optimal reservoir facies association and will also help in defining how to enhance the recovery factor since the productivity is mainly driven by these depositional facies associations, their occurrence and reservoir quality. In addition, this study may have application as an analogue for other hydrocarbon plays, since Australia has a number of fluvial-lacustrine basins with hydrocarbon potential.

Since all of the previous studies concentrated on a group of wells or fields in specific areas and not on the whole Lake Murta, this study covers the regional extent of the Murta Formation wells by selecting a group of representative wells from different geographic locations in both Queensland and South Australia.

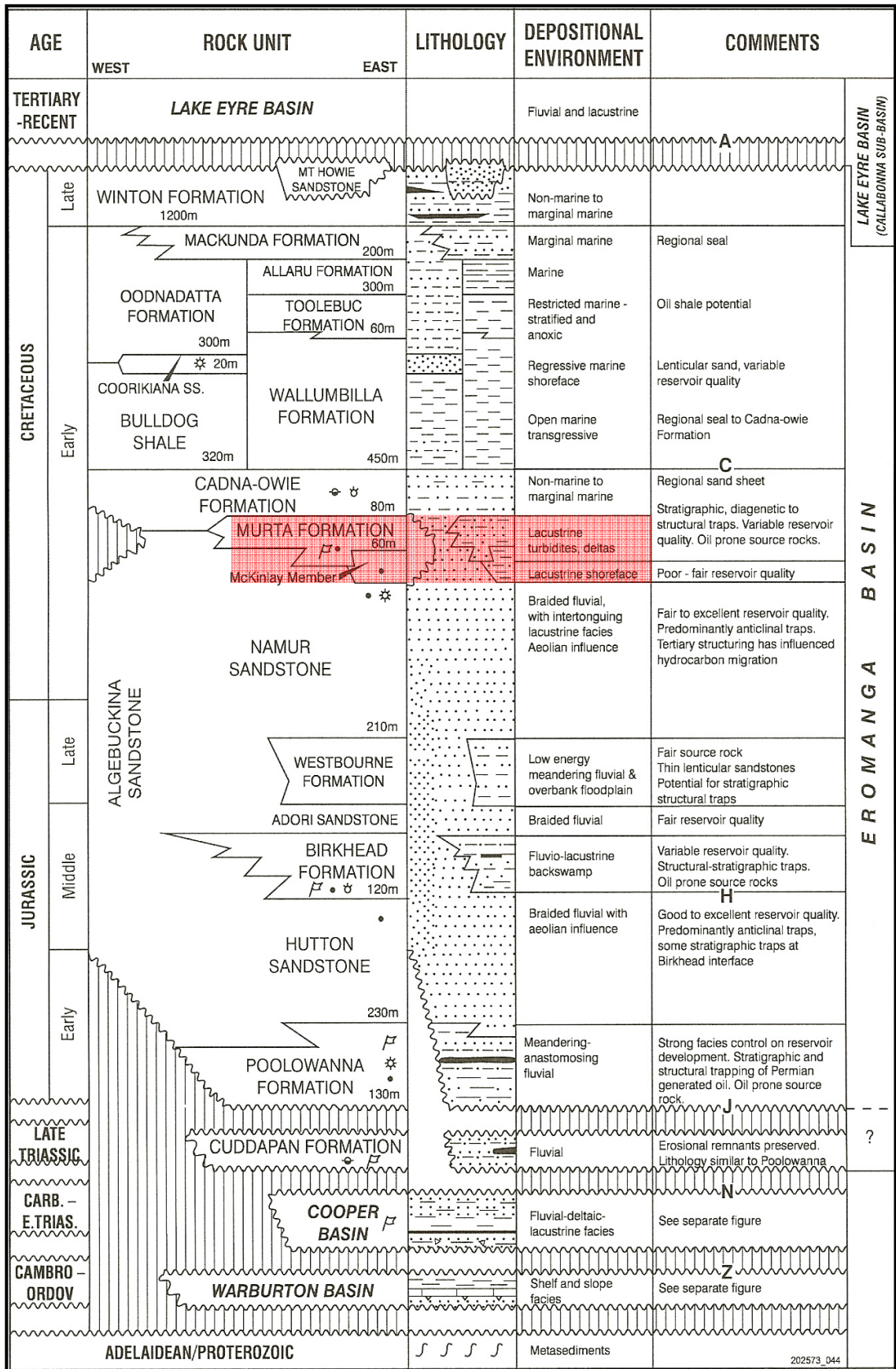


Figure 1.1: Geological summary of the Eromanga Basin. The unit of investigation is highlighted in red (modified from PIRSA, 2006).

### 1.1.2 Aims and significance

The aim of this study is to define those parts of the basin and facies associations where oil productivity and recovery in the Murta Formation are likely to be optimal. This is done through an integrated study to get a better understanding of reservoir quality and geometries for each facies association.

### 1.1.3 Objectives

The objectives of this study cover two parts, namely the sedimentology, sequence stratigraphy and mapping, and reservoir development. Together, the objectives help to define the aim of finding those parts of the basin that are sweetspots for oil accumulations and production.

These objectives are:

- To generate geographically regional log correlation cross sections for every trough and ridge across the basin to show the direction of the sand input/trends
- To identify the core coverage for each interval and perform core descriptions.
- To integrate wireline logs with core descriptions (core to wireline log correlation).
- To interpret the depositional facies associations.
- To identify the key surfaces and stacking patterns from cores and wireline logs for sequence stratigraphy.
- To identify the facies association distribution in the Murta Formation and place them in a sequence stratigraphic model.
- To construct a set of isopach maps for each unit of the Murta Formation.
- To predict the possible sand input into the basin.
- To build a depositional model for the basin for each unit of the Murta Formation
- To determine the reservoir quality for each facies association from petrography analysis.
- To identify the clay types and distribution, and pore geometry.
- To interpret the provenance of the sandy intervals.
- To construct a permeability distribution map for each depositional environment and map the facies associations quality and its extent for the Murta Formation prospectivity.

### 1.1.4 Study area

The Murta Formation/Lake is best developed over the Harkaway Fault area and Nappamerri Trough within the Eromanga Basin with a maximum thickness of 100 m over the southern Nappamerri Trough (Fig. 1.2 & 1.8). The Murta Formation between those areas contains a cluster of hydrocarbon fields extended between the southwestern part of Queensland and the northeastern part of South Australia. Murta Lake is considered to have been a very large lake of at least 300 km by 300 km (Lang *et al*, 2001).

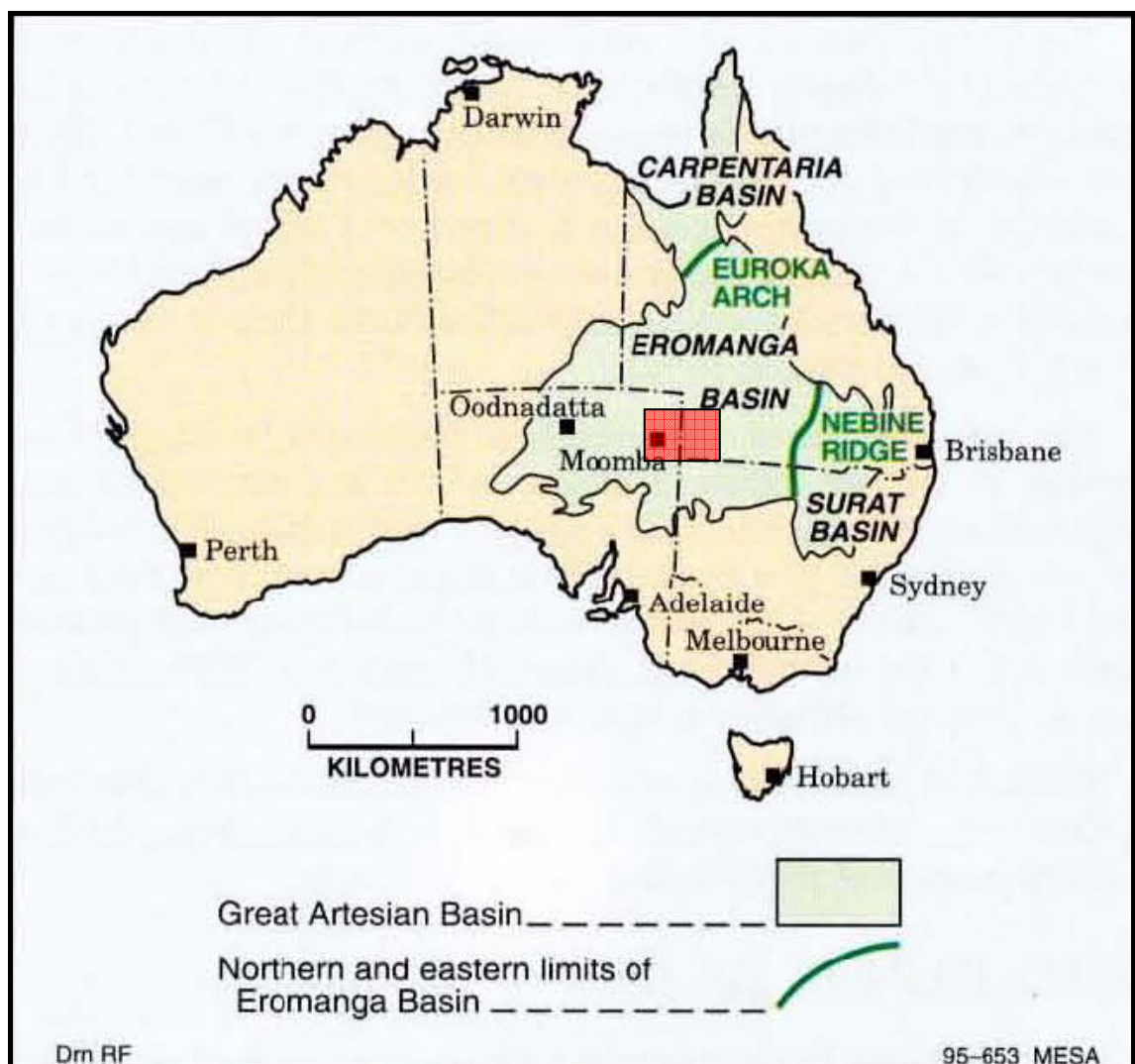


Figure 1.2: Eromanga Basin location map with the study area in red (modified from Krieg *et al*, 1995).

### 1.1.5 Data support

Santos Ltd. gave full access to its database using a workstation with access to the Cooper-Eromanga database (dbmap and Geoframe). Five regional correlation cross sections from 41 wells, and 8 isopach maps were generated with the help of Santos Ltd. database using Geoframe software.

A total of 37 cores were described both from Queensland and South Australia. Fifteen of the 37 cores were from the Queensland part and were logged at Santos Ltd's Gilman core storage in Port Adelaide. The other 22 cores were described using the Primary Industries and Resources of South Australia (PIRSA) core facilities in Glenside, South Australia.

Forty four thin sections and 40 XRD samples were prepared with the help of Santos Ltd. through a contractor. A Santos Ltd. petrographic microscope with image analysis software was used to study the thin sections from both the Queensland and South Australian wells. PIRSA provided an additional 15 thin sections for the petrography study. Forty one SEM samples were analysed through arrangements by the Australian School of Petroleum (ASP) and the University of Adelaide.

### 1.1.6 Methodologies

This study employed a number of techniques, including regional log correlations, core descriptions, sequence stratigraphy, petrography, probe permeability measurements, and palaeogeography mapping.

#### *Regional log correlations*

Gamma ray (GR) and sonic logs (DT) were used to construct 5 regional cross sections (Appendices 3.2, 3.3, 3.4, 3.5 and 3.6) and to correlate between 41 wells for facies relationships determination (Fig. 1.3). One hundred API was used as the sandstone cutoff value on the gamma ray log. A velocity cutoff of 100 microseconds per foot was implemented for carbonate cemented zone determination.



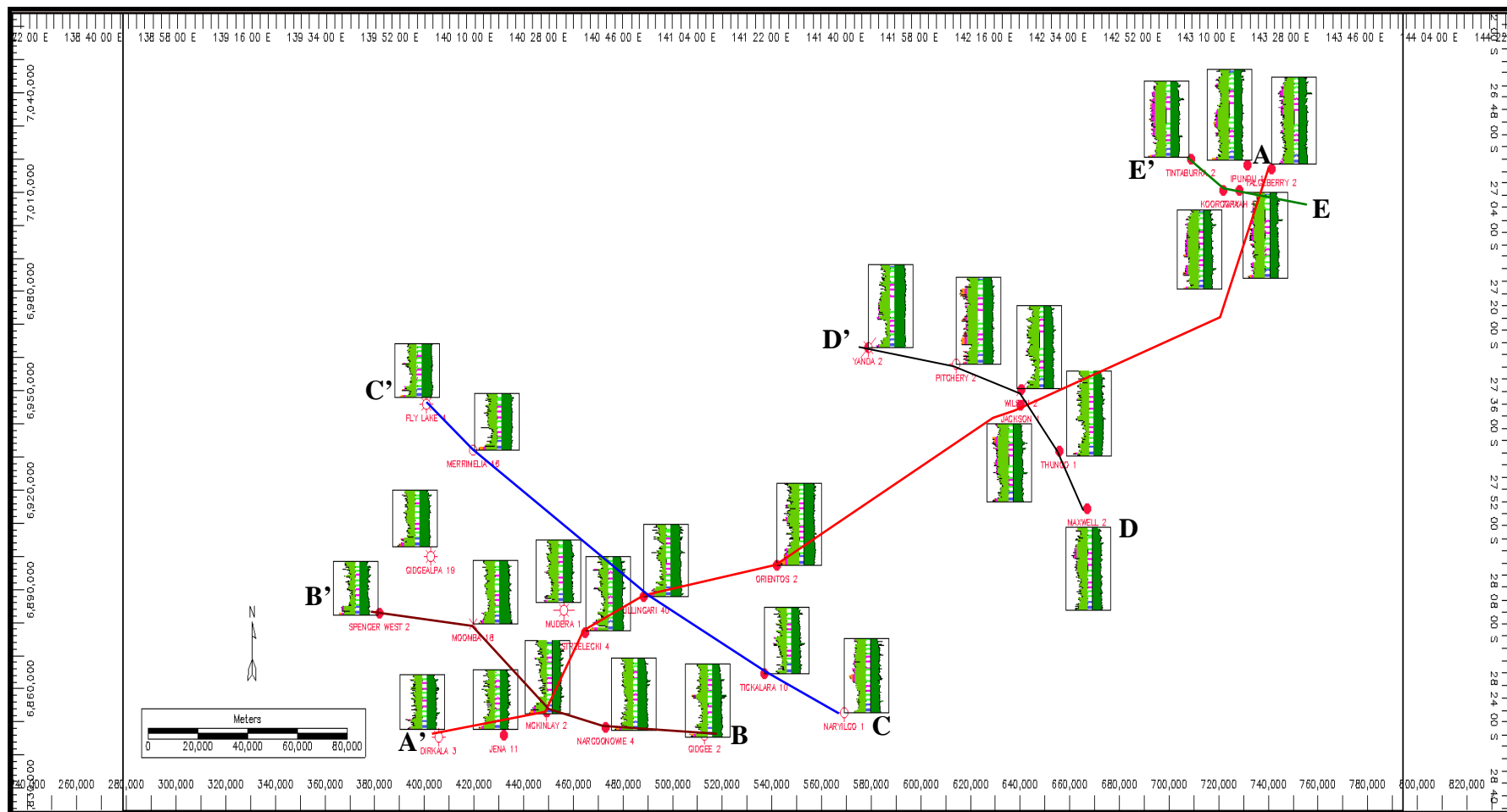


Figure 1.3: Location of the five regional cross sections across the Eromanga Basin showing the Murta Formation cored wells in South Australia and Queensland.

Gamma ray and sonic log signatures were used to subdivide the Murta Formation from both the South Australian and Queensland parts of the basin using Wellpix/Geoframe software. The subdivision of the Murta Formation concentrated more on chronostratigraphy than lithostratigraphy to provide a temporal framework and helped to break out the individual sands from the logs (Fig. 1.4).

This study followed a Santos Ltd. nomenclature for the Murta Formation surfaces (DC notation). DC00 represents the top of the Murta Formation and/or the base of Cadna-owie Formation as marine influence commenced from the Cadna-owie Formation onwards. DC70 is the base of the Murta Formation and/or top Namur Sandstone where lacustrine influence started, and dominant fluvial conditions in the Namur Sandstone below stopped. DC10, DC20, DC40, and DC60 represent the tops of the Murta Formation sandy packages (Fig. 1.4).

After identifying the key surfaces, regional correlations of 41 wells were produced to help in mapping the thickness of each unit in the Murta Formation. A sequence stratigraphic framework was constructed through integrating core descriptions and regional log correlations. A regional schematic palaeogeographic map of each unit was produced using the facies associations interpretations.

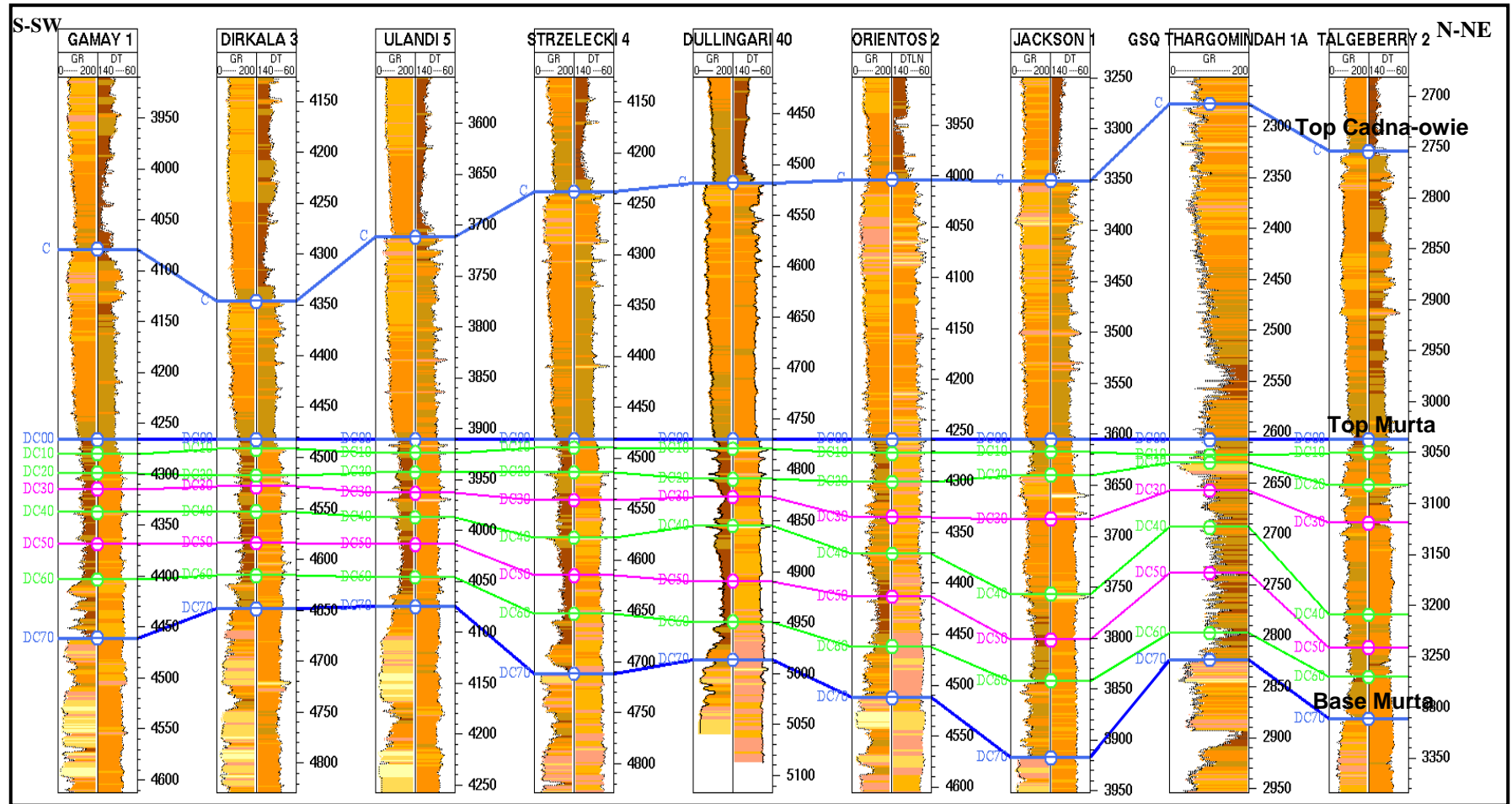


Figure 1.4: Regional log correlation between Gamay-1 in South Australia and Talgeberrry-2 in Queensland showing Murta Formation key surfaces and units (Wells flattened on top Murta Formation) (A-A' cross section in the base map).

### ***Core logging***

After identifying the best possible core coverage using the Santos Ltd. database, 37 representative wells with Murta Formation cores were logged across the basin. The aim was to get a representative coverage for the entire interval for various different geographic locations.

The core information was correlated back to the type sections in Dullingari North 1, Dullingari 9 and Strzelecki 4 concentrating on subdividing the reservoir sands into depositional facies associations (distributary channels, shoreline, protected shoreline, deltaic mouth bars, tempestite and turbidite deposits).

Graphic sedimentological logs including grain size and sedimentary structures, were prepared for all cores to be integrated and/or correlated with wireline logs for facies associations interpretation and sequence stratigraphy (Appendix 2.1). Integration of graphic sedimentological logs with the wireline logs was possible after wireline to core depth matching, by identifying the carbonate-cemented layers of the core and density peaks in logs (Fig. 1.5).

Core depths were used for logging of all cores. There was a minimal core loss in 2 of the 37 wells. However, those core losses were estimated for each of those two wells by correlating the core with wireline log curves.

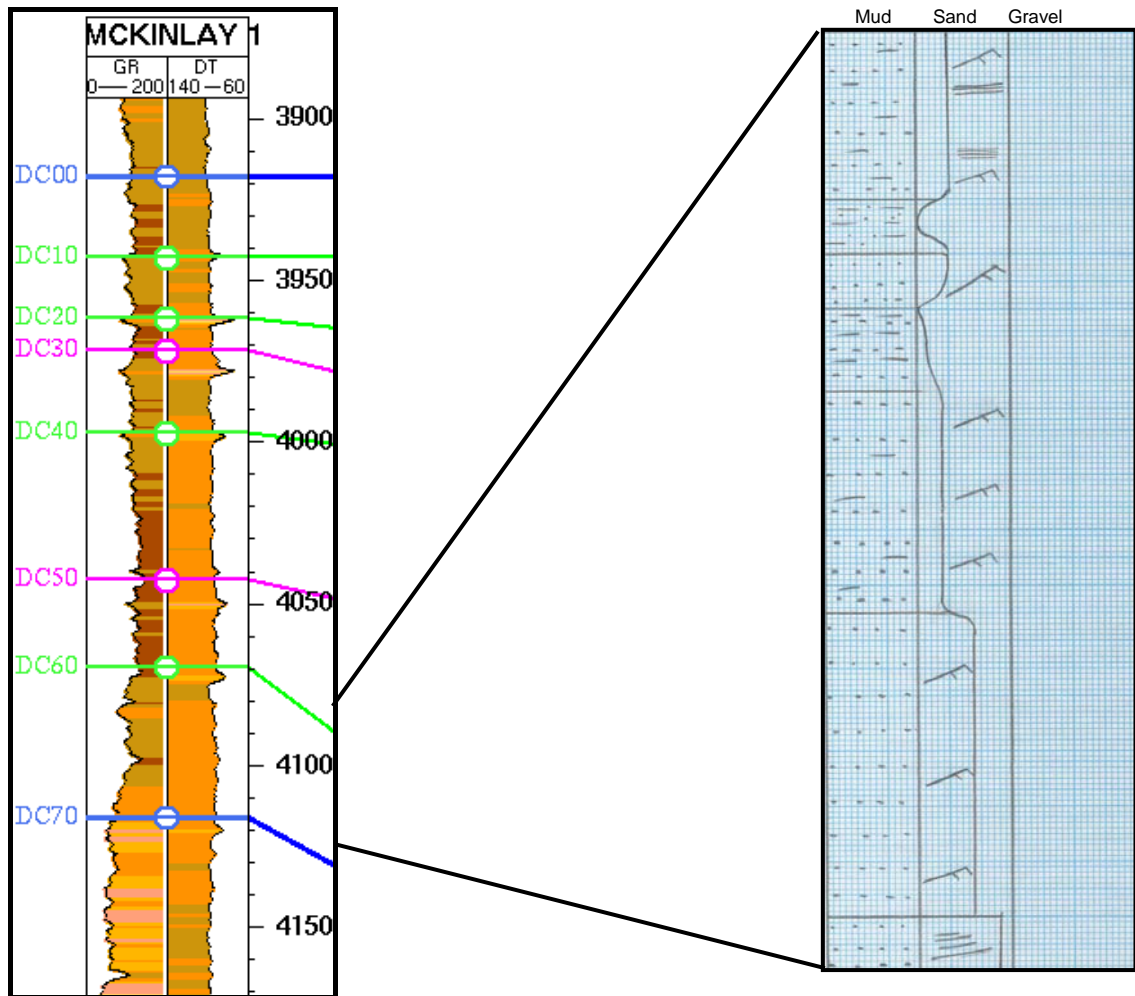


Figure 1.5: McKinlay-1 well (4086-4120') as an example of core to log correlation.

### *Stratigraphic analysis*

A sequence stratigraphic framework for the Murta Formation across the Eromanga Basin was constructed using facies interpretation and regional wireline log correlations. These data were applied to establish regional stacking patterns and system tracts for the Murta Formation.

Eight isopach thickness maps were generated for each unit of the Murta Formation including a general regional isopach map of the Murta Formation for southwest Queensland and northeast South Australia (Fig 1.6). To construct those maps, data from the regional correlations were integrated with facies associations interpretation using a sequence stratigraphic framework.

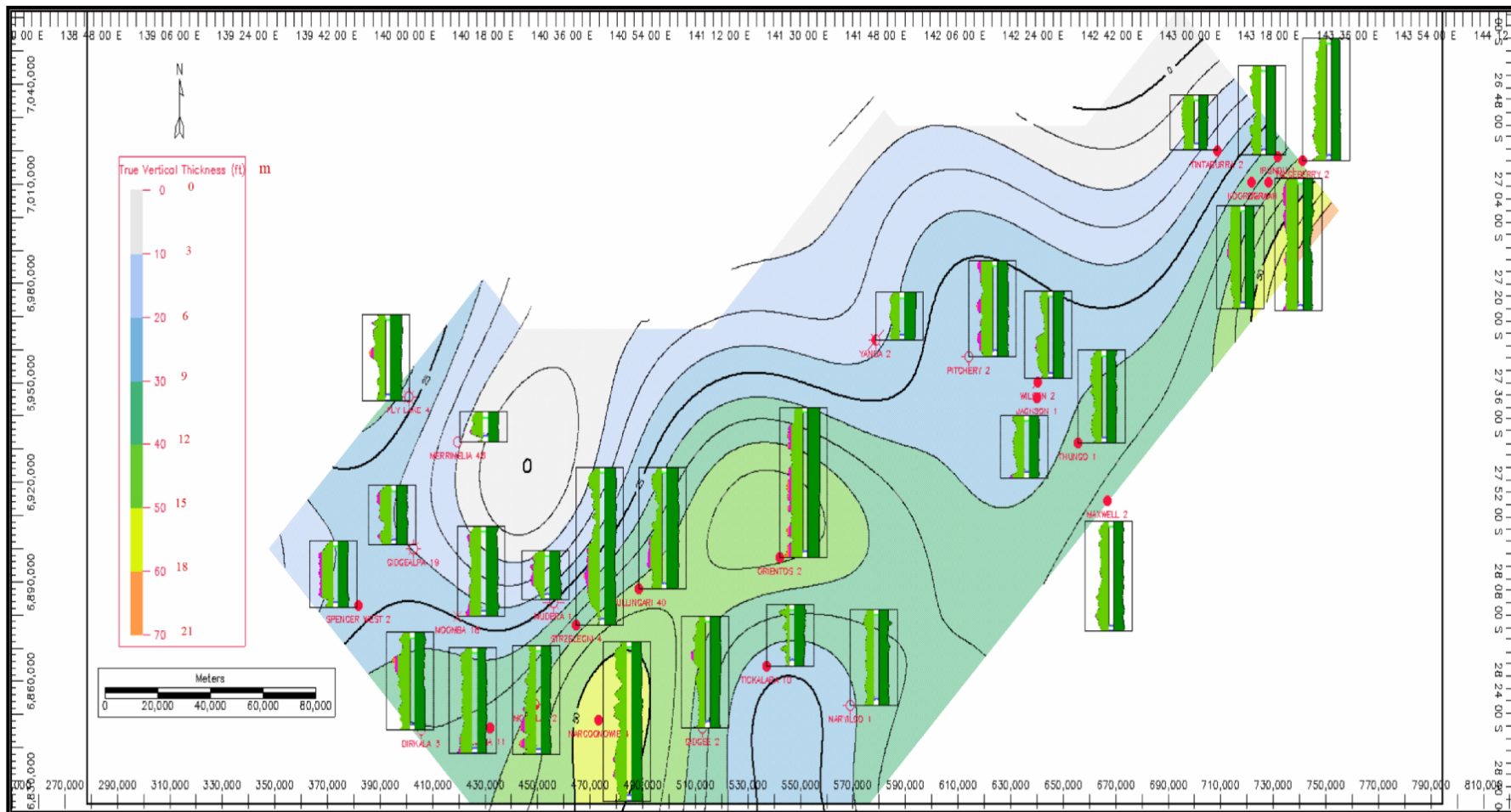


Figure 1.6: Example of Murta DC60-70 unit (McKinlay Mbr. of Murta Formation) thickness map with high sand input mainly from S-SW.

### ***Palaeogeography***

By pulling together the regional geology, sedimentology, and sequence stratigraphy, this study produced schematic palaeogeographic models of the basin taking into consideration its size and shape, position on the continent, palaeolatitude and orientation, likely prevailing winds and wind fetch. This was done to determine where sandy beaches and shorelines might preferentially develop as opposed to muddy shorelines. Twelve schematic palaeogeographic maps were generated for each unit of the Murta Formation (Fig. 1.7).

### ***Petrography***

Fifty nine thin sections were examined from 8 geographic areas across the Eromanga Basin. This was done to define the reservoir characteristics of each facies and to define provenance differences for the gravel intervals developed when the lake level was low.

An Olympus BX41 petrographic microscope was used for thin section descriptions. Identification of the facies and gravel interval distributions were made using the sedimentology and sequence stratigraphy data. The localities of these thin sections were selected to represent all of the Murta Formation facies from different wells. All of the thin sections were prepared by impregnation with blue epoxy resin for porosity recognition.

A standard thin section description form was filled in for every thin section. Texture, detrital grains, matrix, cements, porosity, permeability, and connectivity features were noted (Appendix 4.4). Provenance was interpreted for some thin sections/wells which have grain size from fine to medium sand or coarser.

The statistical function of *analySIS* (Soft Imaging System) software, with its camera linked to the Olympus BX41 petrographic microscope, was used for grain size analysis. For every representative view, 50 grains from different sizes were selected to represent the sample under the petrographic microscope. The *analySIS* software was utilized to provide a grain size mean and its standard deviation (Appendix 4.4).



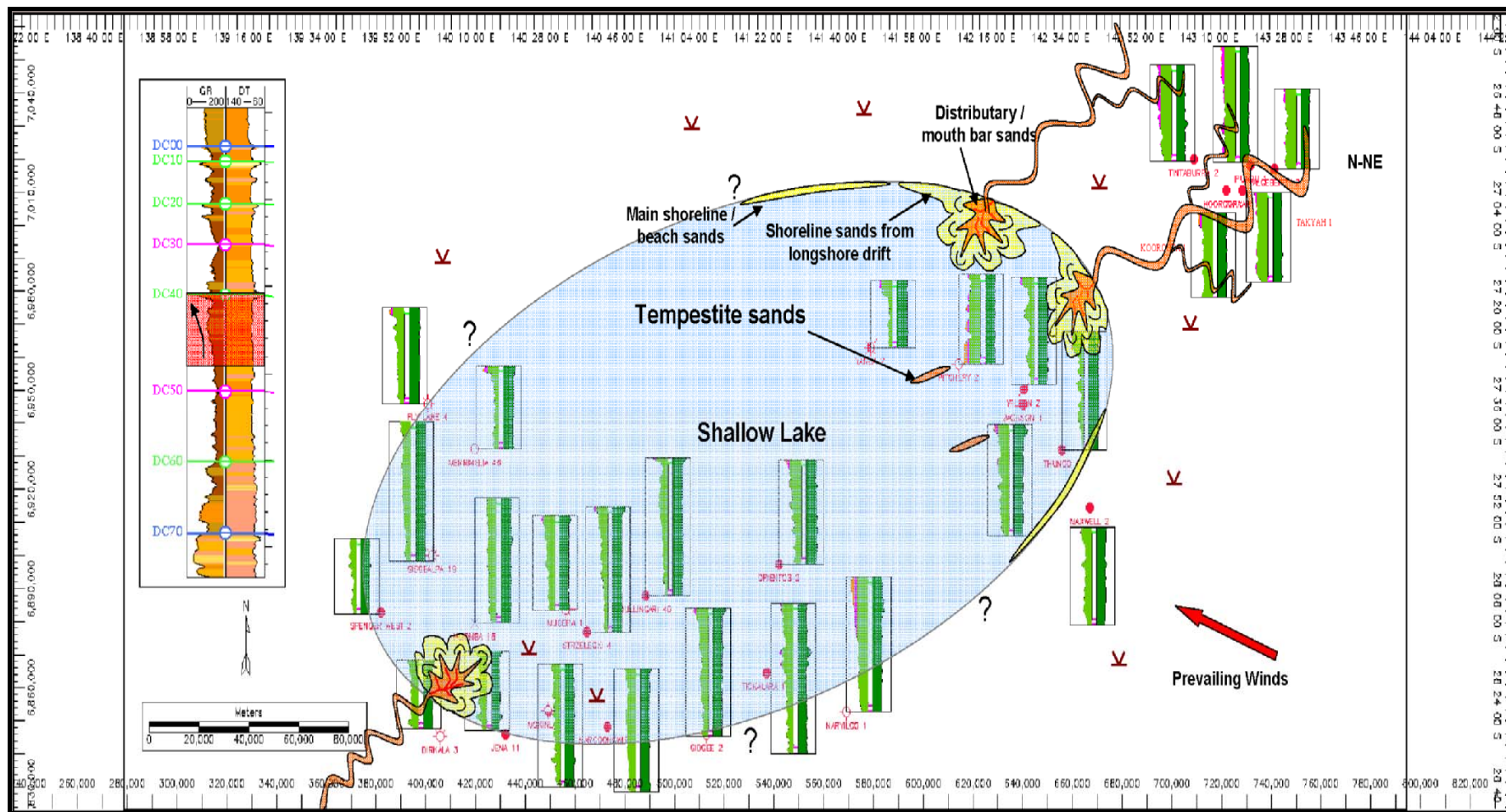


Figure 1.7: Schematic palaeogeographic map of Murta DC40-50 unit showing two sand inputs in Lake Murta. The main sand input was from N-NW, while the secondary sand input was from S-SW.



Visual effective porosity estimations were applied to every thin section using the petrographic microscope (Appendix 4.4). In addition, the *analySIS* software sometimes was able to give a confirmation for the visual porosity estimation. As the software depends on density slicing a grey-scale image, tonal resolution is often insufficient to accurately depict porosity. For this study, the *analySIS* software was used only for grain size analysis and collecting images.

### ***Scanning Electron Microscope (SEM)***

Forty one samples from most of the selected wells across the basin were studied under the Scanning Electron Microscopy (SEM). This was completed to define the pore and grain relationships, clay distribution, cement types, and in turn how they influence the pore geometry/spaces. The advantage of this microscope is to allow viewing the samples at high magnification and resolution.

A Philips XL30 SEM was used to examine all samples and to take photos of each. The samples were glued on stubs and then coated with platinum for high resolution. The operating parameters used were 10 kv with a spot size of 2 or 3 A° depending on the magnification required.

### ***X-Ray Diffraction (XRD)***

XRD was used to define the clay types, mineral content, and type of carbonate of all facies groups. The XRD work concentrated on the origin/provenance of the coarse input to the basin at times of lowered lake levels and on the nature and controls on the carbonate cemented zones. Most of the samples were tested for clay content and some for whole rock analysis (Appendix 4.5).

Twenty seven samples were tested for clay types and prepared by crushing the sample by mortar and pestle in 1 M Magnesium Chloride (MgCl) solution. The suspended clays were partially separated from the granular quartz and carbonates and saved for washing. The washed clay concentrate was settled on to a glass slide and dried ready for XRD analysis. The MgCl solution exchanges ions with swelling clays to sharpen the peaks for more accurate definition.

The 13 samples selected for whole rock mineralogy were from coarse grained intervals. These samples were also crushed using a mortar and pestle and slurried with water before being smeared on a glass slide then dried for XRD examination.

Whole rock samples were run as air-dried samples. Clay separates were run as air-dried samples and repeated after the addition of ethylene glycol to expand the smectitic clays.

All samples were analyzed using a Siemens PW 1050 X-Ray Diffractometer. The operating conditions used were Cobalt K $\alpha$  radiation as a source, scan length of 5-40°, scan angle of 2 $\theta$ , and at a resolution of 0.05° (for clay content samples) and 0.08° (for whole rock samples) increments.

### ***Core analysis (Permeametry)***

Permeability measurements were conducted on all of the identified sandstone facies with an emphasis on the tempestite facies. Permeametry was used to determine the vertical and lateral permeability variability for each facies.

The surface of slabbed core samples was divided into squares with an area of 2cm x 2cm. The measurements were centered on each of those squares to get a good representation of the permeability measurements (Appendix 4.3).

Some permeability readings were removed from the data set because they fall on fractured parts of the core sample. Some of those readings have been estimated by visual comparison with other parts of the core slab.

A plot representing the relationship between silt percentages versus permeability measurements was produced (Appendix 4.4).

### 1.1.7 Basin setting and tectonics

The Eromanga Basin covers an area of about 1 million km<sup>2</sup> in central Australia. (Wecker, 1989) (Fig. 1.8). It is a broad intracratonic basin with up to 3000 m of middle Triassic to Late Cretaceous sediments. It is one of three basins which comprise the Great Artesian Basin. The other two basins are the Carpentaria and Surat Basins. (Wecker, 1989).

There was minimal syndepositional tectonic activity in the Eromanga Basin apart from subsidence and the main depocenters largely coincide with those of the preceding Permo-Triassic basins (Wecker, 1989). However, there was an Early Tertiary structuring phase which led to uplift and erosion of the eastern margin of the Eromanga Basin and developed broad northwesterly to northeasterly-trending anticlines within the basin (Wecker, 1989). Some high angle faults are associated with those anticlines. These structural deformations have been strongly effected by the underlying Palaeozoic structural elements (Fig. 1.8) (Wecker, 1989).

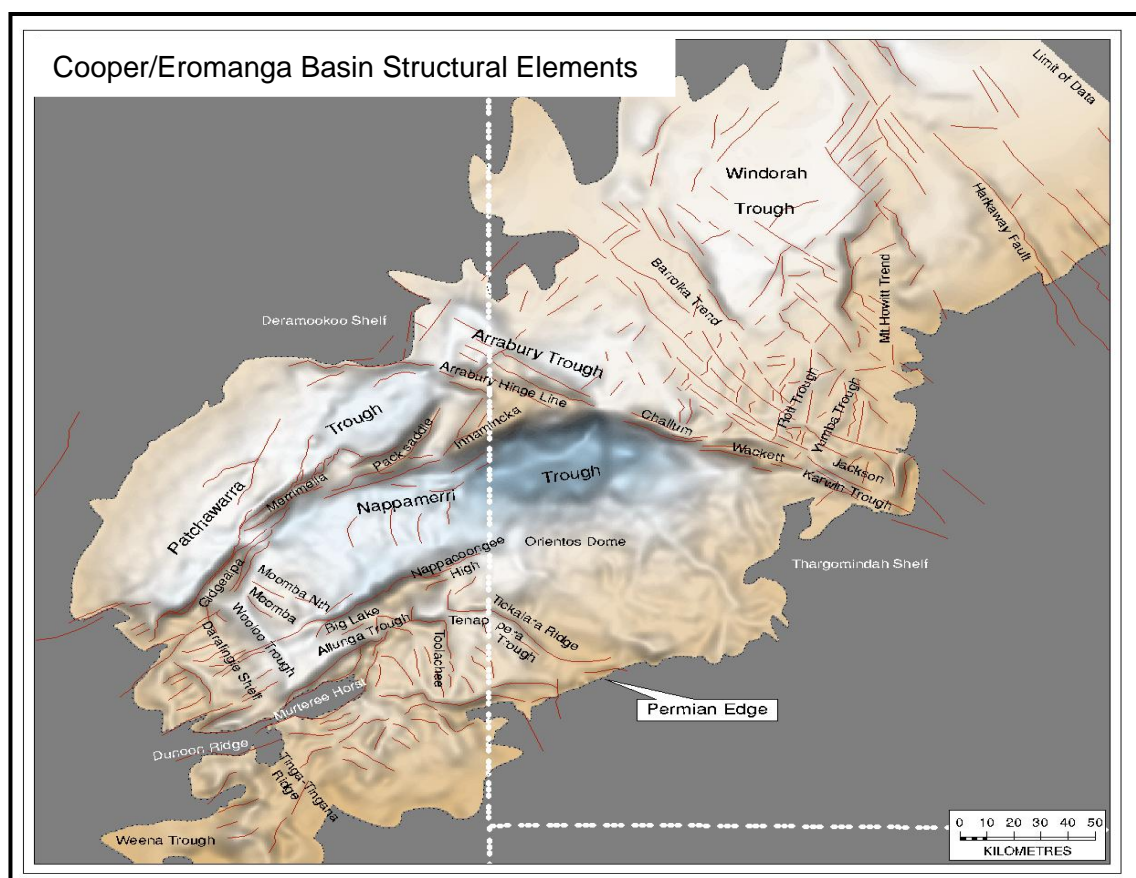


Figure 1.8: Structural elements of the Cooper/Eromanga Basins (Santos Ltd., 2003).

The main reservoirs in the Eromanga Basin are non-marine to fluvial and lacustrine rocks (Poolowanna Formation, Hutton Sandstone, Birkhead Formation, Adori Sandstone, Westborne Formation, Algebuckina Formation, Namur Sandstone, and Murta Formation) capped by shallow marine deposits (Cadna-owie Formation, Wallumbilla Formation, Bulldog Shale, Coorikiana Sandstone, Toolebuc Formation, Oodnadatta Formation, Allaru Formation, and Mackunda Formation). These are overlain by more fluvial-lacustrine and coal swamps successions (Winton Formation, and Mt. Howie Sandstone) (Fig. 1.9) (Wecker, 1989).

The lower interval (Fig. 1.9) contains the main reservoirs and source rocks of the Eromanga Basin with most of the commercial hydrocarbon accumulations (Wecker, 1989). The trap types in this basin are a combination of structural and stratigraphic traps, but mainly structural.

Most of the major discoveries to date were drilled in the basin centre adjacent to and overlying the Permo-Triassic Cooper Basin (Fig. 1.10). The Cooper Basin is believed to have contributed most of the hydrocarbons in the Eromanga Basin (Wecker, 1989). Methane carbon isotope compositions of the Eromanga gases suggest derivation from the more thermally-mature Permian Cooper Basin section (Wecker, 1989). In addition, the Eromanga Basin section is only marginally mature for gas generation. Thus, vertical migration of Permian gas and oil facilitated by Tertiary faults is believed responsible for the hydrocarbon accumulations in the Eromanga Basin (Wecker, 1989).



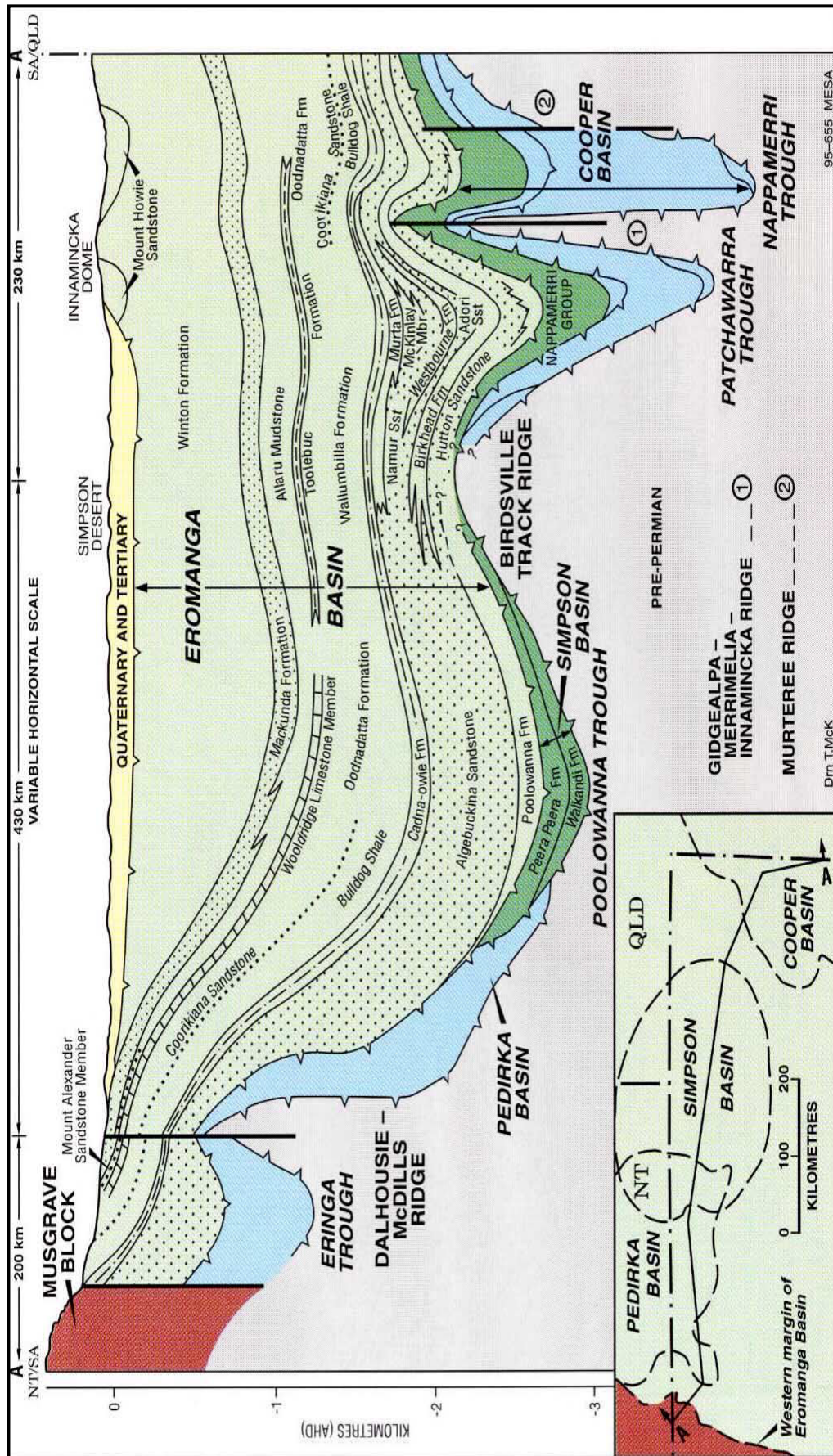


Figure 1.9: Cross section through the Eromanga Basin (Krieg *et al*, 1995).



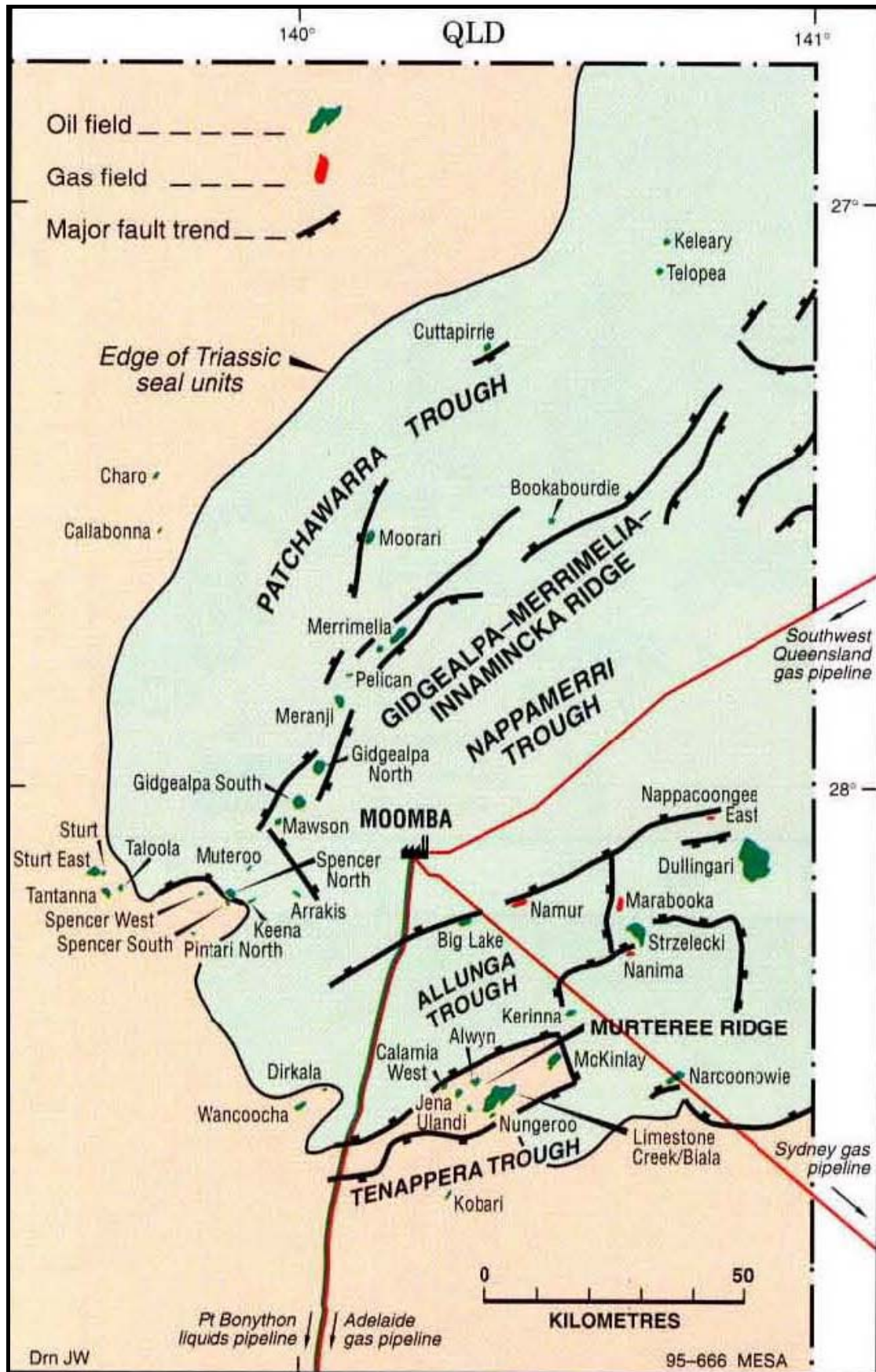


Figure 1.10: Location of the Eromanga Basin hydrocarbon discoveries in the Cooper region (Krieg *et al*, 1995).

## 1.2 Literature review of the Murta Formation

### 1.2.1 Definition of the Murta Formation

Ambrose *et al* (1986) defined the Murta Formation as a mainly fine-grained lacustrine sequence intervening between braided-fluvial sediments of the Namur Sandstone and the overlying, marginal marine Cadna-owie Formation. The lower and upper contacts of the Murta Formation with Namur Sandstone and the Cadna-owie Formation are gradational. Ambrose *et al* (1986) proposed a reference section for the Murta Formation in Dullingari 9 well.

Mount (1982) was the first to introduce the McKinlay Member of the Murta Formation as silty sandstone transitional between the fluvial Namur Sandstone below and the overlying lacustrine siltstone of Murta Formation. Zoellner (1988) indicated a possible marine influence in the upper Murta Formation.

According to this definition, Ambrose *et al* (1986) kept the Murta as a member of the Mooga Formation. However, Gravestock *et al* (1995) upgraded Murta to a Formation and proposed Strzelecki-4 well as a type section for the McKinlay Member of the Murta Formation and the Namur Sandstone (Fig. 1.11) (Krieg *et al*, 1995).

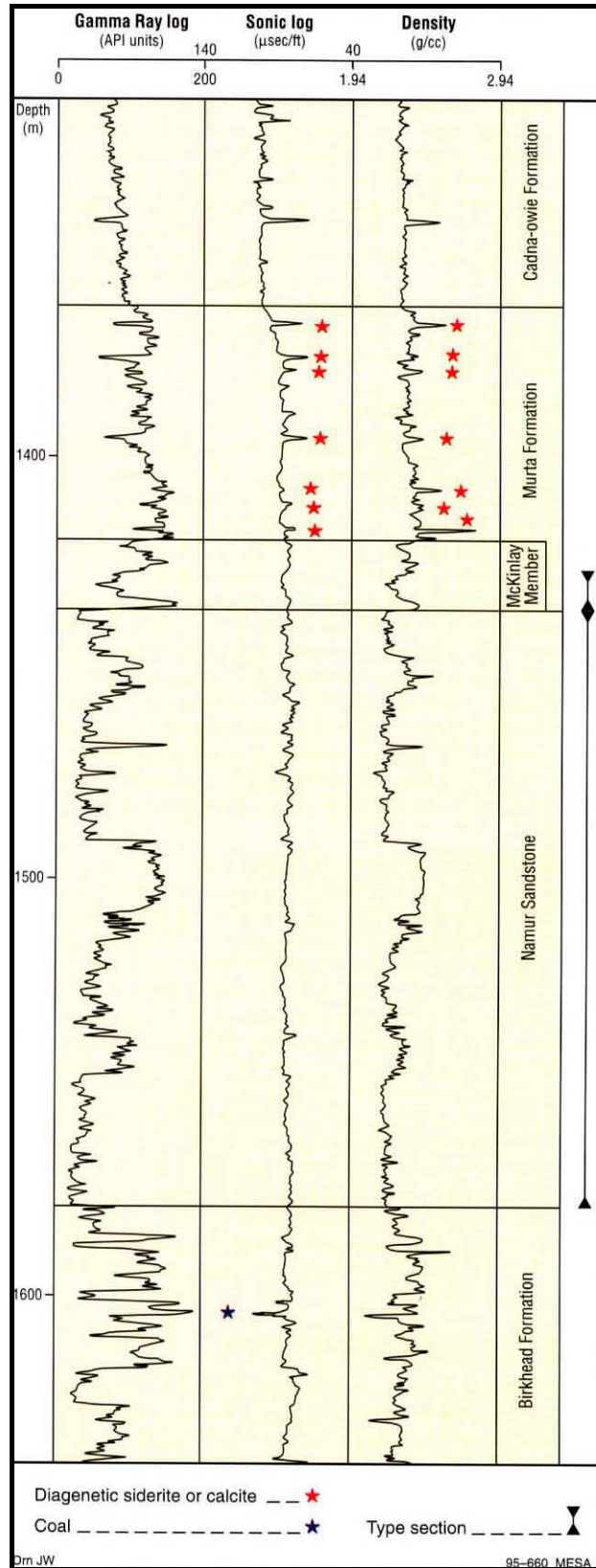


Figure 1.11: Stratigraphic subdivision and lithologic features from Strzelecki-4 drill-log interpretation, McKinlay Member and Namur Sandstone type section by Gravestock *et al* (1995) (Krieg *et al*, 1995).



## 1.2.2 Murta Formation units

Four units have been recognized by Ambrose *et al* (1986) in the Murta Formation reference section in Dullingari 9 well (Fig. 1.13-B&1.14). The basal unit, unit 1, is an upward-coarsening lacustrine delta sequence capped by delta front sands. Unit 2 has similar graded fine sand and silt deposited in a shallow water environment. A basinward progradation of a fan sequence is named unit 3 by Ambrose *et al* (1986). Unit 3 is a shallowing trend which finished with the development of a thin shoreline bar. Unit 4 represents a return to offshore sedimentation. The unit 4 sequence is fining-upward which could reflect a deep water environment prior to a marine incursion (Ambrose *et al*, 1986).

Gorter (1994) proposed a model based on dividing the Murta Formation into six units in Nockatunga wells based on log characteristics and lithology. These units were numbered M1 to M6 sequentially downward (Fig. 1.12 & 1.13-C).

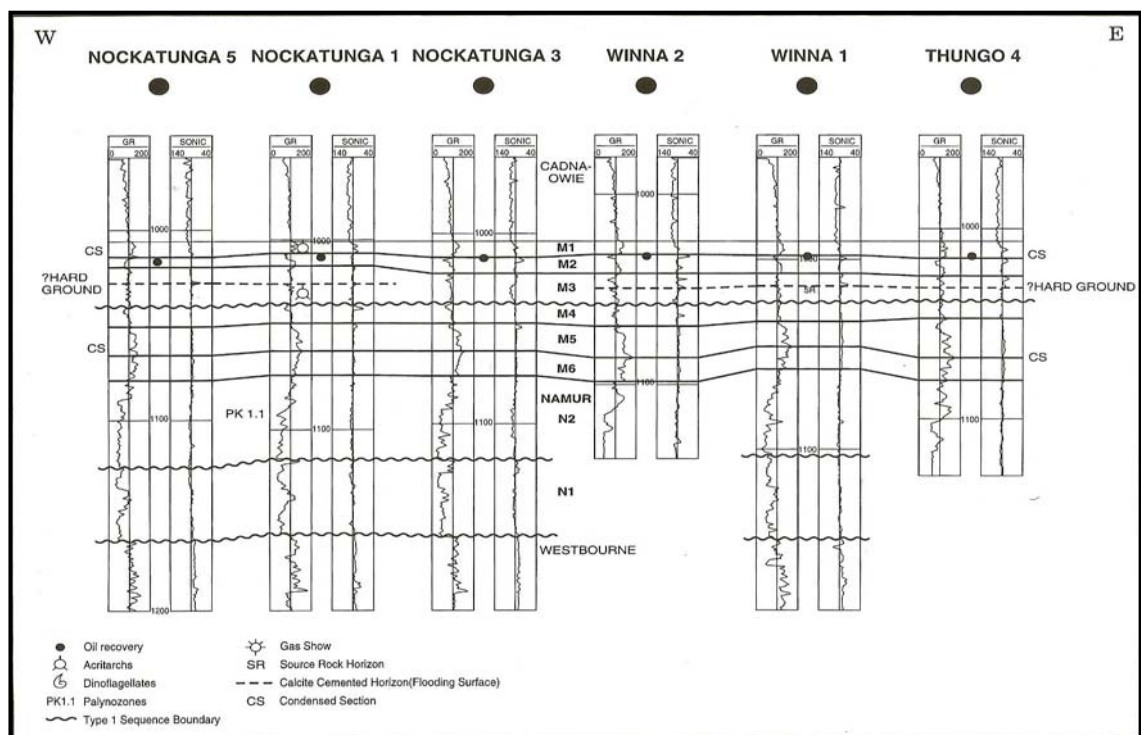


Figure 1.12: West to east cross section from Nockatunga-5 to Thungo-4 showing Murta Member M1 to M6 units and Namur sandstone Member N1 and N2 units. Also shown the zones of oil recovery, palynology control, Type 1 sequence boundaries and the Winna-1 source rock horizon (Gorter, 1994).

The Gorter (1994) units are slightly different to the five subunits proposed by Mount (1981) for the Dullingari field.

Gorter's (1994) M6 is a fining-upward succession and is equivalent to the M5 unit of Mount (1981) (Fig.1.13). This fining-upward succession unit is interpreted in response to the transgression of the Murta waterbody at this time. Dark brown carbonaceous claystone is the main lithology of Gorter's (1994) M5 unit. It is a coarsening upward succession from high gamma ray shale to fine grained sandstone. The presence of dinoflagellates was reported from the M5, unit suggesting a marine influence. This unit is correlated with the Ambrose *et al* (1986) M4 at Dullingari field (Gorter, 1994) (Fig. 1.13). The M4 unit of Gorter's (1994) classification is equivalent to the upper part of Mount's (1981) M4 unit (Fig. 1.13). It is also a coarsening upward succession from shale to sandstone.

The base of Gorter's (1994) M3 unit represents a type 1 sequence boundary. M3 unit correlates with Mount's (1981) M3 and is most likely the lower part of Unit 2 of (Ambrose *et al*, 1986) (Fig. 1.13). The M2 unit of Gorter (1994) can be correlated with Mount's (1981) M2 unit. It is also a coarsening upward succession. The M1 unit is a fining upward succession of shale and its upper part is directly correlated with Mount's (1981) M1.

### 1.2.3 Sequence stratigraphy

In his study, Gorter (1994) proposed a sequence stratigraphic model for the Murta Formation including the Namur Sandstone in Nockatunga field (Fig. 1.13-C). A type 1 sequence boundary developed during the lowstand in Namur Sandstone. Two sequences were recognized within the Namur Sandstone (N1 & N2) with a type 1 sequence boundary interpreted within the member. The upper Namur is gradational with the lower Murta Formation M6 unit. This M6 unit represents a transgressive system tract (Gorter, 1994).

The M5 and M4 have been interpreted as high stand system tract sediments deposited over the maximum flooding surface at the base of M5. At the end of M4, there was a drop in sea level leading to incisions of channels which represents a sequence boundary. After that, sea level rose leading to filling of these incised channels gradually in the middle of M3 (Gorter, 1994). The sandstone reservoirs were developed with the basal M3 incised valley fill sand, while the transgressive microtidal barrier facies developed at the top of the M3. A microtidal environment formed at the top of M2 under a seasonal climate.

After the flooding of the barrier islands during the M2 and M1 times, a high amount of organic matter was supplied to the Nockatunga field (Fig. 1.13-C). There is a condensed section in the M1 represented by “hot gamma” shale as a source rock for the formations overlying the Murta Formation (Gorter, 1994).

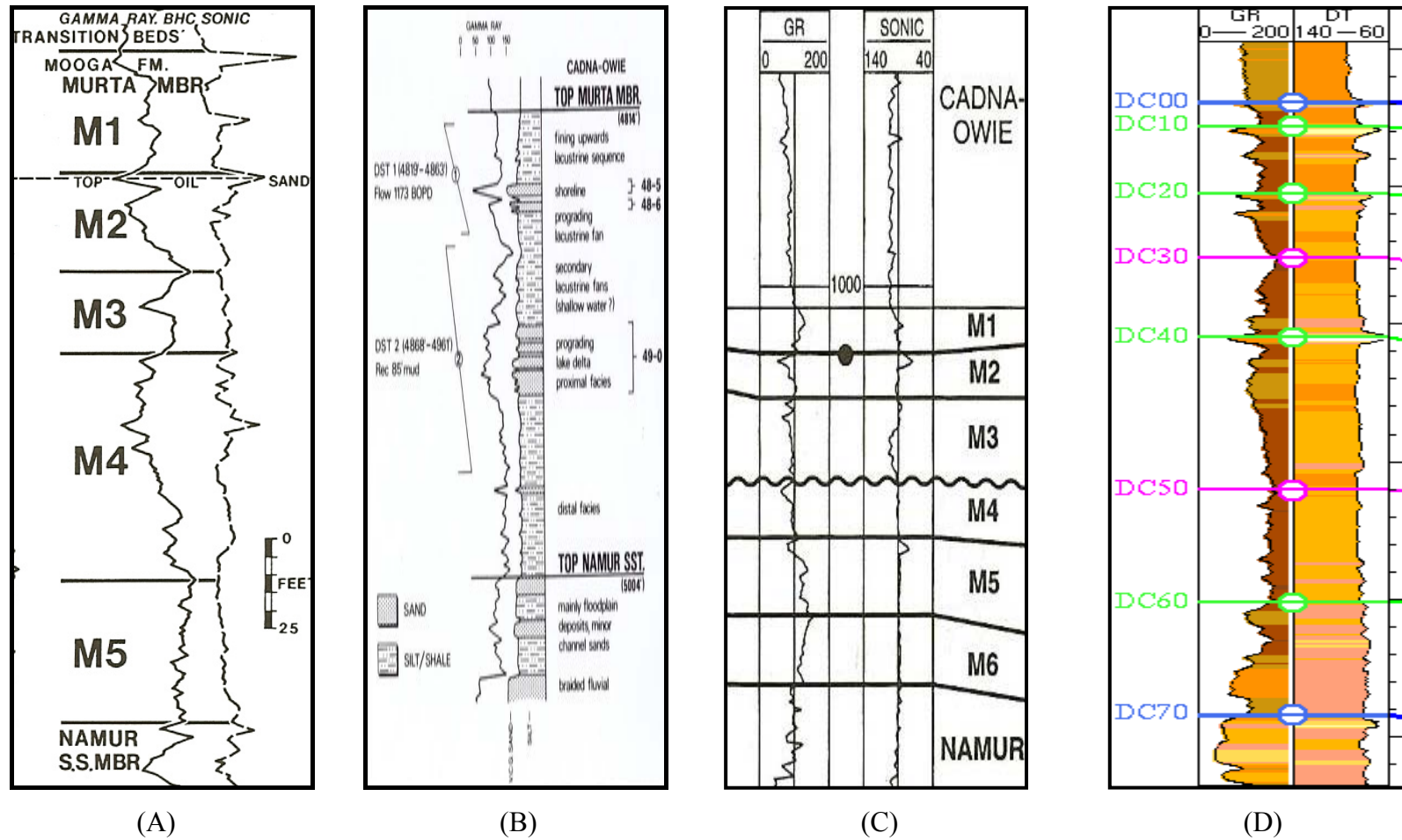


Figure 1.13: Murta Formation units from: (A) Dullingari North-1 well, by Mount (1981). (C) Nockatunga-3 well, by Gorter (1994). (B) Dullingari-9 well, defined by Ambrose *et al* (1986). (D) Dullingari-40 well, this study (2007).

#### 1.2.4 Facies and reservoirs

Mount (1982) and Ambrose *et al* (1986) interpreted different facies in the Murta Formation. Their interpretations included: open lacustrine, lacustrine fan delta, distributary channel, and lacustrine shoreline. The difference in reservoir quality from different sands in the Murta Formation is interpreted to be differences in their depositional environment “facies” (Fig. 1.14 & 1.15).

The main reservoirs in the Dullingari-Murta field are shoreline-bar sands (Ambrose *et al*, 1986) (Fig. 1.14 & 1.15). Little oil has been produced from proximal turbidite and delta distributary channels due to quartz-calcite cementation and discontinuous behavior of the reservoir (Ambrose *et al*, 1986). On the other hand, the main reservoir in the Jackson field was interpreted to have been deposited in a proximal delta front (Ambrose *et al*, 1986). Ambrose *et al* (1986) reported that the 49-0 sand was deposited as a proximal delta slope with fine to occasionally medium grained sand. The 48-6 sand, according to Ambrose *et al* (1986) was deposited as a proximal turbidite at the head of the lacustrine fan with very fine to coarse grained sand (Fig. 1.14 & 1.15). The facies interpretation for the 48-5 sand, which has the best reservoir quality of the three sands, was shoreline-bar sand (Ambrose *et al*, 1986) (Fig. 1.14). Due to thin pay sands, they can not be detected on seismic sections (Mount, 1982). The source of the Murta oil is interpreted to be the dark siltstones that are interbedded with the reservoir sandstones (Mount, 1982).

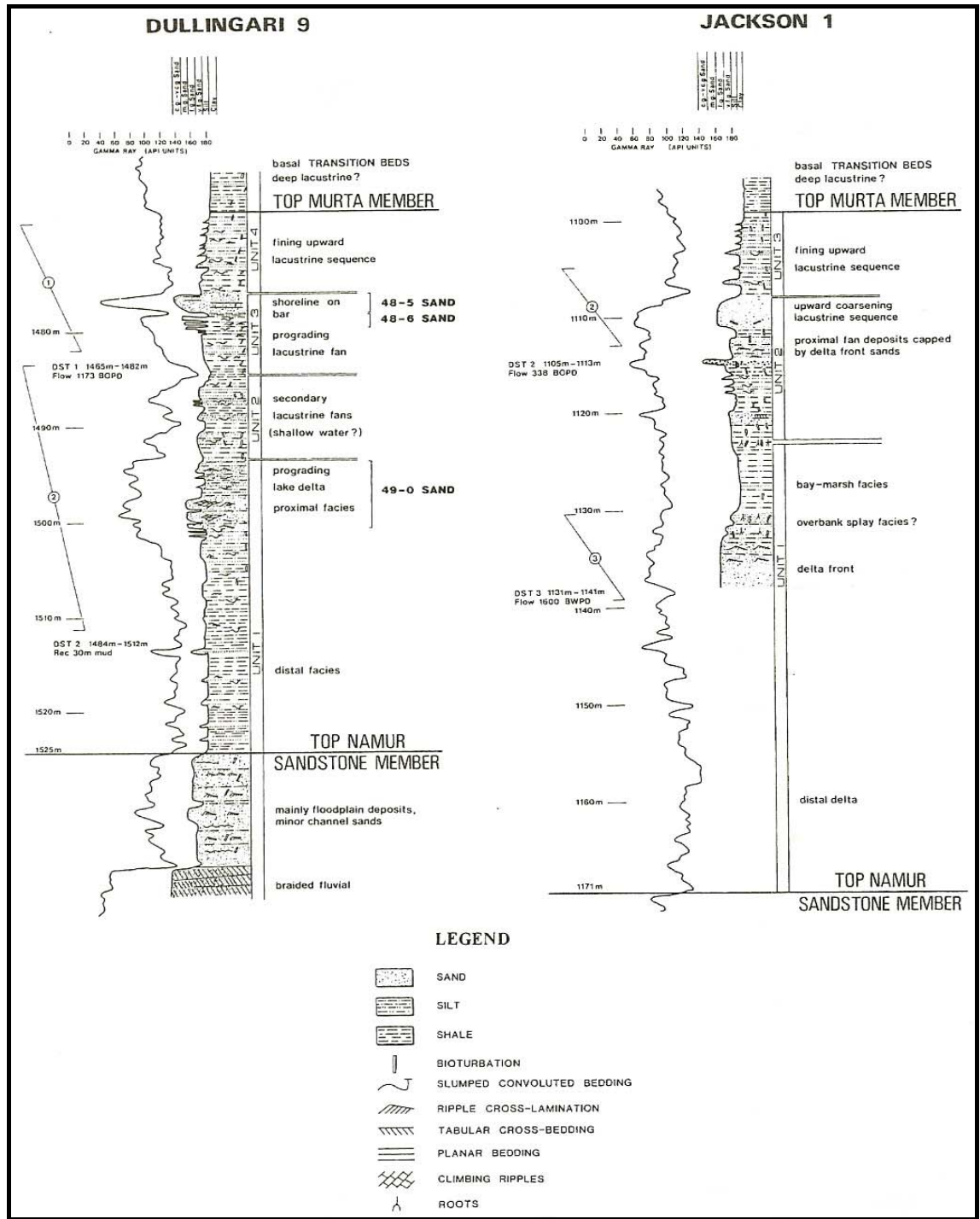


Figure 1.14: Murta Member lithofacies, Dullingari 9 and Jackson 1 (Ambrose *et al*, 1986).

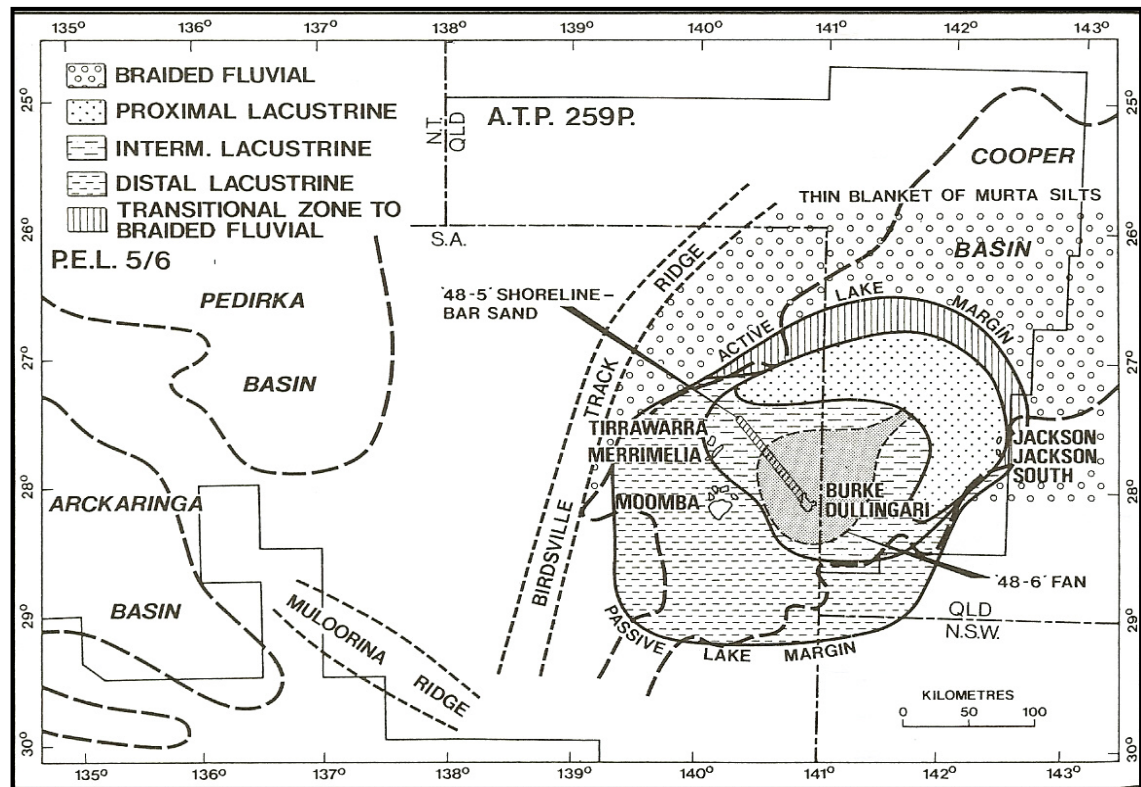


Figure 1.15: Generalised regional lithofacies interpretation, Murta Member, southern Eromanga Basin (Ambrose *et al*, 1986).

### 1.2.5 Isopach maps and depositional models

Ambrose *et al* (1986) constructed a regional isopach and sand:shale ratio maps to show the gradual trend of decreasing thickness and sand content from the north and east to the southwest (Fig. 1.16). The isopach maps produced by Ambrose *et al* (1986) were used in his depositional model which stated that there is a regional reduction in thickness and sand content from the north-northeast to the southwest reflected a depositional pattern where the main sand input into “Lake Murta” was from north and east (Fig. 1.17).

Mount (1981) mentioned that the Murta Formation can be accommodated in a model that proposed the Murta Formation as a shoreface facies in between the braided fluvial environment of the Namur Sandstone in the hinterland and the advancing waters of the first marine transgression in the Cadna-owie Formation.



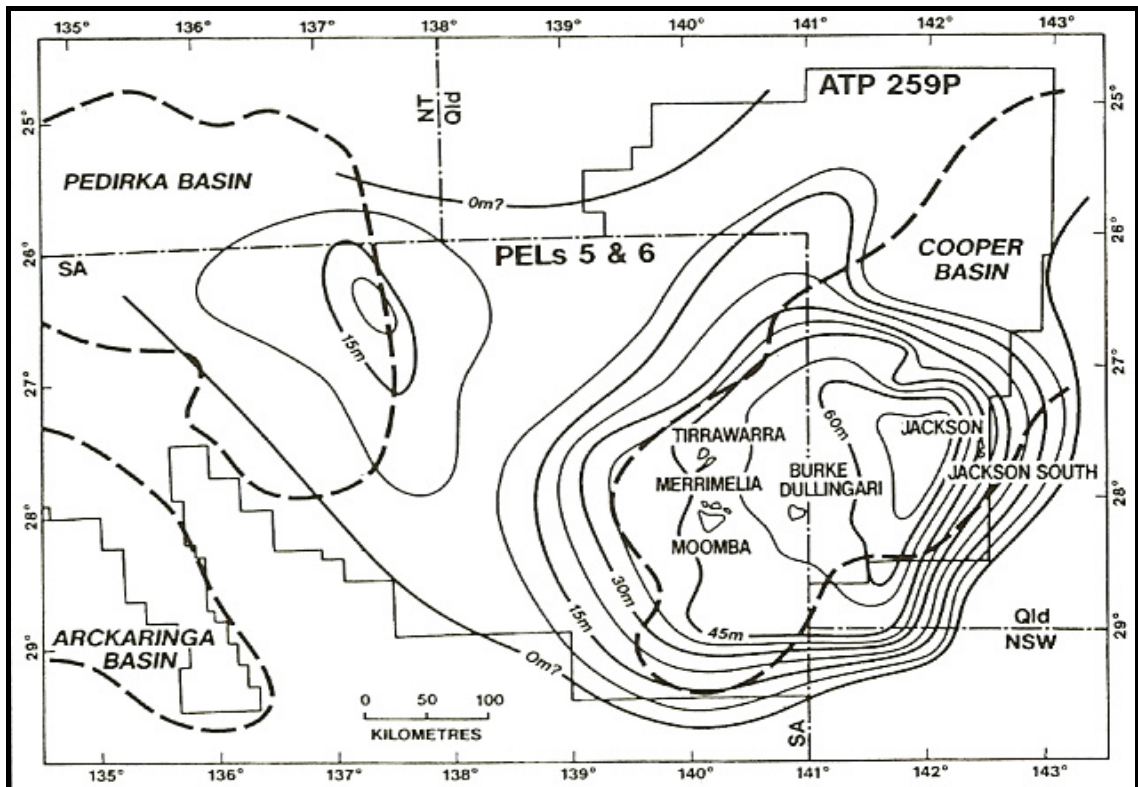


Figure 1.16: Isopach map of the Murta Member, southern Eromanga Basin. Isopach interval is 7.5 m (Ambrose *et al*, 1986).

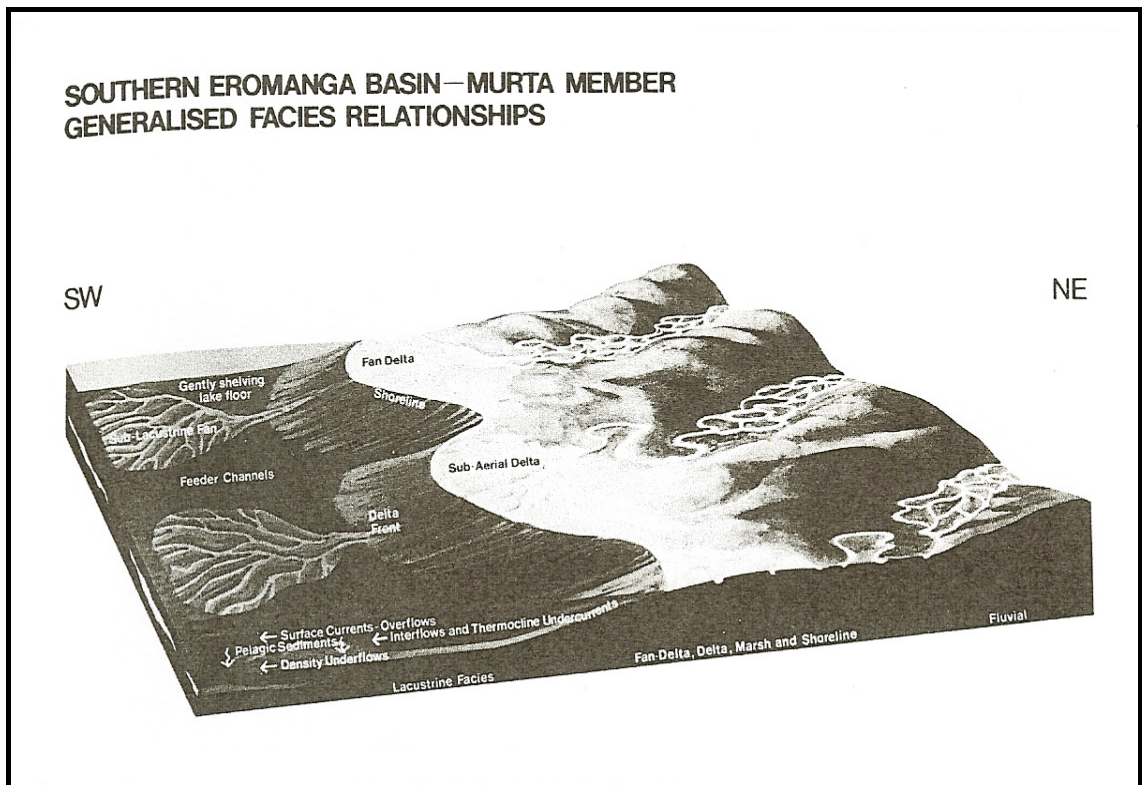


Figure 1.17: Generalised depositional model, Murta Member, southern Eromanga Basin (Ambrose *et al*, 1986).



In his 1994 paper, Gorter included an isopach map for each subunit he proposed to show the development of the Murta Formation units through time. From the isopach maps along with geological information from cores, cuttings, and palaeontology, Gorter (1994) was able to produce a depositional model for the upper part of Murta Formation (Fig. 1.18).

Gorter (1994) disagreed with Ambrose *et al* (1986) model and he provided some inconsistencies with their model. The problem with Ambrose *et al's* (1986) model was that Ambrose *et al* (1986) put, according to their lithofacies maps, the Nockatunga-Thungo fields on a braided fluvial facies, but no such facies were found from these fields (Gorter, 1994) (Fig. 1.18).

Gorter (1994) suggested instead a lake system with vegetated islands southeast of the Maxwell area in mid Murta time. Channel incision and erosion took place because of a rapid drop in the base level directly after M4 time (Fig. 1.18). Then, rising base level and filling of the channels with sediment reworked by the transgression formed the basal M3 as estuarine deposits. The transgression continued during M3 and M2 time forming a basin-wide shoaling cycles and calcite cementation (Gorter, 1994). At the base of M1, there was a maximum transgression resulting in a condensed section.

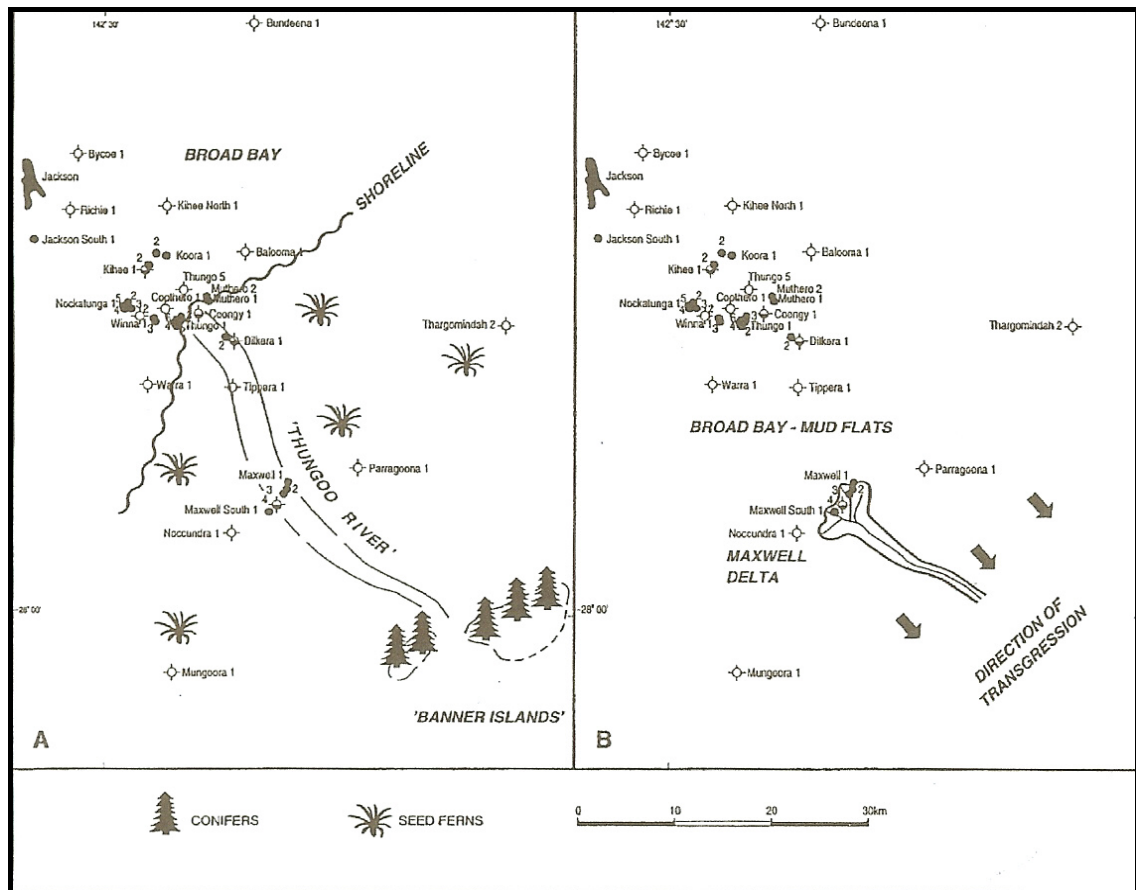


Figure 1.18: Murta Formation depositional model in southeastern Eromanga Basin (Gorter, 1994).

### 1.2.6 Palaeoclimate and palaeogeography

For a schematic palaeogeographic model construction of the Murta Formation, there was a need to be aware of the Eromanga Basin size, shape, position on the continent, palaeolatitude, and orientation. Furthermore, knowing the direction of prevailing winds and wind fetch (Figure 1.19) will play a role in predicting where sandy beaches and shorelines might preferentially develop as opposed to muddy shorelines.

The palaeoclimate of the Early Cretaceous has been identified using palynofloral and megafloal indicators (Gorter, 1994). There was a sudden change in climate conditions and flora from the warm and wet Jurassic to the cold Early Cretaceous when Gondwana started to break apart causing eustatic sea level rise. The climate then warmed during the late Cretaceous as Australia drifted northwards (Alexander & Sansome, 1996).

Frakes *et al* (1987) concluded that a major marine transgression occurred mainly in central and Western Australia during Murta Formation time (Canning and Officer Basins in the west and the Eromanga and Carpentaria Basins in the east). These basins have elongate shapes which reflect structural influence controlled by older, non-marine sedimentation in the Jurassic and earlier Cretaceous. Twelve Cretaceous shoreline maps of Australia have been introduced by Frakes *et al* (1987) including the Eromanga Basin shoreline maps in Murta Formation time (Barremian) (Fig. 1.20).

During the Early Cretaceous, Central Australia was positioned in high latitudes and was occupied by a large intracratonic basin, the Eromanga Basin, in which marginal marine sandstone and mudstones were deposited (Frakes & Francis, 1988) (Fig. 1.20). The palaeolatitude investigations of the southeast Eromanga Basin during the time of Murta deposition is comparable to the present-day latitudes of Norway and Alaska (Gorter, 1994) (Fig. 1.20). Since there is evidence to support cold climate conditions in southeast and central Australia during the Early Cretaceous (Frakes & Frances, 1988), it is possible that periglacial conditions existed during the Early Cretaceous. This will possibly lead to a seasonal run-off of melted fresh water into a marine environment resulting in stressed environments with low biological diversity and changing salinities structures (Gorter, 1994).

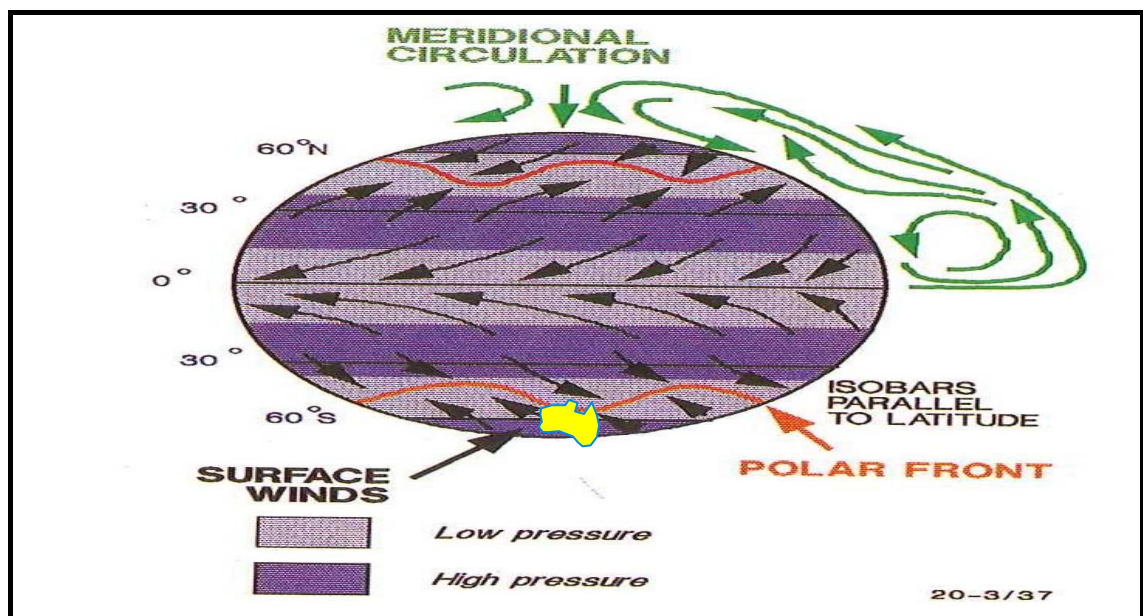


Figure 1.19: Australia's position in the Early Cretaceous suggests winds should have been from what is now the E-SE end of Lake Murta towards the W-NW direction (Struckmeyer & Totterdell, 1990).

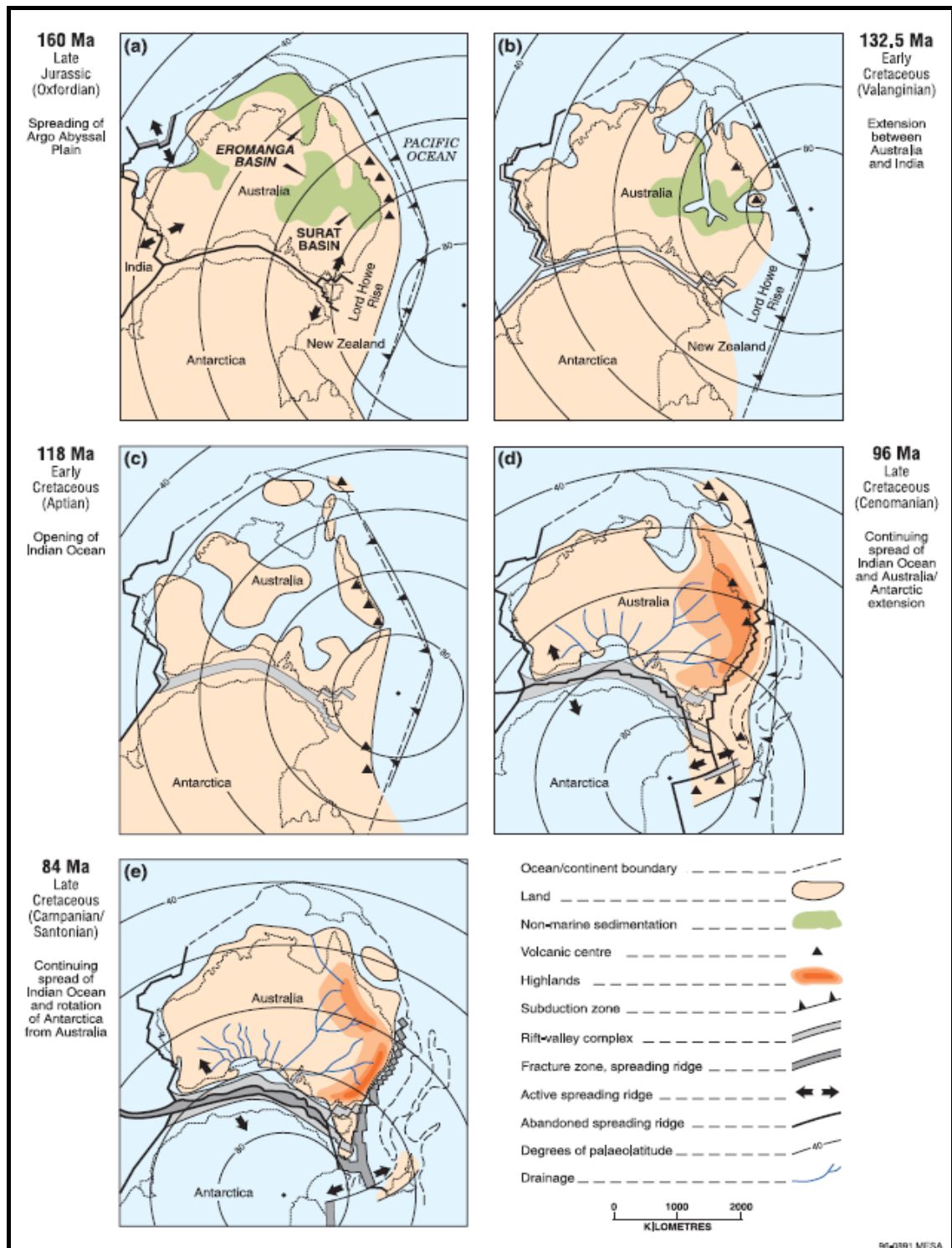


Figure 1.20: Palaeogeographic change through the Jurassic to Cretaceous: (a) Algebuckina Sandstone-Birkhead Formation time (b) Cadna-owie Formation-Murta Formation time (Bulldog Shale-Wallumbilla Formation time (d) Winton Formation time (e) post Winton Formation erosion (Alexander & Sansome, 1996).

## Chapter 2 Sedimentology and Facies Analysis

### 2.1 Review on lake sedimentation

Lakes are inland standing water bodies occupying a depression in the Earth's crust (Gierlowski-Kordesch & Kelts, 1994). Although it seems to be an accurate definition of a lake, many authors have proposed different definitions of a lake based on lake settings, sizes, chemistries, concentrations and morphologies (Reineck & Singh, 1980; Fouch & Dean, 1982; Selley, 1985; Gierlowski-Kordesch & Kelts, 1994; Bohacs *et al.*, 2002).

(Gierlowski-Kordesch & Kelts, 1994) simplified the classification of lake basins into three categories: event basins, paralic basins and tectonic basins. Event lake basins are characterized by short-term processes and thus most likely will not preserve thick lake deposits in the geological record. Paralic lake basins are controlled by the fluctuations of the sea level and include cut-off marine embayments and shoreline depressions. Tectonic lake basins are commonly encountered in the geological record. These include broad regional sags, foreland deeps, orogenic-collapse basins, or rift and strike-slip basins.

Lacustrine sequences are characterized by cyclic sedimentation. This is as a result of the expansion and contraction of lake margins (lake volume). In a sag basin setting, where there are gentle slopes, small volume changes will give large changes in shoreline and rapid vertical facies changes (N. Lemon, Santos Ltd., pers. comm.). Because many lakes are fault controlled as a result of subsidence, their preservation potential within a fluvial succession is relatively high.

A combination of a topographical depression and a hydrological balance (input-output) are the most important conditions for a lake (Fig. 2.1). The hydrological balance, in turn, depends on the climate which is controlled by latitude-dependent zonal winds, geography, and altitude (Gierlowski-Kordesch & Kelts, 1994). Thus, lacustrine sequences are considered to be valuable records of global climate history.

Climate controls the amount of the clastic sediment input delivered into a lake during the fluctuations in the seasonal discharge of the rivers. In addition, it controls the physical and chemical characteristics of the lake deposits (Reineck & Singh, 1980).

Two types of lakes may be considered depending on the balance of input versus evaporation, either hydrologically open or closed. Hydrologically-open lakes have an outlet and are dominated by clastic input sedimentation unlike potential evaporites in a closed lake (Fig.2.2). Consequently, the input plus precipitation is balanced by output plus evaporation and this will prevent severe fluctuations in the shorelines (Allen & Collinson, 1986). On the other hand, those lakes which lack an outlet are hydrologically closed and are dominated by chemical and biochemical sedimentation with frequent and rapid change in their shorelines (Allen & Collinson, 1986). It is possible, however, that every lake could pass through both of these two hydrological settings through their lifetime because of the dynamic behaviour of the lakes in terms of tectonic settings, water chemistry, and bathymetry (Allen & Collinson, 1986).

“Lake Murta” appears to be a hydrologically-open lake for most of its time, becoming closed when water level drops below the outflow point. “Lake Murta” developed as an interior sag basin but became paralic late in its history as it eventually joined to the open ocean during deposition of the Cadna-owie Formation (N. Lemon, Santos Ltd., pers. comm.).



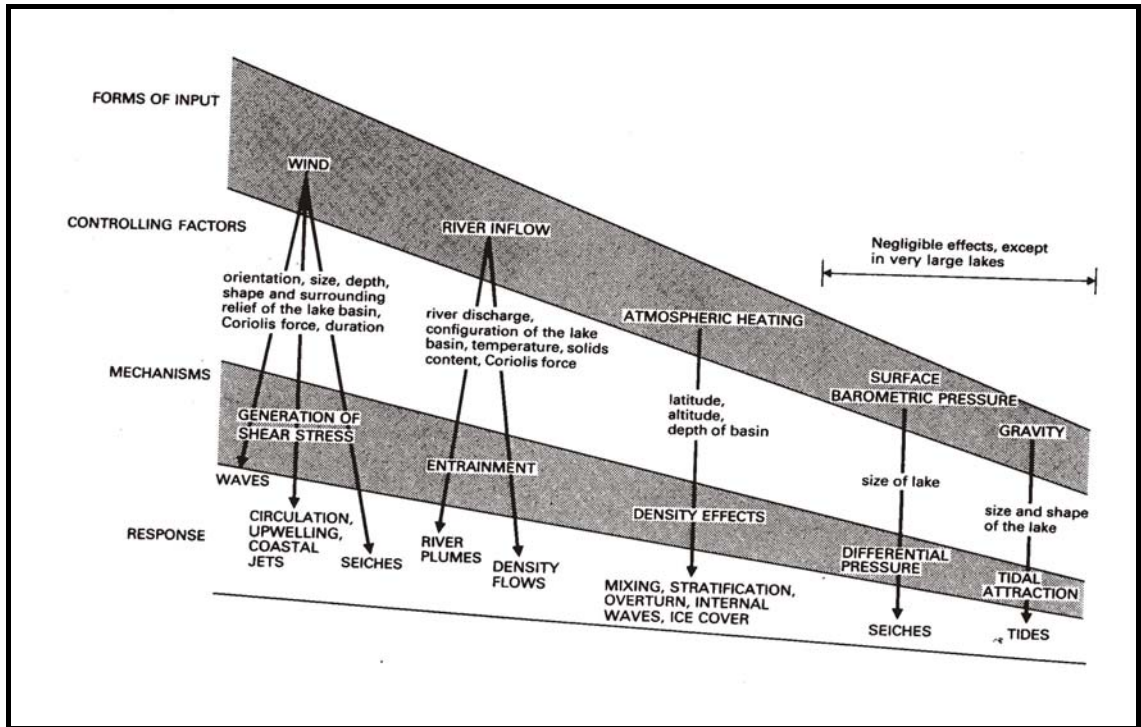


Figure 2.1: Lake response to various forms of physical input (after Sly, 1978).

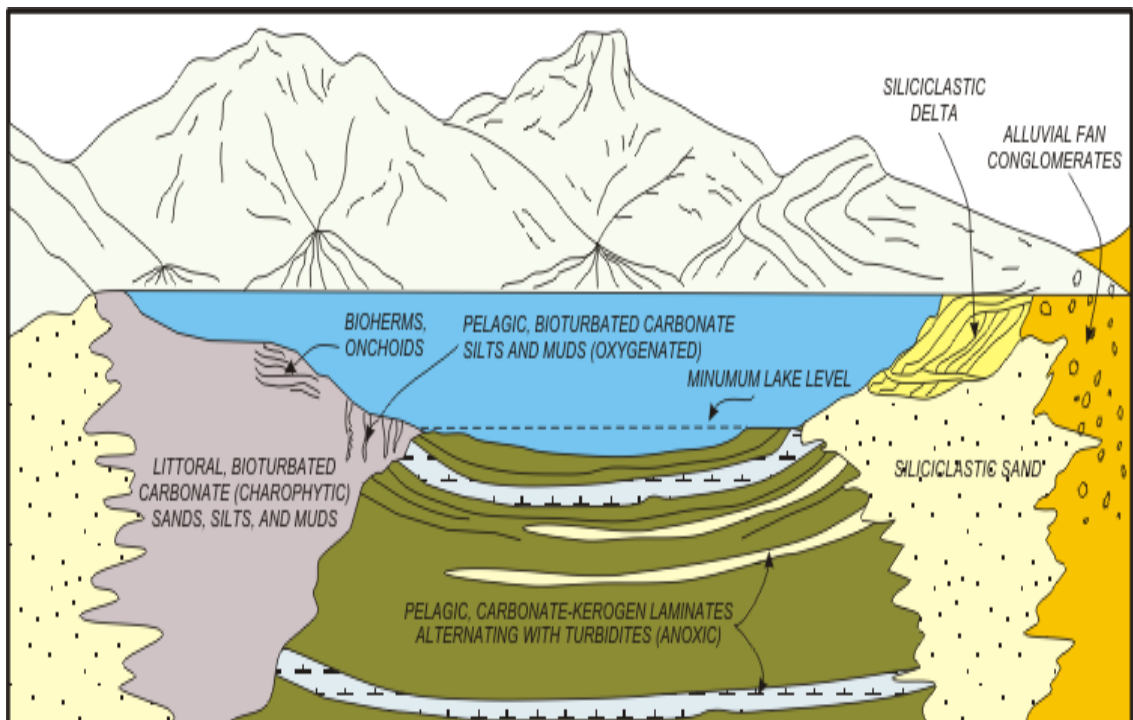


Figure 2.2: Depositional elements in a hydrologically-open, freshwater lake (after Eugster and Kelts, 1983).

## 2.2 Facies associations of the Murta Formation

Detailed core logging is a fundamental part of any reservoir description study. The aim of this core logging was to describe the vertical distribution of facies associations in the Murta Formation. This was done in regards to sedimentary, biological, and diagenetic characteristics of each facies association.

Reading (1986) defined facies as a body of rock with specified features. A facies is defined according to its colour, bedding, composition, texture, fossils, and sedimentary structures. Facies associations consist of genetically and environmentally related groups of facies (Boggs, 1995).

Six facies associations were recognized in the Murta Formation using core description (Table 2.1). A detailed core description for all wells can be seen in Appendix 2.1. The Miall (1978) logging scheme was added to the core description (Appendix 2.2). The outcomes of this core description have a direct impact on interpreting the depositional environment of each facies association and its lateral continuity and, in turn, help in predicting the palaeogeographic distribution of each facies association.

Table 2.1: Summary table of facies associations of the Murta Formation with lithology, sedimentary structures and depositional environment interpretations.

Facies Assoc.	Lithology	Sedimentary Structures	Depositional Environments
Facies Assoc. 1 (St, Sm, Fm, Fd)	Sandstone and mudstone	Trough cross bedding, massive sandstone and deformed mudstone	Distributary channels
Facies Assoc. 2 (Sr, Sh, Srb)	Sandstone	Wave ripple lamination and parallel lamination	Lacustrine shoreline
Facies Assoc. 3 (Sb, Fb, (Sbr))	Sandstone	Bioturbated protected sandstone	Bioturbated shoreline
Facies Assoc. 4 (Sr, Sb, Fb, Fl)	Sandstone with minor mudstone	Laminated microhummocky ripples , coal clasts, bioturbation	Deltaic mouthbar
Facies Assoc. 5 (Ss, Sr, Sb, Fb)	Sandstone and siltstone with minor mudstone	Lenticular-bedding, ripple lamination, hummocks, bioturbation, soft sed. defor.	Offshore transition
Facies Assoc. 6 (Fl, Ss, Sb)	Mudstone and minor sandstone.	Linsen beds in mud, ripple lamination in sand lenses, minor bioturbation in mud, bioturbation in sand	Lacustrine offshore



### **2.2.1 Facies association 1: Distributary Channels - Trough cross bedded and massive sandstone with massive and deformed mudstone (St, Stt, Sp, Sm, Fm, and Fd)**

#### **Description**

This facies association comprises trough cross-bedded (St) and minor planar-tabular (Sp) well-sorted medium-grained sandstone. The thicker trough cross-bedded sandstone described from this facies association has a sporadic thickness from 1.2-3 m. A general fining-upward in the grain size is typical for this facies association. The contact between this facies association and the overlying facies association is gradual.

The thickness of the very coarse thin beds of the trough cross-bedded sandstone (Stt) is about 10 cm. The base and the top of these very coarse thin beds are erosive and sharp respectively. This facies association also consists of fine to medium-grained massive sandstone (Sm) (Table 2.1).

The sedimentary structures observed in the (St) and (Sm) facies were trough cross-bedding and massive (structureless) sandstone. Quartz pebbles, mud rip-up clasts, coal chips, and scour surfaces were also common characteristics of the St facies. The facies association of St and Sm was presented in many cores such as: Challum-1#1, Dirkala-3, Dullingari-40#1, Gidgealpa-19#1, Gidgee-2#1, Ipundu-1#1, Jackson-1#1, Jena-11#2, Maraboka-1#1, Orientos-2#1, McKinlay-1 & 2#1, Moomba-18#1, Merrimelia-6#1, Merrimelia-46#1, SpencerWest-2#1, Strzelecki-4#1, Talgeberry-2#1, Ulandi-3 & 5#1, and Wilson-2#1.

The massive and deformed mudstone (Fm and Fd respectively) represented in this facies association is highly oxidized. Rootlets and carbonate cement are very common in the mudstone facies. A good example of rooted highly oxidized mudstone was described from Merrimelia-6#1 and Jena-11#2. A mudstone with roots can be seen in Figure 2.4-C.

There were no shelly fossils or ichnofossils features within the cored section of this facies association apart from rootlets. Carbonate cements were the most common diagenetic feature in this facies association.

### **Discussion and interpretation**

The bounding surfaces of trough cross-bedding structures are curved. These surfaces have an elongate scour filled with curved laminae with tangential relationship to the base of the set (Boggs, 1995). They usually form through migration of three-dimensional bedforms and modify when the flow velocity or depth change during bedform migration. An erosion surface will be present within the cross strata known as a reactivation surface (Tucker, 1995).

The trough cross-bedding sedimentary structure (St) is common in fluvial-deltaic cross-bedded sandstones as a result of bedload transport (Fig. 2.4-A) (Tucker, 1995).

Hydrocarbon stain recorded from this (St) facies suggested it to be one of the Murta Formation reservoirs. The trough cross and planar-bedded sandstone is best featured in the distributary channels of the McKinlay Member of the Murta Formation, deposited across the lake shoreline (Fig. 2.3). This environmental interpretation supported the clear fining-upward succession of this facies from logs.

The very coarse thin beds facies (Stt) with about 10 cm thickness represents fluvial sand sheets delivered to the basin when the lake level is low (Fig. 2.4-B). These very thin beds have a very high sonic response because of the carbonate cement in the bed, while the gamma ray response is very low because of the sandy nature of this facies.

Massive bedding (Sm) refers to beds lacking of any visible structure. This massive sandstone is possibly formed as a result of rapid deposition or sediment-gravity flow deposits. However, these beds are only poorly developed and associated with trough cross-bedded structures and are grouped according to their underlying and overlying facies, so they were grouped with trough cross-bedded features in one facies.

Massive and deformed mudstone (Fm) and (Fd) is associated with the very thin fluvial sand sheets of the (Stt) facies. This association takes place when the fluvial systems make their way to the basin during drying out of Lake Murta. The (Fm) and (Fd) facies represent the lacustrine exposure surface with rootlet structures and have a high gamma ray log response (Fig. 2.4-C). The associated carbonate represents incipient soil formation.

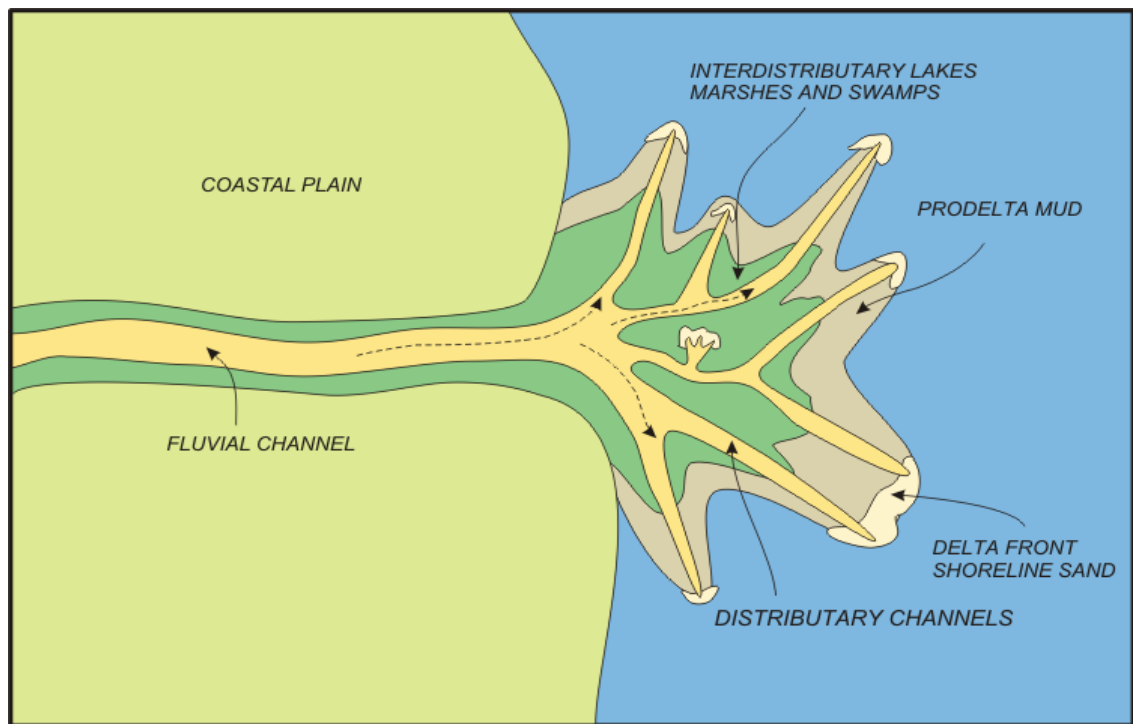


Figure 2.3: Schematic model of fluvial-dominated delta and its depositional elements (modified from Elliott, 1986). Fluvial-dominated deltas are found in environments where the influence of fluvial processes is greater than the influence of wind or tide and are common in lacustrine settings. Sand is dominantly deposited in subaqueous mouthbars at the terminal end of distributary channels and within the channels upon abandonment (Riordan *et al*, 2006).

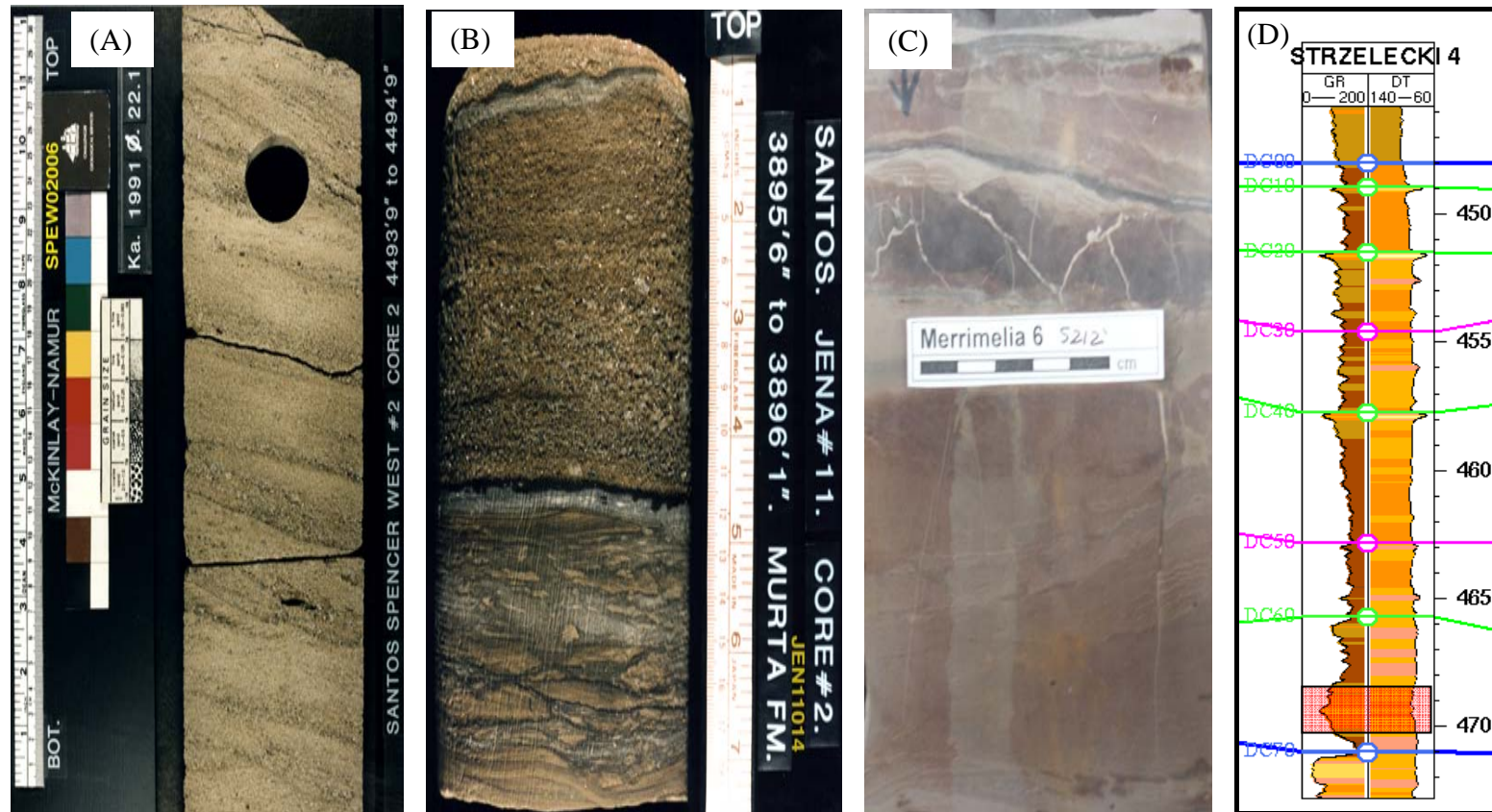


Figure 2.4: (A): Facies association-1 core photograph with trough cross bedded medium-grained sandstone to represent finning-upward cycle and interpreted to be distributary channel. (B): Thin fluvial sand sheets delivered to the lake basin when it dries out. (C): Highly oxidized mudstone with rootlets representing a period of exposure of lake bed sediment. The rootlets have been replaced by carbonate during incipient soil formation. (D): Strzelecki-4 log signature (4683-4702') showing the distributary channel environment in the highlighted red box.

### **2.2.2 Facies association 2: Shoreline - Wave ripple laminated sandstone (Sr, Sh, Srb, and Fl)**

#### **Description**

This facies association consists of wave ripple-laminated (Sr), well-sorted, clean, fine-grained sandstones with undulating laminae patterns. Each ripple unit ranges from few millimetres to few centimetres. The thickness of this facies association varies from 0.6-2.7 m.

This facies association frequently alternates with very thin-laminated mud (Fl). The base of this facies association shows a gradual increase in wave-generated depositional structures from a massive and trough cross-bedded medium-grained sandstone. However, the facies association changes at the top appear to be abrupt since there is a sudden increase in the mud content of the overlying facies (Table 2.1).

Sedimentary structures identified include: wave ripple-laminations, swaley ripple-laminations, and parallel-laminations. Most of the laminations from this facies association show relatively high mica content (Fig. 2.5).

Biological features are infrequently observed in this facies association with some small horizontal and vertical burrowings. Diagenetic features also are uncommon from this facies.

This facies association was noted in many cores, for example, Gidgee-2#1, Jackson-1#1, Jena-11-1#1, Marabooka-1#1, Orientos-2#1, McKinlay-1#1, Merrimelia-6#1, Mudera-1#1, Namur-1#1, SpencerWest-2#1, Tintaburra-1#1, Tickalara-10#1, Ulandi-5#1, and Wilson-2#1.

#### **Discussion and interpretation**

Ripples from (Sr) facies are formed by the migration of small bedforms with mainly sinuous crests. The presence of wave ripple-laminations, swaley ripple-lamination, parallel-laminations, and minor bioturbation suggests a deposition in wave-dominated shoreface setting. Waves rework the upper-shoreface sands resulting in the formation of ripple-lamination, while the swaley ripple-lamination and parallel-lamination will form under wave conditions in shallow water (Fig. 2.6).

The wavelength of the wave-formed ripples depends on many factors, such as sediment grain size, diameter of water-particle orbits in the waves, and the water depth (Tucker, 1995). Ripples may vary in their internal structures depending on flow velocity and sediment supply (Allen, 1984). The foresets in the wave ripples are usually composed of cross-laminae arranged in groups. Therefore, the cross-bedded unit will show bundle-wise up-building (Reineck & Singh, 1980).

This facies association shows an obvious coarsening-upward succession in the log (Fig. 2.7). It is hard to distinguish between a mouth bar log signature and shoreline log signature since both of them have a coarsening-upward profile. This applies also to the tempestite depositional environment which has an overall coarsening-upward log profile. The only way to differentiate between these depositional environments is through a detailed core description of their distinctive features.

Some wells show a hydrocarbon stain from this facies association nominating it to be a very good reservoir.

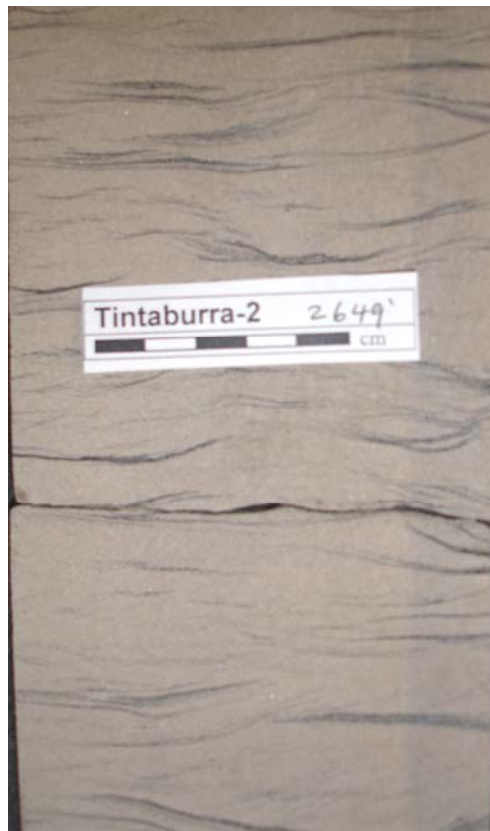


Figure 2.5: Facies association-2 wave ripple-laminated fine-grained sandstone deposited in lacustrine shoreline environment.

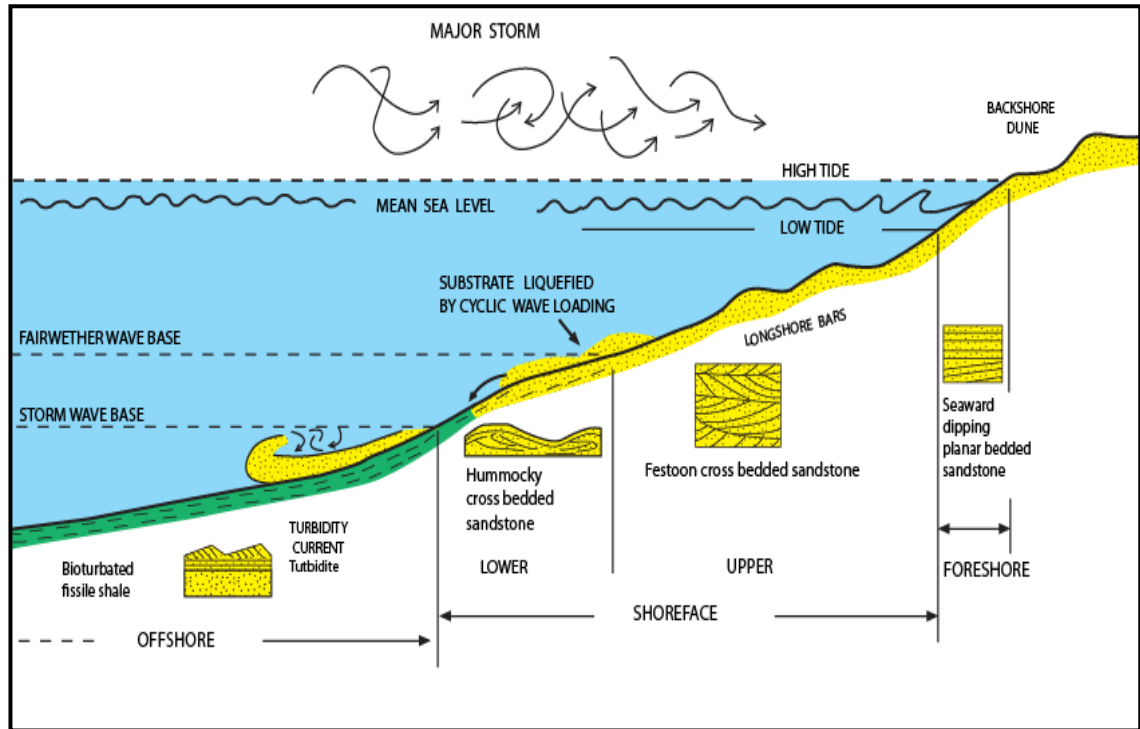


Figure 2.6: Offshore profile locating foreshore, shoreface, and offshore, as well as fair-weather wave base (modified after Walker, 1984).

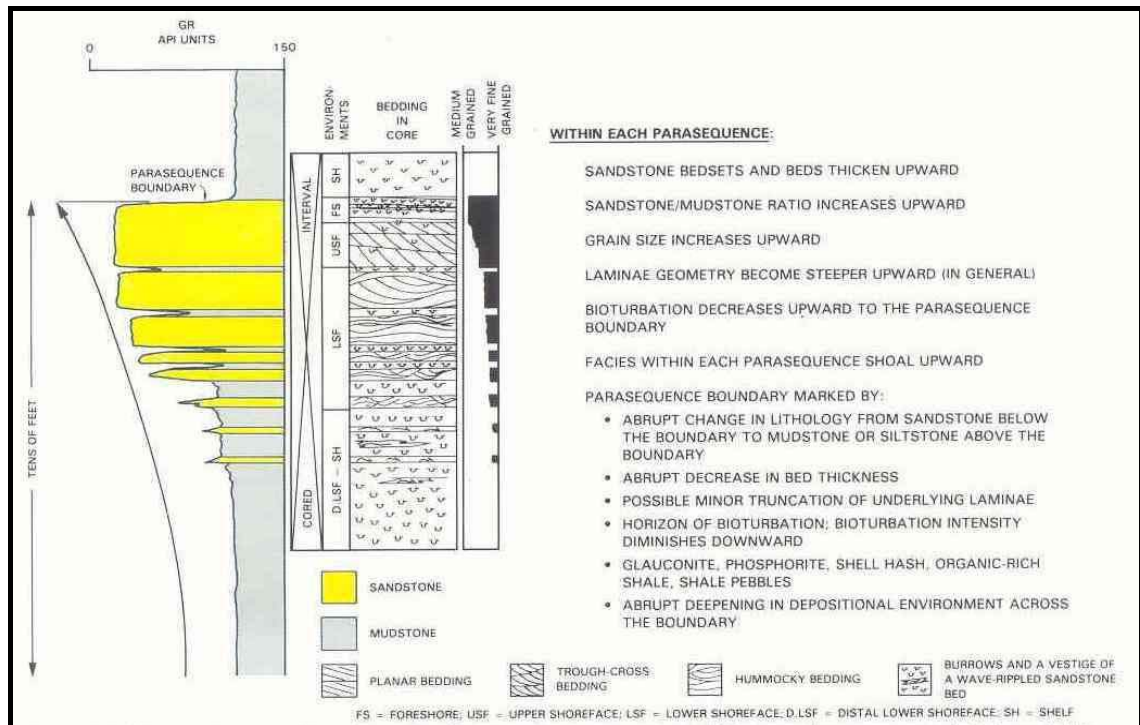


Figure 2.7: Stratigraphic characteristics of an upward coarsening parasequence. This type of parasequence is interpreted to form in a beach environment on a sandy, fluvial or wave dominated shoreline (Wagoner *et al*, 1990).



### 2.2.3 Facies association 3: Bioturbated shoreline (Sb, Sr, Fb)

#### **Description**

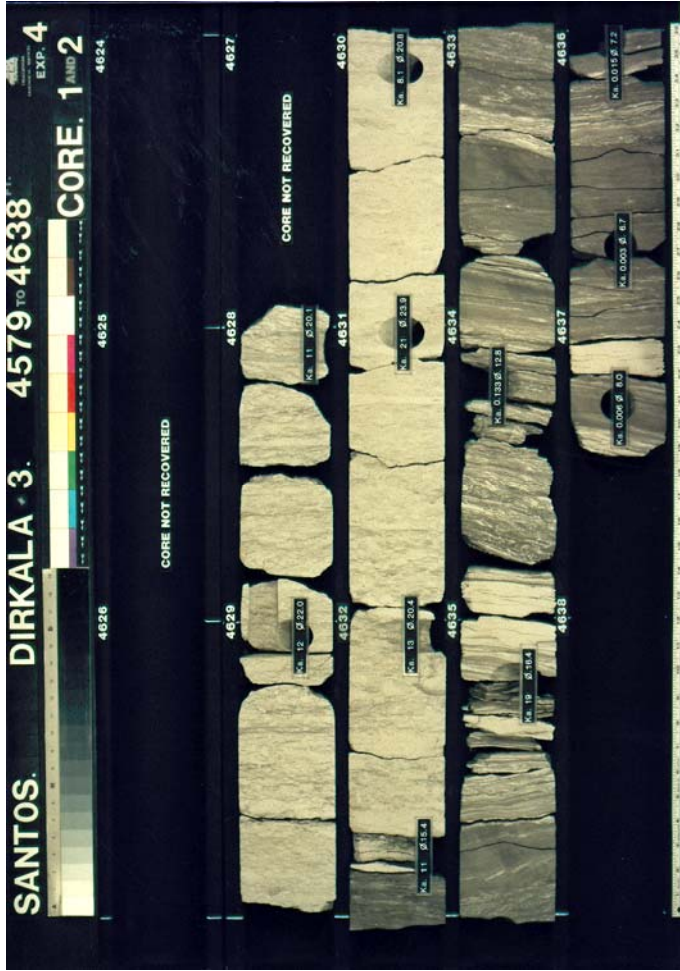
This facies association is considered to be an extremely bioturbated, clean, faintly-rippled, fine-grained sandstone. The thickness of this bioturbated sandstone reached over 2.4 m in some wells, but in general it is around 1m in thickness. This bioturbated sandstone was recognized to have high mica content and is occasionally interbedded with mudstone. An overall increase in sand content was noted from the underlying muddy facies.

The mechanical sedimentary structures in this facies association were often destroyed by the intense burrowing. These possible previous structures include wave ripple-lamination and parallel-lamination. Slumps were recorded from the muddy part of this facies association (Table 2.1).

This facies association was identified in many cores such as: Bogala-1#1, Challum-1#1, Dullingari-40#1, Gidgealpa-19#1, Gidgee-2#1, Jackson-1#1, Jena-11-1#1, Koorroopa-1#1, McKinlay-1#1, Namur-1#1, Pitchery-2#1, and Takyah-1#1.

#### **Discussion and interpretation**

Some of this facies association may have originally been associated with facies association 2 (wave ripple-laminated sandstone) of the shoreline environment, but has been deposited in a protected embayment away from the wave action and then disturbed by fauna (Fig. 2.8). A coarsening-upward trend, similar to facies association 2, marks the log response of this facies association. Bioturbation is common where sedimentation is not disturbed by events such as slumps and storm beds (N. Lemon, Santos Ltd., pers. comm.). Some zones may have a high degree of wave reworking, and, as a result, the species diversity will be low like in the shoreline environment of facies association 2.



Bottom



Figure 2.8: Bioturbated “wave rippled” laminated fine-grained sandstone of facies association-3 deposited in a possible lacustrine shoreline environment with coarsening-upward sequence.

#### **2.2.4 Facies association 4: Deltaic mouthbar – Laminated microhummocky rippled sandstone (Sr, Sb, Fb, Fl)**

##### **Description**

Facies from Sr and Sb are characterized by ripple-laminated, clean, well-sorted, and fine-grained sandstone. This facies ranges from 4.7-6 m in thickness. Bioturbation is not that obvious or intense in this ripple-laminated sandstone. The base of this facies association is marked by a gradual increase in silt and sand content from bioturbated mudstone (Fb). There is an increase in coal clasts size towards the top of this facies association (Table 2.1).

Slumps and microfaults were documented in a number of intervals from the lower part of this facies association. Small-scale hummocks were recognized in this facies association especially in the interbedded mud, silt, and sand sequence (Fig. 2.10-A). Starved ripples were associated with the rippled-laminated sandstone at the top of the facies association.

Siderite concretions were noted and associated with the small hummocks and mudstone intervals. This facies association shows a high concentration of micaceous minerals especially in the ripple-laminated sandstone.

The laminated microhummocky rippled sandstone (Sr) facies was recognized in the following cores: Bogala-1#1, Challum-1#1, Dirkala-3#1, Dullingari-40#1, Fly Lake-4#1, Gidgealpa-19#1, Ipundu-1#1, Jackson-1#1, Kooroopa-1#1, McKinlay-1&2#1, Moomba-18#1, Pitchery-2#1, Strzelecki-4#1, Takyah-1#1, Talgeberry-2#1, Thungo-1#1, and Wilson-2#1.

##### **Discussion and interpretation**

The bioturbated mudstone (Fb) in the lower part of this facies association suggests deposition below the wave base from suspension. The overlying ripple-laminated sandstone is interpreted to be deposited in relatively low energy subaqueous delta environment.

The coal and wood clasts described from this facies association are supposed to be delivered to the basin in times of flood and discharged into the nearshore zone, where wave action grinds the coarser wood particles into large concentration of organic debris sometimes referred to as “coffee grounds” (Fig. 2.10-B) (Coleman & Prior, 1982). In this case, a constructive lobate or elongate delta will form with the lack of tides or effective waves. These delta lobes will show a lateral shifting of delta distributaries resulting in lakeward construction of the delta front by overlapping lobes of sediment (Ambrose *et al*, 1986) (Fig. 2.3).

As a result, the best possible environmental interpretation of this ripple-laminated sandstone with coarsening-upward succession is a prograding distributary mouth bar. The facies association from a mouth bar environment shows a coarsening-upward succession on logs (Fig. 2.9 & 2.10-C). However, shoreline environments can also show the same coarsening-upward profile; therefore log responses must be complimented by core description to tell the difference.

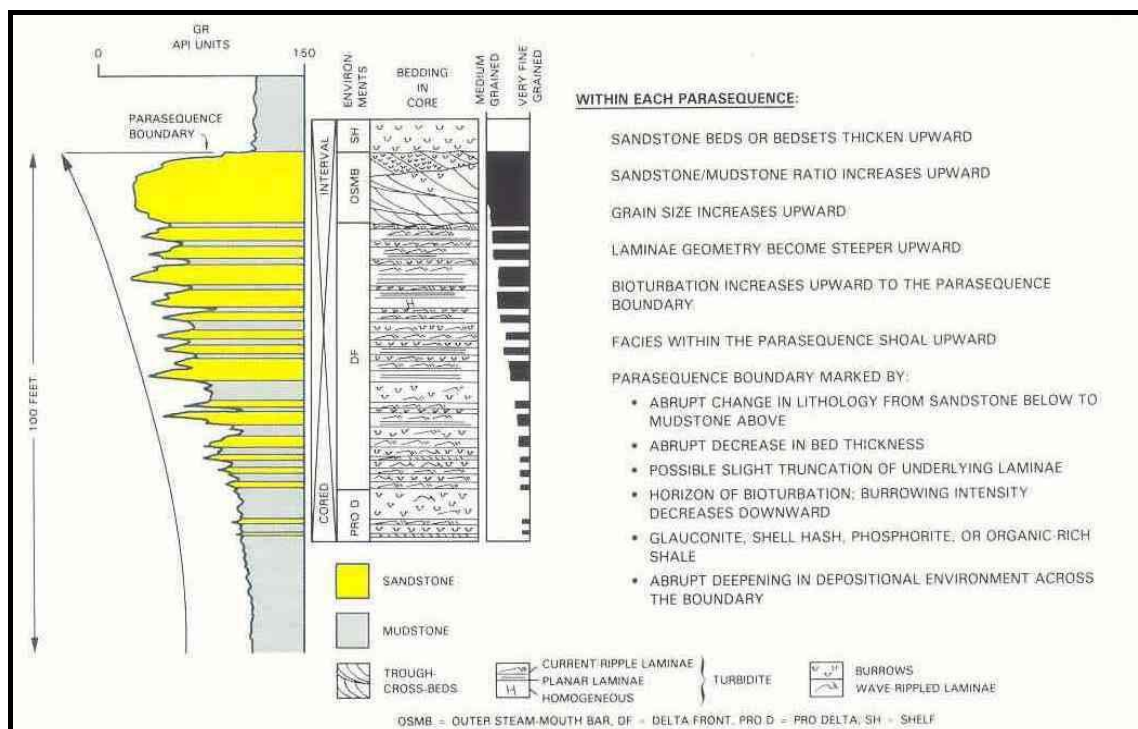


Figure 2.9: Stratigraphic characteristics of an upward coarsening parasequence. This type of parasequence is interpreted to form in a deltaic environment on a sandy, fluvial or wave dominated shoreline (Wagoner *et al*, 1990).

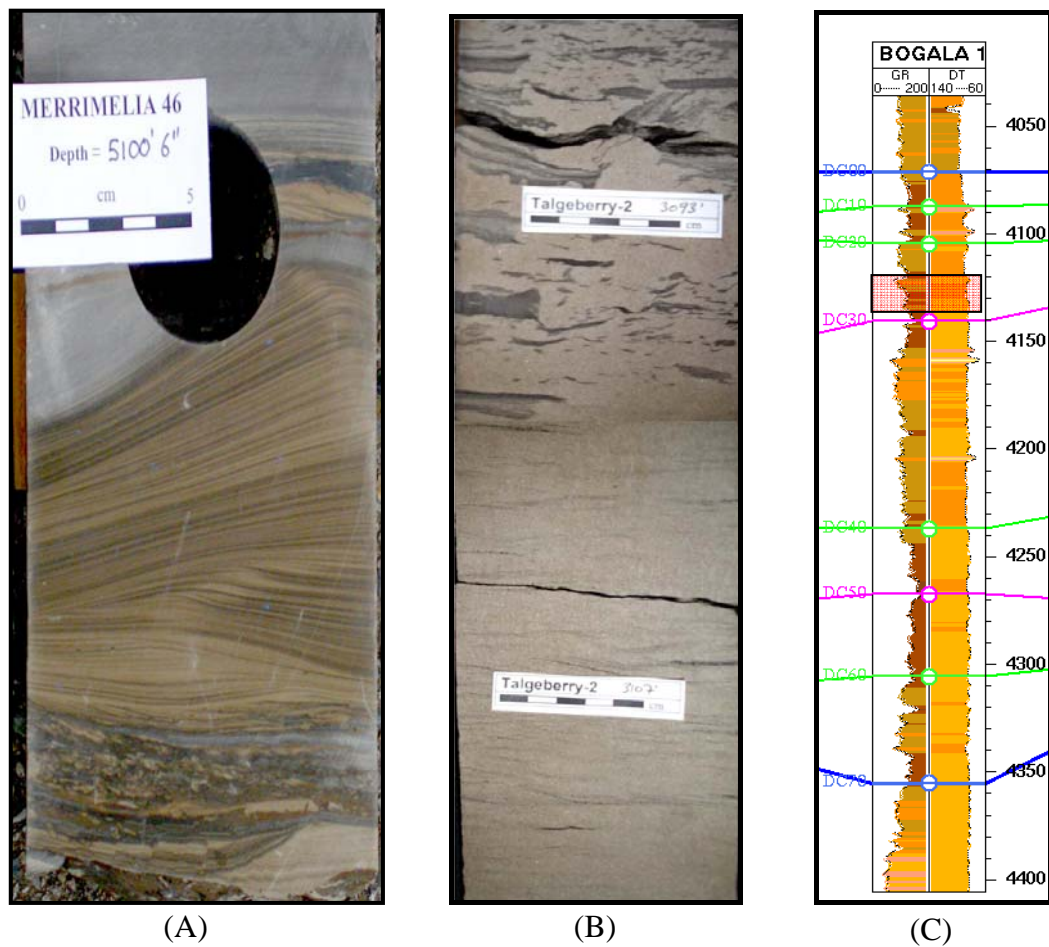


Figure 2.10: Facies association-4 core photographs, (A): ripple-laminated sandstone from the upper part of Sr, Sb, Fb facies association represent a coarsening-upward cycle and interpreted to be a deltaic mouth bar. (B): The coal clasts “coffee grounds” are very clear at the top of this facies association. (C): Bogala-1 log signature (4120-4138’) showing a typical coarsening-upward cycle from bioturbated lacustrine muds to ripple cross-laminated fine to lower medium-grained sands, interpreted to be a deltaic mouth bar.

### **2.2.5 Facies association 5: Offshore transition - Bioturbated lenticular-bedded sandstone and siltstone with minor mudstone (Ss, Sr, Sb, Fb)**

#### **Description**

Facies association 5 consists of lenticular-bedded sandstone and siltstone with minor mudstone drapes. The thickness of the clean sandstone lenses ranges from 5 cm to 10 cm. These lenticular beds are discontinuous and isolated in both horizontal and vertical directions. Some of the larger clean sand lenses have erosional bases with fining-upward profiles. Nevertheless, this facies association show a general coarsening-upward succession, since an upward increase in the sand content was noted from this facies association (Fig. 2.12-A).

Sedimentary structures encompass lenticular bedding, clean sand ripples, climbing ripples, mud flaser bedding, starved ripples, and well-defined hummocky laminae. Hummocks have low angle (<10°) curved cross lamination arranged in convex upward style and combined with climbing ripples (Table 2.1).

The facies association 5 overlies facies association 6 with a sharp increase in sand content and sharp increase in bioturbation upward. The bioturbation style is of small vertical and horizontal burrows. Many intervals in this facies association have suffered from the bioturbation destruction of their primary sedimentary structures. The cleaner sandstones lenses are generally unbioturbated, well-sorted, and very fine to fine-grained. However, some cases showed reworking of the lenticular sandstone by biota in the lower part of this facies association at the contact with facies association 6.

Soft sediment deformation was also recognized in this facies association. Slumps are common in the muds while microfaults were seen in the interbedded sands (Fig. 2.12-B). Dewatering structures were also common as a result of water escape. Siderite concretion is very common especially at the top of this facies association and has affected the primary sedimentary structures. Oil stains were noted from many cores of this facies association indicating it as a target reservoir.



This facies association was described from the following cores: Dullingari-40&37#1, Gidgealpa-19#1, Gidgee-2#1, Ipundu-1#1, Jena-11#1, Maxwell-2#1, Orientos-2#1, McKinlay-1&2#1, Moomba-18#1, Merrimelia-6,16,&46#1, Narcoonowie-4#1, Pitchery-2#1, SpencerWest-2#1, Takyah-1#1, Talgeberry-2#1, Tickalara-10#1, Tintaburra-2#1, Ulandi-3&5#1, and Yanda-2#1.

### **Discussion and interpretation**

The above recorded sedimentary structures specified deposition in storm-dominated shoreline (tempestites) with associated silt and mud drapes. The deposition of these features is interpreted to be above the storm wave base.

The lenticular bedding developed when incomplete sand ripples deposited in a mud layer and then have been preserved by an overlying muddy layer. On the other hand, preservation of the mud in the troughs of the ripples is best described as flaser bedding (Reineck & Singh, 1980).

Hummocky cross stratification is considered to be developed between fair-weather wave-base and storm wave-base as a result of wave-generated oscillatory flows or combined flows (Fig. 2.11) (Walker, 1982). Hummocks sometimes are difficult to be identified from logs since it gives a coarsening-upward succession similar to the ones with deltaic/distributary mouth bar and shoreline environments.

The intense burrowing in the lower part of this facies association indicates slow sedimentation from suspension. The soft sediment deformation in this facies association formed a result of rapid deposition of sandstone. Slumps and microfaults show sediment movement soon after deposition.



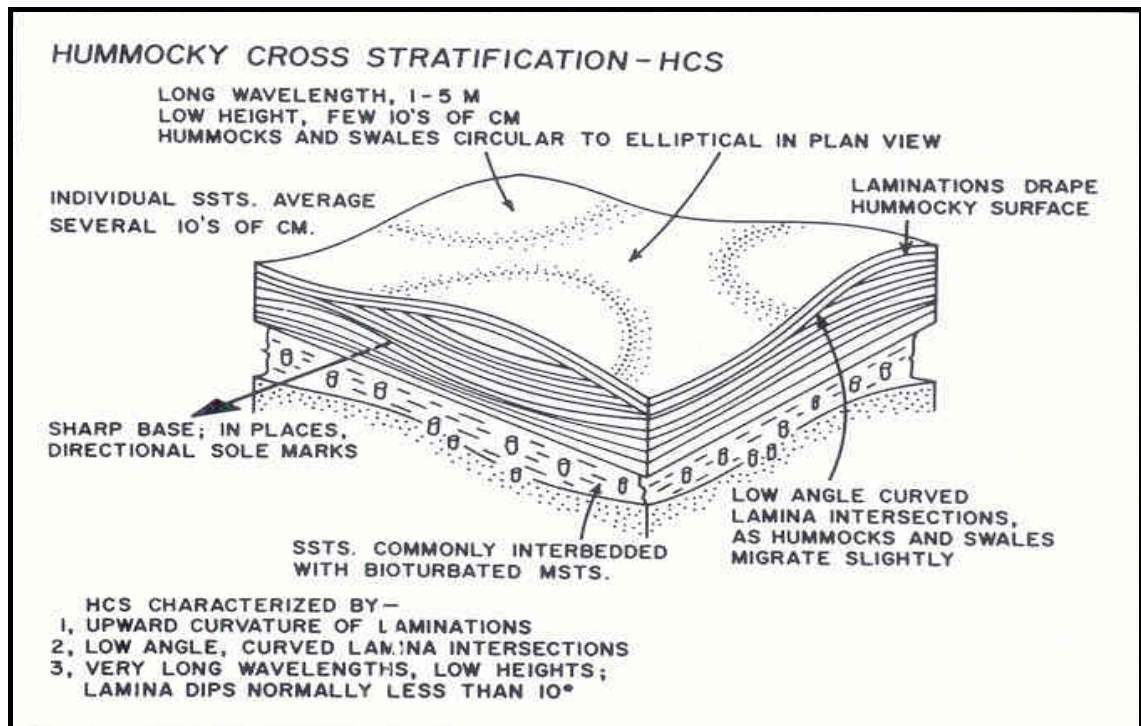
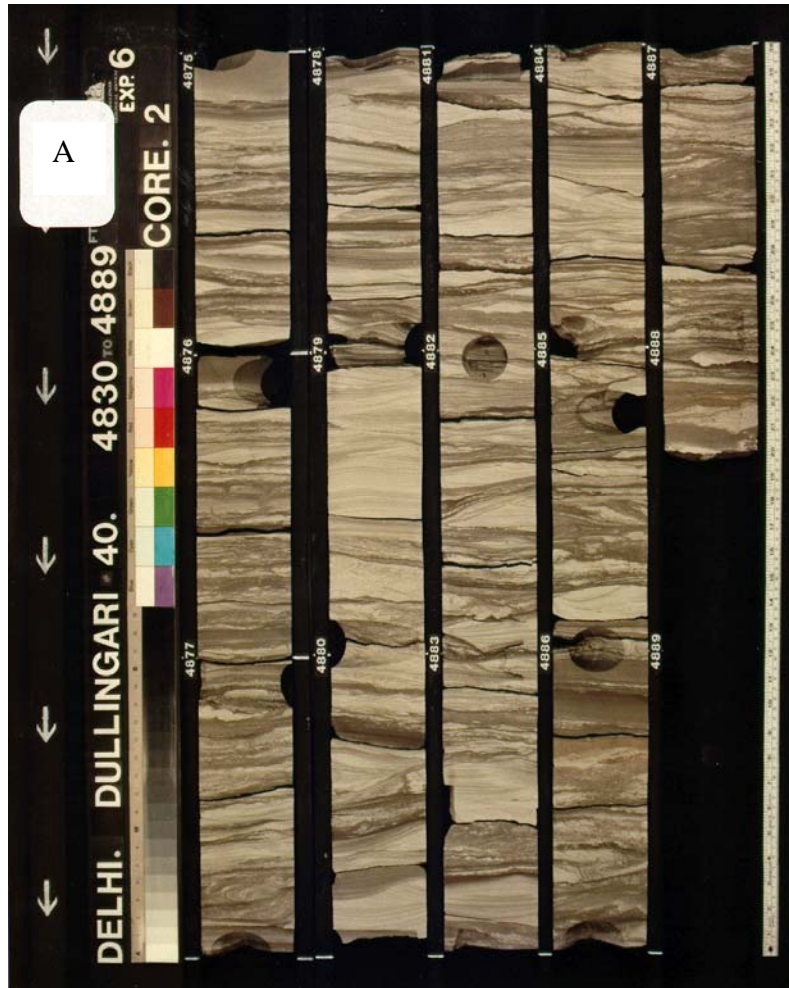


Figure 2.11: Block diagram of hummocky cross stratification, showing its typical occurrence in the interbedded HCS sandstone/bioturbated mudstone facies (Walker, 1982).



Bottom

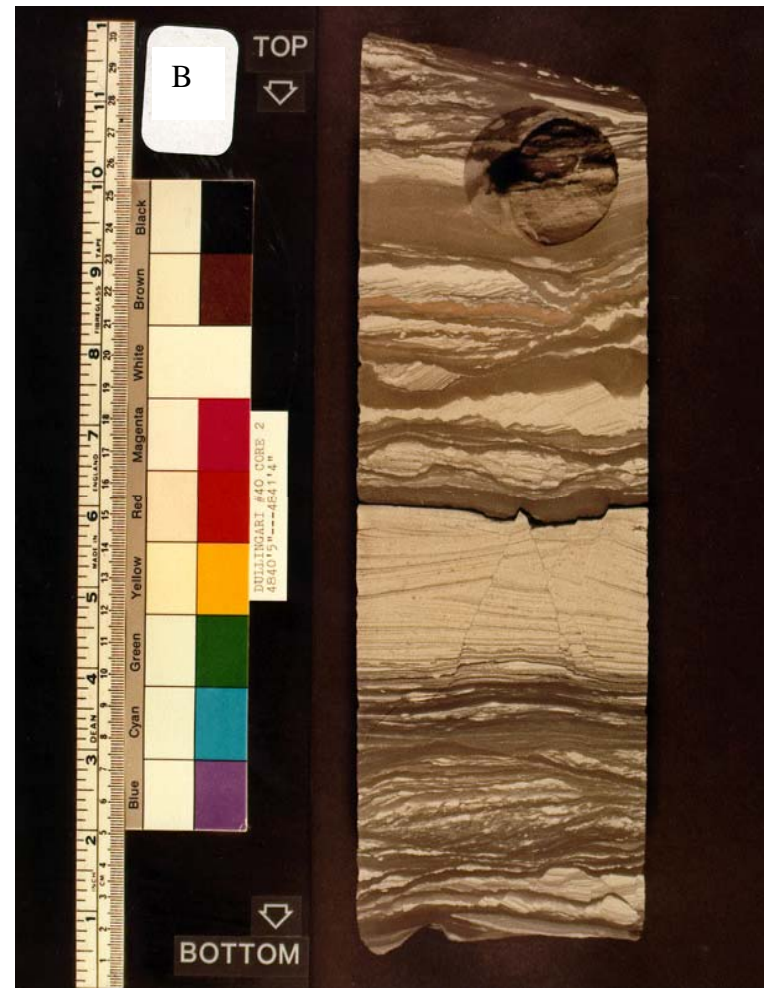


Figure 2.12: (A): Facies association-5 core photograph with convex-upwards laminae combined with climbing ripples which can be interpreted as storm-generated hummocky cross stratification. They commonly occur in coarsening-upward sequences. (B): Note slumps, microfaults, bioturbation, and siderite concretion at the top.

### **2.2.6 Facies association 6: Lacustrine offshore - Linsen laminated mudstone with minor siltstone and sandstone (Fl, Ss, Sb)**

#### **Description**

This facies association is characterized by linsen-laminated mudstone with minor hummocky cross-stratified, clean, well-sorted, thin, and fine-grained sandstone. The thickness of these clean lenses of sandstone does not exceed a few centimetres. Linsen-lamination, parallel-lamination, climbing ripple-lamination, starved ripples, and flaser bedding are the mainly observed sedimentary structures from this facies association. Burrowing in this facies association is intensive and found mainly in the thin silty and sandy layers. This bioturbation is so extensive in a degree where it disrupts the sedimentary structures of the thin sandy layers, while the linsen-laminated mudstone is lightly bioturbated (Table 2.1).

Soft sediment deformation including dewatering and slumps are found in this facies association. Microfaults were noted in the silty sand layers. Siderite concretions were recognized in both thin sandy layers and laminated mudstone.

Facies association 6 was identified from almost all of the described cores: Challum-1#1, Dullingari-40&37#1, Gidgealpa-19#1, Fly Lake-4#1, Gidgealpa-19#1, Gidgee-2#1, Ipundu-1#1, Jackson-1#1, Jena-11#1, Koorroopa-1#1, Marabooka-1#1, Maxwell-2#1, Orientos-2#1, McKinlay-1&2#1, Moomba-18#1, Merrimelia-6,16,&46#1, Namur-2#1, Narcoonowie-4#1, Pitchery-2#1, SpencerWest-2#1, Strzelecki-4#1, Takyah-1#1, Talgeberry-2#1, Three-Queens-1#1, Thungo-1#1, Tickalara-10#1, Tintaburra-2#1, Ulandi-3&5#1, Wilson-1#1, and Yanda-2#1.

### **Discussion and interpretation**

Based on the above facies association description, this facies association is interpreted to be deposited below the wave base in a low energy deep lake environment.

This environmental interpretation is supported by minor ripple laminated sandstone, lack of bioturbation, laminated character, and linsen bedding within the dominated mudstone facies association (Fig. 2.13). This facies association is interpreted to occur below the biogenic abundance level where sedimentation occurs from suspension with little or no currents. The deposition of this facies association is interpreted to occur in a moderately deep quite water environment (2-10m) (Moore & Castro, 1984). Alternatively, a deposition in a pro-delta environment should not be excluded. This facies association shows a high gamma ray log response because of its muddy nature.

The minor, very thin, clean, hummocky and ripple-laminated sandstones have a sharp erosive base with a general fining-upward pattern. This is interpreted as density flow deposits associated with storm and slump events which occurred below the wave base. This facies association is likely to have been deposited as storm and slope-generated turbidites (Fig. 2.13).

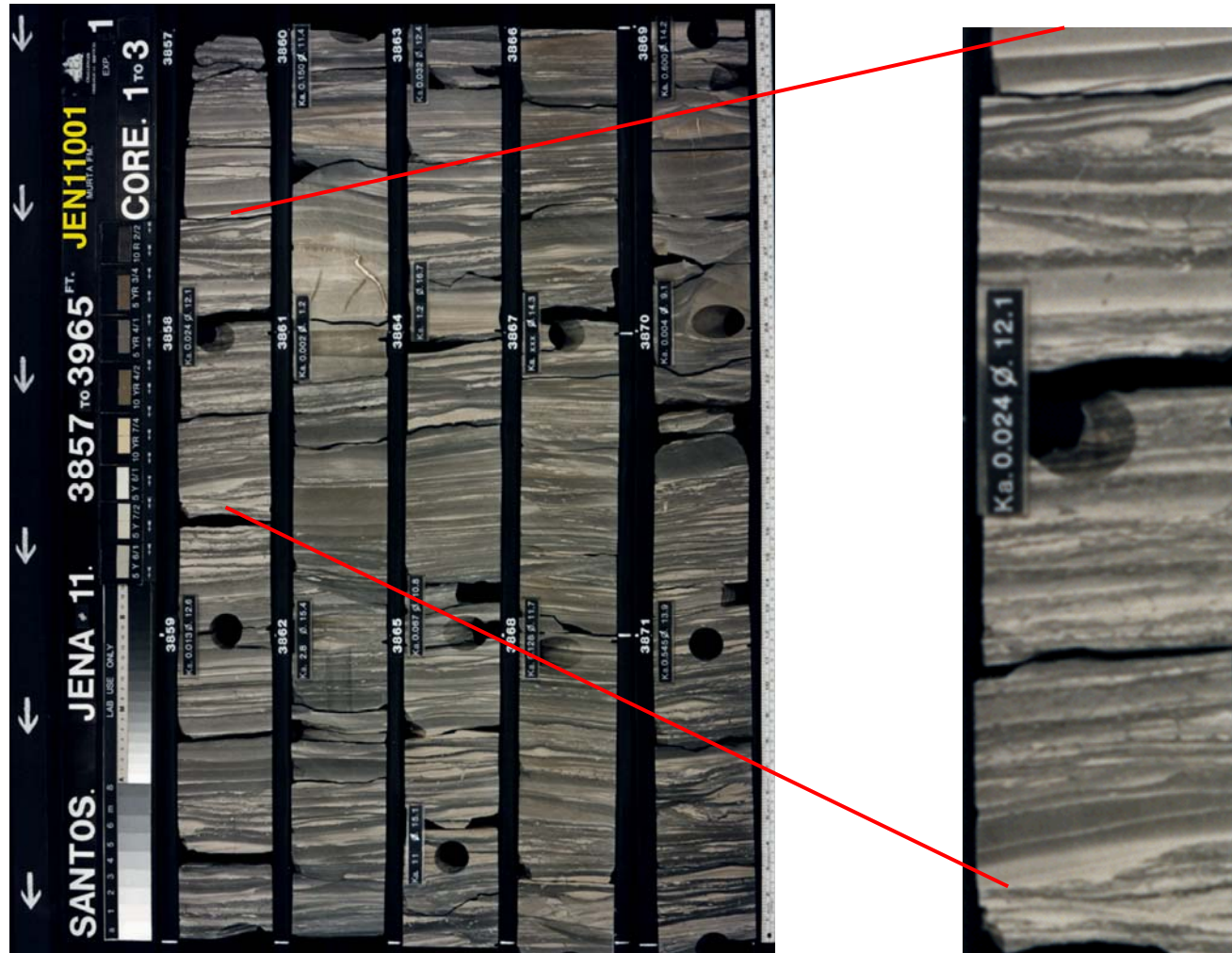


Figure 2.13: Facies association-6 core photograph with linsen-laminated mudstone with minor clean sandstone lenses interpreted to be deposited in a deep lake environment.



### 2.3 Summary of facies associations and depositional environments

The facies association concept was used and facies related to one another can lead to an environmental interpretation of the Murta Formation sequences. The deposition of the facies associations in the Murta Formation indicates a non-marine influence in the succession and suggests a fluvial-deltaic-lacustrine setting. This non-marine depositional setting was suggested by many previous authors who studied the Murta Formation (Mount, 1981 & 1982; Gravestock, 1982; Moore & Castro, 1984; Ambrose *et al*, 1986; Gorter, 1994; Theologou, 1995). On the other hand, Zoellner (1988) reported a marine influence in the uppermost part of the Murta Formation close to the Cadna-Owie Formation.

A repeated general coarsening-upward sequence was very clear through combining the vertical succession of the facies associations identified in cores. This coarsening-upward sequence starts with facies association 6 which represents deep/offshore lacustrine, facies association 5 as storm-dominated lacustrine shoreline, facies association 4 was interpreted as deltaic/distributary mouth bar setting, facies association 3 has a bioturbated/protected lacustrine shoreline sedimentation characteristics, facies association 2 was deposited across a lacustrine shoreline environment, and finally facies association 1 which represents a fluvial-deltaic system deposited close to the sand input. However, local incised valley fills were interpreted from the logs and are best represented in Pitchery-2, although they were not covered in cores. A conceptual diagram illustrating the Murta Formation facies associations is shown in Figure 2.14.

The thickness of each coarsening-upward cycle in the Murta Formation could reach 9 m and are very extensive, representing a progradation into a lake of shallow-moderate depth (4.5-9 m) with considerable areal extent. This coincides with Ambrose *et al*'s (1982) findings.

As a result of weak wave activity and negligible tidal influence, a lack of distinctive coastal zone was endorsed (Moore & Castro, 1984).

Due to fluctuations in the base level of Lake Murta and the influx of fluvial sediments, the depositional environments of the Murta Formation can be interpreted from cores and wireline logs as a prograding fluvial-dominated delta into a lacustrine basin with a minor marine transgression toward the top of the cored sections.

For instance, a base level change happens at the contact between facies associations 6 and 5. The contact is sharp, but not erosive with change in depositional setting from offshore/deep lacustrine in facies association 6 to storm-dominated shoreline setting in facies association 5. A series of base level changes took place in many wells locations when the lake dried out, letting the fluvial deposits to enter the lake area. This clearly represents the specifications of the fluvial sheets of facies association 1 as a regressive profile (Fig. 2.14).



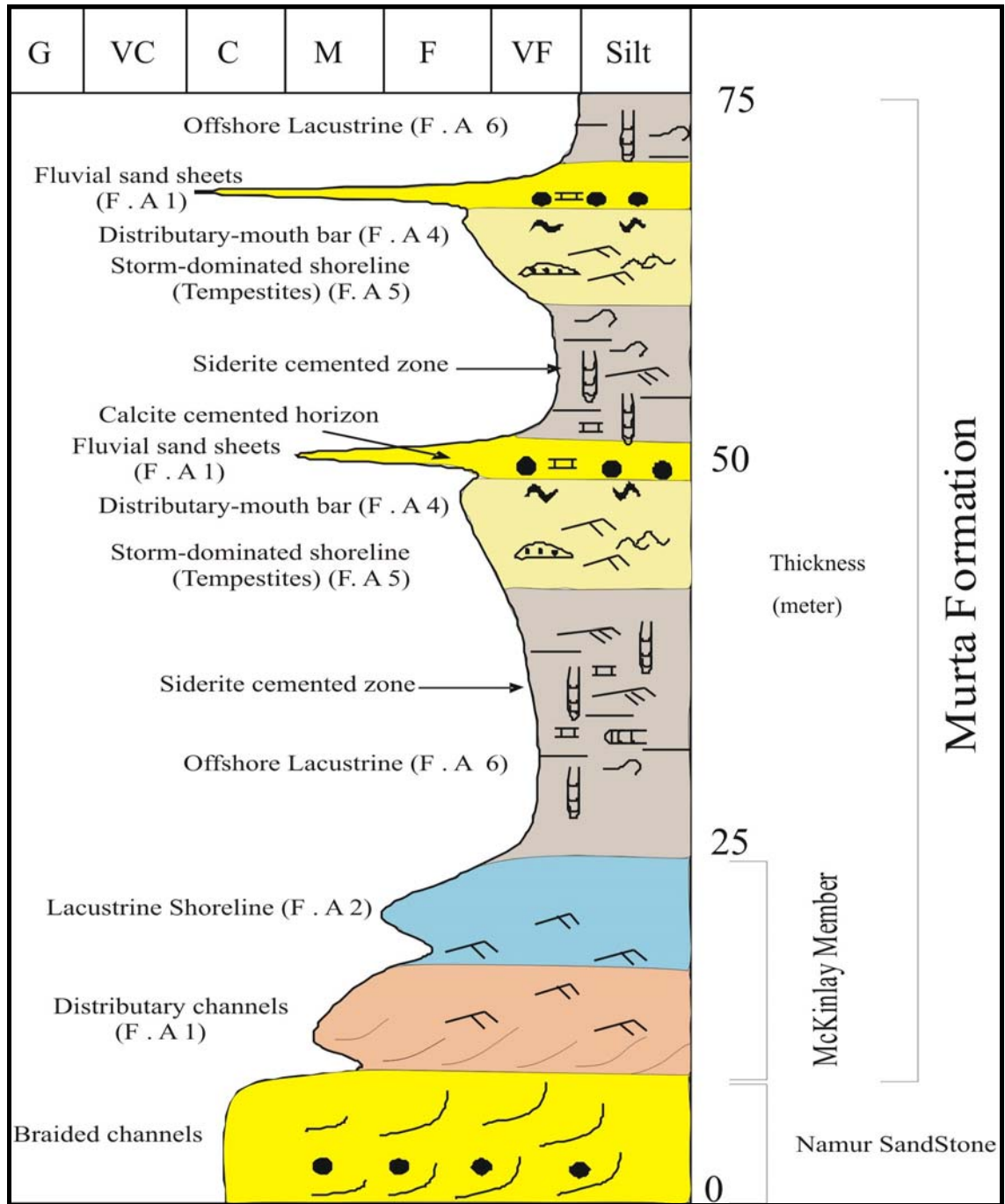


Figure 2.14: Interpreted conceptual diagram for the Murta Formation facies associations including the McKinlay Member. Namur Sandstone is also represented as braided fluvial.

## 2.4 Lake Murta sedimentation patterns and modern analogues

Murta lake is interpreted to be a hydrologically-open lake since sedimentation is dominated by material introduced by fluvial inflow. Deltas (generally fluvial-dominated in morphology) and shoreface zones are also common features in Murta lake sedimentation.

Variation in climate, tectonic setting, and lake morphology influences the distribution of depositional elements around a lake (Fig. 2.15). It is important to remember that in smaller lakes, wave and tide action is minimal and therefore lacustrine deltas have mainly fluvial dominated (birdfoot) morphology. When wave action is significant, lacustrine shorelines can develop at the downwind end of the lake (Riordan *et al*, 2006). Lake Murta is considered to be a mixed, mainly fluvial and partially wave dominated, hydrologically-open, freshwater lake.

Various depositional elements are found within a lacustrine setting, such as shorelines, deltas and their associated fluvial and distributary channels as well as occasionally deepwater deposits (Fig. 2.15). Distinguishing between the different depositional elements is important for establishing reservoir and seal dimensions and relationships. Lacustrine depositional systems provided hydrocarbon reservoirs, seals, and significant source material (Riordan *et al*, 2006).

Three major facies have been recognised within a lake environment: river facies, delta facies, and lake facies (Reineck & Singh, 1980).

Most clastic sediments deposited in the lakes are transported by rivers, either in suspension or bedload (Fig. 2.15). The size and the nature of the drainage basin will play a major role in the sediment input. Australia during Murta Formation/Lake time (Early Cretaceous) was in high latitude (60°-70°) similar to present-day Alaska and Norway and thus, Murta Lake is interpreted to be a hydrologically-open, freshwater lake. The input of clastic sediments is controlled by seasonal fluctuations of high latitude lakes when the glacial meltwaters discharge during summer. The organic matter is interpreted to be delivered to the basin during the flood discharges (Allen & Collinson, 1986).

Clastic sediments at the lake margins are commonly deposited around river mouths, while beach and barrier sediments are deposited by wave action reworking (Fig. 2.15).

The reworking of the lacustrine shoreline depends on many factors, such as the height of the waves, depth of water, type of material forming the shoreline, and the change in the lake water levels (Allen & Collinson, 1986).

Deltas of frictional processes become dominant where high bedload rivers discharge into shallow lakes (Allen & Collinson, 1986) (Fig. 2.15 & 2.16). This describes the Murta Formation nearshore depositional patterns where sediments are deposited over a wide area.

Clastic sediments are generally deposited in offshore zones by three ways; turbidity flows, pelagic fall-out and mass flows (Allen & Collinson, 1986). Murta Formation offshore zones were deposited by turbidity flows (Fig. 2.15). The percentage of the bottom lake clastic sediments is related to the circulation patterns of the lake (Allen & Collinson, 1986). The circulation patterns of Lake Murta in the southern hemisphere were clockwise (N. Lemon, Santos Ltd., pers. comm.).

These circulation patterns, in turn, are strongly controlled by river currents and geostrophic effects (Allen & Collinson, 1986).

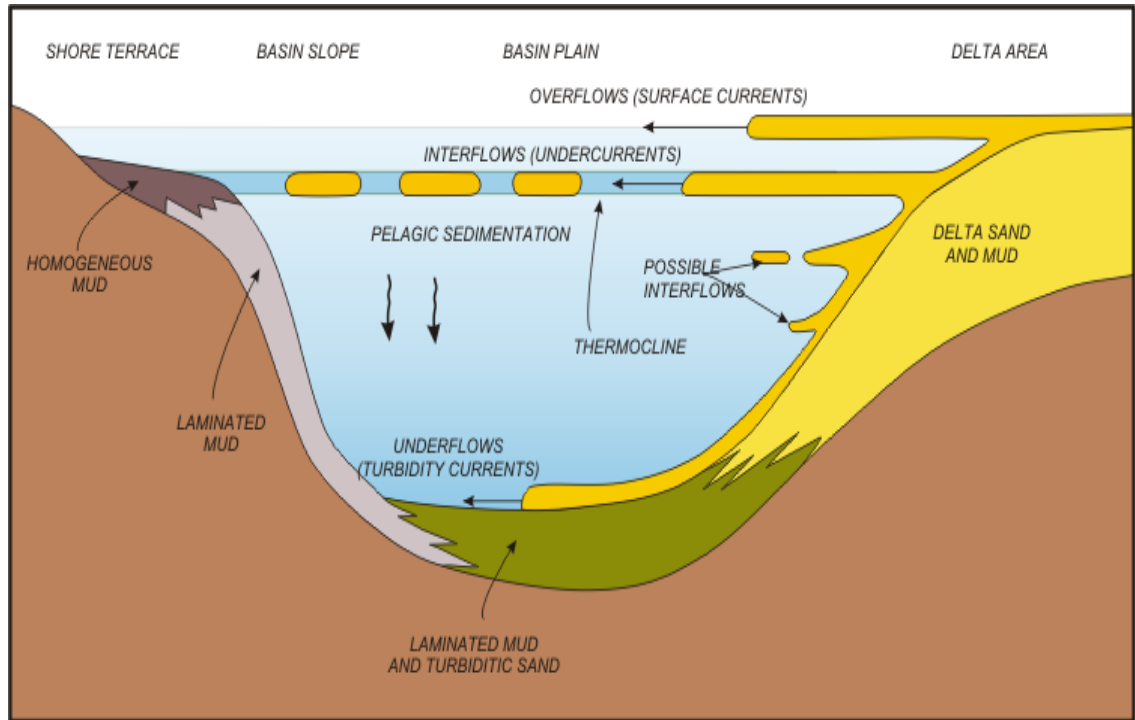


Figure 2.15: Distribution mechanism and resulting sediment types proposed for clastic sedimentation in lacustrine environment (after Sturm and Matter, 1978).

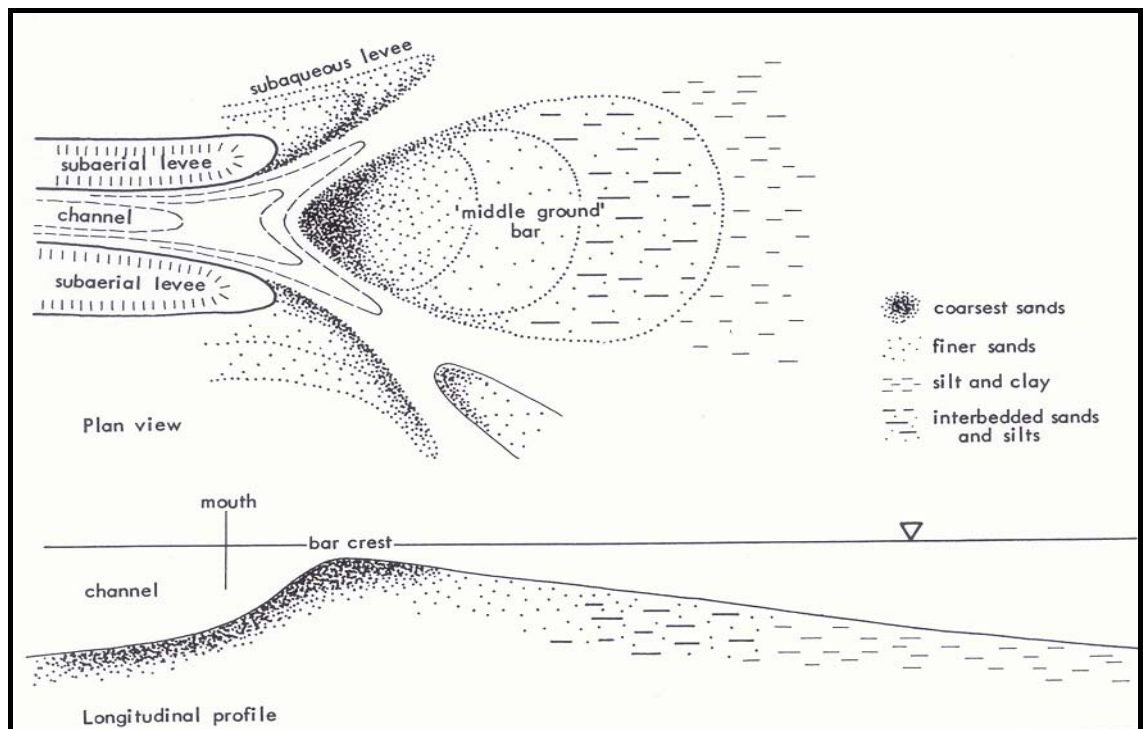


Figure 2.16: Depositional patterns associated with friction-dominated river-mouth outflow (Wright, 1977).

Bohacs *et al* (2002) proposed three classifications of lacustrine facies associations based on empirical observations of lacustrine basin strata: Fluvial-lacustrine facies associations, Fluctuating profundal facies associations, and evaporitive facies associations (Table 2.2). According to this classification, Murta Formation/lake, as fluvial-deltaic dominated, hydrologically-open freshwater lake, can fit on Fluvial-lacustrine facies associations with overfilled lake basin-type and dominantly progradational stacking pattern of its parasequences (Table 2.2 & 2.3). The word “overfilled” is influenced by accommodation space and water plus sediment supply. The fluvial-lacustrine facies association, as in Murta Formation/lake study, is characterized by freshwater lacustrine mudstones interbedded with fluvial-deltaic deposits (Fig. 2.17). These deposits are widespread regionally with lateral discontinuities (Bohacs *et al*, 2002).

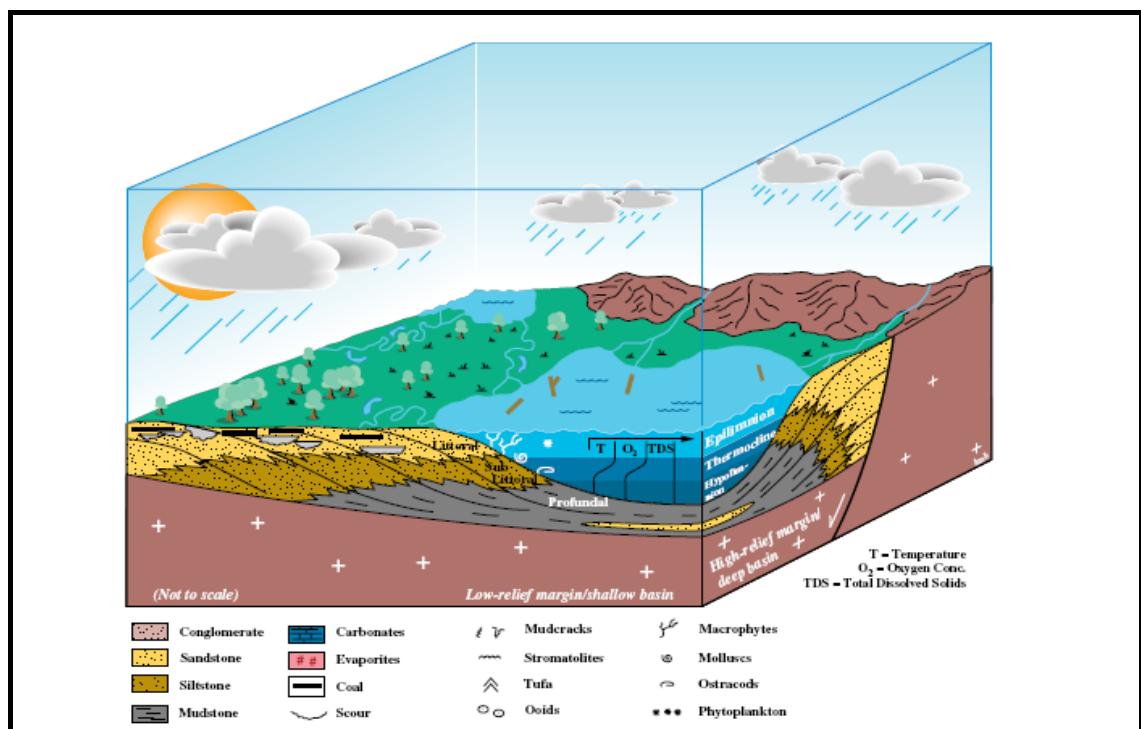


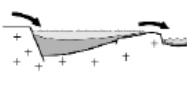

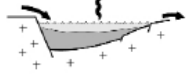

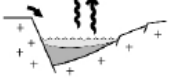
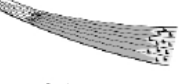
Figure 2.17: Schematic diagram highlighting major features of overfilled lake basins: persistently open hydrology, freshwater lake chemistry, progradational shoreline architecture, and a close relationship to fluvial system. This lake-basin type occurs when the rate of supply of sediment plus water consistently exceeds potential accommodation. Climatically, lake level fluctuations are minimal because water inflows are in equilibrium with outflows (Bohacs *et al*, 2002).

Table 2.2: Representative attributes of three major lacustrine facies associations (Bohacs *et al.*, 2002).

Lacustrine Facies Association	Stratal Stacking Patterns	Sedimentary Structures	Lithologies	Organic Matter
Fluvial-Lacustrine	Dominantly progradation Indistinctly expressed parasequences	Physical Transport: ripples, dunes, flat bed Root casts Burrows (infaunal & epifaunal)	Mudstone, marl Sandstone Coquina Coal, coaly shale	Freshwater biota Land-plant, charophytic and aquatic algal OM* Low to moderate TOC* Terrigenous & algal biomarkers
Fluctuating Profundal	Mixed progradation & aggradation Distinctly expressed parasequences	Physical & Biogenic: flat bed, current, wave, & wind ripples; stromatolites, pisolites, oncolites Mudcracks Burrows (epifaunal)	Marl, mudstone Siltstone, sandstone Carbonate grainstone, wackestone, micrite Kerogenite	Salinity tolerant biota Aquatic algal OM* Minimal land plant Moderate to high TOC Algal biomarkers
Evaporitive	Dominantly aggradation Distinctly to indistinctly expressed parasequences	Physical, Biogenic, & Chemical: climbing current ripples, flat bed, stromatolites, displacive fabrics, cumulate textures	Mudstone, kerogenite Evaporite Siltstone, sandstone Grainstone, boundstone, flat- pebble cgl*	Low-diversity, halophytic biota Algal-bacterial OM* Low to high TOC Hypersaline biomarkers

\*OM = organic matter, TOC = total organic carbon, cgl = conglomerate.

Table 2.3: Characteristics of lake-basin types: strata, source facies, and hydrocarbons (Bohacs *et al.*, 2002).

Lake Type & Lacustrine Facies Association	Stratigraphy	Source Potential	Hydrocarbon Characteristics
<b>OVERFILLED</b>  <i>Fluvial-Lacustrine Facies Association</i>	Maximum progradation:  <ul style="list-style-type: none"> <li>Parasequences related to lateral progradation (relatively subtle)</li> <li>Maximum fluvial input</li> </ul>	<ul style="list-style-type: none"> <li>Low to moderate TOC</li> <li>Mixed type I-III kerogen</li> <li>Marked organic facies contrasts</li> <li>Distinct lateral changes in organic facies</li> </ul>	<ul style="list-style-type: none"> <li>Generate both oil and gas</li> <li>Very waxy, low-sulfur oils</li> <li>Terrigenous biomarker assemblage dominant</li> </ul>
<b>BALANCED-FILL</b>  <i>Fluctuating-Profundal Facies Association</i>	Mixed progradation and desiccation:  <ul style="list-style-type: none"> <li>Distinct shoaling cycles common</li> <li>Fluvial input variable</li> </ul>	<ul style="list-style-type: none"> <li>Moderate to high TOC</li> <li>Predominantly type I kerogen, with type I-III mixtures near flooding surfaces</li> <li>Relatively homogeneous and laterally consistent organic facies</li> </ul>	<ul style="list-style-type: none"> <li>Mostly oil generative</li> <li>Paraffinic but relatively nonwaxy oils; low sulfur</li> <li>Algal biomarker assemblage dominant</li> </ul>
<b>UNDERFILLED</b>  <i>Evaporative Facies Association</i>	Maximum desiccation:  <ul style="list-style-type: none"> <li>High-frequency wet-dry cycles</li> <li>Minimum fluvial input</li> </ul>	<ul style="list-style-type: none"> <li>Low overall TOC (w/ some high TOC intervals)</li> <li>Type I kerogen</li> <li>Minimum organic facies contrasts</li> <li>Laterally consistent organic facies</li> </ul>	<ul style="list-style-type: none"> <li>Mostly oil generative</li> <li>Paraffinic oils; moderate to high sulfur</li> <li>Distinctive "hypersaline" biomarker assemblage</li> </ul>



Murta Formation depositional patterns are associated with shallow and deep events in the lake. A modern analogue of deep intervals could be matched with Selenga River entering Lake Baikal at a shallow depth. This setting is accompanied by relatively high interaction between the fluvial-deltaic inputs and lake shoreline across the southern part of Lake Baikal (Fig. 2.18).

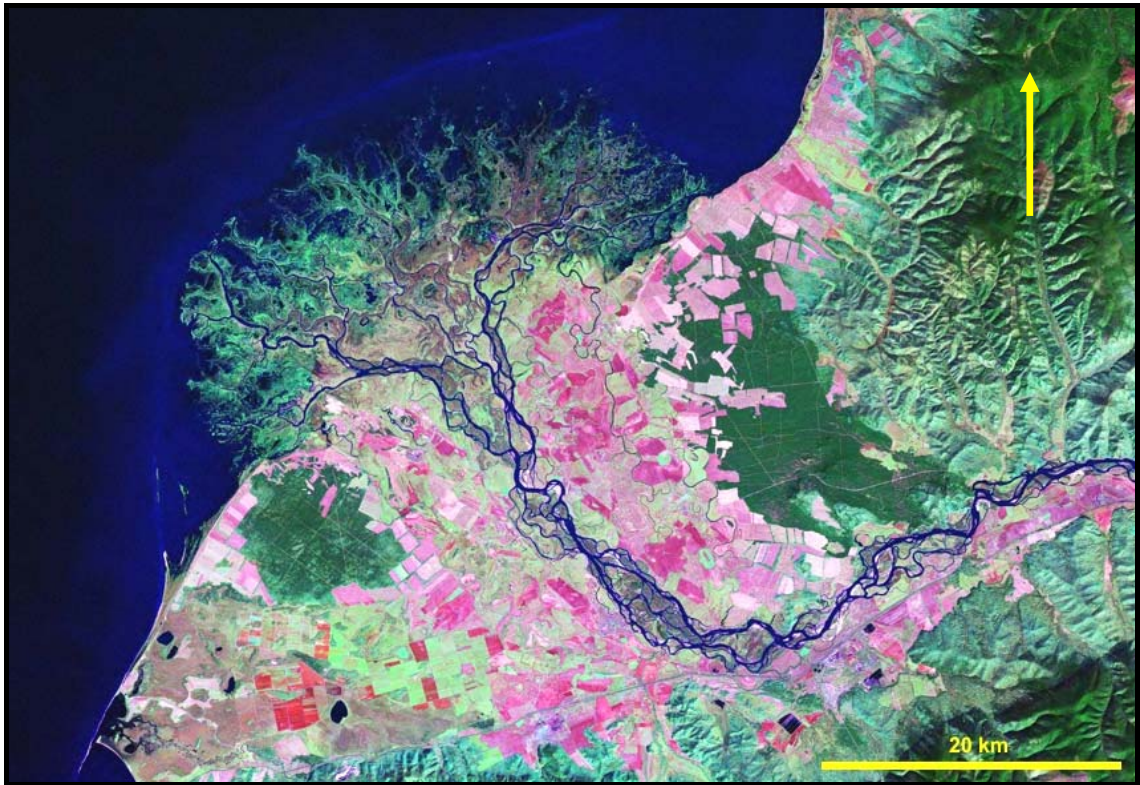


Figure 2.18: Fluvial-dominated delta example from Selenga River delta of the southeastern part of Lake Baikal. Little delta front reworking is evident, indicating that wave processes are minimal in this part of the lake (Riordan *et al*, 2006).

On the other hand, a modern analogue for extreme shallow intervals in Lake Murta is Lake Eyre (Neales and Kalawereena) in Central Australia (Fig. 2.19). During such a period, there is nearly no water and the fluvial sand inputs make their way to the basin when the lake dried out.





Figure 2.19: The Kalawereena terminal splay complex in the dry of July 2003 looking SE. Note the darker muddy patches along the numerous distributary channels, and highstand shoreline (Krapf & Lang, 2005).

## Chapter 3 Sequence Stratigraphy

### 3.1 Introduction

Sequence stratigraphy deals with the analysis of cyclic sedimentation patterns that are present in stratigraphic successions, as they develop in response to variations in sediment supply and space availability for sediment to accumulate (Posamentier & Allen, 1999). In the simplest sense, sequence stratigraphy studies the sedimentary response to the changes in base-level (Fig. 3.1), which can be analysed from the scale of individual depositional systems to that of entire basins (Catuneanu, 2006).

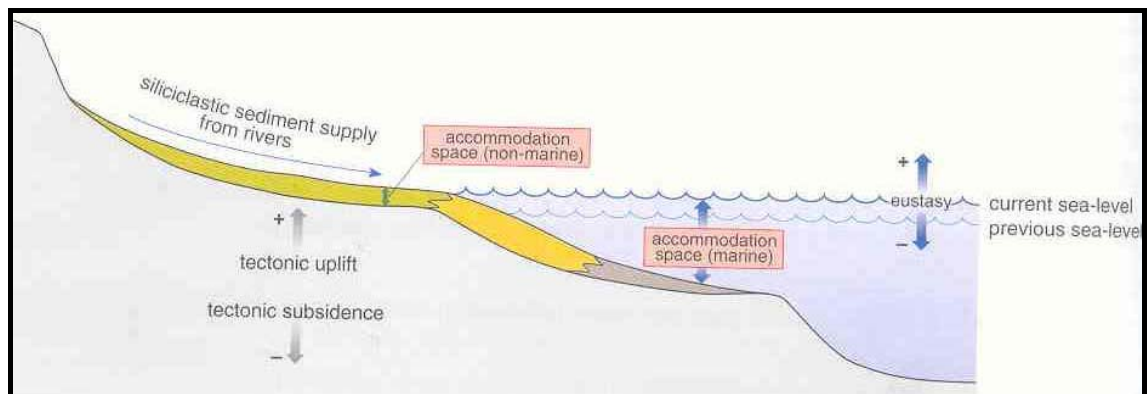


Figure 3.1: Sediment accommodation space and its relationship to eustatic sea level and tectonic uplift and subsidence (Coe & Church, 2003).

The use of sequence stratigraphy implies the recognition and correlation of coeval stratal units based on the event significance of their bounding surfaces. This will be irrespective of the lateral changes of facies that commonly occur across the basin. Additionally, the palaeoenvironment interpretation using facies analysis is most important for sequence stratigraphy. In contrast, lithostratigraphy does not require knowledge of palaeoenvironments, but only mapping of lithological contacts. This, in turn, will cause potential problems that could confuse the lithostratigraphy. Some of the lithostratigraphic contacts may coincide with sequence stratigraphic surfaces; others may just reflect diachronous lateral facies changes. Therefore, lithostratigraphic units provide a lithology description of different sedimentation products regardless of the depositional environments. Figure 3.2 shows an offset relationship of sequence stratigraphic units compared to lithostratigraphic units due to emphasis on different rock attributes (Catuneanu, 2006).

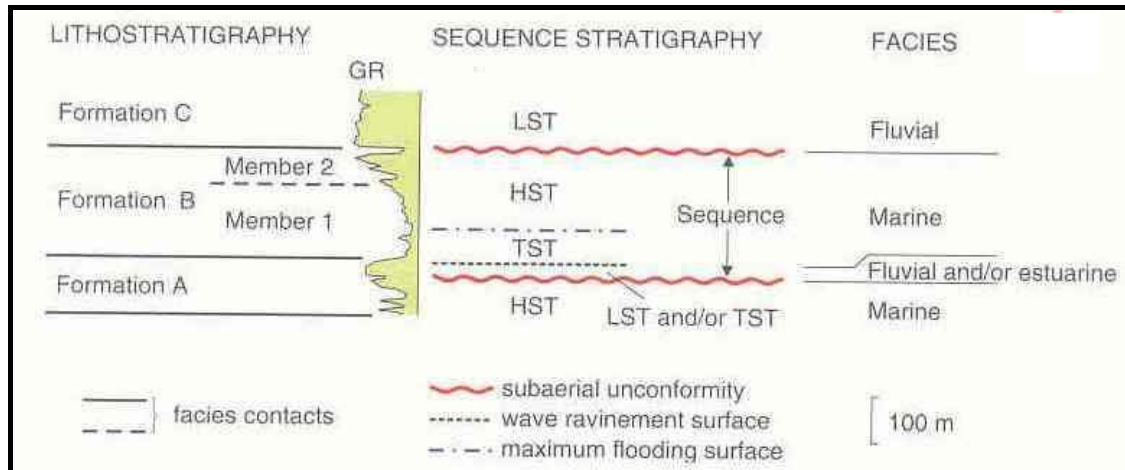


Figure 3.2: Lithostratigraphic and sequence stratigraphic interpretations of a gamma ray (GR) log (modified from Posamentier and Allen, 1999). Lithostratigraphy defines rock units on the basis of lithology, often irrespective of the depositional environment. Sequence stratigraphy defines rock units based on the event significance of their bounding surfaces (Catuneanu, 2006).

Sedimentation patterns in any sedimentary basin are governed by the accommodation space and the amount of sediment supplied. Accommodation space is what is made available within a basin for sediment to be deposited and preserved. Accommodation space is measured by the distance between base level and the depositional surface (Catuneanu, 2006). The amount of accommodation space, in turn, is controlled by changes in relative sea level. Changes in relative sea level, sequentially, are controlled by both eustatic sea level fluctuations and tectonic subsidence and uplift which are acting independently (Coe & Church, 2003).

The interaction between sediment supply and accommodation space is a two way process. Sedimentation not only consumes accommodation space, but also can create additional space as sediment aggradation and loading continues and this will determine the sedimentation styles (Fig. 3.3) (Coe & Church, 2003).

A prograding lacustrine/marine shoreline will develop as a result of increase in sediment supply compared to constant or decrease in accommodation space. The shoreline in this case has moved in a basinward direction and parasequences are described to have prograded and the succession of parasequences called progradational parasequences (Coe & Church, 2003). These kinds of parasequences are common in Highstand System Tracts (HST).

On the other hand, a retrograding lacustrine/marine shoreline will develop as a result of increase in accommodation space compared to constant or decrease in sediment supply. The shoreline in this case will shift landward and parasequences are said to have a retrogradational pattern and associated with a Transgressive System Tracts (TST) (Bohacs *et al*, 2002). Equal accommodation space and sediment supply will result in an aggradational pattern of the parasequences deposited in this succession with no net movement of the shoreline. Usually, they are related to a Lowstand System Tracts (LST) (Bohacs *et al*, 2002). Definition of selected sequence stratigraphic terms used in this study can be seen in Appendix 3.1.

### **3.2 Lacustrine sequence stratigraphy**

Application of sequence stratigraphy in lacustrine systems is very important since it helps in correlation and mapping of lithofacies and hydrocarbon play elements (Bohacs *et al*, 2002).

Similar to all depositional sequences, lacustrine depositional sequences are controlled by the combined influence of lake base level, sediment supply, and tectonics. Although, lacustrine systems vary rapidly and widely, this will not affect the application of sequence stratigraphy on these sequences since the rocks are still deposited in layers bounded by physical surfaces which can be used as time lines (Bohacs *et al*, 2002).

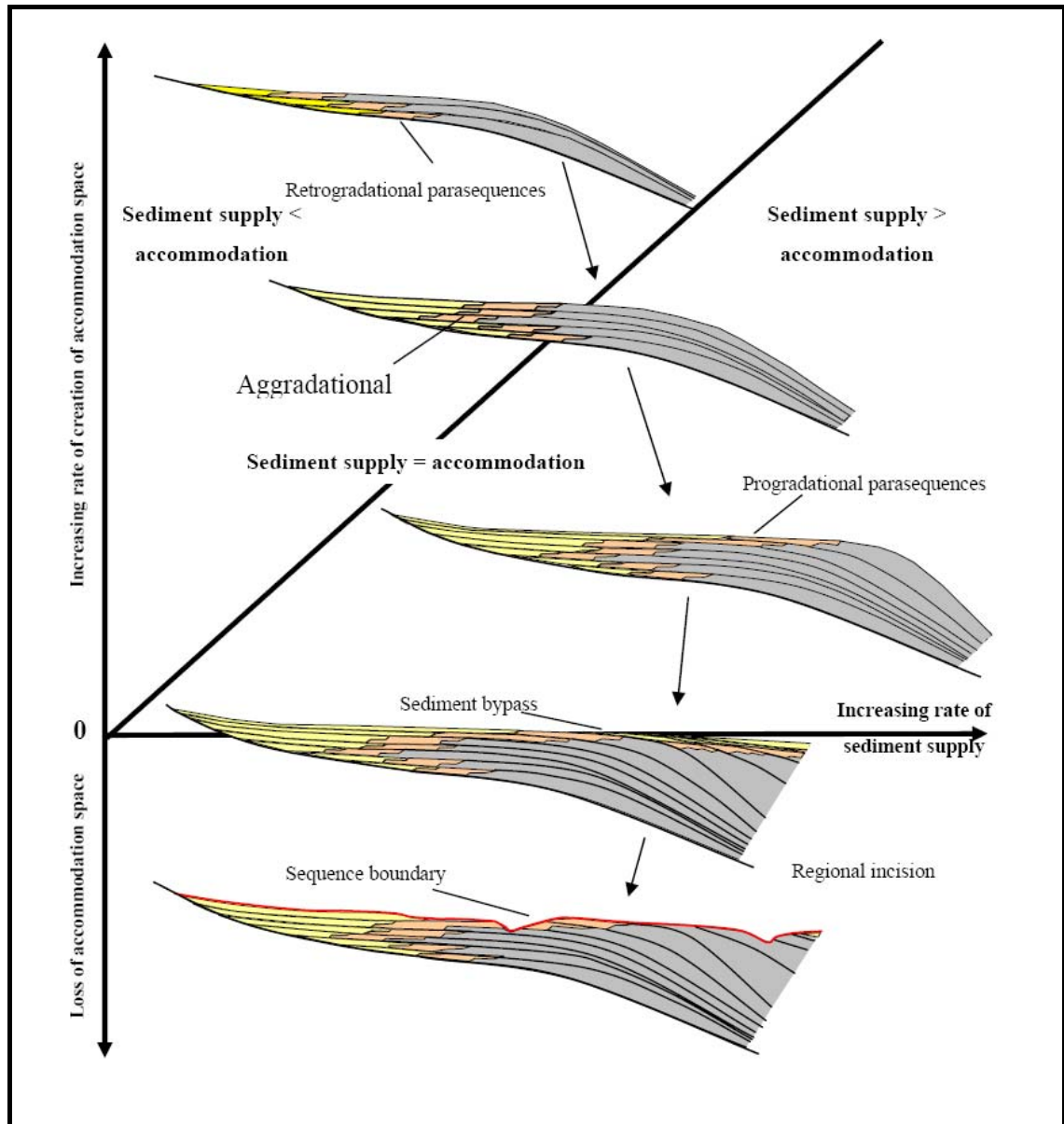


Figure 3.3: Interplay between accommodation space and sediment supply and the resultant stacking patterns (after Shanley & McCabe, 1994, and Hill, 1999).

Due to the different scale of lacustrine system cyclicality, these systems trace their reaction to regional and local activities. Small-scale parasequence packages deposited over short time are interpreted to represent by changes in climate (water+sediment supply), while large-scale packages deposited over longer time can disclose the changes in subsidence, tectonic, and landscape evolution (Bohacs *et al*, 2002).

The depositional patterns in lacustrine environments represent the interaction between sediment supply and lake level changes. Accommodation space in this case is commonly controlled by climatic or tectonic activities that are isolated from the changes in sea level (Shanley & McCabe, 1994).

Parasequences in overfilled lake basins, like in the Murta Formation case, are very similar to shallow marine sequences although they are generally thinner (Fig. 3.4) (Bohacs *et al*, 2002).

In lacustrine settings, lake levels play a major role in fluvial-lacustrine stratigraphy regardless the type of the lake (open or closed). The fluctuations in lake levels will be acting in the same manner as marine environment respond to changes in relative sea level, although, lake levels fluctuations are considered to be more frequent than eustatic fluctuations (Posamentier & Allen, 1999).

Allen *et al.* (1996) suggested that if there is a very low sediment supply and rapid subsidence, this will lead to a development of a lacustrine system (Fig 3.5). Therefore, an increase in accommodation space will encourage the expansion of the lake which later on will be noticeable through its Maximum Flooding Surfaces MFS.

Sequence Boundaries (SB) are well defined in non-marine and lacustrine sequences. They are characterized by channel fills which deeply erode the underlying lacustrine successions or rapid lakeward shifts in facies in general (Bohacs *et al*, 2002).

A Maximum Flooding Surface (MFS) is relatively easy to interpret in lacustrine settings either from logs or cores. MFS can often be correlated across the basin because of their regional extent. Shaly and mudstone intervals from cores and a high gamma ray response in logs will clearly establish a MFS (Fig 3.5).

There is an accepted impression of an easy application of sequence stratigraphic concepts to lacustrine successions due to the cyclic nature of lakes. Some sequences, however, do not embrace the idea of being bounded by unconformities or their correlative conformities. For example, the switching of the delta lobes as a result of different sediment supply can send a false message of the possible occurrence of a regional Maximum Flooding Surface, although they are just local flooding surfaces (Oviatt *et al*, 1994). To overcome this problem, a regional stratigraphic study should be conducted to define the true sequences (Posamentier & Allen, 1999).

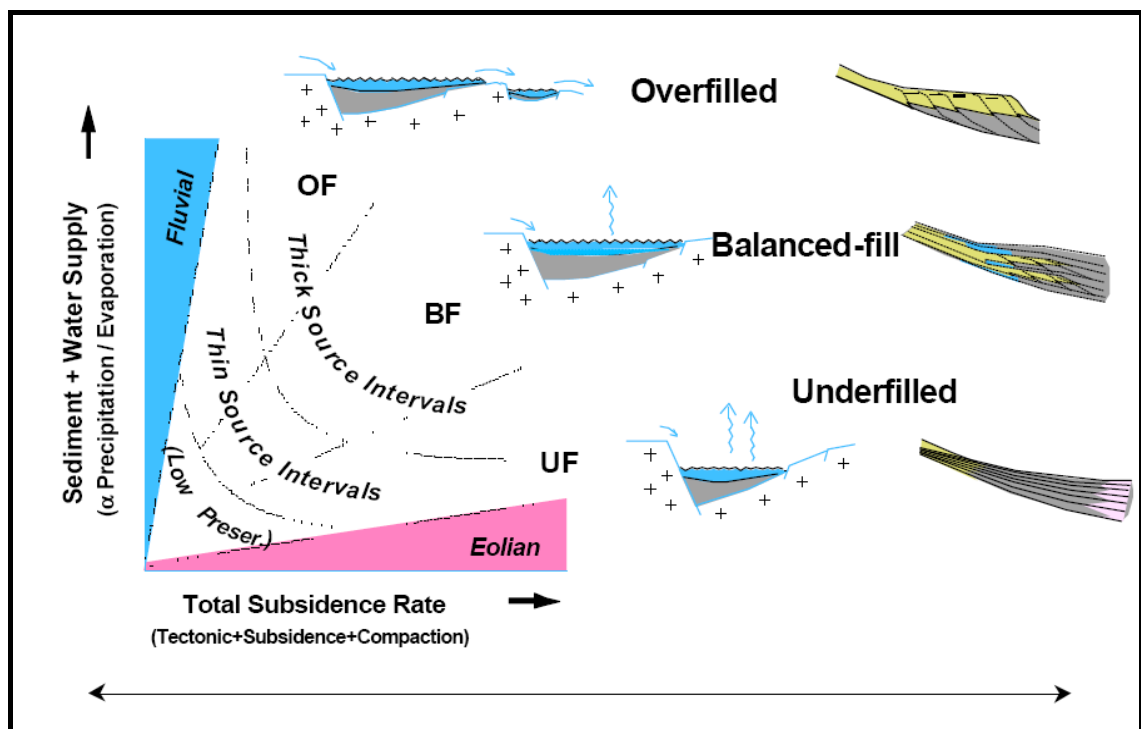


Figure 3.4: Relationship between sediment+water supply and total subsidence rate and the resulting lake basin type (Bohacs *et al*, 2002).



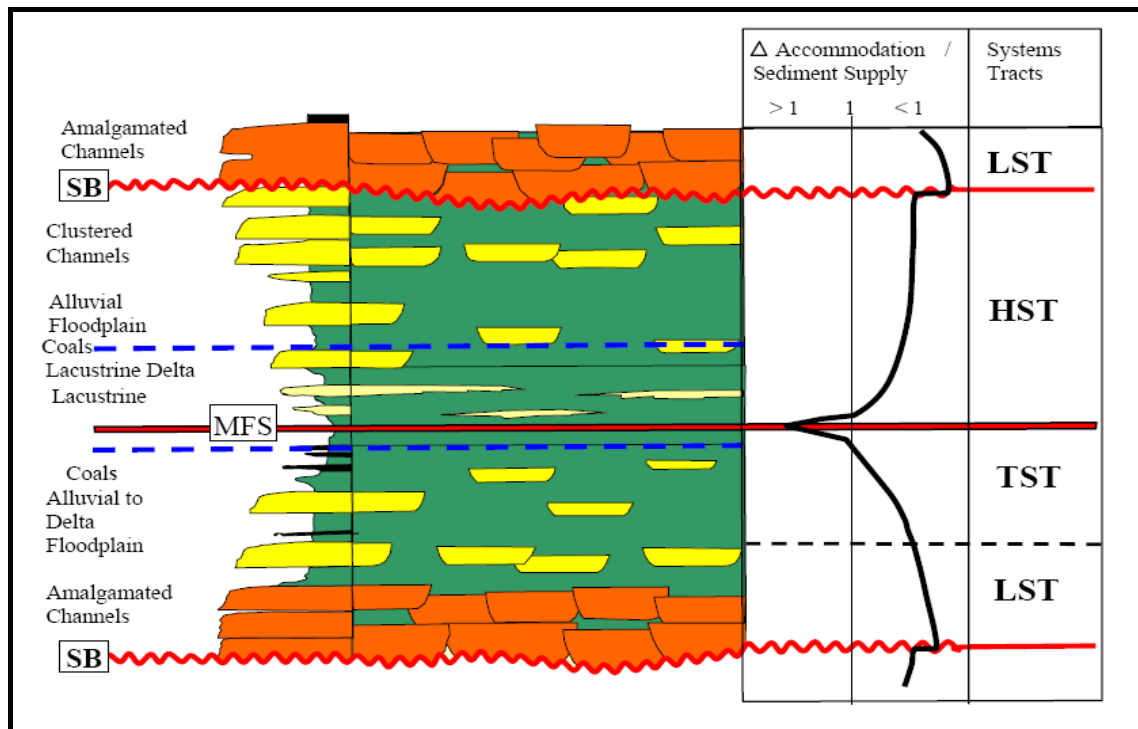


Figure 3.5: The position of key surfaces in relation to systems tracts and their relationship to the ratio of accommodation to sediment supply (Legarreta *et al*, 1993). Note the amalgamated fluvial deposits which represent the Lowstand System Tract (LST) and indicate low accommodation are overlying the sequence boundary and topped by a transgressive surface (TS). This transgressive surface, in turn, marks the start of lacustrine or coal sediments. The Transgressive System Tract (TST) is characterized by coarsening upward sequences of lacustrine deltas and topped by Maximum Flooding Surface (MFS). The Highstand System Tract (HST) is characterized by progradational stacking pattern and associated with the infilling of the lacustrine delta and decrease in the accommodation space (modified from Legarreta, 1993, Allen, 1996).

### 3.3 Murta Formation sequence stratigraphy

The deposition of the Murta Formation represents a phase of increase in the accommodation space in the Early Cretaceous (Gierlowski-Kordesch & Kelts, 1994). An overall transgressive lacustrine setting explains the deposition of the Murta Formation in the Eromanga Basin, an intracratonic sag basin.

A regional transgression was recognized across the Eromanga Basin from the fluvial Namur Sandstone to lacustrine Murta Formation. This regional and gradual transgression started at the contact between the Namur Sandstone and the McKinlay Member of the Murta Formation. Another regional and gradual contact defines the contact between lacustrine setting of the Murta Formation and the overlying increasingly marine setting of the Cadna-owie Formation.

Two Maximum Flooding Surfaces (MFS) within the Murta Formation, identified clearly from the wireline logs with high gamma ray readings, were documented from all of the cored wells across the entire study area, and were correlated regionally (Fig. 3.6). Nevertheless, in the north and northeastern part of the study area, close to the main sand inputs, it is hard to identify the (MFS) either from logs or from cores as it lies within thick fine to medium-grained sandstones. These MFS represent a period of decrease in sediment supply and an increase in the accommodation space of the lacustrine basin. Two minor Maximum Flooding Surfaces (mMFS) were identified also within the Murta Formation (Fig. 3.6).

The regional and gradual contacts between the Murta Formation and the underlying Namur Sandstone, and the Murta Formation and the overlying the Cadna-owie Formation are represented by two normal Transgressive Surfaces (TS) (Fig. 3.6). The deposition between these two transgressive surfaces is mainly lacustrine deltaic and shoreline settings which propose the depositional environment of the Murta Formation and its basal McKinlay Member. However, local incised valley fills within the Murta Formation sequences were interpreted from logs. They are best represented in Pitchery-2 well, although there are no cores in this well. Incised valley fills can indicate localized sequence boundaries (SB) within the lacustrine setting of the Murta Formation (Fig. 3.6).

By constructing several regional cross sections across the study area, sediment supply points were interpreted to deliver sediment to the lacustrine basin from different directions. Specifically, wireline log motifs showed that the main sand input to the basin came from the north-northeastern direction of the study area in Queensland and nominated a main depocentre in that area. This implies a regional reduction in sand content from the north-northeastern (main sand input) part of the study area towards the southwest in South Australia (Fig. 3.7). This reduction in sand content fits in the Murta Formation depositional pattern which is fluvial-dominated delta prograding into a lacustrine setting. Theologou (1995) suggested another sand input from a northwestern direction of the study area to explain the thick sandy facies of Merrimelia-6. The major possible outflow of Lake Murta was located to the southwest of the study area (N. Lemon, Santos Ltd., pers. comm).

Regional analysis of the Murta Formation facies showed variations in wireline log signatures and thicknesses in the Murta Formation which have been recorded across the study area. These variations could be as a result of variations in sediment supply, rapid base level changes, differential compaction or different shoreline morphologies. Facies associations close to the central part of the basin and to the type and reference sections did not show that many facies associations variations compared to the type and reference sections log signature (Fig.3.7). Nevertheless, facies associations near the south and southerwestern part of the basin show an increase in shale and mudstone (Fig.3.7). In addition, facies close to the main sediment inputs in the north and northeast direction of the basin are more sand-rich than elsewhere (Fig.3.7).

The Murta Formation was divided into seven units based on the key surfaces (MFS, TS, and maximum shallowing events) correlated across the study area. These key surfaces or time lines encompass chronostratigraphic units which later will be used in reconstructing the isopach and palaeogeographic maps of each unit of the Murta Formation. These units followed Santos nomenclature and the prefix is based on naming conventions in the Eromanga Basin.

A sequence stratigraphic model of the Murta Formation was established using all of the above data from core description, facies associations, and wireline log motif facies scheme (Fig. 3.6).

This sequence stratigraphic model was correlated back to the Murta Formation, the McKinlay Member, and the Namur Sandstone type and reference sections in Dullingari North-1 defined by Mount (1981), Dullingari-9 defined by Ambrose *et al* (1986) and Strzelecki-4 defined by Gravestock *et al* (1995) respectively.

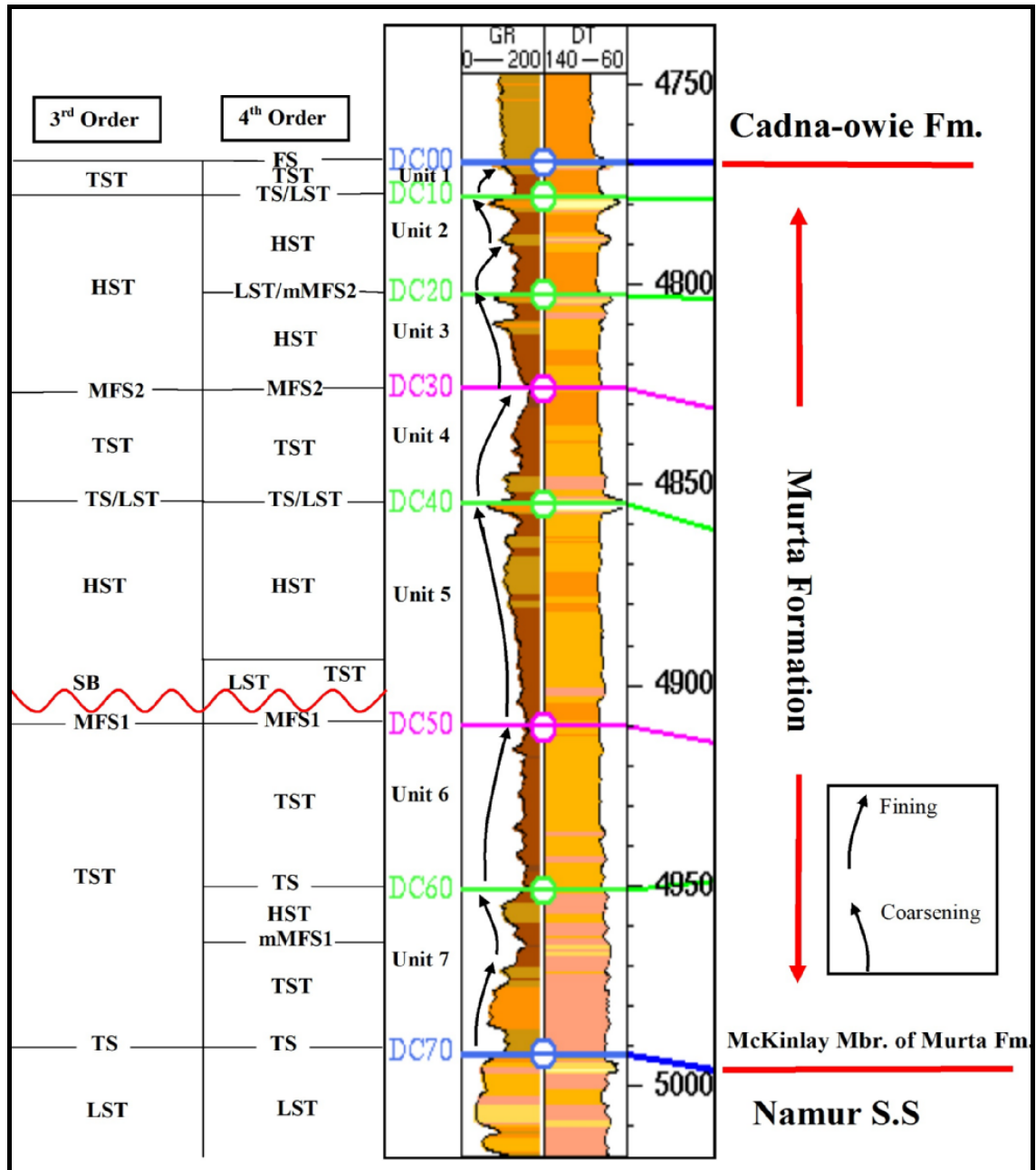


Figure 3.6: Murta Formation sequence stratigraphy elements from Dullingari-40 well. The squiggly lines represent the fluctuations in lake level. DC10, DC20, and DC40 represent the tops of shallowing events in the Murta Formation, while DC60 represents a transgressive surface before the first Maximum Flooding Surface (MFS) which is DC50. The second MFS in the section is DC30. There are 7 units between the Murta Formation surfaces.

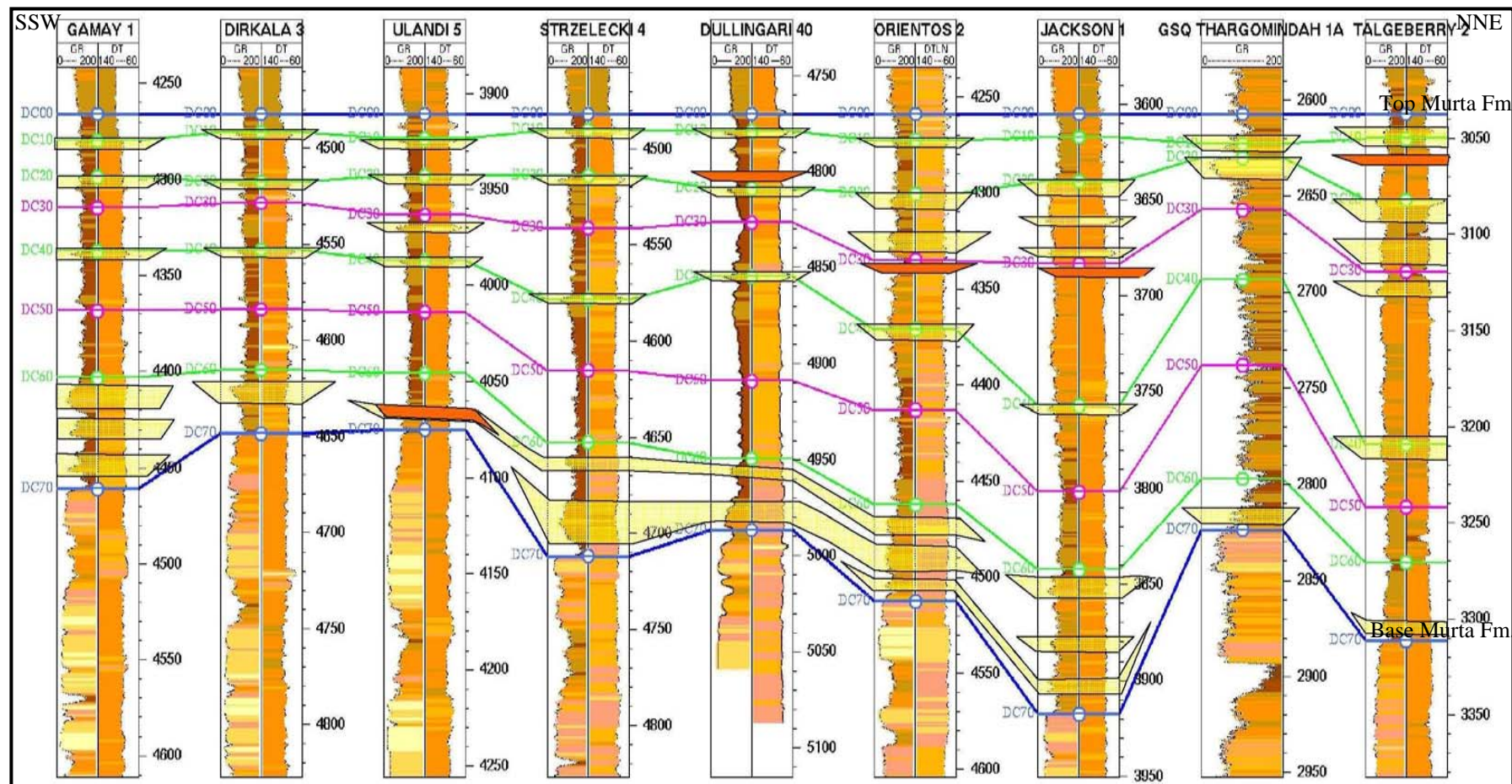


Figure 3.7: A regional cross section from the Harkaway Fault area in Queensland (N-NE) to Murteree Ridge in South Australia (S-SW). This regional cross section shows a general reduction in sand content from N-NE to S-SW in the upper section. The sand content of the McKinlay Member of the Murta Formation is concentrated in the S-SW. In the middle section, sand is coming from either direction. A map showing this line of cross section (A-A') is shown in Fig. 1.3. Red intervals represent the thin coarse sandstone channels.

### 3.4 Description of chronostratigraphic intervals

#### 3.4.1 Unit 7 (DC60-DC70)

##### **Core description**

The lithology description of this unit can be summarized as (St) and (Sp) of facies association 1, and Sr of facies association 4 (Table 2.3). Examples of these fining (St & Sp) and coarsening (Sr) upward cycles can be seen in cores from Strzelecki-4, Wilson-2, McKinlay-1 & 2, Ulandi-5, Moomba-18, Dirkala-3, Jena-11, Merrimelia-6, and Gidgealpa-19.

Strzelecki-4 type section shows two coarsening-upward cycles starting from two muddy intervals with a general fining-upward trend from the fluvial Namur Sandstone. The lower cycle gradually increases its grain size from fine-grained sandstone interbedded with mud to coarse grained sandstone. The upper cycle also gradually increases its grain size from the muddy interval to fine grained sandstone.

##### **Wireline log**

This unit comprises fining and coarsening-upward cycles in various wells. It shows an overall gradual increase in fine and medium grained sandstone from the underlying blocky, braided fluvial Namur Sandstone. However, a sharp and sudden change in lithology from blocky sand packages of the Namur Sandstone to the muddy intervals of the lower part of the McKinlay Member was also noticed in some wells in the South Australian part of the study area.

Unit 7 can be differentiated from the overlying muddy unit by the sudden decrease in the sand content toward the overlying Unit 6 of the Murta Formation, although Unit 7 is interbedded with thin muddy intervals especially in the south and southwestern part of the study area. However, wells in the north and northeastern part of the study area do not show much difference in lithology and log responses between Units 7 & 6 in general.

This is as a result of similar facies association within these units because of a steady sediment input in this portion of the basin. This makes it hard to pick and differentiate between the Murta Formation, the McKinlay Member, and the Namur Sandstone in that area. Commonly, an overall increase in fine grained sandstone from north-northeast toward south-southwest can be identified from the wireline logs (Fig.3.7).

The thickness of this unit varies from 9-24 m, while its thickness at its type section (Strzelecki-4 well) is 15 m (Fig. 3.7).

### **Sequence stratigraphy interpretation**

Unit 7 represents an overall fining-upward, transgressive succession from the fluvial Namur Sandstone associated with flooding of Lake Murta. This unit is a 3<sup>rd</sup> order Transgressive System Tract (TST) with a minor 4<sup>th</sup> order Maximum Flooding Surface (mMFS) between the 4<sup>th</sup> order Transgressive Surface (TS) and the 4<sup>th</sup> order Highstand System Tract (HST) with fine sand packages (Fig. 3.6). The depositional environment of this unit was interpreted to be mainly distributary channels. Though, some wells especially in the South Australian part of the study area showed stacked mouth bars with coarsening-upward sequences beside the distributary channel interpretation. As a result, this unit was interpreted as prograding fluvio-deltaic sequence into lacustrine basin. This unit describes the depositional environment of the McKinlay Member of the Murta Formation before flooding the lake and depositing of Unit 6 (Fig.3.7).

### **Isopach mapping**

Two sand inputs were noted from this Unit 7. The main one was from the northeast, while the secondary one was from the southwest during the deposition of the McKinlay Member of the Murta Formation. The “typical” McKinlay Member is noticed only in South Australia with Strzelecki-4 as a type section. However, a sandier McKinlay Member represents a 4<sup>th</sup> order TST in the north-northeastern direction within Lake Murta. This unit shows also that the deepest part of the lake was located in the southwestern part of the study area (Murteree Ridge and Tenappera Trough) where the first flooding started. This deepening was due to a combination of subsidence and lake level rise. Sediment input maintained shallower water depths at the northeastern end of Lake Murta (Fig. 3.8).



### **Schematic palaeogeographic mapping**

A schematic palaeogeographic map for this regional study of the Murta Formation was established based on core description, facies associations, wireline logs, sequence stratigraphy, and isopach mapping.

The above data shows the basin axis is running from north-northeast towards southwest, while the palaeo-depocentre was located towards the north-northeast (Fig. 3.8). The direction of sandy lithologies from wireline log motifs and isopach mapping validates these palaeo-dipping and palaeo-basin directions (Fig. 3.7 & 3.8). It is suggested that this lacustrine basin has many secondary sand inputs in addition to the main one coming from north-northeastern and northwestern direction of the study area. Shoreline sands from longshore drift were deposited along the lake margins by the prevailing northwesterly wind. The main shoreline sands were concentrated at right angles to the main sediment input in the north-northeastern direction (Fig. 3.9-A & B).

An early progradation of fluvio-deltaic into a relatively shallow lacustrine basin can be accommodated here as a depositional environment (Fig. 3.9-A & B). The main sand input interpreted from this unit was from a north-northeastern direction, while the secondary sand input from a southwestern direction in the South Australian part of the study area.

Two schematic palaeogeographic maps were generated for this unit to represent the transgressive setting as the deep lake increases its areal extent (Fig. 3.9-A & B). Gradually, Lake Murta increased its deep basin area until it reached the 3<sup>rd</sup> order Maximum Flooding Surface (MFS) during the deposition of the overlying unit 6.

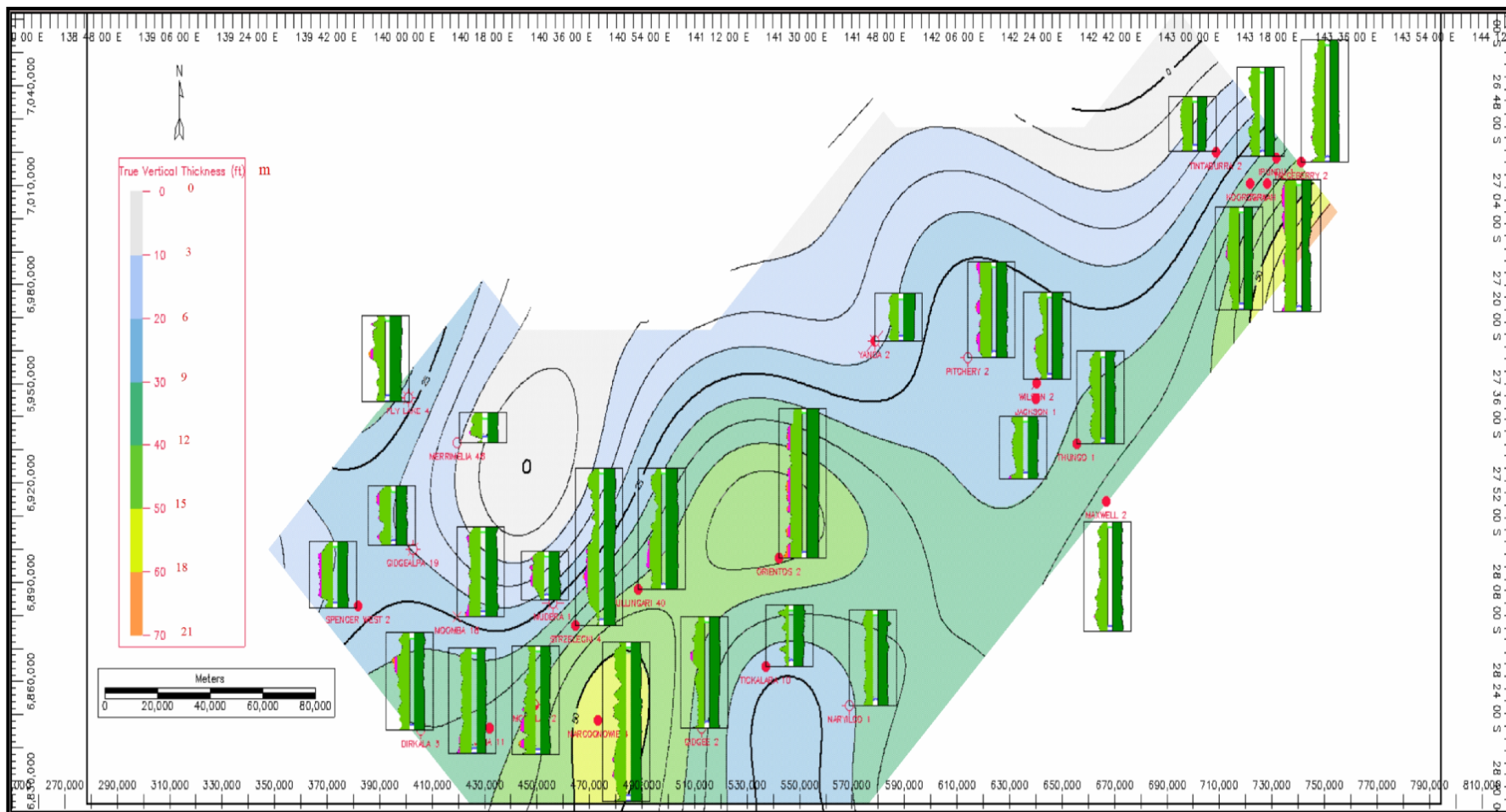


Figure 3.8: Isopach map overprint of Unit-7 with log profiles that show the thickest sediments deposited in the southwest direction of the study area. These basemaps were supplied by Santos Ltd. A better wells names resolution can be seen in Fig. 1.3.

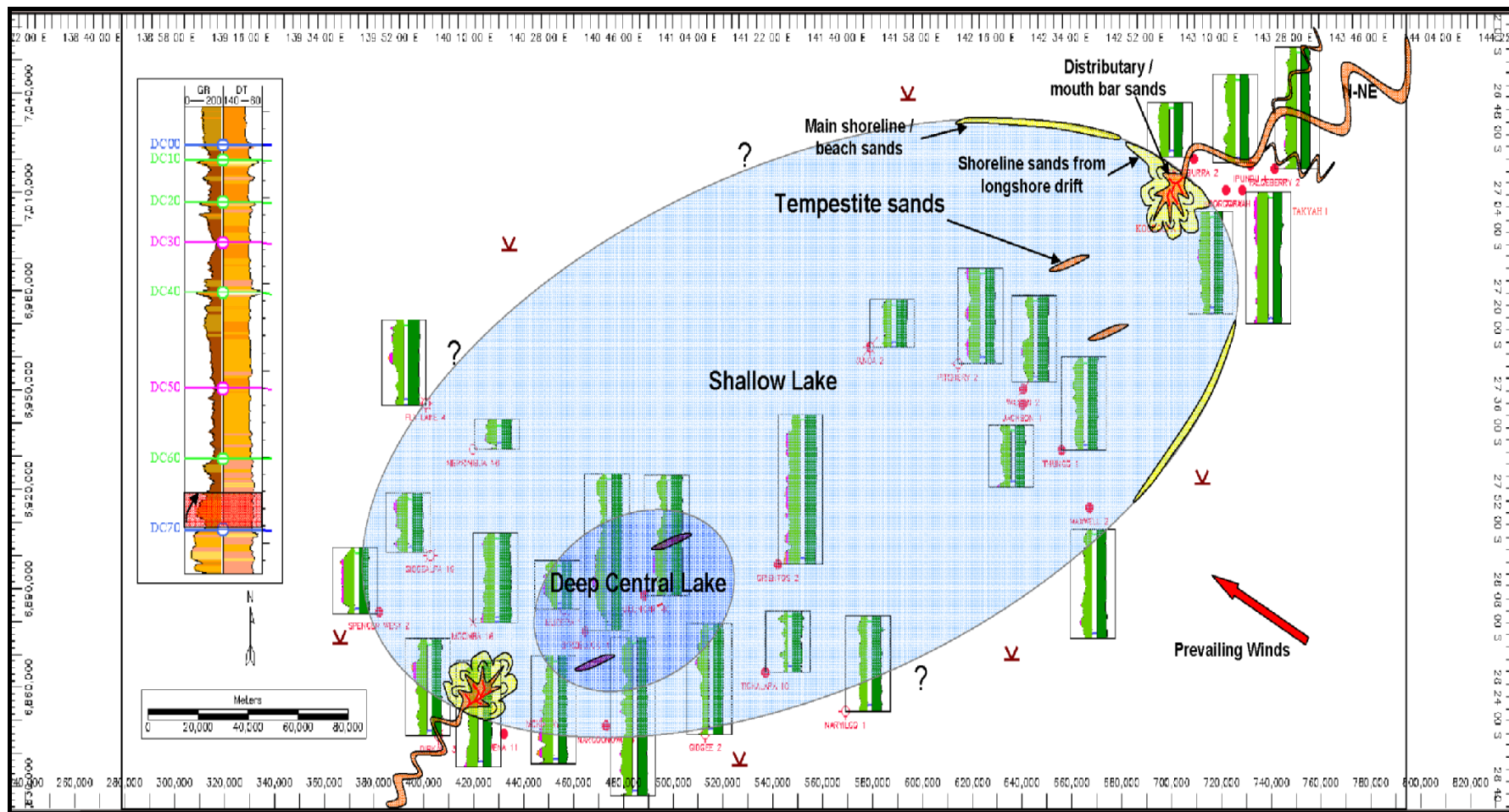


Figure 3.9-A: Schematic palaeogeographic map of Unit-7 representing the deposition of the McKinlay Member of the Murta Formation associated with the first transgression in Lake Murta. Dullingari-40 well wireline log signature is shown at the left side as an example for the Murta Formation. The question marks represent the uncertainty in the borders of Lake Murta. Red box interval shown represents depth (4972-4992’).



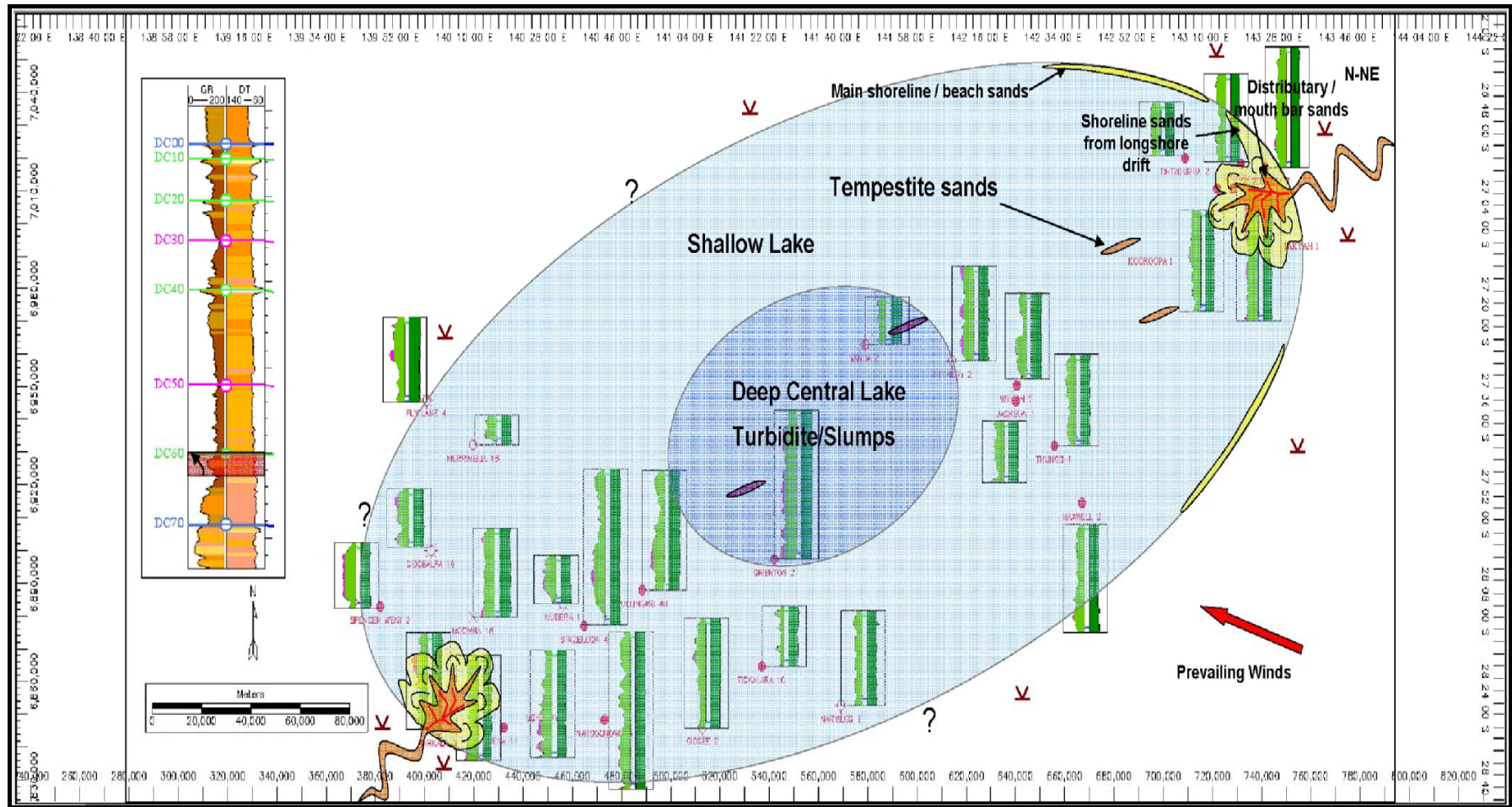


Figure 3.9-B: Schematic palaeogeographic map of the upper McKinlay Member of the Murta Formation before the Maximum Flooding Surface (DC50).

### 3.4.2 Unit 6 (DC50-DC60)

#### **Core description**

Lithological characteristics of this unit are prominent in facies association 6 (Table 2.3). Facies association 6 is best described as linsen-laminated mudstone with minor siltstone and sandstone lithologies.

#### **Wireline log**

The consistent log signature of this unit makes it easy to be identified from the wireline log and core description. The base of this unit marks a relatively sharp contact with the underlying sandstone of Unit 7 with an overall decrease in sand content and increase in mud-dominated lithologies. This sharp contact was recorded as a high gamma ray log response. However, the contact with the overlying unit 5 is transitional. The boundary between this unit and Unit 5 is characterized by a gradual upward increase in sand content. It is suggested that a localized incised valley fill made its way down the basin and cut the upper part of this unit. This was noticed from the log response of wells located in the northern part of the study area (for example Pitchery-2), although there was no core coverage from that interval.

The top of this unit can be mapped regionally with confidence to mark the first Maximum Flooding Surface (MFS) in the Murta Formation. However, recognition of this (MFS) becomes difficult towards the north and northeast (main sand input) from the Murta Formation type section (Dullingari-9, defined by Ambrose *et al*, 1986). In spite of the mud-dominated lithologies of this unit, occasionally it shows alternating muddy intervals with very fine to fine grained sandstone and siltstone in many wells especially close to the secondary sand input in the southwestern part of the study area (Murteree Ridge).

The maximum thickness of this unit was between 15 and 18 m, and was recorded in the Challum-1 and Yanda-2 area. The average thickness recorded in South Australian part of the study area was 9-12 m (Fig.3.10).

### **Sequence stratigraphy interpretation**

This unit represents a continuation of the regional transgression that started from the underlying Unit 7 before flooding Lake Murta. The deposition of this unit is interpreted to be associated with a 3<sup>rd</sup> order Transgressive System Tract (TST). This unit shows a general fining upward trend compared to the coarser Unit 7 below. The top of this unit marks the first 3<sup>rd</sup> order Maximum Flooding Surface (MFS) in the Murta Formation (Fig.3.6). This unit deposited in offshore/deep lake environment and could be considered as a good source rock (Mount, 1982). However, organic matter within the Murta Formation in the Murteree Ridge area is only marginally mature and not considered to be the source of the oil (Theologou, 1995). Instead, oil is thought to have migrated from the Permian sediments probably from the northern side of the Murteree Ridge where seals are very thin or absent (Theologou, 1995).

### **Isopach mapping**

This unit covers a period of increased accommodation and areal extent of deep Lake Murta with an open lacustrine setting. The thickest section of this unit was noticed in Nappamerri Trough, western Tennaperra Trough, and Murteree Ridge (Fig. 3.10). On the other hand, a general thinning was recognized from Gidgealpa-Merrimelia-Innamincka (GMI) Ridge, Patchawarra Trough, Harkaway Fault area wells, eastern Tennaperra Trough, and southern part of Jackson-Naccowlah Trend. Difference in sediment thicknesses has led to subdivision of the basin into highs and lows (Fig. 3.10).

### **Schematic palaeogeographic mapping**

During the sedimentation of this unit, sand input ceased into the Lake Murta included in this study and most of the lithologies were mud-dominated. However, sand input was identified from the north-northeastern direction. The large areal extent of deep Lake Murta from this unit indicates a lack of tectonism between the deposition of this unit and the underlying Unit 7 (Fig. 3.11) (Zoellner, 1988). However, this could happen as a result of not only increase in water volume, but also from subsidence to give more accommodation.

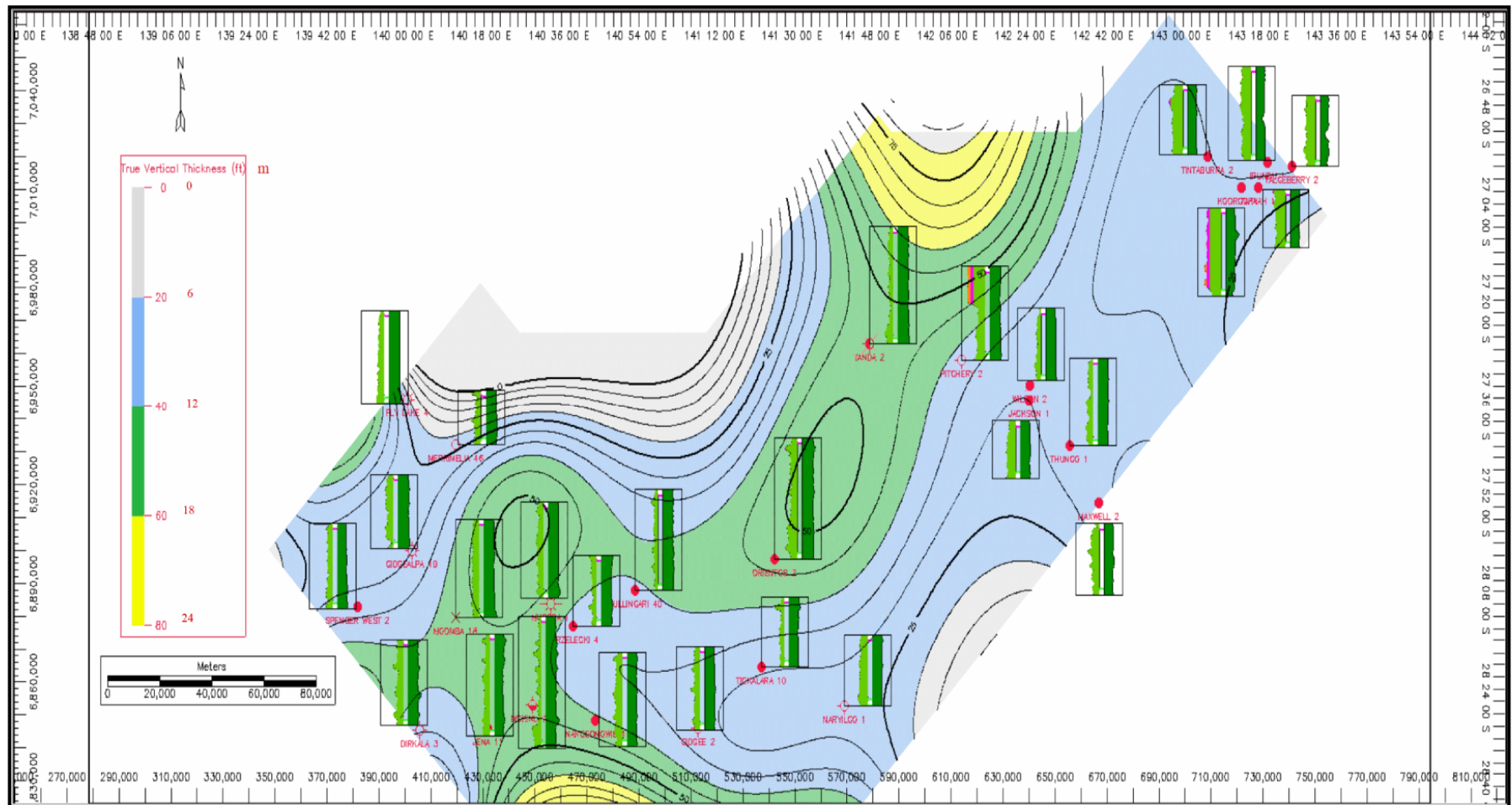


Figure 3.10: Isopach map of Unit-6 to represent a high degree of accommodation or high rise in lake level. Deepest parts of the lake are concentrated in the central and southwest part of the study area.



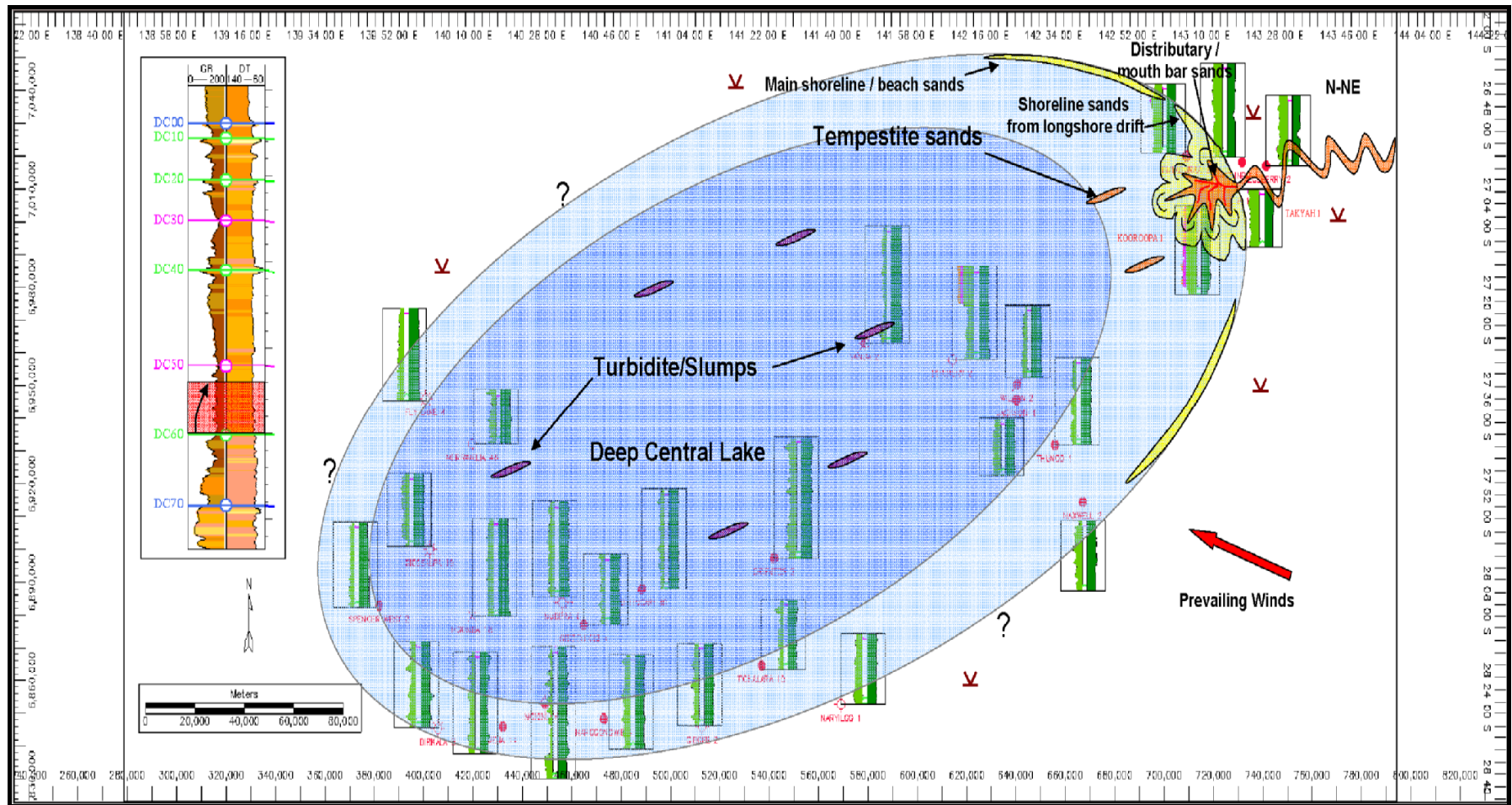


Figure 3.11: Schematic palaeogeographic map of Unit-6 during the first Maximum Flooding Surface (DC50) of Lake Murta. Note a very low sediment influx in this unit. Depth highlighted in red box is (4920-4950’).

### 3.4.3 Unit 5 (DC40-DC50)

#### **Core description**

The overall coarsening-upward sandstone packages described from this unit (Fig. 3.6) fit in facies associations 2, 3, 4 & 5. The lower part of this unit is best described as facies association 6. Fluvial sand sheet and blocky sand reported from facies association 1 are considered in this unit (Table 2.3).

#### **Wireline log**

This unit shows high variations in its coarsening-upward log signatures with lateral variation in thickness and sand content across the study area. However, it generally has a sharp base with the underlying Unit 6 (Fig.3.7). Facies associations from logs of this unit can be classified into 6 facies associations similar to the ones defined earlier. The below facies associations are similar to the facies association of M4 unit reported by Zoellner (1988).

- 1- Facies associations 2 & 3 are similar to the type section coarsening-upward sequence. These facies associations show alternating sandstone and siltstone at the base and topped by well-defined sandstone packages. Examples of these facies associations are from Tenappera Trough wells (Dullingari-40, Strzelecki-4, and Gidgee-2).
- 2- The second facies associations present in this unit are facies associations 4 & 5. They are similar to the above ones, but with less sand content and less obvious coarsening-upward trends. In these facies associations, the sandstone at the top is thinner compared to the one in the type section (Dullingari and Strzelecki wells). Examples of these facies associations are from Murteree Ridge wells (McKinlay-1, Ulandi-5, Dirkala-3, and Jena-11) and Maxwell-2 well.
- 3- Facies association 6 can be seen clearly in this unit from logs. It is very similar to the underlying Unit 6 and overlying Unit 4 with mainly muddy intervals with little thin sandstone beds. Examples can be seen in Big Lake-57, Spencer West-2, and McKinlay-2.

- 4- Facies association 1 shows a blocky signature and occasionally cuts the underlying Unit 6 (Fig.3.13-B). Other blocky units also may be added to this type which is characterized by mainly sandy facies close to the main sand supply in the north and northeastern direction of the study area. Examples of these blocky facies can be seen in Moomba-18, Merrimelia-6, Three Queens-1, Namur-2 in South Australia, and wells from the Harkaway Fault area (Talgeberry-2, Koorroopa-1, Tintaburra-2, Ipundu-1, and Takyah-1) in Queensland. Additionally, very thin sandstone (10 cm) beds of facies association 1 are present at the base of this unit. These thin sandstone beds show an abrupt base with a fining-upward profile. It is interpreted to be thin channels. Example of these channels is from Merrimelia-6 well.

The lateral facies variations of this unit have a regional significance. Sandy facies occur close to the sand input in north-northeast with muddy/shaly facies in the southwest of the study area (Appendices 3.2, 3.3, 3.4, 3.5 & 3.6). The channels in the north-northeast are replaced by the coarsening- upward sequence sandstone packages in the central part of the study area, which in turn, are replaced by the muddy/shaly facies in the southwest part of the study area. The muddy/shaly facies increase distally from the channels toward the deepest part of the basin. The incised valley fill noticed in the lower part of this unit indicates the maximum progradation of the Murta delta (Fig.3.13-B) (Theologou, 1995).

The thickness of this unit is 9-18 m, while its thickness at the type section is 16 m (Fig.3.6).

### **Sequence stratigraphy interpretation**

This unit marks the beginning of a progradational stacking pattern with a relative drop in lake level toward its top representing a Sequence Boundary (S.B) (Fig.3.6). It could also be that the lower muddy part of this unit may represent a retrogradational stacking pattern. Sandstone packages deposited in this unit are interpreted to belong to the 3<sup>rd</sup> order Highstand System Tract (HST) after earlier flooding of Lake Murta. These coarsening-upward sand packages could be interpreted as delta mouth bars.

The base of this unit and the top of the underlying Unit 6 represent the first 3<sup>rd</sup> order Maximum Flooding Surface (MFS) in the Murta Formation. However, an incised valley fill was identified in Pitchey-2 well log marking a sequence boundary cutting from the middle of this unit all the way down to the top of the underlying Unit 6 (Fig.3.13-B).

### **Isopach mapping**

This unit shows a general shallowing of Lake Murta primarily in the north-northeast direction of the study area with high sediment influx (Fig. 3.12).

### **Schematic palaeogeographic mapping**

A very shallow lake setting was dominant in this unit and more prograding delta mouth bar sands over the underlying muddy unit entered the lake mainly from the main sand input in the north-northeast (Fig. 3.13-A & B). Deposition of this unit was as a series of broad, lobate delta mouth bars, vertically stacked and overlapping each other, and intercalated with dark lacustrine silt and mud that have much greater lateral continuity (Mount, 1981). These delta mouth bars may be constructed over very large areas on very gentle slopes (Mount, 1981).

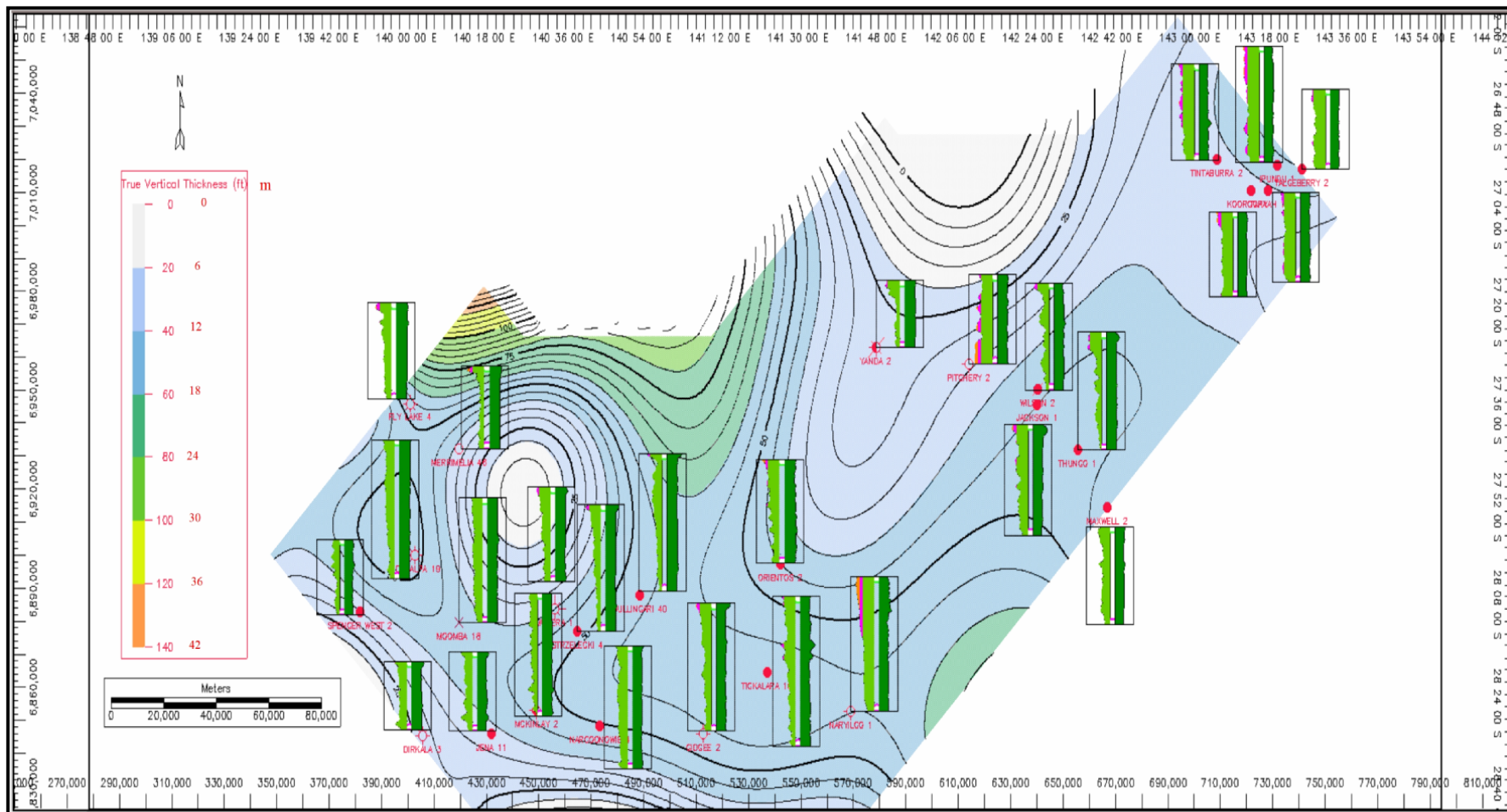


Figure 3.12: Isopach map overprint with log profiles that show a shallowing lake character of Unit-5.



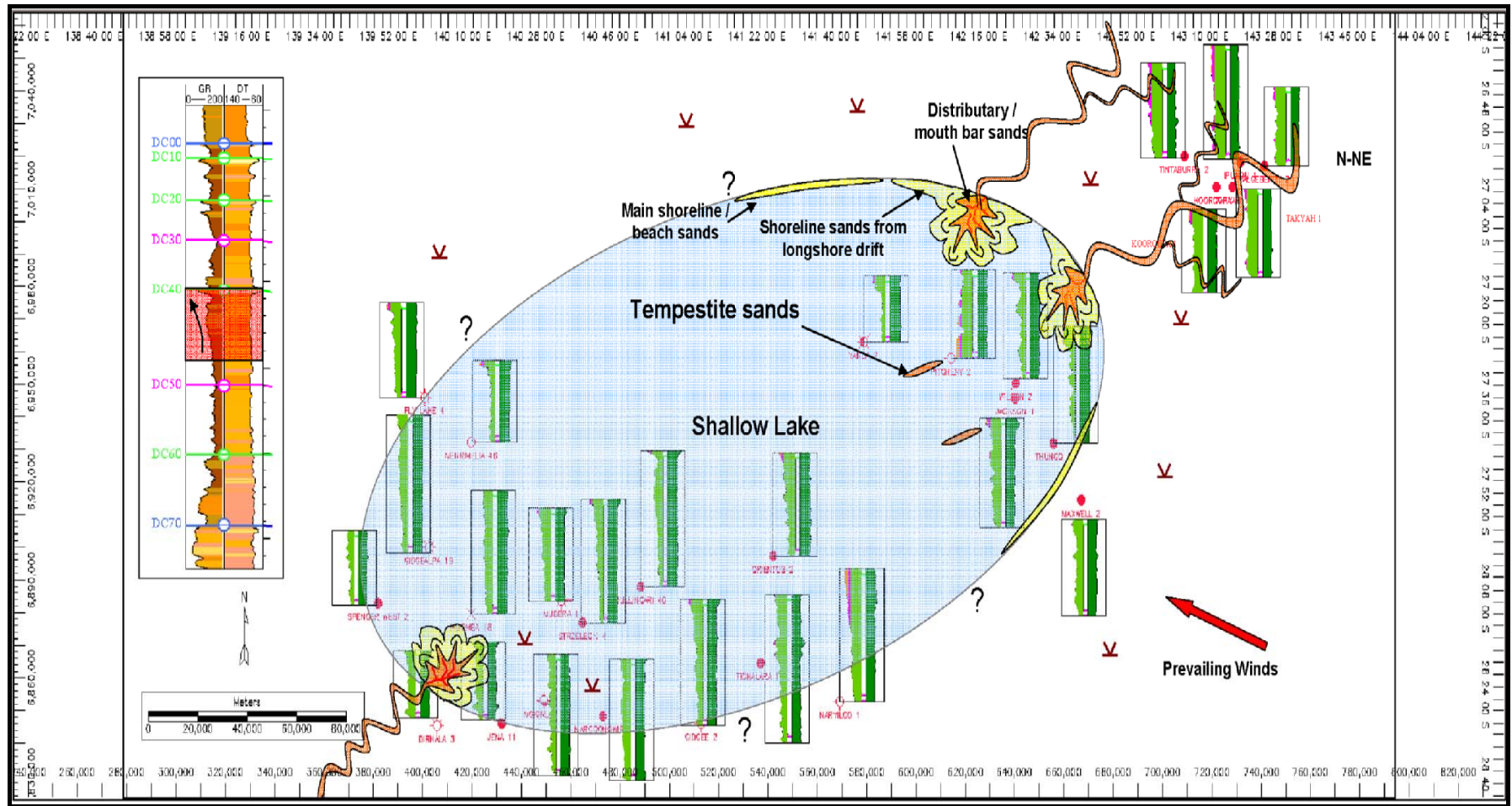


Figure 3.13-A: Schematic palaeogeographic map of Unit-5 to illustrate the shallowing in Lake Murta with high sediment input mainly from north-northeast direction of the study area. The map shows the possible depositional environments associated with the shallowing of Lake Murta. Depth highlighted in red box is (4855-4895')

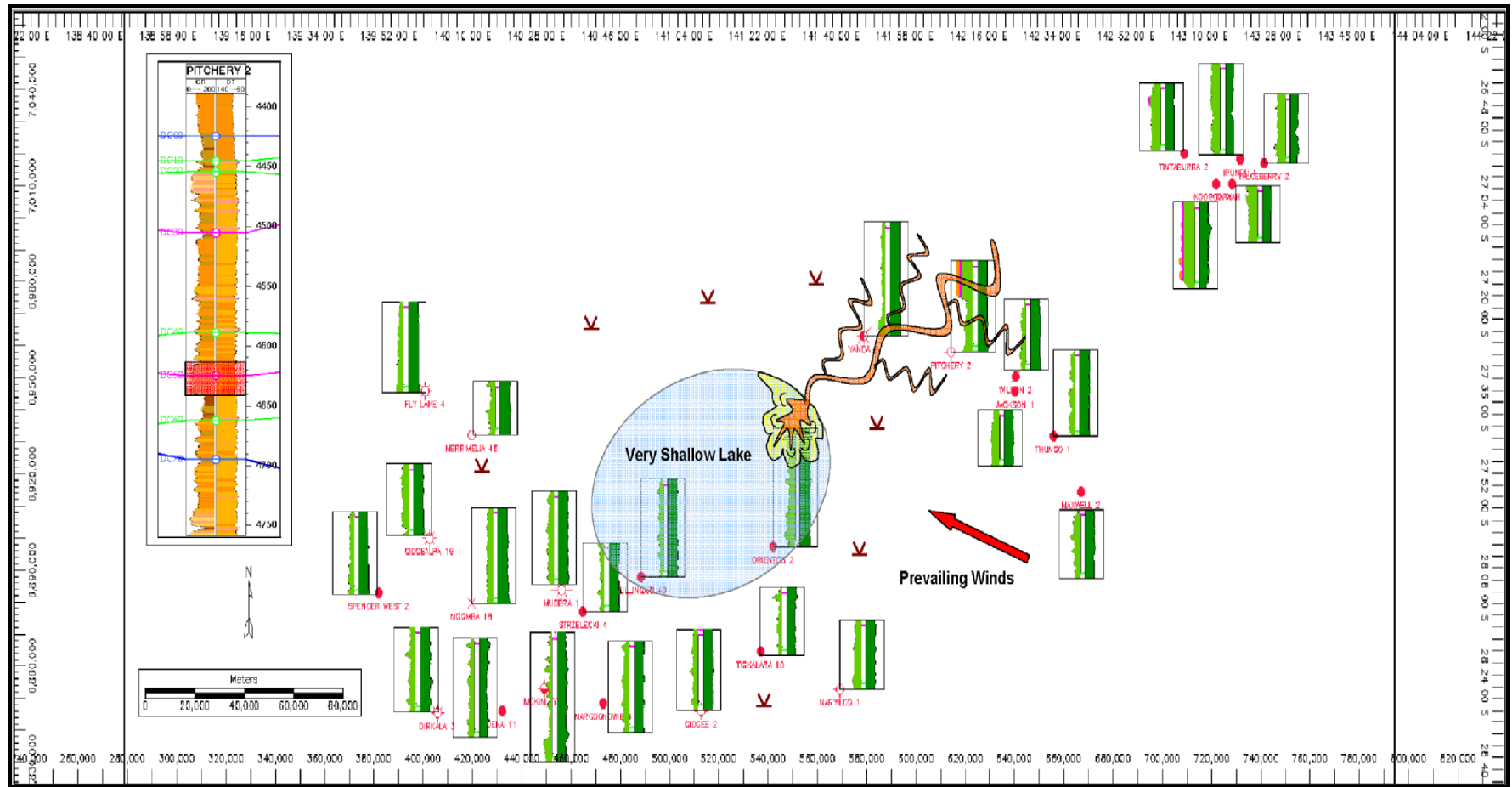


Figure 3.13-B: Schematic palaeogeographic map of the localized incised valley fill cutting the lower part of Unit-4 all the way down to the upper part of Unit-5. At that time, Lake Murta was very shallow or almost no lake existed. Example from Pitchery-2 log at depth range 4613-4640’.



### 3.4.4 Unit 4 (DC30-DC40)

#### **Core description**

The best facies associations to describe this unit are facies associations 6 & 5 for southwest part of the study area and facies association 1 (St, Sp) for the north-northeast (Table 2.3).

#### **Wireline log**

The muddy and fining-upward profile of Unit 4 can be easily picked from most of the wireline logs (Fig.3.7). This unit is very similar to Unit 6 (DC50-60); both of them are easy to recognize from logs as a high gamma ray reading and from cores as muddy-dominated lithologies. However, it is hard to pick close to the sand source in the north and northeast where the boundary lies within the sandy lithologies (Appendices 3.2, 3.3, 3.4 & 3.5). The top of this unit is characterized by high gamma ray readings and can be mapped regionally with confidence to mark the second (MFS) in the Murta Formation (Fig. 3.6).

The base of this unit marks a relatively sharp contact with the underlying sandstone of Unit 5 with an overall decrease in sand content and increase in mud-dominated lithologies. However, the contact with the overlying unit 3 is transitional. The boundary between this unit and Unit 3 is characterized by a gradual upward increase in sand content. In spite of the mud-dominated lithologies of this unit, occasionally it shows alternating muddy intervals with very fine to fine-grained sandstone and siltstone in many wells especially close to the secondary sand input in the southwest part of the study area (Murteree Ridge).

The wireline log cross sections (Appendices 3.2, 3.3, 3.4, 3.5 & 3.6) show that the sandy facies were concentrated in the northeast part of the study area, while the muddy facies were common in the southwest.

Harkaway Fault area wells and those along the Jackson-Naccowlah Trend show pure thick sandy lithologies of this unit, that make it difficult to identify the MFS at the top of this unit. Nevertheless, the lithology of this unit in the south and southwest part of the study area has a fairly high sand content compared to the type section in central area which is interpreted to be muddier.

Very thin sand sheets were delivered to the basin before flooding the lake. These coarse sand sheets were identified in cores particularly from Murteree Ridge wells.

The maximum thickness of this unit is about 24 m in eastern and Jackson-Naccowlah Trend wells (Fig.3.7). The average thickness in South Australian part of the study area is 6-10 m, close to the Murta Formation type section (Dullingari-9 defined by Ambrose *et al*, 1986).

### **Sequence stratigraphy interpretation**

This unit indicates a fining-upward trend toward its top before flooding the lake. This 3<sup>rd</sup> order Maximum Flooding Surface is the second 3<sup>rd</sup> order MFS in the Murta Formation/Lake. This unit can be interpreted to be deposited during a 3<sup>rd</sup> order Transgressive System Tract (TST). Infrequent very thin fluvial sandy sheets were deposited within this unit could be interpreted as a 3<sup>rd</sup> order Lowstand System Tract (LST) (Fig. 3.6).

Overall, the deposition of this unit indicates dominantly deep lacustrine conditions with very little sediment supply.

### **Isopach mapping**

This unit marks the return to deep lake conditions after flooding the lake. Deep lake sediments covered most parts of the lake particularly in the southwest direction (Fig. 3.14).

**Schematic palaeogeographic mapping**

The deepening of the lake was in response to basin subsidence or rise of lake level. The flooding of Lake Murta started as a gradual event before the Maximum Flooding Surface commenced. This unit characterizes a period of very little sediment influx (Fig. 3.15-A & B).

This unit and the overlying units are interpreted to be deposited during a tectonically quiet period during which the depositional centres remained stable. These conditions prevailed until deposition of the Cadna-owie Formation (Zoellner, 1988).

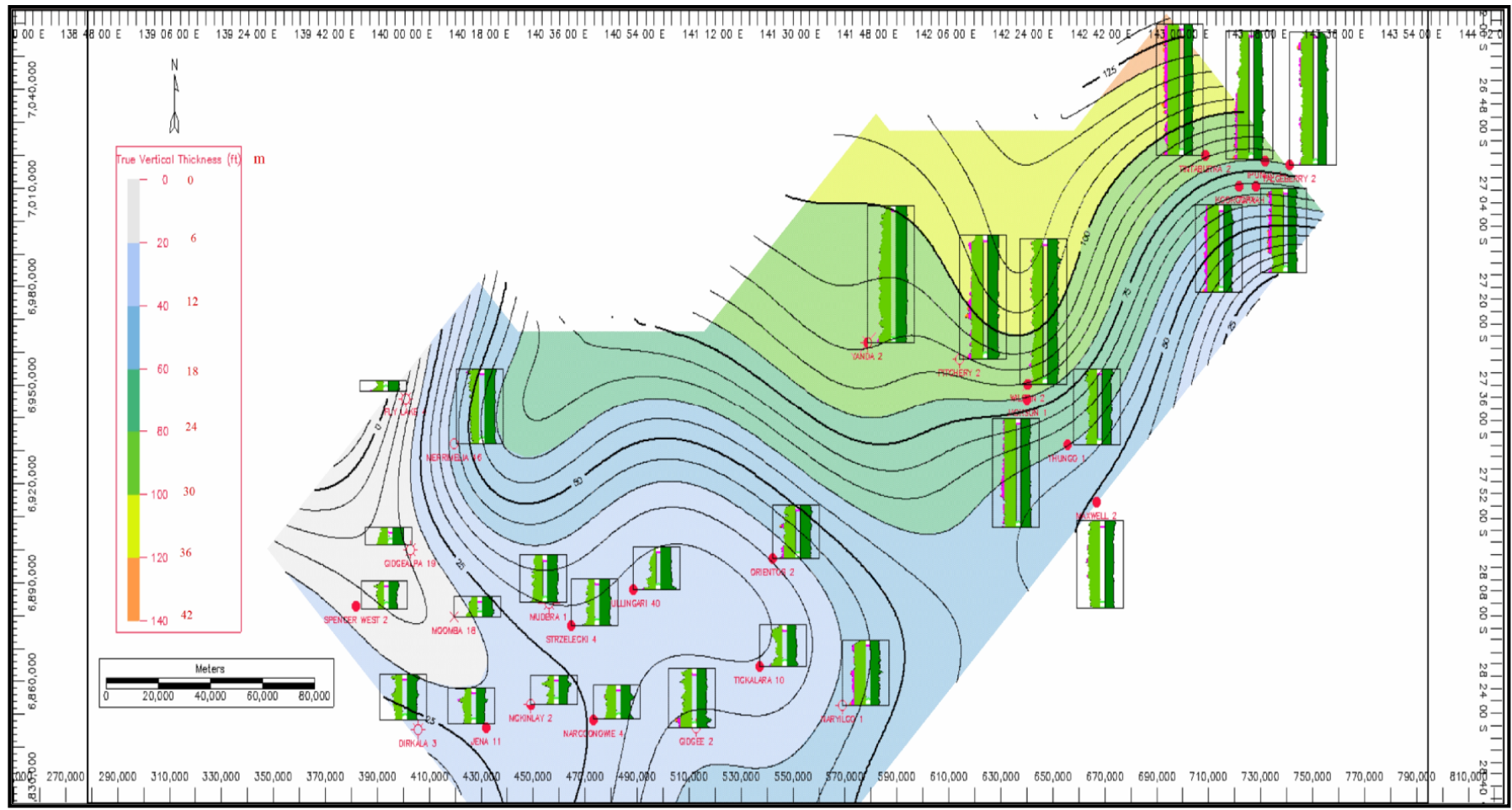


Figure 3.14: Lake Murta Isopach map shows a return to a deep lake conditions after flooding the lake to mark the second 3<sup>rd</sup> order Maximum Flooding Surface MFS in Lake Murta.

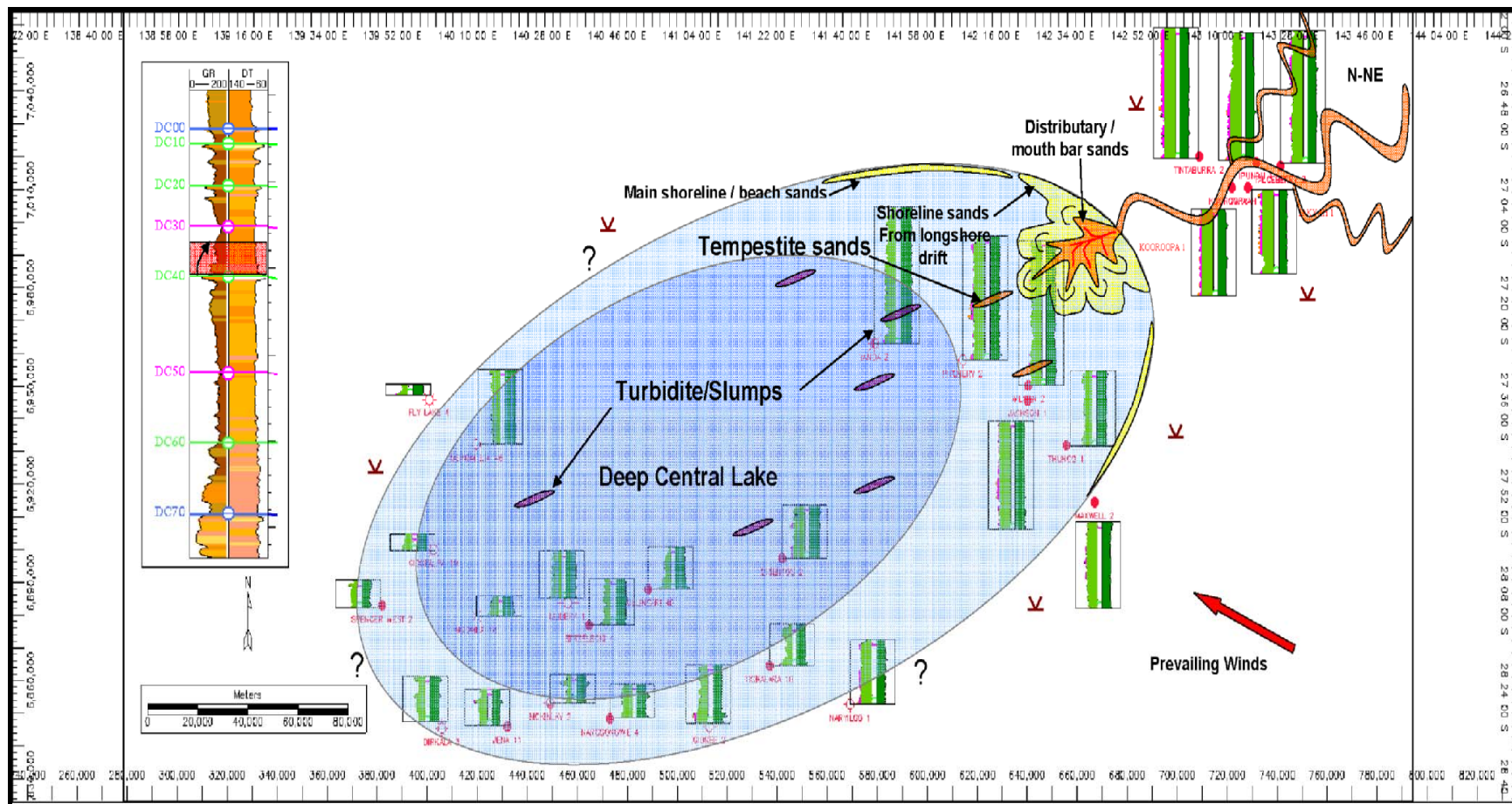


Figure 3.15-A: Schematic palaeogeographic map of the lower part of Unit-4 directly before flooding of the lake. This unit characterized by its muddy lithologies to mark the deep lake setting during the flooding stage. Depth highlighted in red box is (4838-4955’).



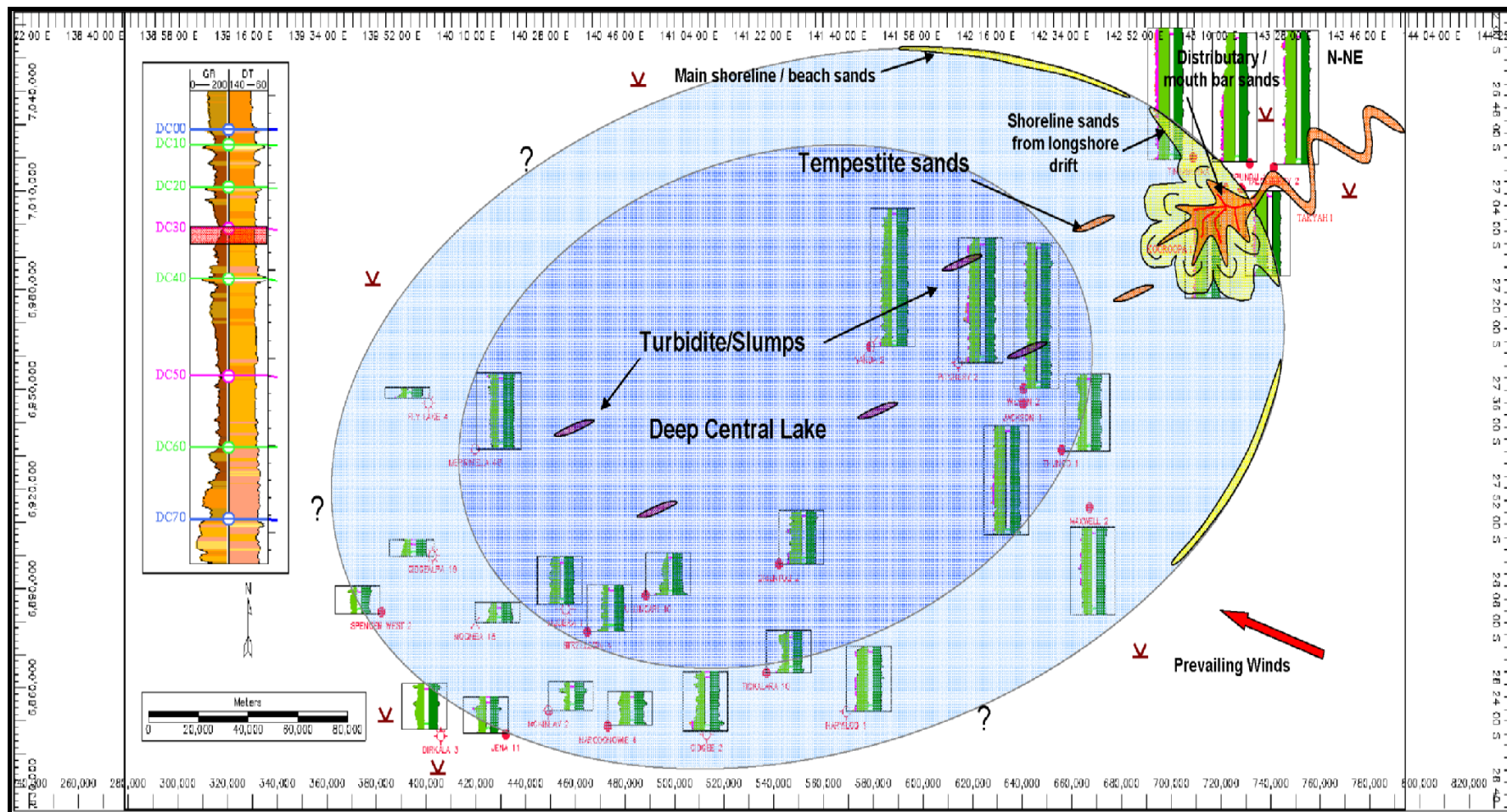


Figure 3.15-B: Schematic palaeogeographic map of the upper part of Unit-4 defining the second 3<sup>rd</sup> order Maximum Flooding Surface MFS in Lake Murta. Depth highlighted in red box is (4827-4838’).



#### 4.4.5 Unit 3 (DC20-DC30)

##### **Core description**

Facies association 2 and facies association 4 are best represent the lithologies of this unit apart from the fluvial sandy sheets of facies association 1. Facies associations 5 & 6 represent the muddier part of this unit (Table 2.3). Sand packages of this unit deposited closer to the main sand inputs in the north-northeast were interpreted to be of fluvio-deltaic environment. On the other hand, the muddier facies deposited away from the main sand inputs was interpreted to be from lower shoreface-offshore environments.

##### **Wireline log**

This unit is similar to Unit 5 in a way that both of their sandstone packages show a coarsening-upward profile. However, the top of this unit is thinner and the sand is coarser. In its type section in Dullingari-9, this unit shows a coarsening-upward trend which extends over of the entire study area. Therefore, it can be mapped regionally with confidence. This unit can be correlated over a large area indicating a fluvial sand sheets represented by high permeability streaks or tightly cemented zones of facies association 1 (Ambrose *et al*, 1986).

Many wells show that this ideal coarsening-upward cycle has been replaced by blocky then fining-upward sands with a sudden erosional base interpreted associated with fluvial channel deposits. This blocky and fining-upward log character was identified from many wells mainly from the north-northeast and southeast part of the study area (Appendices 3.2, 3.3, 3.4, 3.5 & 3.6). On the other hand, this unit becomes muddier with less sand in Murteree Ridge and Patchawarra Trough areas, close to the proposed deep lake basin in the southwest part of the study area.

This unit embraces many thin sands which were deposited as thin channels. Alternatively, these thin sands (10 cm) could have been deposited as mouth bars or restricted shorelines. It is proposed that the braided fluvial ‘Namur’ regime fed coarse detritus into the ‘Murta’ lake from the east (Ambrose *et al*, 1986). These sand sheets are dispersed everywhere in the section. However, they are noticed to be deposited mainly in Unit 3 and 2. The lateral continuity of these thin sands is limited.

The base of this unit shows a gradual and transitional contact with the underlying unit, while the contact with the overlying unit appears to be sharp with a rapid transgressive event (Fig. 3.6). The sonic log suggests that the lower portion of the sand has a good effective porosity, while the upper part is strongly cemented and generally tight (Ambrose *et al*, 1986). The sandstone packages located at the top of this unit and below the high sonic response are the main productive reservoir in Murta Formation (Mount, 1982).

The maximum thickness of this unit in eastern wells and Jackson-Naccowlah Trend wells of about 21 m, while it is just 9-12 m in the type section and nearby wells (Fig.3.7).

### **Sequence stratigraphy interpretation**

This unit shows an overall coarsening-upward cycle reflecting the progradational stacking pattern and a 3<sup>rd</sup> order Highstand System Tract (HST) after the second flooding of Lake Murta (Fig.3.6).

This progradational stacking pattern was associated with a relative drop in lake level toward the top of this unit. However, the lower muddy part of this unit may represent a retrogradational stacking pattern.

The top of this unit could represent either a rapid 4<sup>th</sup> order Transgressive Surface (TS) or a minor 4<sup>th</sup> order Maximum Flooding Surface (mMFS) after deposition of the regressive facies (Fig.3.6). In addition, thin channels in this unit could be interpreted as a localized 4<sup>th</sup> order Lowstand System Tract (LST). Nonetheless, they could be interpreted as transgressive sheet sandstone associated with the erosion of the underlying shoreface deposits. The base of this unit and the top of the underlying unit 4 represent the second 3<sup>rd</sup> order Maximum Flooding Surface (MFS) in the Murta Formation (Fig.3.6).

Sandstone packages deposited in this unit are interpreted to belong to a 3<sup>rd</sup> order Highstand System Tract (HST) after earlier flooding of Lake Murta. These packages are interpreted to be deposited either as distributary mouth bar or shoreline deposits.

The sandy part of this unit is deposited as fluvial sand sheets of a 4<sup>th</sup> order Lowstand System Tract (LST) with a spiky signature. It is suggested that this unit and the top of Unit 5 indicate general regressive cycles compared to the general transgression that occurred in Unit 7 to Unit 1 (Mount, 1981) (Fig. 3.16).

The thinning of this unit indicates a shallower lake and marks the maximum regression compared to unit 5 which shows moderately deep lake conditions. Figure 3.17 highlight the deposition of the coarse-grained fluvial reservoirs during falls and lowstands of lake level in overfilled lake basins.

Lake Murta during deposition of this unit is believed to be very shallow with very low-angle slopes and the wave energy was low (Mount, 1982). This description coincides with the broad, thin, linear geometry of the uppermost reservoir sand (Mount, 1982).

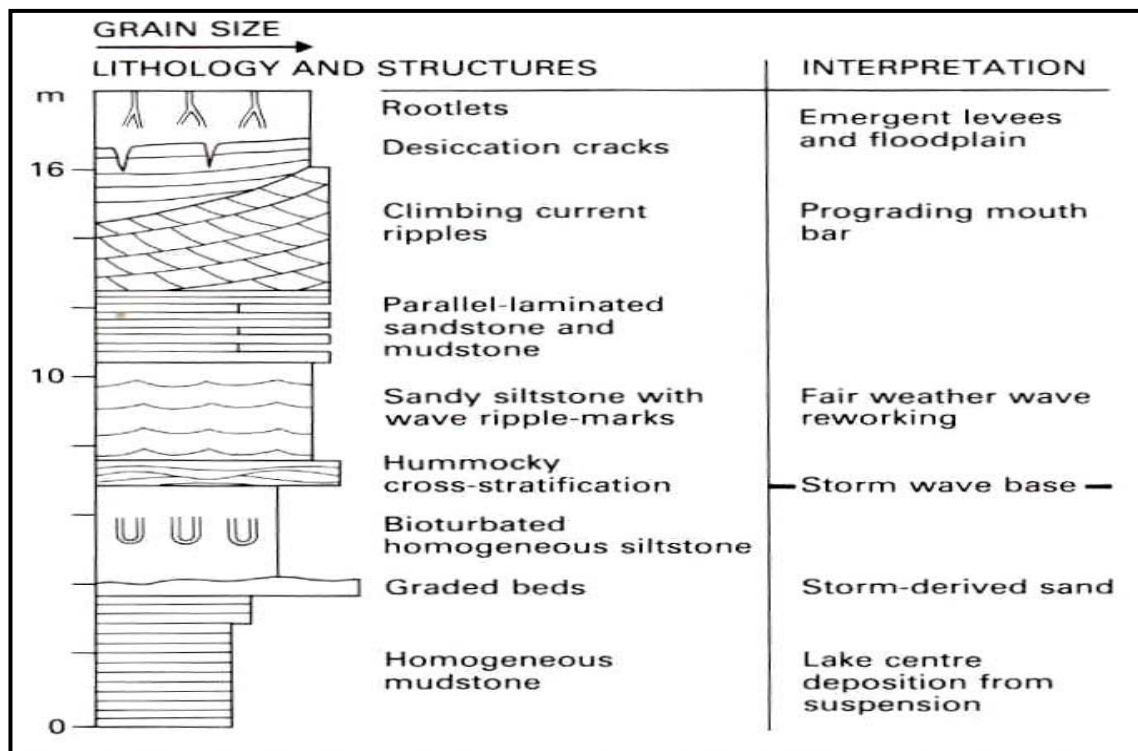


Figure 3.16: Idealized sequence produced by regression in siliciclastic-dominated, hydrologically open lake, eastern Karoo Basin. (after Van Dijk, Hobday and Tankard, 1978).

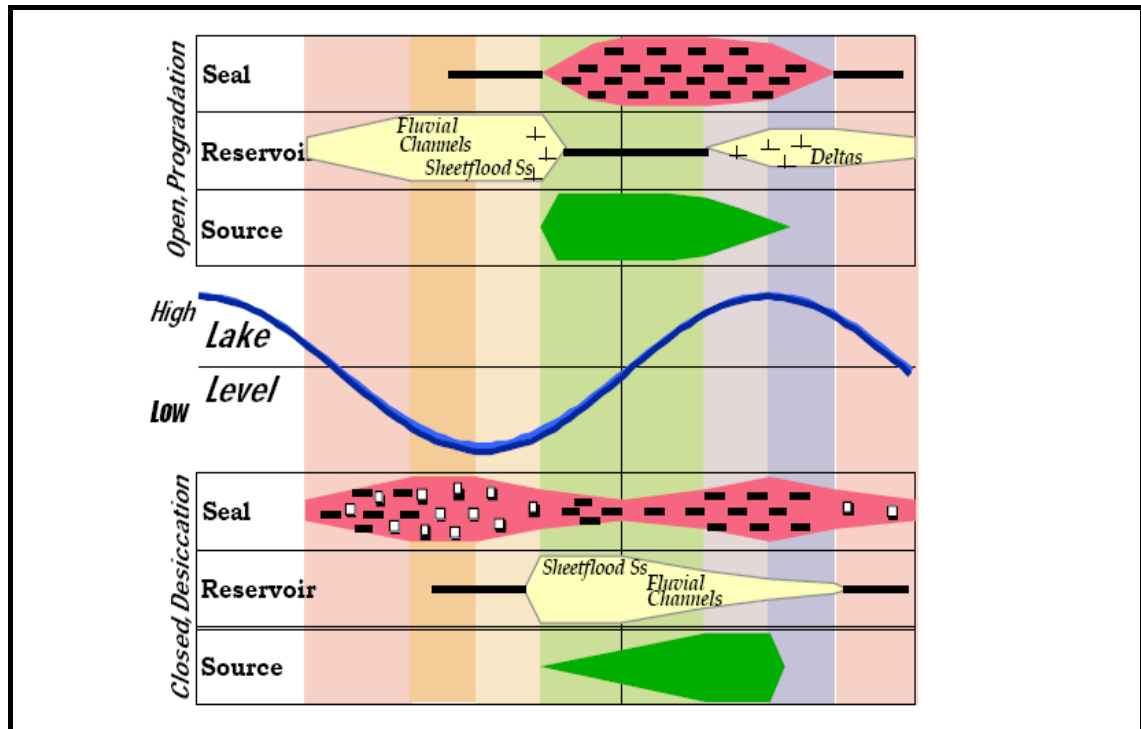


Figure 3.17: Contrast in timing of play-element deposition between end-member lake types. For example, overfilled lake basins are most likely to accumulate coarse-grained fluvial reservoirs during falls and lowstands of lake level (Bohacs *et al*, 2002).

### **Isopach mapping**

The isopach map of this unit shows a general thinning, particularly in the southwestern part of Lake Murta. Sediments of this unit entered the lake when very shallow or about to dry out. Thick sediments are represented in the north-northeast, close to the main sand input in Queensland. The isopach map shows a gradual decrease in thickness toward the southwest (Fig. 3.18).

### **Schematic palaeogeographic mapping**

A relative drop in lake level is interpreted to be the main cause of shallowing of Lake Murta. Deposition during this unit is interpreted to take place in a very shallow lake setting with very low-angle slopes and low wave energy (Mount, 1982). This description coincides with the broad, thin, linear geometry of the uppermost reservoir sand (Mount, 1982). The lake level in Lake Murta during deposition of this unit drastically dropped from moderately deep to very shallow and near exposure (Fig. 3.19-A & B).

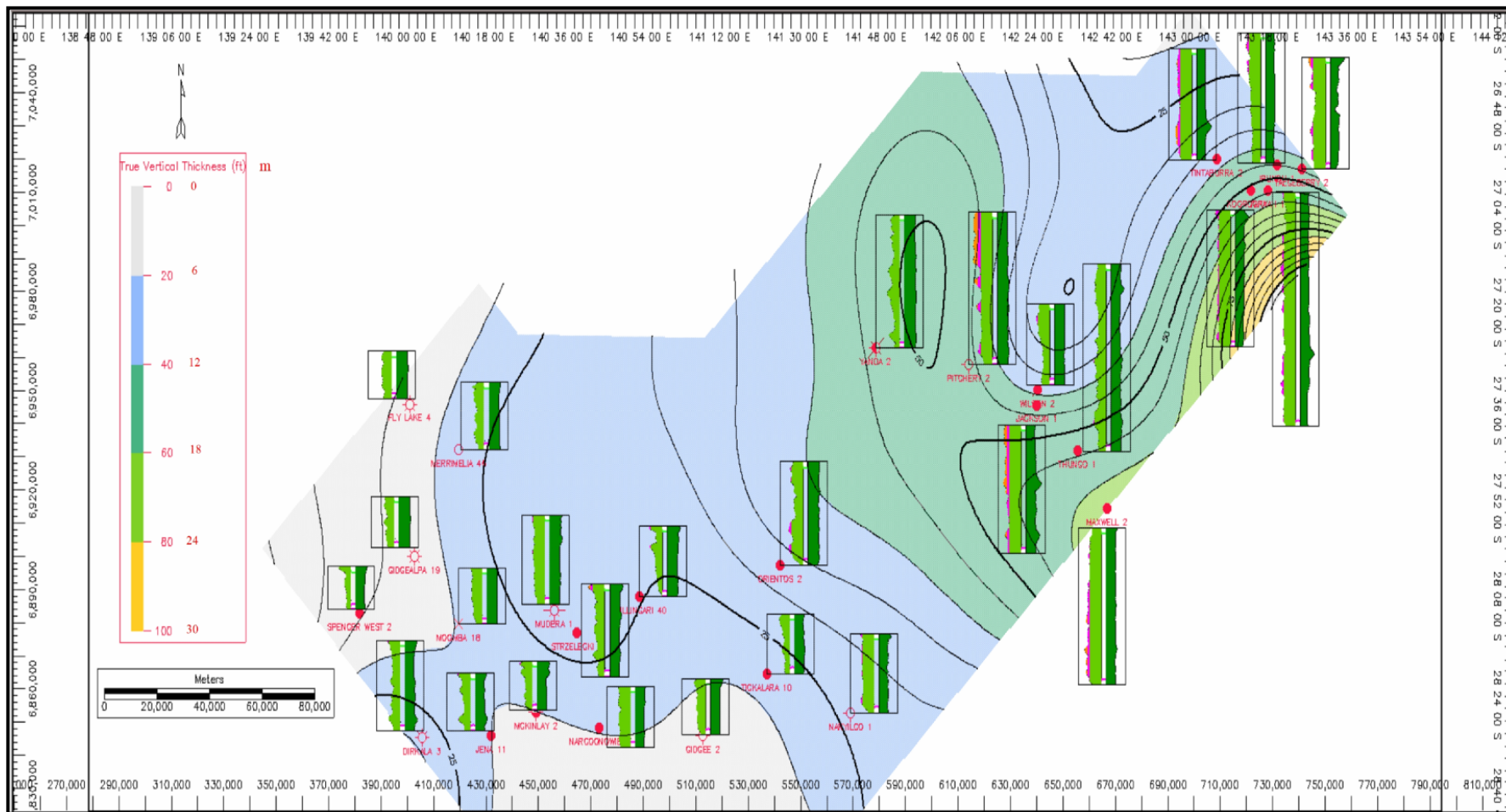


Figure 3.18: Isopach map of Unit-3 representing thick sediments located at the northeast of the study area, while the very thin sediments are in southwest with a general shallowing event.



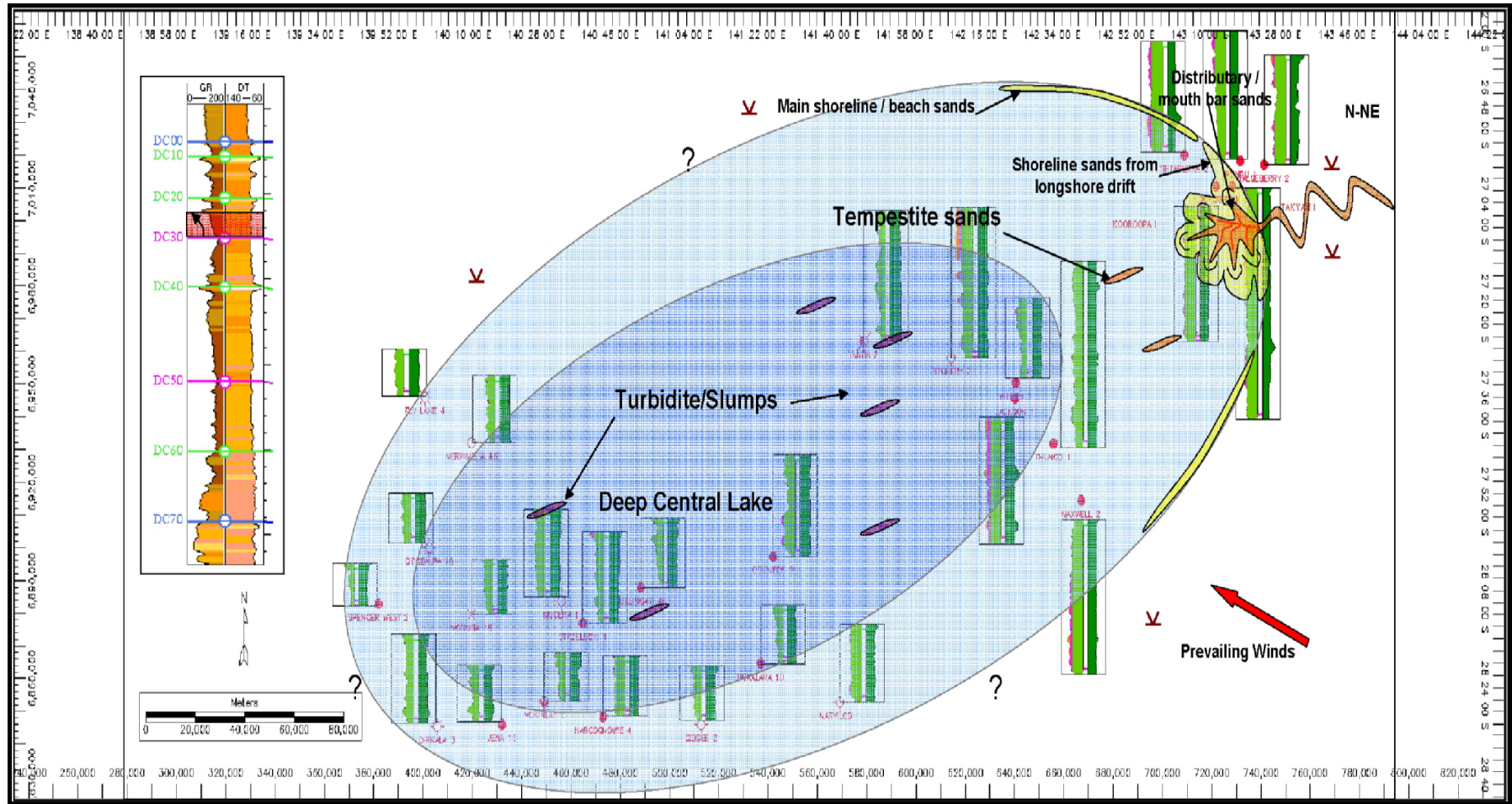


Figure 3.19-A: Schematic palaeogeographic map of the lower part of Unit-3 directly after the second 3<sup>rd</sup> order Maximum Flooding Surface (DC30) in Lake Murta. This sub-interval will be followed by a drop in lake base level. Depth highlighted in red box is (4810-4827’).



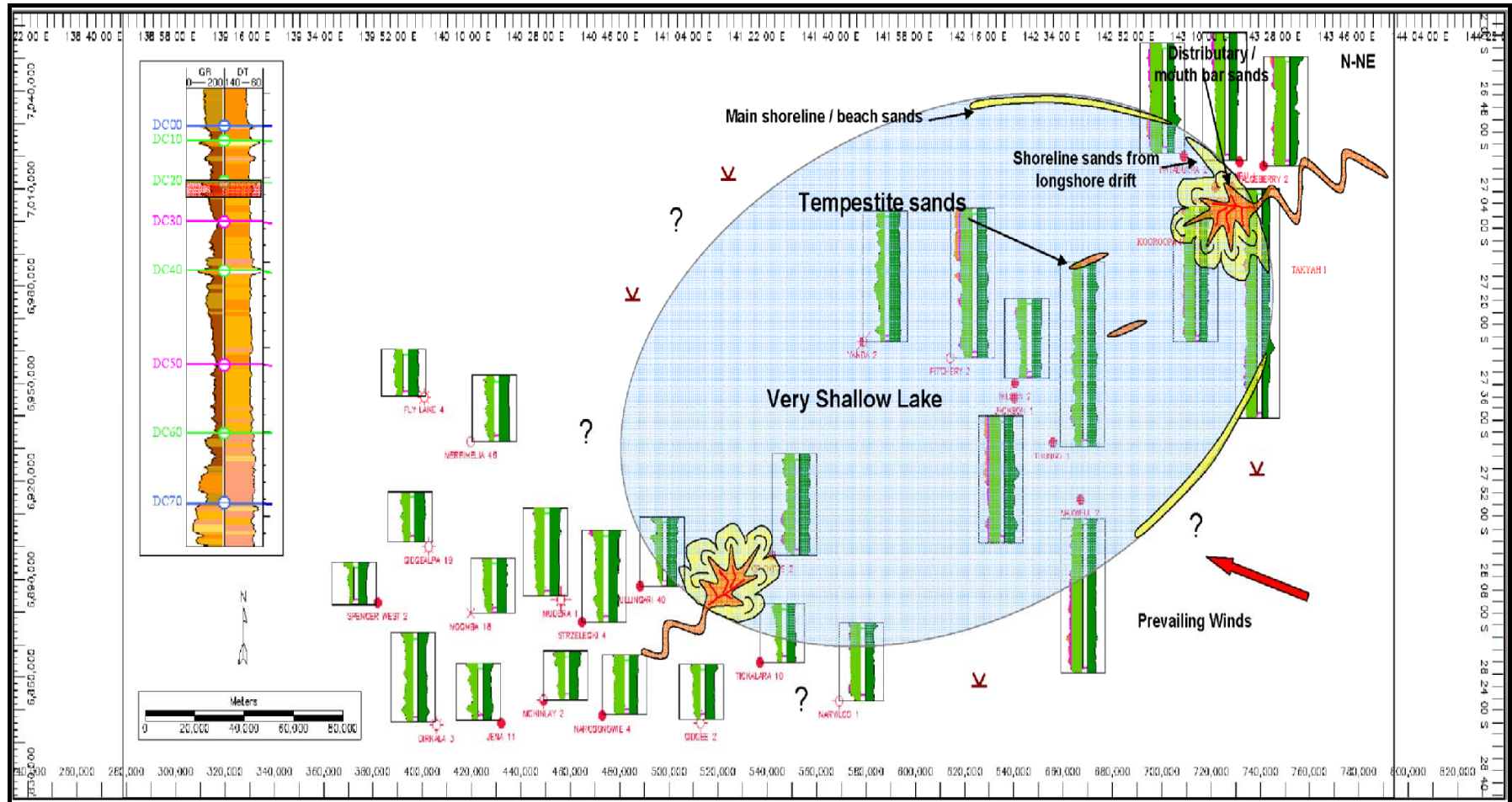


Figure 3.19-B: Schematic palaeogeographic map of the upper part of Unit-3 identifying the deposition of the sediments to take place in very shallow lake. Sediments were delivered by rivers to the lake basin when the lake about to dry out. Depth highlighted in red box is (4803-4810’).

### 3.4.6 Unit 2 (DC10-DC20)

#### **Core description**

A combination of facies associations 2 & 4 with the thin fluvial sand sheets of facies association 1 are common in the sandy part of this unit. Facies associations 5 & 6 represent the lithological and environmental interpretation of the muddy part of this unit (Table 2.3).

#### **Wireline log**

This unit and the underlying Unit 3 are very similar in their log character, particularly in the upper part. However, dissimilarities arise from the lower part of both of them at least in the type section. Unit 2 shows an abrupt contact with the underlying Unit 3, while the lower part of Unit 3 shows a relatively transitional contact with its underlying Unit 4. This lower part is muddier and represents a 4<sup>th</sup> order minor Maximum Flooding Surface (mMFS) or a 4<sup>th</sup> order Transgressive Surface (TS) before flooding of the lake. An overall coarsening upward trend is noticed from this unit. This unit covers the entire study area and can be mapped easily. It represents an abrupt decrease in the coarse sand compared to the underlying unit.

Similar to Unit 3, Unit 2 changes its nature both lithologically and in the wireline log signatures across the study area (Fig. 3.7). It has a blocky, then fining-upward profile close to the main sand input in the north-northeast and northwest of the study area. However, it has less sand and more mud in some wells in Jackson-Naccowlah Trend especially in the northern part of this trend (Challum-1, Yanda-2, Bogala-1, and Wilson-2). Although it is mainly a muddy facies, it has a spiky sand signature close to the type section in South Australia near the Murteree Ridge (Appendices 3.2, 3.3, 3.4, 3.5 & 3.6).

Minor very thin sandy intervals were identified within this unit in some wells, representing fluvial sand sheets. These intervals have sharp base and gradually they fine upward.

The average thickness of this unit recorded was 9-12 m.

### **Sequence stratigraphy interpretation**

This unit shows an overall coarsening-upward cycle to demonstrate the progradational stacking pattern and 3<sup>rd</sup> order Highstand System Tract (HST). Similar to Unit 3, the progradational stacking pattern in Unit 2 is associated with a relative drop in lake level toward the top of this unit. However, the lower muddy part of this unit may represent a retrogradational stacking pattern (Fig.3.6).

The top of this unit could represent a deposition of a regressive facies of a thin sand sheet channels eroding the lower shoreface deposits. These channels could be interpreted as localized 4<sup>th</sup> order Lowstand System Tract (LST). However, these thin sands could have been deposited as transgressive sheet sandstone of mouth bars or restricted shorelines, and thus could be interpreted as 4<sup>th</sup> order TS/LST. The unit is bounded by two 4<sup>th</sup> order Transgressive Surfaces (TS) and in between it contains deposits of a 3<sup>rd</sup> order Highstand System Tract (HST) (Fig.3.6). These deposits are interpreted to be either as distributary mouth bar or shoreline deposits. The thinning of this unit indicates a shallower lake and marks the maximum regression.

### **Isopach mapping**

The thickness patterns of the Unit 2 are the reverse of the underlying Unit 3. Thick sediments were deposited in the southwest of the study area. On the other hand, thin sediments were deposited in a north-northeast direction (Fig. 3.20).

### **Schematic palaeogeographic mapping**

The same palaeogeographic interpretation in the underlying unit can be applied to this unit. Lake Murta went significantly from a moderately deep lake at the base of this unit to very shallow or almost no lake setting at the top of this unit. This will explain the deposition of the coarse sand at the top of this unit beside the coarsening-upward sequences of prograding shoreline or mouth bars (Fig. 3.21-A & B).

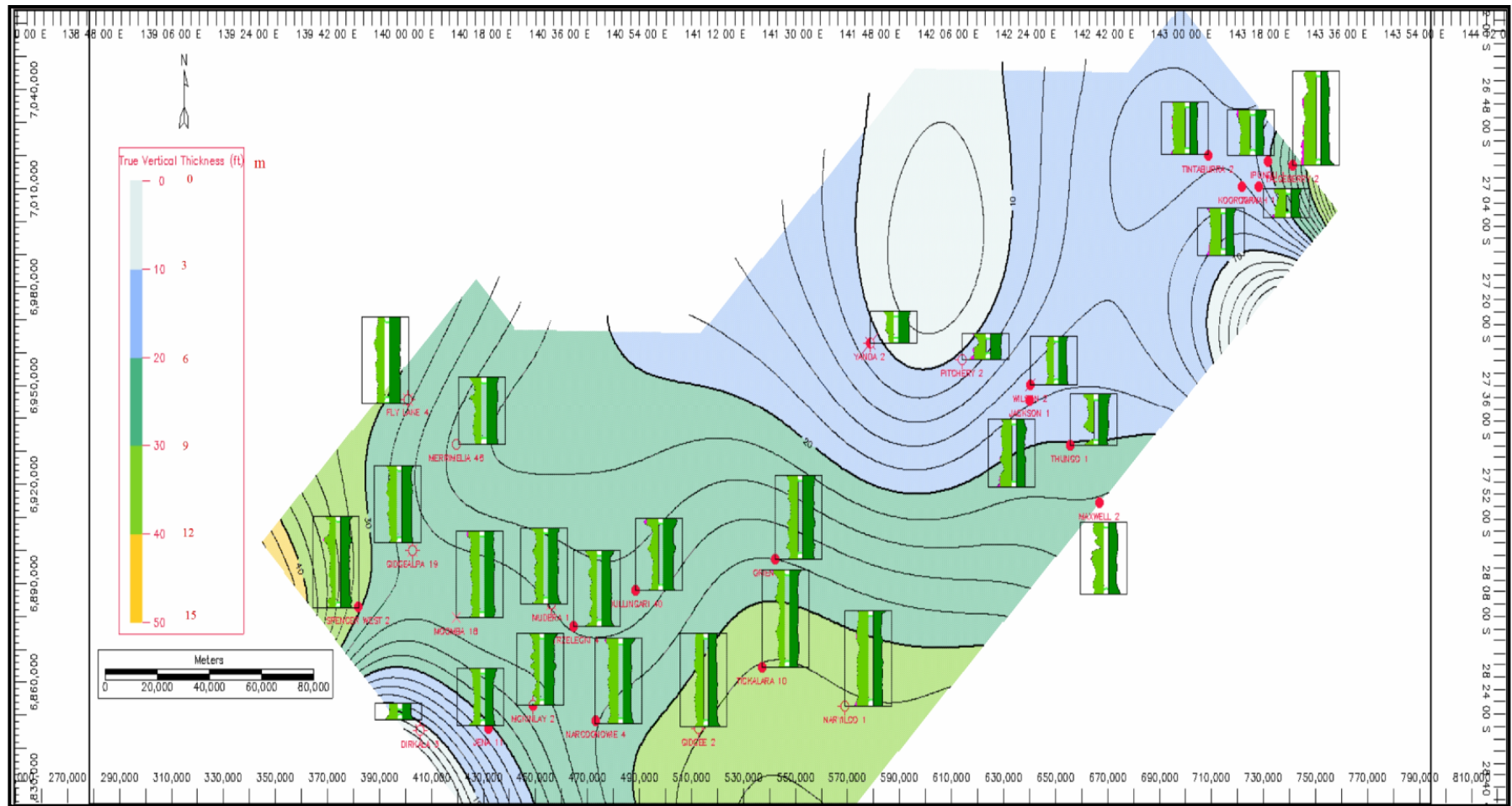


Figure 3.20: Isopach map of Unit-2 showing thick sediments deposited in the southwest part of the study area close to the proposed deep lake basin. There could be a subsidence in that part of the lake or an increase in lake base level.



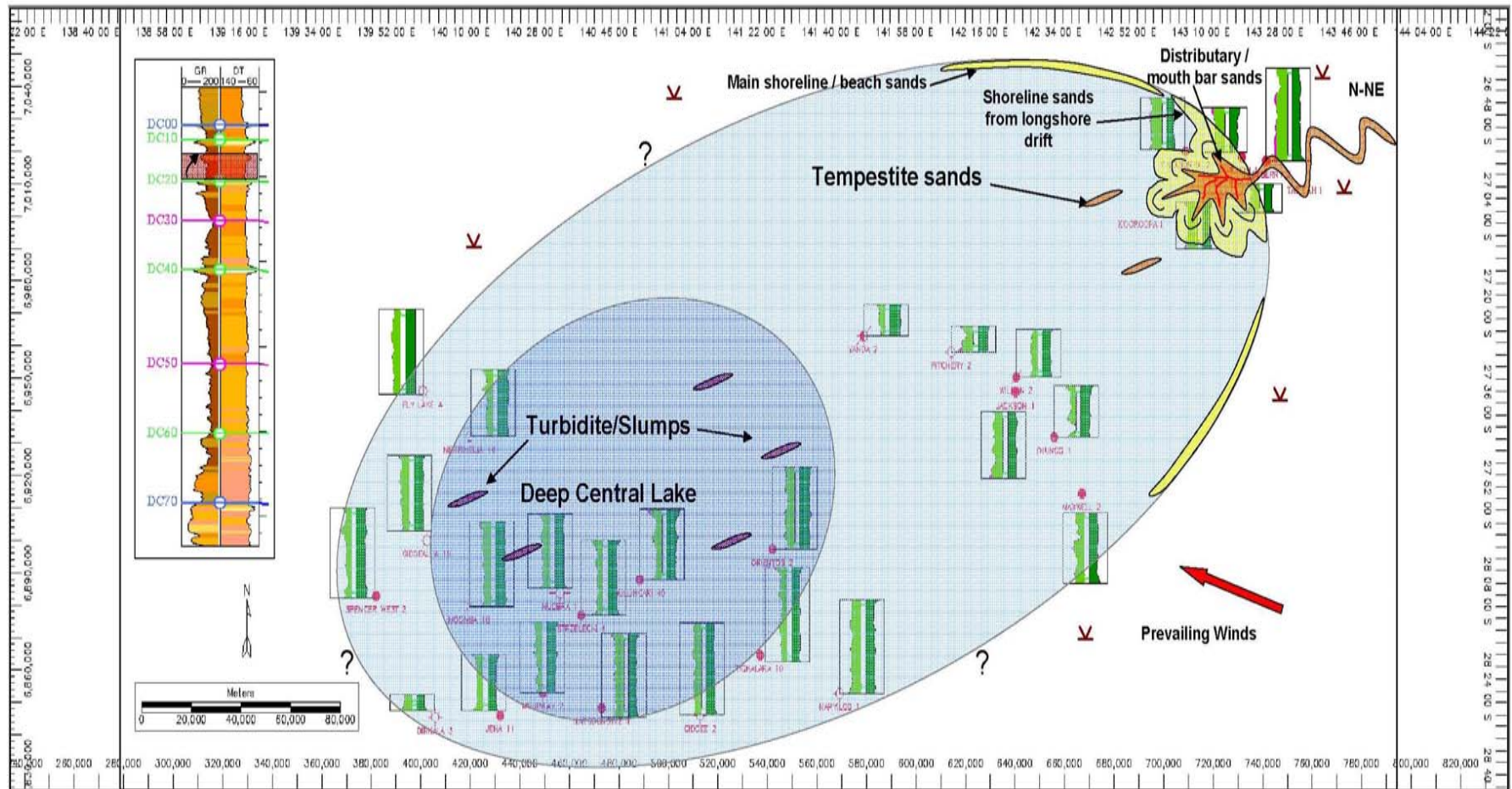


Figure 3.21-A: Schematic palaeogeographic map to characterize the deposition in early stages of Unit-2. This was characterized by a deep lake setting before the drop in lake base level in late Unit-2. Depth highlighted in red box is (4790-4803’).

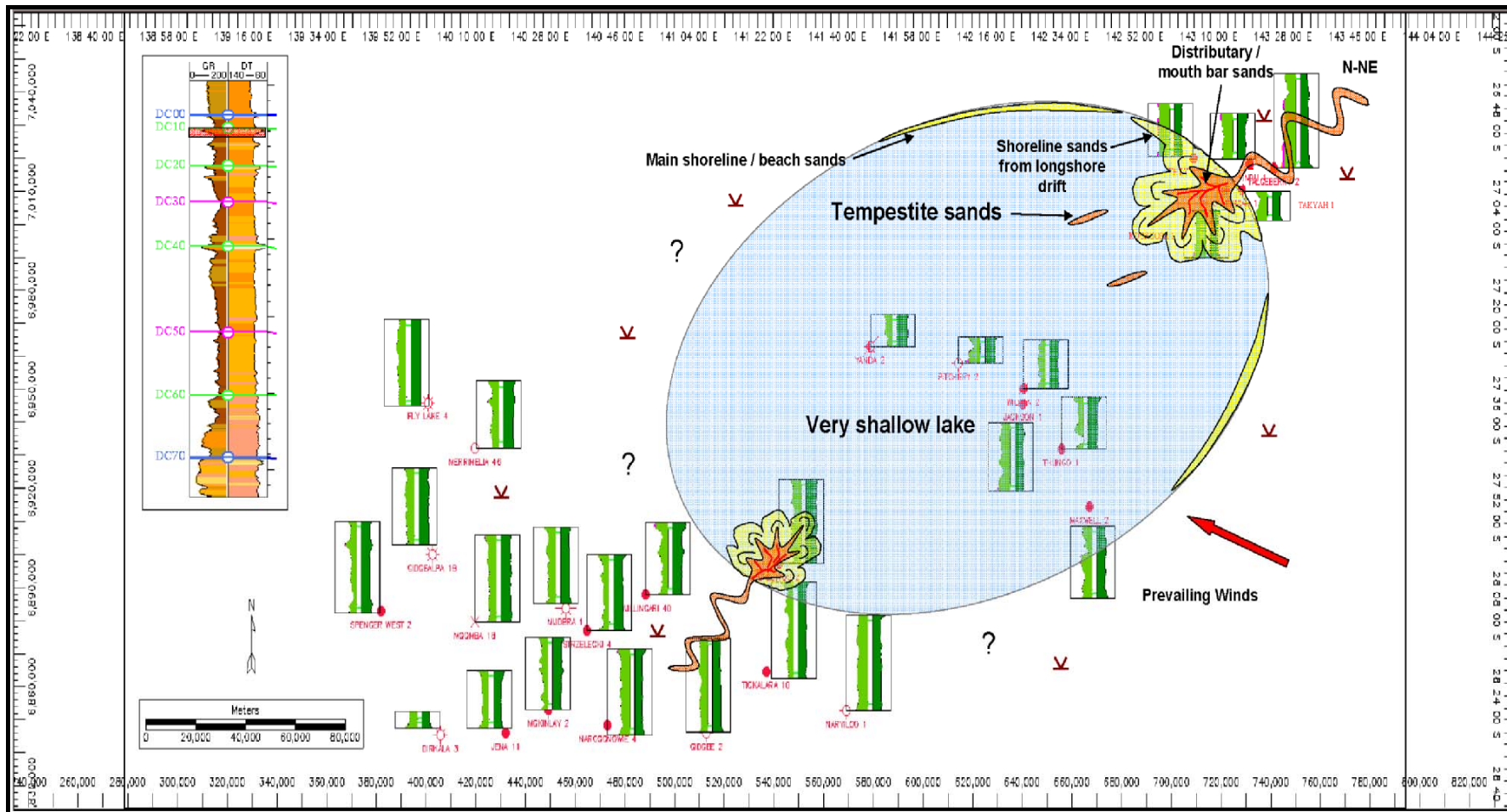


Figure 3.21-B: Schematic palaeogeographic map representing the deposition of sediments during late Unit-2. This was marked by a very shallow with possible exposure during which fluvial sheets moved into the very shallow lake. Depth highlighted in red box is (4779-4801’).



### 3.4.7 Unit 1 (DC00-DC10)

#### **Core description**

Facies associations 5 & 6 are well pronounced in this unit (Table 2.3). Sometimes it is hard to distinguish from cores between sediment from this unit of the Murta Formation and the overlying Cadna-owie Formation. However, (Zoellner, 1988) reported a distinctive colour change in these two formations. The upper Murta Formation has dark grey mud/shale, while lithology from the Cadna-owie at the contact with the Murta Formation has a reddish tinge.

#### **Wireline log**

The topmost unit of the Murta Formation contains muddy sediments deposited from its lower 4<sup>th</sup> order transgressive surface up to the 4<sup>th</sup> order Flooding Surface (FS) of the Cadna-owie Formation. These muddy intervals act as the ultimate upper seal of the Murta Formation sandstone reservoirs. Its lower contact is sharp and abrupt with the coarse thin sandy underlying Unit 2, while its upper contact is relatively gradual/transitional with the Cadna-owie Formation (Fig.3.7).

The average thickness of this unit is 3-7 m.

#### **Sequence stratigraphy interpretation**

This unit shows continuous deposition in a regional 3<sup>rd</sup> order Transgressive System Tract (TST) (Fig.3.6). This unit represent a return to an offshore lake environment as the lake transgressed the underlying sandy unit, adding significantly to the accommodation space. These facies were deposited in deep water before flooding of the basin by the sea (Ambrose *et al*, 1986). It was suggested by many authors that this flooding could represent the starting of a regional marine transgression of the Cadna-owie Formation (Ambrose *et al*, 1982 & 1986; Mount, 1982; Gorter, 1994). There is no lithological proof of the marine influence in the transitional zone suggesting the marine flooding took place higher in the succession.

This facies occupied a large area as Lake Murta level rose before the marine transgression which came from the north through the Carpentaria Basin (Ambrose *et al*, 1986). This unit, like Unit 6, was deposited in a deep lake setting.

### **Isopach mapping**

Isopach map from this unit represents a high accommodation space either due to subsidence or rise in lake level. This map shows very thin muddy intervals with little or no coarse sediments input into the lake (Fig. 3.22).

### **Schematic palaeogeographic mapping**

A deep lake setting is preferential for this unit. Murta Lake started its last transgressive phase before flooding by the marine setting of the Cadna-owie Formation (Fig. 3.23).

The gradual onset of marine conditions in the Cadna-owie Formation is recorded by the appearance of gradual increase in marine palynomorphs (dinoflagellates, acritarchs). An unusual aspect of the change to marine sedimentation is the decrease in the gamma log values at this point. One might expect a deepening associated with the influx of the sea but this is not accompanied by high gamma readings. The increase in salinity with connection of Lake Murta to the sea may have altered the clay mineralogy of the siltstones and shales leading to the unexpected gamma log profile.

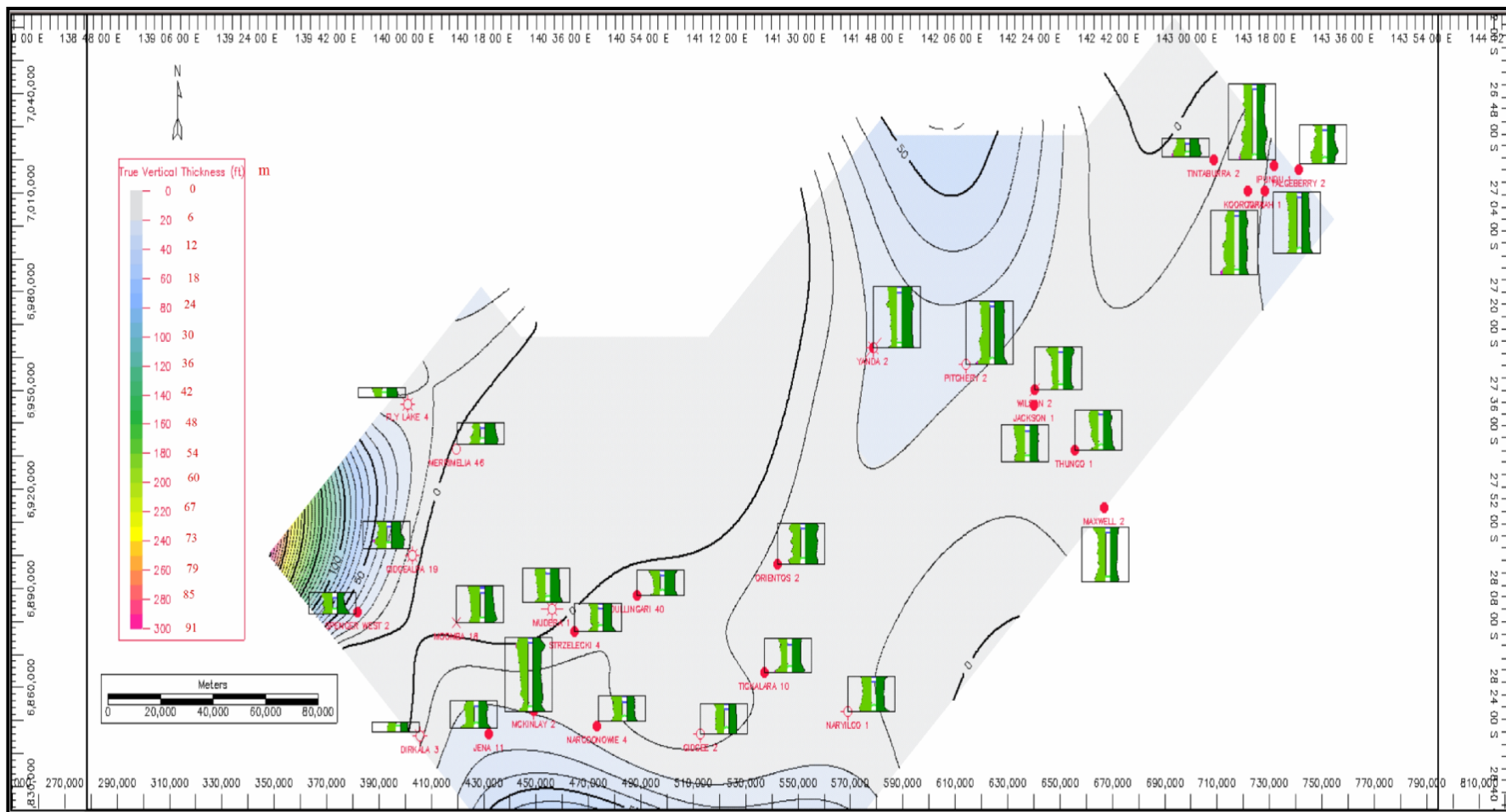


Figure 3.22: Isopach map of Unit-1 during the maximum rise of the lake base level with little sediment input. Note that due to lack of control data, some high thickness values are recorded at the western edge of the study area.

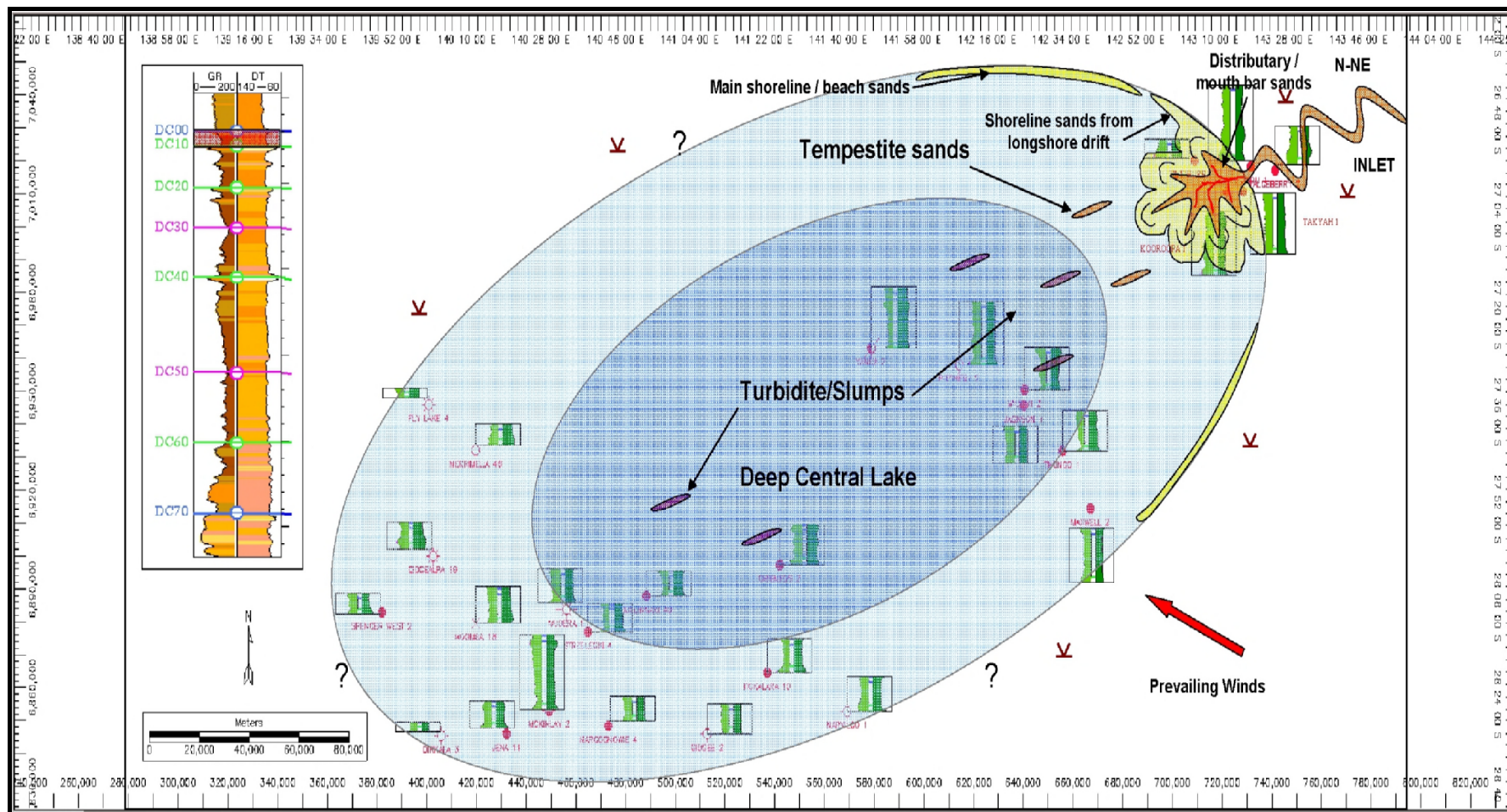


Figure 3.23: Schematic palaeogeographic map representing the deposition of muddy sediments during Unit-1. This was recognized by an increase in accommodation space either due to a rise in lake base level or subsidence. Depth highlighted in red box is (4770-4779’).

## Chapter 4 Petrographic Analysis

### 4.1 Introduction

To establish a study of reservoir quality for any area, a petrographic study should be conducted. This petrographic study includes compositional, depositional, and diagenetic features which, in turn, control the hydrocarbon flow of the targeted reservoirs. This was done based on the relationship between grain size, mineralogy, texture, cementation and matrix, porosity, and permeability for each facies to nominate the facies association with the best production potential in the Murta Formation. XRD, SEM, and point counting of thin sections were integrated to get the best possible interpretation of the reservoir characteristics.

The reservoir rocks in the study area are largely moderately-well sorted to well sorted very fine- to fine-grained sandstones. However, a few samples were bimodal in their grain size distribution with two different concentrations of coarse sand and silt-sized grains. Quartz with an average abundance of 55.7% is the main framework mineral. Other minerals noted are feldspar with average content of 2.5%, mica (average 2.2%), rock fragments (average 3.5%), heavy minerals (average 0.4%) and opaque minerals (average 0.1%). Clay minerals are important elements in the samples that have an average clay content of 8.7%. Clay types which have been identified from the samples include mainly kaolinite with small amounts of illite, illite-smectite and chlorite. These clays are mostly authigenic in origin. Carbonate cements, including calcite, siderite, and dolomite were recognized as an important constituent with an average of 9.3%. Pyrite was noted to be associated with siderite in most samples with an average of 0.9%. Visual porosity of the samples varies significantly, ranging from 0-22% and these variations are due to the variability of the diagenetic features (clay cement, quartz overgrowth, and carbonate cement) in different facies associations.

Diagenetic processes have strongly affected the reservoir quality and led to porosity reduction. These processes include cementation by quartz overgrowths and carbonate cements with the formation of micro-stylolites which have been identified from many samples and resulted in reservoir degradation. Moreover, the formation of authigenic clays from the breakdown of feldspar and mica have occupied some pore spaces to increase microporosity, and thus decrease permeability. In addition, the occasional

dissolution of the detrital grains and carbonate cement has resulted in development of secondary porosity which has been filled by kaolinite and fibrous illite.

The diagenetic processes have almost removed the primary porosity from the very fine to fine-grained sandstone facies. Examples of these diagenetic affects in fine-grained sandstones were noted from facies associations 5 & 6 (Fig.4.1-A). On the other hand, the primary porosity in the coarser grained sandstones has been preserved because of the low clay content and partial cement by quartz overgrowth (Fig.4.1-B). Secondary porosity was identified in most samples, especially in medium to coarse-grained sandstones, resulting from the dissolution of feldspar and carbonate cement. Secondary porosity adds to the effectiveness of the primary porosity by increasing the interconnected pores and therefore increasing permeability.

Due to the overall relatively uniform fine grain size of the Murta Formation sandstones, grain size is interpreted to be not the major control on porosity distribution. The above discussed diagenetic features are the main control on the porosity distribution and reservoir quality.

## 4.2 Texture

Textural data for all samples with grain size analysis are listed in Appendix 4.1. To facilitate the statistical analysis of parameters such as sorting, all grain size analysis results are expressed in Phi ( $\phi$ ) units and millimetres. A Wentworth and Phi grain size comparison is given in Appendix 4.2.

### 4.2.1 Grain size

Grain size analysis was conducted on 49 samples from all facies associations of the Murta Formation based on 50 counts using *analySIS* software. Mean grain size of sandstones ranges from coarse silt (0.022 mm, 5.50 $\phi$ ) to medium sand (0.470 mm, 1.08 $\phi$ ). The main grain size for the 48 samples is fine sand (0.164 mm, 2.60 $\phi$ ) and this illustrates the generally fine-grained character of the reservoirs in the Murta Formation in the study area. The average grain sizes for each facies association are outlined in Table 4.1.



Table 4.1: Grainsize averages for each facies association in the Murta Formation. Note the fine-grained nature of the Murta Formation.

Facies Association	No. of samples	Mean grainsize		Size class
		( $\phi$ )	(mm)	
Facies Assoc. 1	16	1.97	0.254	medium sand
Facies Assoc. 2	11	3.04	0.121	very fine sand
Facies Assoc. 3	2	3.13	0.115	very fine sand
Facies Assoc. 4	5	2.96	0.128	fine sand
Facies Assoc. 5	8	2.78	0.145	fine sand
Facies Assoc. 6	7	4.26	0.052	very coarse silt

Average grain size changes from the N-NE (coarser) toward the S-SW (finer) of the study area suggesting a regional reduction in sand content. This indicates a more distal location of the sand input towards the S-SW. It has been noted that the main reservoir in the Murta Formation has fine upper to medium lower grain sizes. Frequently, it shows generally rounded grains with a diagenetic overprint.

#### 4.2.2 *Sorting*

Sorting as expressed by the ( $\phi$ ) standard deviation can be divided into the following classes in Table 4.2. However, a visual estimation of sorting was conducted using visual comparators chart (Fig. 4.2).

Table 4.2: Sorting classification, based on the standard deviation of the grain size ( $\phi$ ) (Friedman and Sanders, 1978).

Standard deviation ( $\phi$ units)	Sorting class
<0.35	very well sorted
0.35-0.50	well sorted
0.50-0.80	moderately-well sorted
0.80-1.40	moderately sorted
1.40-2.00	poorly sorted
2.00-2.60	very poorly sorted
>2.60	extremely poorly sorted

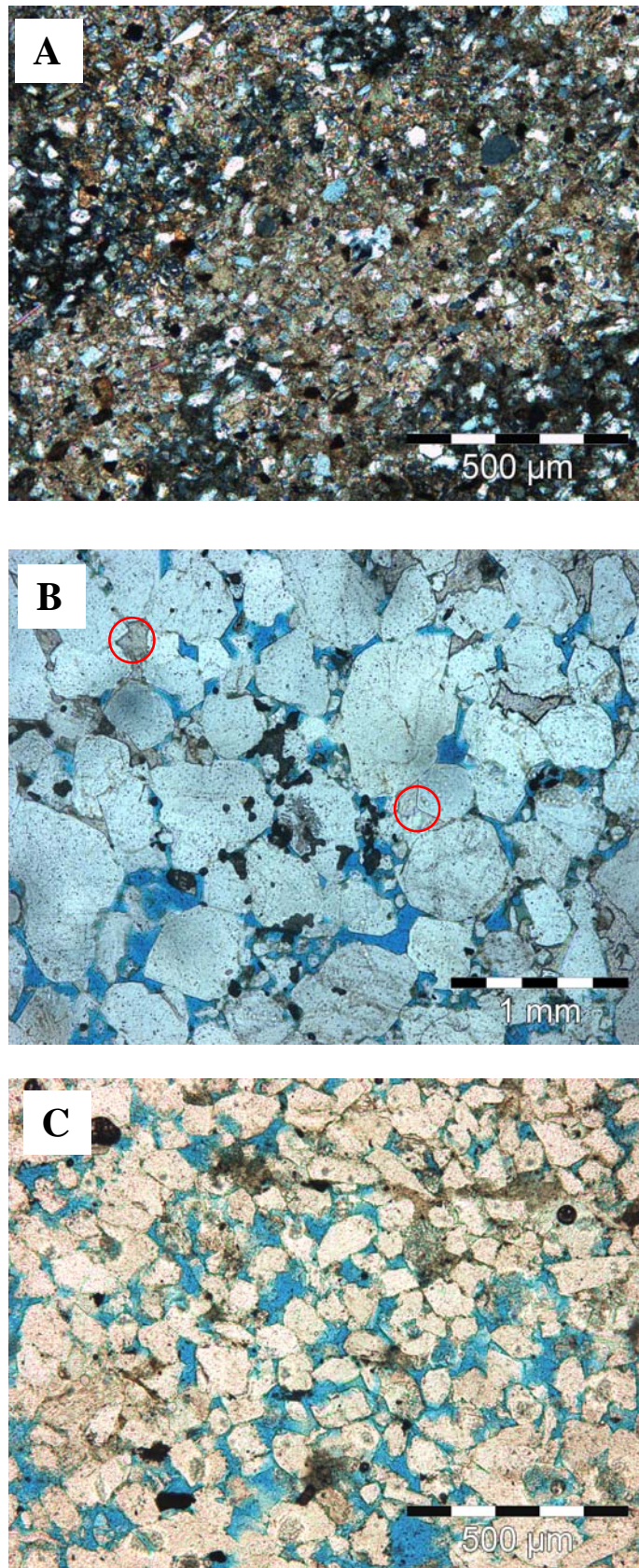


Figure 4.1: (A): High carbonate cement with associated pyrite seen under cross polar light from Three Queens-1 @ 4809' (facies association 6). Note the silt-size to very fine grain nature of the sample. (B): Quartz overgrowth cement and calcite patches seen under plane polar light from Jackson-1 @ 3674' (facies association 1). (C): Excellent reservoir quality with good intergranular porosity seen under plane polar light from Spencer West-2 @ 4470' (facies association 1).

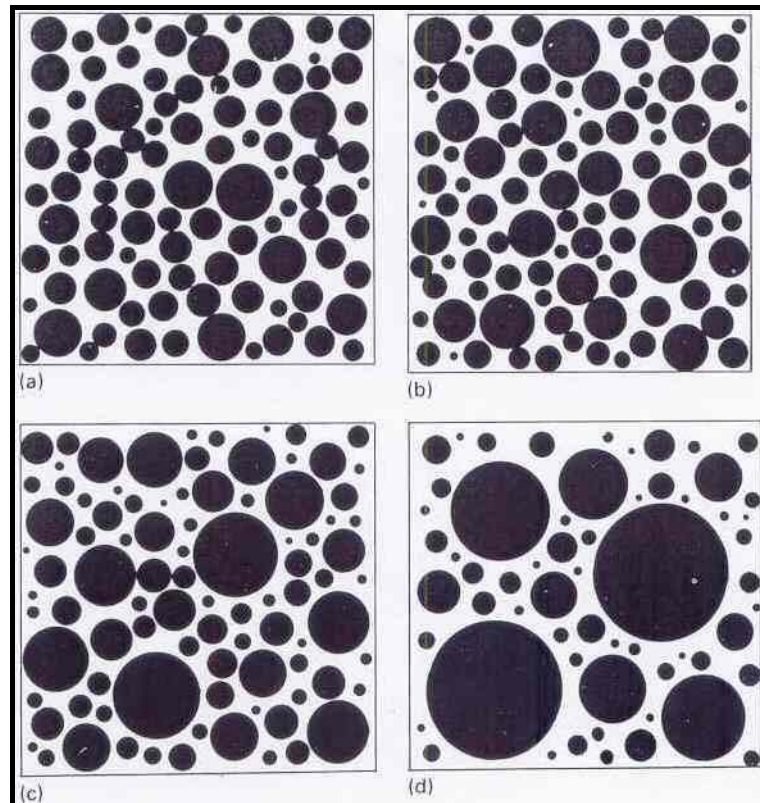


Figure 4.2: Visual comparators for random sections through log-normally distributed sets of spherical grains. Actual sorting in (a) is 0.35 (well sorted), in (b) 0.5 (moderately-well sorted), in (c) 1.00 (moderately sorted) and in (d) 2.00 (poorly sorted) (Tucker, 1995).

Most of the samples analysed for grain size fall in the moderately-well sorted class. The best sorted sample is in facies association 1 of Spencer West-2 @ 4470' with an average grain size of (0.093 mm, 3.43 $\phi$ ) (Fig. 4.1-C). On the other hand, the poorest sorting was noted from facies association 6 of Yanda-2 @ 4995.6' with an average grain size of (0.122 mm, 3.03 $\phi$ ). Although these two samples have same mean grain size type, they show a lack of any apparent relationship between mean grain size and sorting. The poorly sorted samples resulted from mixing of two different grain size concentrations. They are represented in bimodal grain sizes of coarse and very fine grain size types. Few transitional grains have been noted to fall between these two grain size concentrations.

Nevertheless, from facies associations comparison, most of the very fine grain character samples present in facies association 6 usually show poor sorting because the alteration of feldspar grains to clay can mask the sorting. The relatively best sorted samples are noted from facies associations 1 & 2. Facies associations 3, 4 and 5 are generally moderately sorted.

### **4.2.3 Porosity, permeability and textural relationships**

The visual estimation of porosity usually involves only the large pores. The microporosity is often not counted as it is associated with authigenic clays. This results in low readings of the visual estimated porosity compared to core analysis porosity (Wilson & Stanton, 1994). Nonetheless, visual estimation is useful as it is a good estimation of effective porosity, pores likely to reservoir and deliver hydrocarbons.

Visual porosity readings from thin sections show no consistent relationship between the visual porosity and the fine grain sizes of facies associations 2, 3, 4 & 5; however, the only two exceptions came from facies associations 1 & 6. Facies association 1 has a medium grain size with the highest average porosity estimate of 9.5%. On the other hand, facies association 6 has a generally silt to very fine grain sizes with very low average porosity estimate (averages 2.6%).

The above relationship also applies to the permeability readings studied from all facies associations (Appendix 4.3). In general, the finer the grain sizes, the lower permeability readings. The highest average permeability reading (36.8 mD) was recorded from facies association 1 as a result of coarser grain sizes compared to other facies associations. In contrast, the lowest average permeability reading (0.25 mD) was noted from facies association 6 with silt to very fine grain sizes.

The fine-grained laminae in all facies association except in facies association 1 were identified to prevent vertical permeability because they deposited parallel to the bedding planes. As a result, the horizontal permeabilities will be much higher than vertical permeabilities in all the oil-bearing zones (Halyburton & Robertson, 1984).

There is a direct proportional relationship between porosity estimates and permeability readings especially in facies associations 1 & 6. There is an increase in porosity readings associated with increase in permeability readings from the medium sand-sized facies association 1. Furthermore, there is a decrease in porosity estimates accompanied by decrease in permeability readings noted from the silt to very fine sand-sized facies association 6.

Plots representing the relationship between the silt content and the correspondent average permeability readings from all facies associations show a clear increase in permeability readings with decrease in silt content (Appendix 4.4). Facies association 1 was identified to have almost zero silt content with high average permeability readings. Facies association 6 has the highest average silt content with very low average permeability readings. No clear relationship can be established between average permeability reading and average silt content in facies associations 2, 3, 4 and 5.

Sorting in sandstones has an important influence on porosity and permeability. Commonly, reservoir quality increases with better sorting. This applies to facies association 1 being the best sorted facies association in the Murta Formation.

From the above textural discussion, it is clear that the sorting plays a major role in the reservoir quality of the Murta Formation reservoirs. Due to the overall fine-grained nature of the Murta Formation facies associations, no obvious impact of the grain size has been noticed on the reservoir quality parameters. However, facies association 1 has the best reservoir quality having medium grain sizes.

### **4.3 Composition**

Petrographic point counting was used to determine the mineralogy of the sandstone reservoirs in the Murta Formation. The mineral averages were analysed based on 300 counts per slide. The mineral types recognized were: monocrystalline quartz, polycrystalline quartz, K-feldspar, plagioclase, mica, rock (lithic) fragments, heavy minerals, opaque minerals, clays, carbonate cement, pyrite, and porosity. Detailed thin section descriptions/mineralogical results can be seen in Appendix 4.5. These mineralogical results were put in a summary chart for each facies association (Fig.4.3). A summary histogram has been established for each constituent identified in every facies association (Fig.4.4).



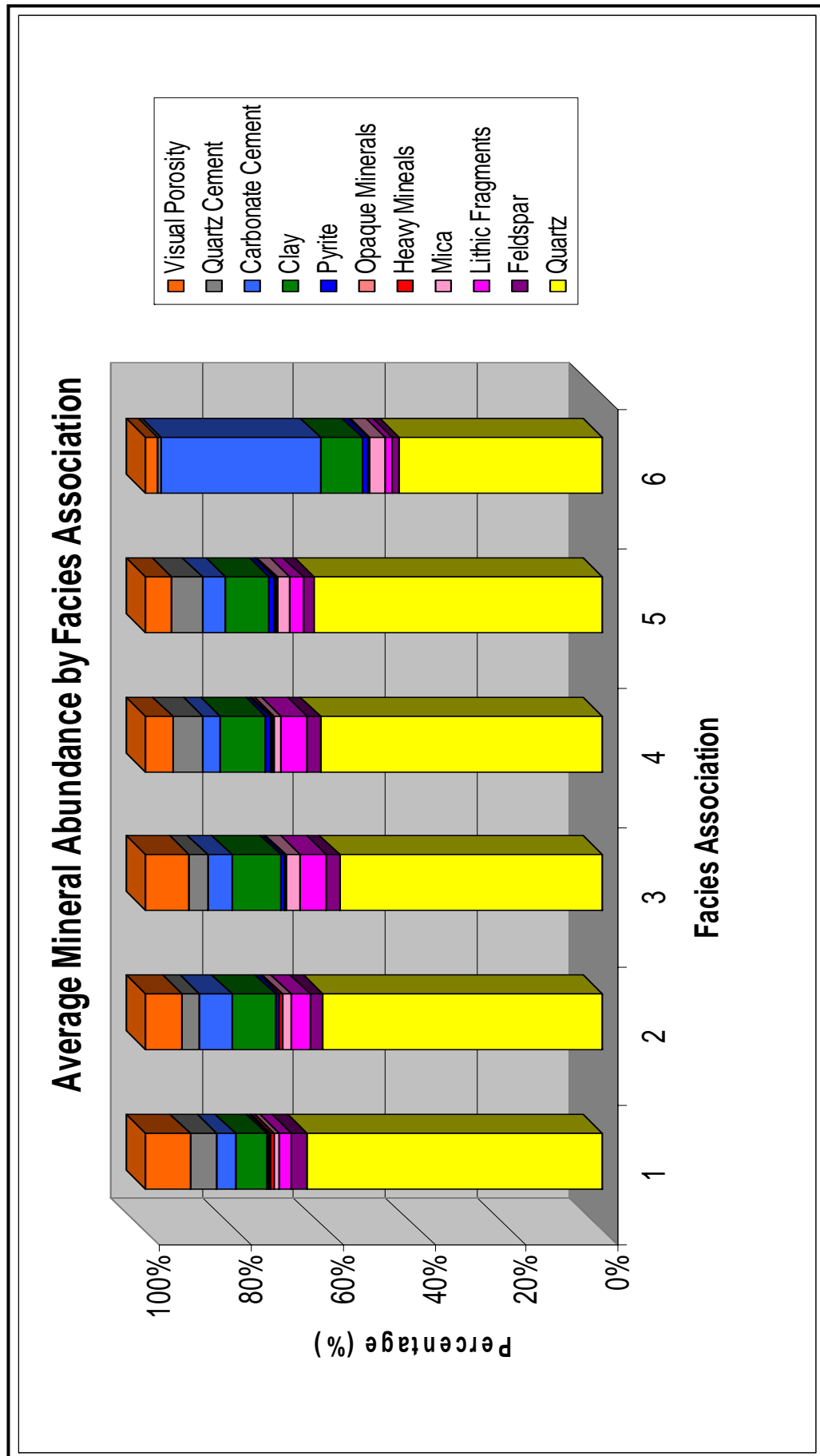


Figure 4.3: Summary chart shows the mineralogical results from each facies association. Note the quartzarenite nature of the sandstones. Also note the high carbonate cement in facies association 6, while facies association 1 has the lowest carbonate cement.



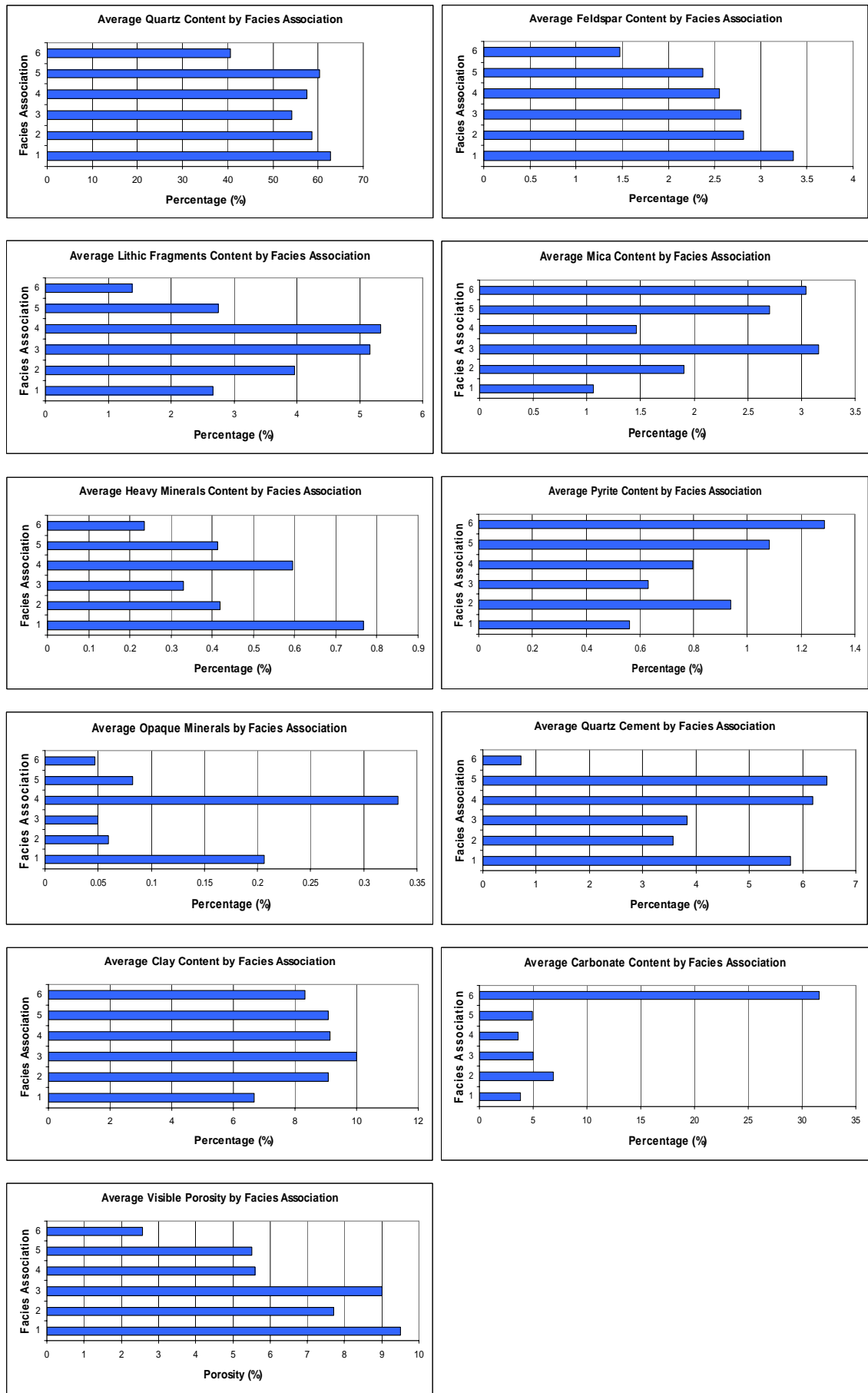


Figure 4.4: Summary histograms for each constituent identified in every facies association.

A modified Folk classification (1980) was used to classify the samples (Fig. 4.5). This classification is based on the population of three end members: quartz, feldspar, and rock (lithic) fragments. The rock type of each facies association was identified after plotting the samples on the Folk (1980) ternary plot. The sandstone reservoirs in the Murta Formation are mainly quartzarenite. Yet, some samples show subarkose and sublitharenite rock type. Samples from facies associations 1, 3, 5 and 6 fall on quartzarenite part of Folk (1980) ternary plot. As a result of having more lithic fragments, facies association 2 falls into the sublitharenite rock type, while facies association 4 with relatively good feldspar concentrations recorded as subarkose.

### 4.3.1 Quartz

Quartz grains have been recognized in all samples to be the main framework grain type. Their content ranges from 10.3% to 78.8% of the total rock with an average abundance of 55.7%. Most of the quartz grains are of monocrystalline type, however, a small amount of polycrystalline quartz grains were identified (average 1.4%). Although, most of the monocrystalline grains have even extinction, grains with undulose extinction are also observable in most samples. Facies association 1 samples contain the highest average quartz content of 62.7%, while facies association 6 has the lowest quartz percentage (40.6%) among the other facies associations (Fig.4.4).

Quartz overgrowths cement were noted in the majority of the samples, although the percentage of the quartz overgrowths cement varies broadly from <1% to 15%. Figure 4.6 shows example of quartz overgrowths in thin section. It was marked that the quartz overgrowth developed in more sandy laminae which contain little clay and mica. However, in some places, the development of the quartz overgrowths has been prevented by carbonate cement, especially in some coarser sands. In finer-grained samples, the amount of quartz overgrowths depends on the abundance of clay-coated quartz grains which, in turn, will inhibit the formation of quartz overgrowths (Wilson & Stanton, 1994).

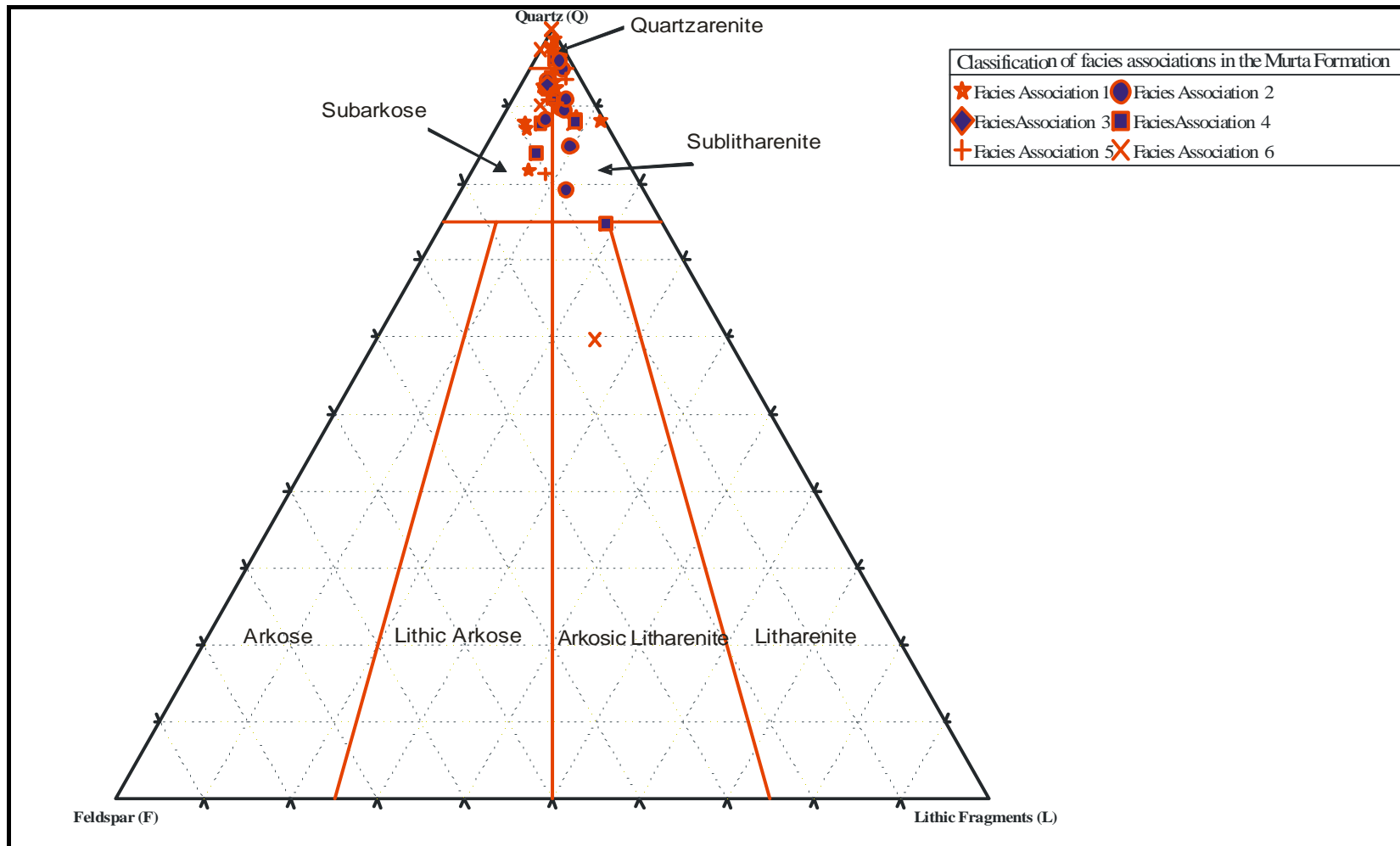


Figure 4.5: Classification of the Murta Formation sandstones based on a modified Folk (1980) classification. Note that most of the samples are Quartzarenite, although some samples fall on sublitharenite and subarkose sandstone type.

Wilson & Stanton (1994), based on laboratory studies, reported that the quartz grain size is an essential factor in overgrowth development. In monocrystalline quartz grains, the finer the grain, the faster the development of overgrowths. Polycrystalline quartz grains show the slowest development of overgrowths in the finer grain sizes. The quartz overgrowths initially started as rapid development of its rhombohedral crystal faces, then the development rate drops to a fraction of the initial rate. An example of well-developed rhombohedral crystal faces is recognized in Figure 4.6.

Usually, quartz overgrowths reduce pore spaces, but they do not completely fill all the intergranular pore spaces leaving some primary porosity between planar overgrowth crystal faces. Thus, quartz overgrowths are not the only major control on reservoir quality reduction knowing that most of the samples have quartz overgrowths and still considered to be a good reservoir quality. In more micaceous and clay-rich samples, overgrowths are not well developed. Therefore, the porosity loss results from grain suturing and the presence of the authigenic clay (Martin, 1984).

### **4.3.2 Feldspar**

Feldspar is considered to be the second most abundant constituent detrital grain in the samples. It's content ranges from <1% to 8% with an average abundance of 2.5% (Fig.4.4). Potash feldspar is the main feldspar type present with microcline and orthoclase. Plagioclase was also identified only in minor amounts with an average content of less than 1% and sometimes it is not present at all.

Thus, potash feldspars are more common in the samples than plagioclase. There are two reasons for this. Potash feldspar has a greater chemical stability than plagioclase, and so the latter is altered preferentially in the source area (Tucker, 1995). In addition, potash feldspars are more common in continental basement rocks which are the provenance of the continental interior Eromanga Basin.

Feldspar grains have been altered either completely or partially and have been replaced by clays or carbonate (Figure 4.7 A&B). The alteration of feldspar to clays is well recognized and it is interpreted to be the main process in feldspar content degradation. The alteration of feldspar grains has resulted in the formation of the secondary porosity in most of the samples (Figure 4.7-C).

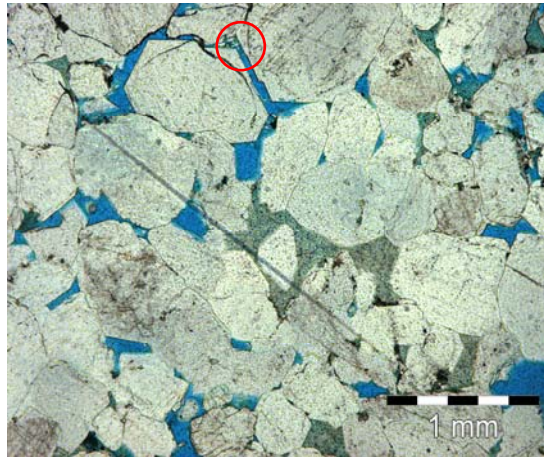


Figure 4.6: Well-developed rhombohedral crystal faces of quartz overgrowths seen under plane polar light from Merrimelia-6 @ 5185' (facies association 1).

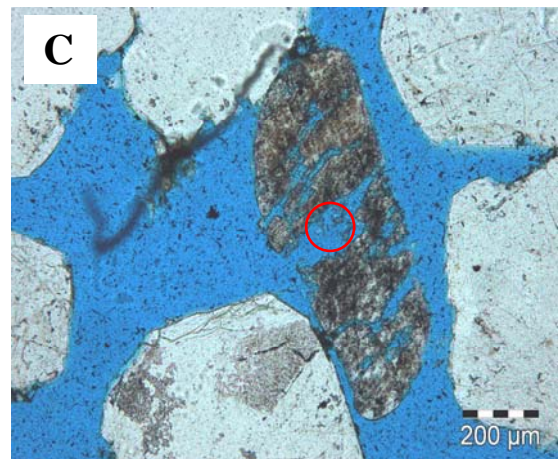
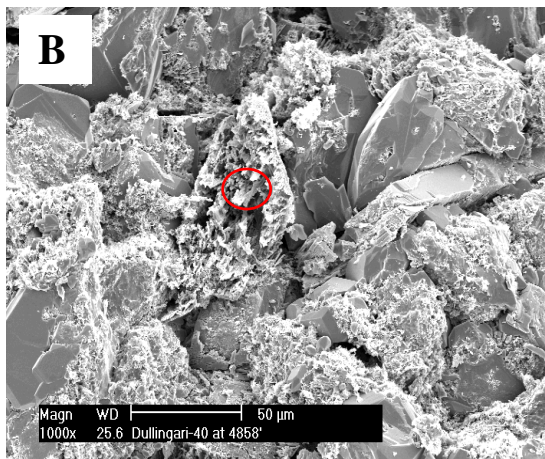
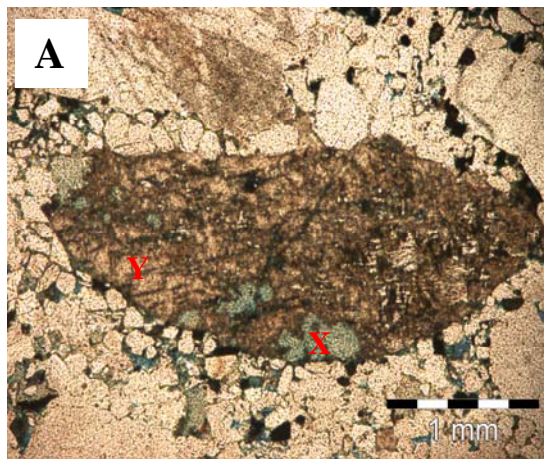


Figure 4.7: A: feldspar grain partially altered to kaolinite (X) and in the same time replaced by carbonate (Y) seen under plane polar light from Moomba -18 @ 5833.7' (facies association 1). B: SEM image shows a dissolved feldspar grain altered to kaolinite in Dullingari-40 @ 4858' (facies association 2). C: Dissolved feldspar grain creating secondary porosity seen under plane polar light from Ulandi-5 @ 4064' (facies association 1).

Facies association 6 is interpreted to have the lowest feldspar content (1.5%) not only because of alteration to clays, but also as a result of high carbonate cement recorded in that facies association. Although facies association 1 has the highest feldspar content (3.3%) and the lowest clay content (6.7%), it still classifies as an overall quartzarenite rock type. There is a general rough trend of decreasing feldspar content with increase in clay content as a result of feldspar alteration to clays.

### **4.3.3 Rock fragments (lithic)**

Rock (lithic) fragments are common and average 3.5% in the analysed samples, although they range from <1% to 12.3%. Facies association 2 & 4 were recorded to have the highest average lithics content of 4% and 5.3% respectively and to be of sublitharenite rock type. These relatively high concentrations of lithics in facies associations 2 & 4 samples are interpreted to be derived mainly from metamorphic and/or recycled orogenic sources, however, all the sediment came from the same source (Figure 4.8-A). The answer lies in the sorting of sand grains by size. The more labile grains (feldspar and rock fragments), the more easily breakdown of finer sand sizes in transport.

### **4.3.4 Mica**

Mica averages 2.2% in most of the samples analysed, more abundant in finer sandstone and siltstone samples. The percentage ranges from <1% to 5.7%. Because of their flaky nature, they are easily removed from coarser sediments and so tend to accumulate in finer sand and silts (Tucker, 1995). They are sheet silicates and concentrated along the finer-grained carbonaceous silty laminae. Biotite is less abundant than muscovite. This could be a function either of the relative abundance in the source area or that biotite is more reactive and alters quickly to chlorite. On the other hand, muscovite is mostly fresh in its appearance and sometimes affected by extensive carbonate replacement (Figure 4.8-B).

An increase in mica content has been recognized to be associated with increase in clay content. This trend was identified in the petrography study as a result of mica alteration to clays (Fig. 4.3 & 4.4).



Facies association 1 samples have the lowest mica content (1%) because of their medium to coarse grain nature. The low mica content associated with the lowest clay content recorded (6.7%) is also in facies association 1. Facies association 3 have the highest mica content with an average of 3.2% and has been noted to be associated with the highest average clay content (10%) reading among all facies associations.

Since mica is interpreted to be grouped in facies associations characterised by very fine to fine grain sizes, this grouping has resulted in low permeability readings of those facies associations. An overall trend has been documented showing a decrease in permeability with increase in mica rich silt samples (Appendix. 4.4).

#### 4.3.5 Clay mineralogy

Clay content is well presented in most of the samples ranging from 3% to 16% with an average of 8.7%.

XRD and SEM techniques were used to study the clay mineralogy and the textural relationships between clays and pores of the reservoirs in the Murta Formation. XRD results showed the occurrence of kaolinite, illite-smectite clays, and illite-mica combination. Most of the clay types appear to be authigenic in origin and resulted primarily from mica or feldspar alteration (Figure 4.8-C). Much of the illite and illite-smectite is allogenic; part of the original matrix of the sediment.

XRD and SEM emphasize the abundance of well-crystallized kaolinite as a dominant clay type with an average of 8.7%. Other clay types change from sample to sample but have extremely low abundances. Illite-smectite and grain-coating chlorite were recognized in very small amounts (<1%), while pore-lining illite averages 1.2%. These clays are very difficult to recognize both in thin section and in SEM because of their fine-grained nature. As a result, point counting method underestimates the clay mineralogy compared to the XRD method (Hill, 1999). Appendix 4.6 shows XRD analysis methods used in all facies associations.

Clay content has been noted to be the lowest in facies association 1 associated with the medium to coarse grain character of its samples. On the other hand, clay content is high in the rest of the fine-grained facies associations, especially in facies association 3.

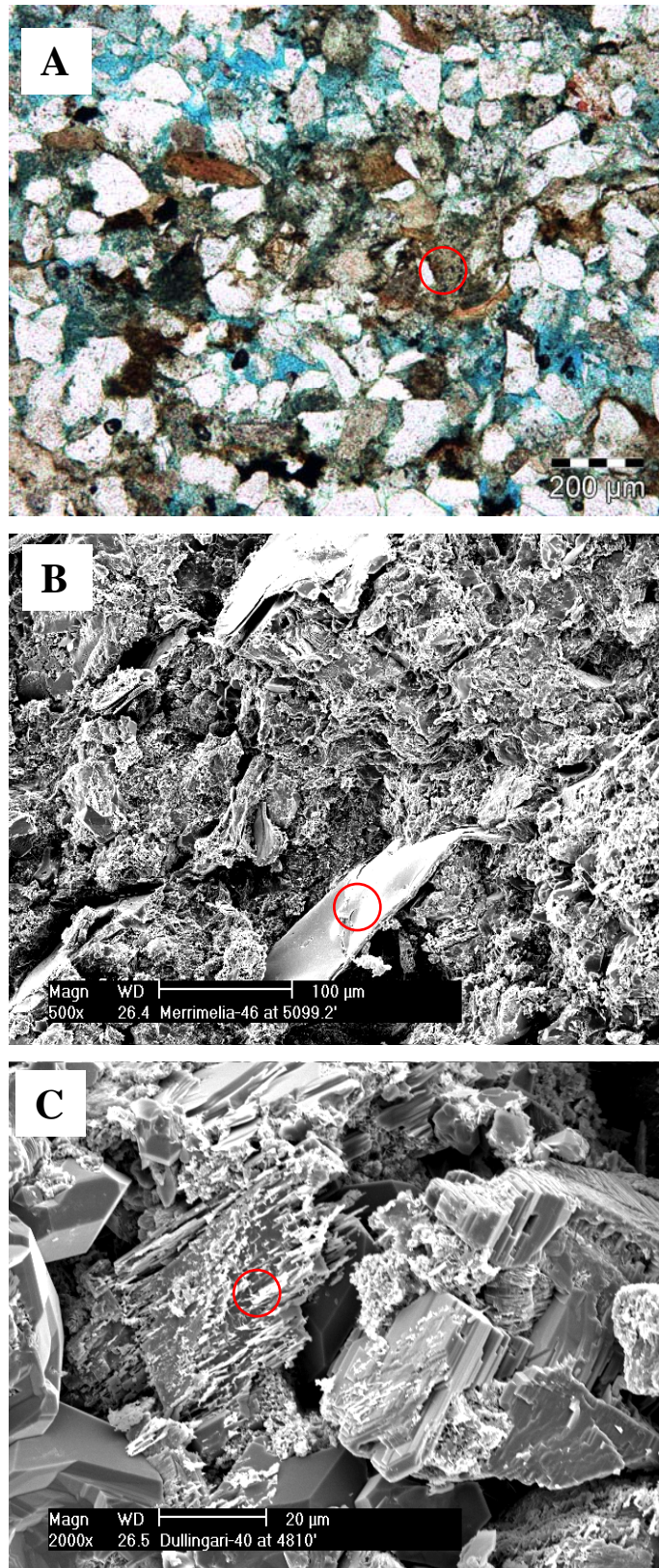


Figure 4.8: A: concentration of lithic grains seen under plane polar light from Talgeberry-2 @ 3082' (facies association 3). B: SEM image from Merrimelia-46 @ 5099.2' (facies association 5) shows a fresh mica grain. Many of the other grains surfaces are covered with kaolinite. C: SEM image shows a feldspar grain in the process of dissolution and alteration to clays, mainly kaolinite. From Dullingari-40 @ 4810' (facies association 5).

#### 4.3.6 Carbonate and associated pyrite

The carbonate types identified by thin section, XRD and SEM analysis are calcite, siderite and dolomite. These carbonate minerals were recorded as cement and grain replacement minerals in most of the samples studied. Their percentage ranges from 1% to 55% with an average of 9.3%. Carbonates often occur in cemented bands 1-2 cm thick. The carbonate minerals, particularly siderite, were identified to be associated with pyrite which, in turn, has an abundance range from <1 to 2%.

Calcite is the dominant carbonate type ranging from 2% to 28%. Calcites occur as irregular patches of coarse crystalline pore-filling cement. Commonly, these calcites partially or completely replace some framework grains and clays (Figure 4.9-A). The later dissolution of these carbonate cements results in the formation of the secondary porosity. Occasionally, calcite was found to be associated with quartz overgrowth in the medium to coarse-grained samples.

Dolomite was documented using XRD and thin section petrography in very few samples. One example is from facies association 6 (Figure 4.9-B). The Murta Formation has a tendency to have more calcite cement, while in the Namur Sandstone more dolomite samples were noted (Martin, 1984). Like calcite, dolomite occurs as coarse crystalline pore-filling cement, which in part replaced some of the framework grains.

Siderite was recorded in association with pyrite. Together, they cemented and replace silts in many samples particularly in finer-grained samples of facies association 6. Siderite abundance ranges from <1% to 12%. Siderite is present as a collection of small rhombic crystals as a result of mica replacement. Siderite partially replaces some of the detrital grains, especially feldspars and fills some pore spaces (Figure 4.9-C).

Zoellner (1988) noted the occurrence of siderite being associated with the shaly/muddy intervals of the Murta Formation, and thus will increase capacity/threshold pressure of shales/muds. The best examples of siderite are from facies association 6 because of its muddy character.



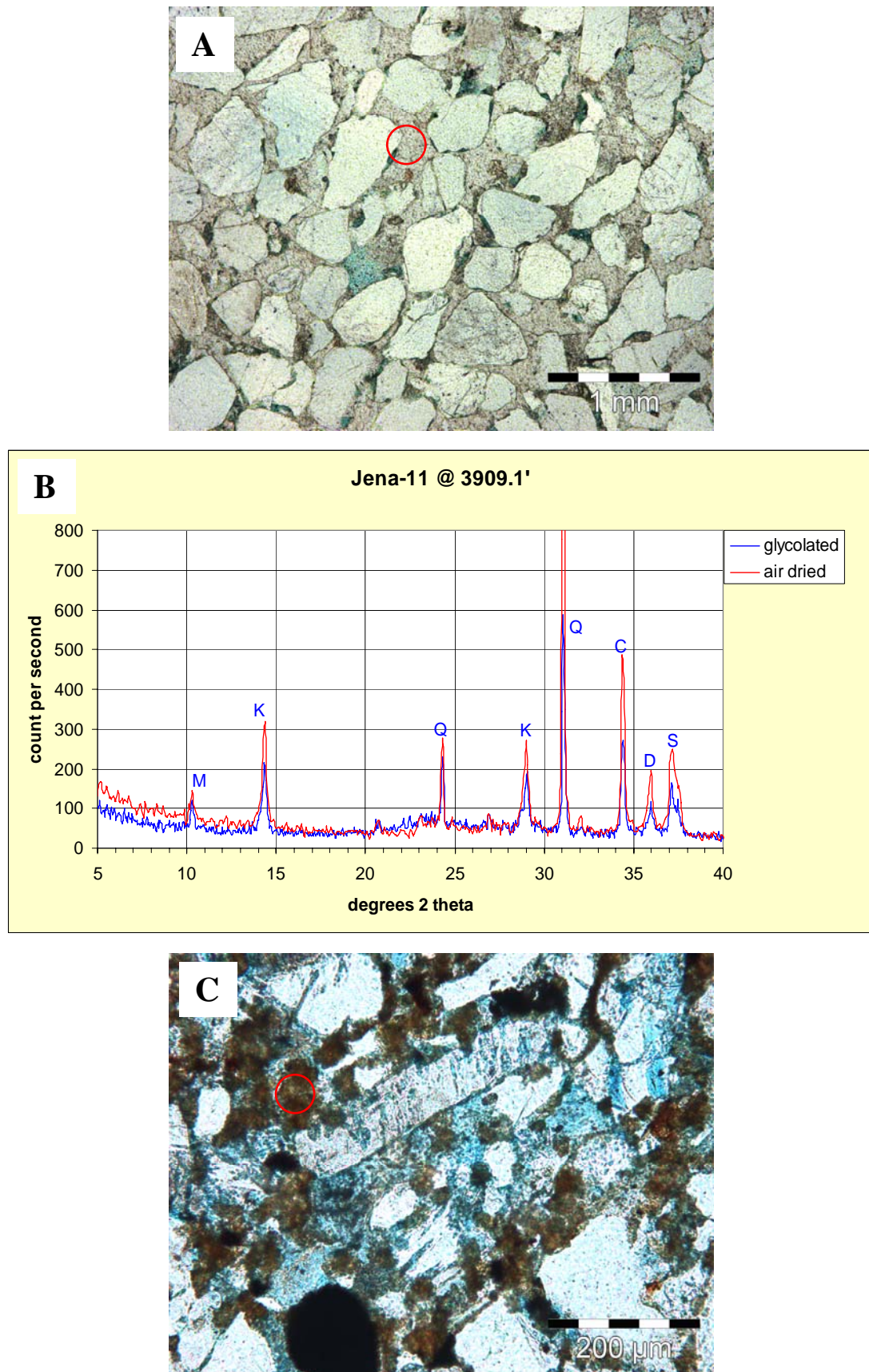


Figure 4.9: A: Intense calcite cementation from Gidgee-2 @ 3904.5' seen under plane polar light (facies association 2). B: XRD trace of very fine-grained sandstone sample showing high concentrations of carbonate including calcite, dolomite and siderite from Jena-11 @ 3909.1' (facies association 6). C: Siderite aggregates of small granular crystals associated with pyrite seen under plane polar light in Gidgealpa-19 @ 5085' (facies association 4).

Facies association 1 has been recognized to have the lowest average percentage (3.8%) of the carbonate content because of its medium to coarse grain sizes. But, facies association 6 has the highest average percentage (31.6%) of the carbonate content (Fig. 4.3 & 4.4).

Based on a carbon isotope study by Staughton (1985), late diagenetic siderite precipitation in connection with oil generation was reported by Zoellner (1988). Due to the common interbedded low permeability shaly and muddy intervals with sandstone, the oil migrates parallel to the bedding planes, not in a vertical direction, and this will inhibit the mixing of neighbouring chemical environments. The precipitation of siderite in the upper part of the sandstones and at the major lithological boundaries supported the late siderite occurrence.

Nevertheless, Martin (1984) suggested an early diagenetic origin started with carbonate cementation and clay formation simultaneously followed by quartz overgrowth cementation and microstylolite formation as a late diagenesis.

Carbon isotope studies by (Schulz-Rojahn, 1993) investigated the origin of extensive patches of calcite cement in the Eromanga Basin. The study concluded that carbon dioxide dissipating upwards from the Cooper Basin was the main factor leading to carbonate precipitation in the Eromanga Basin. He also proposed that the cementation did not take place in the shallow diagenetic setting. Although they studied the underlying Permian succession, Rezaee *et al* (1997) noted several pulses of siderite cement.

#### **4.3.7 Heavy minerals and opaques**

Heavy minerals are a minor constituent in the examined samples and their concentrations average <1%. The most pronounced heavy mineral was zircon because of its well-developed zonation and well-rounded grains suggesting possible mixed sources. Other heavy minerals identified were tourmaline and rutile. Analysis by XRD and SEM did not help in tracing these heavy minerals because of small concentrations.

The study of heavy minerals can give suggestions about the provenance of the sandstones. Because of their high specific gravities, heavy mineral grains tend to be smaller than quartz grains and concentrated in particular laminae (Tucker, 1995).

Opaque minerals average less than 1%. They consist mostly of leucoxene which is resulted from decomposition of rutile or ilmenite (Martin, 1984).

#### **4.4 Diagenetic features**

Diagenetic processes include cementation, replacement and dissolution. These processes can occur separately or together affecting one or more minerals (Tucker, 1995). They begin immediately after deposition and continue until metamorphism takes over. Early diagenetic events take place from sedimentation until shallow burial, while late diagenetic ones occur during deep burial.

Diagenetic changes which have taken place during burial of the Murta Formation include cementation by quartz overgrowths and carbonates, formation of authigenic clays, dissolution of carbonate cement and some of the unstable framework grains to form secondary porosity, and the formation of microstylolites as a result of partial dissolution of quartz. These diagenetic changes were controlled by the original texture and composition of the samples and have been studied using petrographic, SEM, and XRD techniques. Figure 4.10 shows XRD traces used to compare between all facies associations in terms of mineralogical abundances and diagenetic features from selected samples. However, as these samples spread from one end of the study area to the other, there may also be an overprint of different provenance area in the mineralogy included.

##### **4.4.1 Cementation**

Cementation by quartz overgrowths and carbonate is the dominant porosity reducing process especially in clean more sandy laminae with little clay and mica. Commonly, overgrowths reduce the pore sizes but they do not completely fill the pores leaving small pores between planar overgrowth crystal faces (Figure 4.11-A). On the other hand, in fine-grained samples with more mica and clays, the porosity reduction resulted from the formation of authigenic clays, particularly kaolinite.



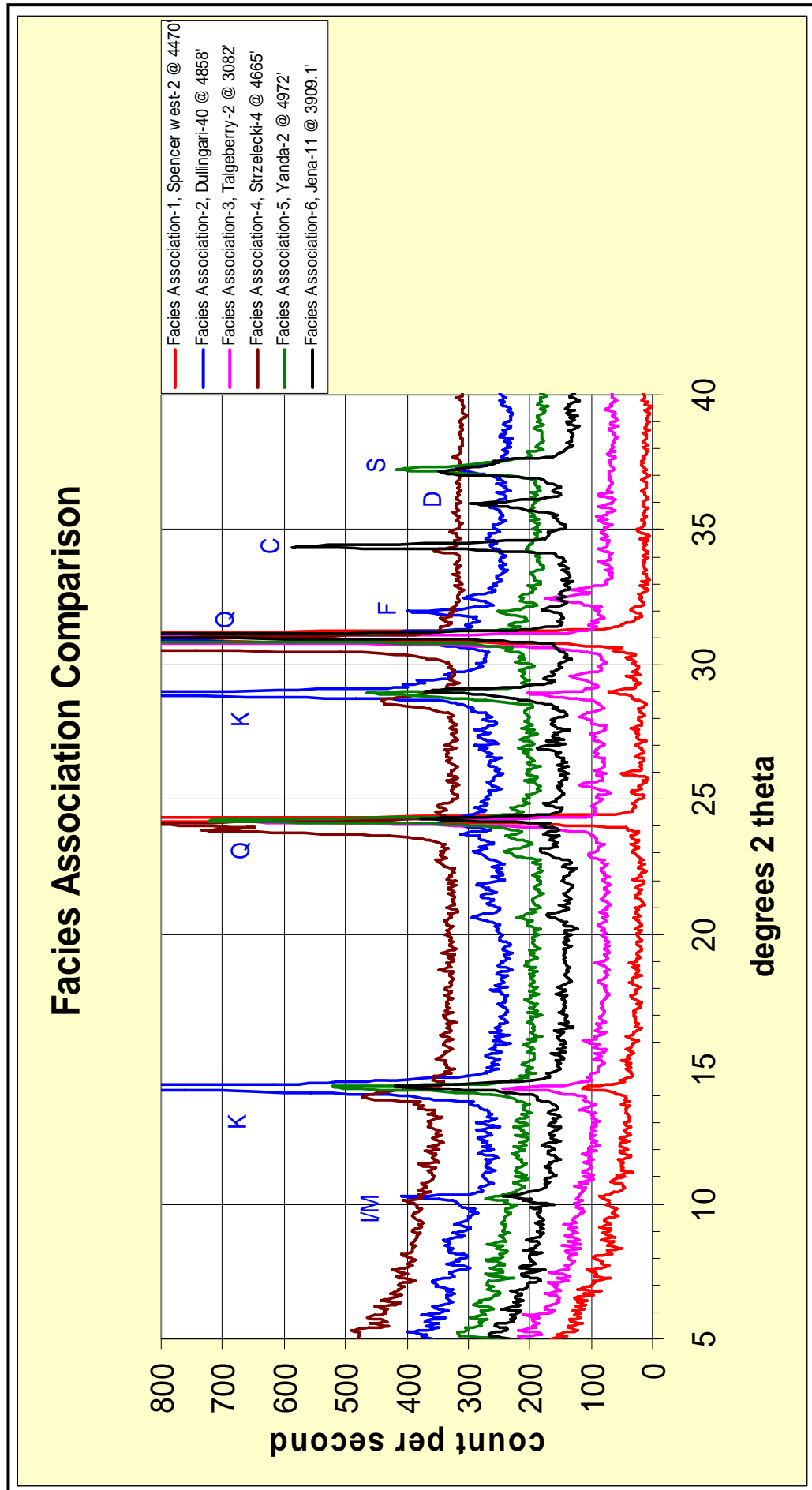


Figure 4.10: XRD traces show mineralogical abundances and diagenetic effects on a representative sample of each facies association.

Overgrowth cementation was noted to be restricted to the parts of the sample where there are framework grains or other cements which allow some porosity to remain. Occasionally, in some samples, overgrowths were recognized to effect silt-sized grains more than the coarser grains. However, bimodal grain samples contain both quartz overgrowth in coarser grains and clay cements in finer grains. Some finer-grained samples show that clays have prevented the development of quartz overgrowth by coating the quartz grain itself (Figure 4.11-B).

Extensive carbonate cementation was noted in some samples as infrequently distributed patches. They are coarse crystalline and mainly of calcite and siderite type, however, dolomite was identified in XRD and in thin section in very few samples.

Carbonates do not fill all the pore spaces and sometimes they replace the framework grains, usually potash feldspar. Siderite occurs in most of the samples as aggregates of small granular crystals replacing mica and lithics rather than as intergranular cementation. Some samples show high calcite and siderite cementation in a way that these carbonate replaced most of the framework grains.

In very silty samples, carbonate, particularly siderite, and associated pyrite, was recognized to fill large burrows that originally contained organic matter and replace most of the silt matrix (Figure 4.11-C).

Carbonate cement is a very common component in facies association 6 samples (average 31.6%). Facies association 1 has the lowest carbonate abundance (average 3.8%).

#### **4.4.2 Formation of authigenic clays**

Authigenic clays formed by the breakdown and alteration of feldspar, mica and rock fragments were found in all samples. These authigenic clays occupy pore spaces leading to porosity reduction. In addition, they increase the microporosity of the total porosity causing a reduction in permeability particularly in fine-grained samples. On the other hand, the interbedded silts and shales in the Murta Formation are, by definition, of detrital origin. Some of the same component is inevitably included in the sands as matrix. While these clays can re-crystallize, they are still of detrital origin.

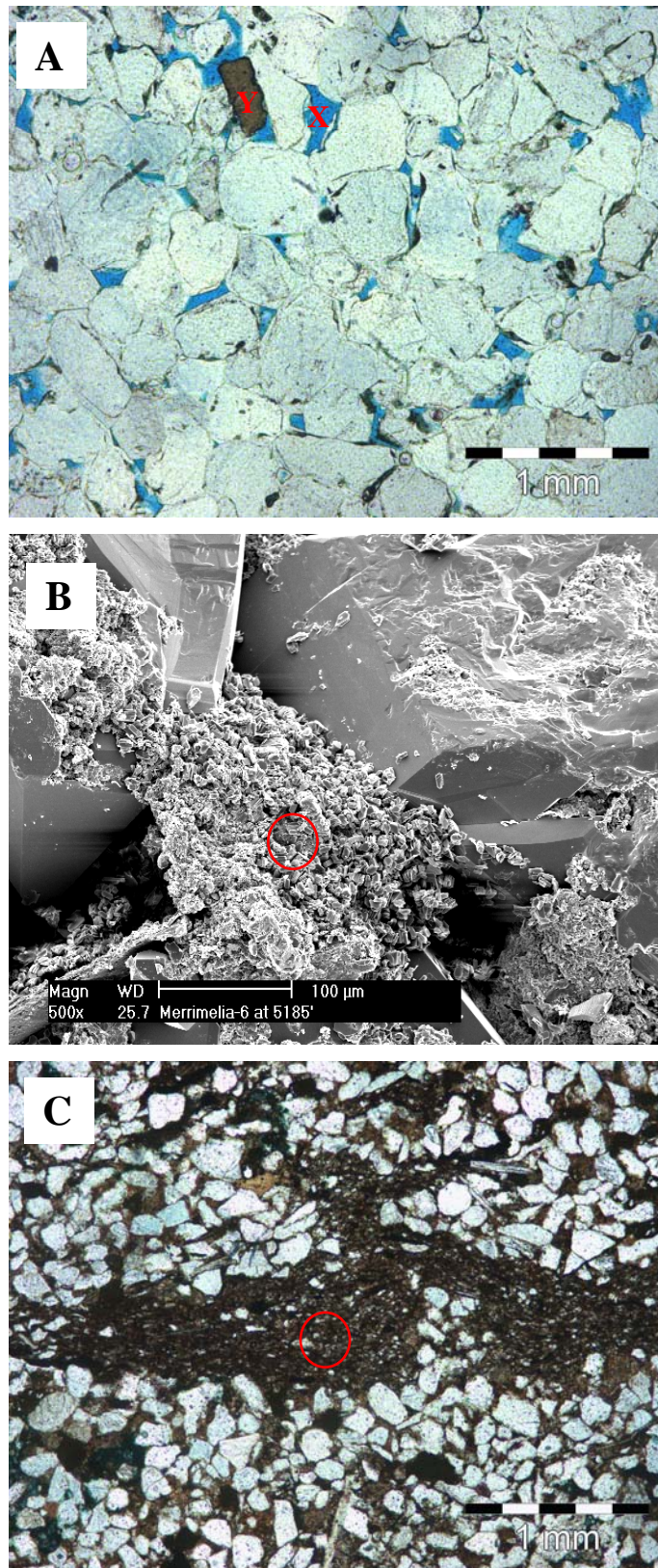


Figure 4.11: A: Example of extensive quartz overgrowth (X) in sandstone from Challum-1 @ 5116' seen under plane polar light (facies association 1). Note the preserved intergranular porosity in spite of aggressive quartz overgrowth cement. Also note the heavy mineral grain (Y) in the upper part of the plate. B: SEM shows well-defined kaolinite cement preventing quartz overgrowths from blocking the pores. Example from Merrimelia-46 @ 5158' (facies association 1). C: Big burrows were identified to be filled with siderite and organic matter seen under plane polar light. Example from McKinlay-1 @ 4118.5' (facies association 2).

Kaolinite as a dominant clay type, occurs as booklets or vermicular shape and forms a loosely packed pore filling in random orientations marking the position of the decomposed feldspar grains. Microporosity was observed under SEM of this arrangement of kaolinite. Kaolinite is authigenic in origin with an average size of 100-200 $\mu$  and usually fills large intergranular spaces where detrital grains were dissolved. Quartz overgrowths are limited in the presence of kaolinite formation (Figure 4.12-A).

Some illite and illite-smectite layers are considered to have originated from the breakdown of mica and feldspar and associated with micaceous fine-grained samples. Both of these clay types occur as pore filling and grain coating. In XRD charts, some illite peaks are not well defined because of a range of composition between mica and smectite (Figure 4.12-B).

Chlorite with a rosette form (Figure 4.12-C) was recorded from the SEM of one sample (Maxwell-2 @ 2920') and has a very low abundance compared to the other clay types. The development of chlorite resulted from biotite alteration, however, Martin (1983) suggested this has occurred in mica source rock and not during the sandstone diagenesis.

SEM imaging also shows the role of these clays on the formation of quartz overgrowths. Many quartz grains were coated by clays and this, in turn, prevents the development of quartz overgrowths.

Zoellner (1988) noted that there is a decrease in kaolinite and increase in smectite over the boundary between the Murta Formation and the Cadna-owie Formation. Moreover, these findings were supported by a later clay mineralogy profile study in the Cretaceous succession by Poonawala (2006) (Appendix 4.7). As mentioned previously, smectite and neoformed illite in the Murta Formation is of very low abundance and this coincides with the Zoellner (1988) and Poonawala (2006) clay mineralogy results.



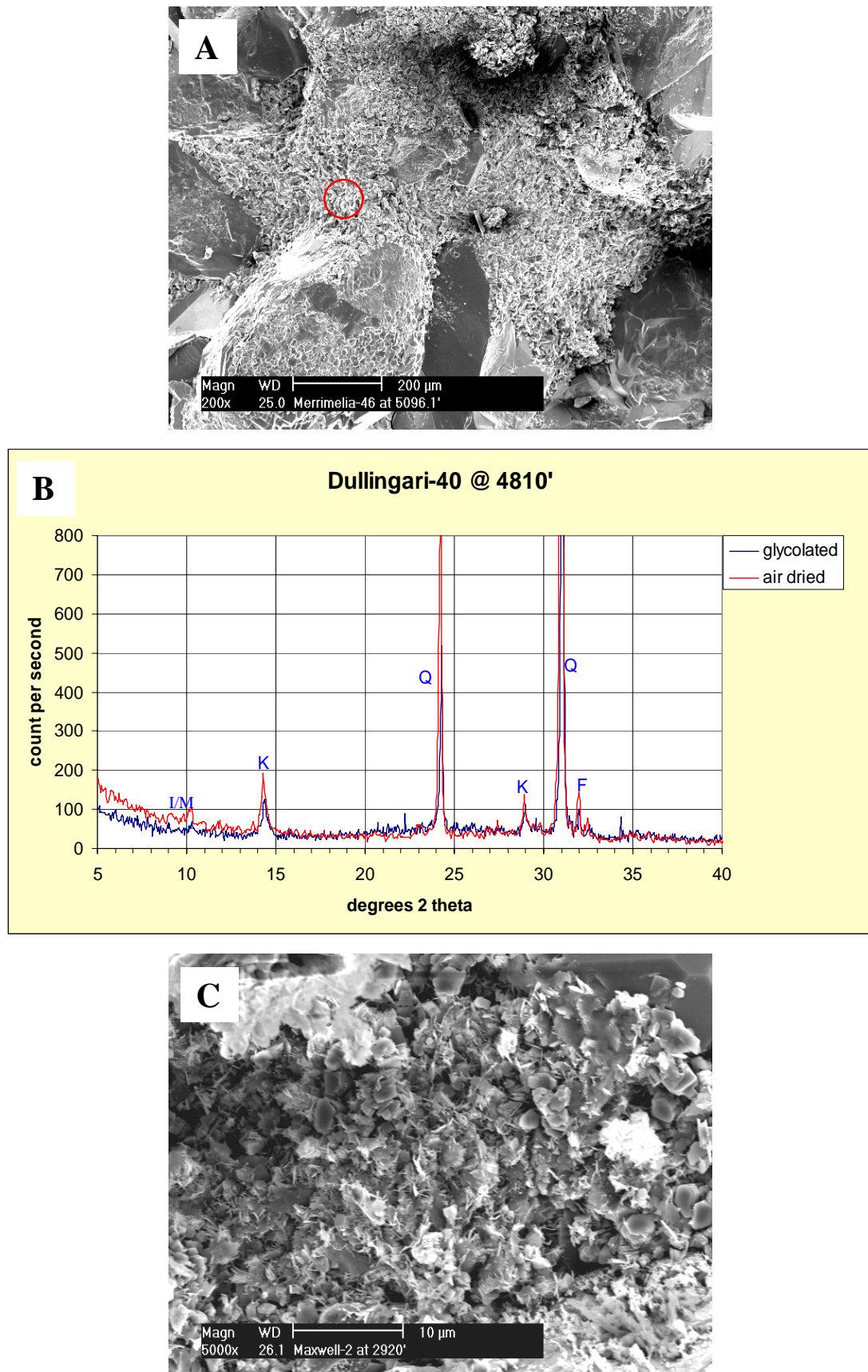


Figure 4.12: A: SEM shows kaolinite coating quartz grains and restraining the development of quartz overgrowth (facies association 1). B: XRD trace shows feldspathic quartz sandstone. Note the mixed peak of mica and illite. This result from the fact that illite developed from mica decomposition (facies association 5). C: SEM image shows edgewise, plate-like chlorite grains from Maxwell-2 @ 2920' (facies association 5).

### 4.4.3 Dissolution

The dissolution noted in the samples studied was the major factor for both porosity reduction and improvement.

The reduction in the porosity resulted from the dissolution of quartz grains to form sutured contacts between the quartz grains and the formation of microstylolites. This kind of pressure dissolution (microstylolites) was marked to be associated with the alteration of mica to illite acting as rim cement in the silty layers (Martin, 1983; Tucker, 1995).

This alteration process encouraged the silica dissolution to form microstylolites which, in turn, are lined with illite and illite-smectite. These microstylolites have a crenulate shape and are normally filled with organic matter and mica. They are formed parallel to the bedding planes and will inhibit the vertical permeability. Examples of microstylolites can be seen in figure 4.13-A.

In coarser-grained samples, the abundance of grain sutures becomes very low. The dissolution of calcite cement and feldspar grains which are responsible for the development of secondary porosity becomes apparent. The secondary pores vary in size depending on whether they originated from cement or framework grain dissolution (Martin, 1984).

Feldspar grain dissolution, partial, or complete alteration to clays creates some pores (Fig. 4.13-B). In some cases, complete feldspar grains were dissolved creating large secondary pores, the same size as the original feldspar grain. This secondary porosity adds to the primary porosity and results in a good interconnected pore system with higher permeability. Generally, the dissolution of carbonate cement produced large irregular-shaped pores (Figure 4.13-C).

The fine-grained sandstones lost their primary porosity as a result of clay cements and quartz dissolution, however, in coarse-grained sandstones, the primary porosity has been preserved and secondary porosity developed from dissolution of feldspar and carbonate cements.



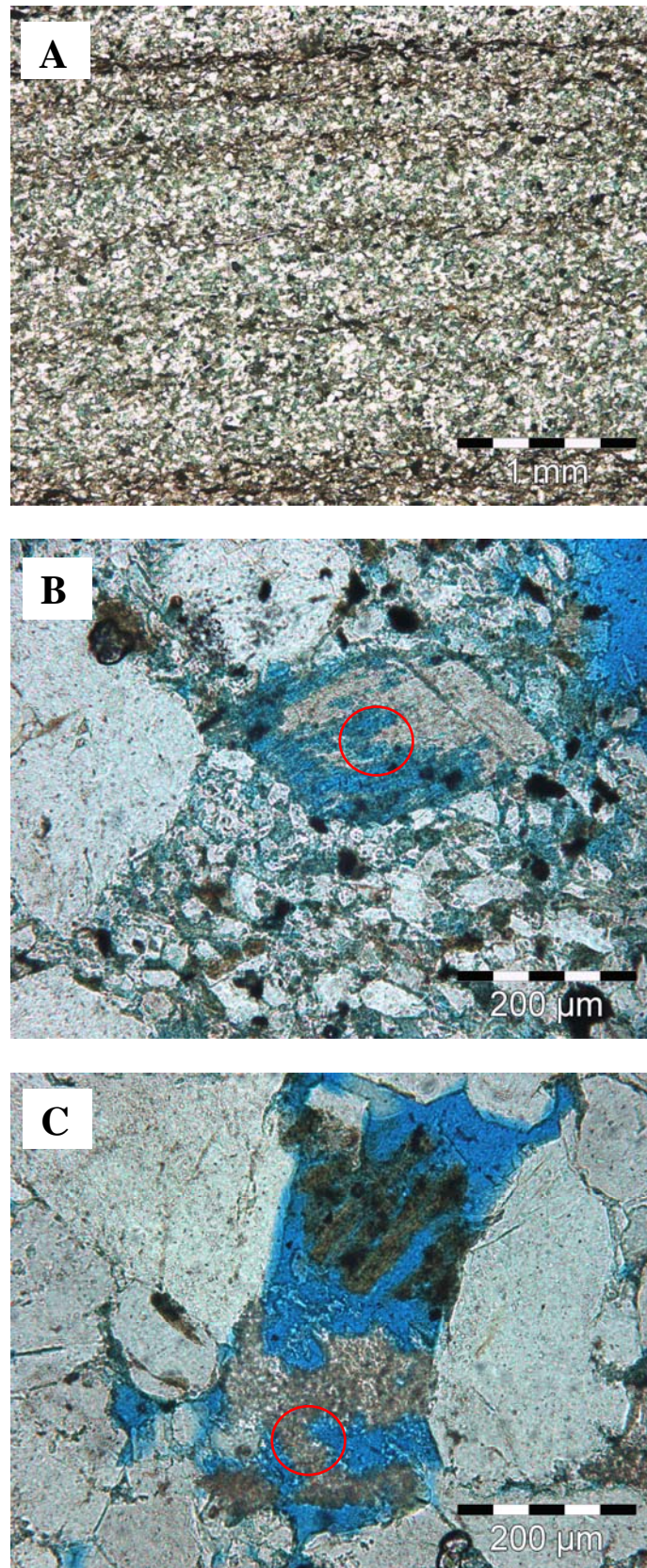


Figure 4.13:A: Microstylolites associated with mica develop parallel to the bedding planes inhibiting the vertical permeability. It shows also interlaminated bands of low porosity with bands of good porosity. Example seen under plane polar light from Merrimelia-46 @ 5099.2' (facies association 5). B: Feldspar grain partially dissolved to create secondary pores from Dullingari-40 @ 4808.5' of facies association 5. C: Example of carbonate dissolution to form secondary porosity after replacing feldspar grain seen under plane polar light from Challum-1 @ 5116' of facies association 1.

## 4.5 Provenance Discussion and Interpretation

### 4.5.1 Discussion

The provenance study makes use of the sediment detrital mineral composition. These minerals provide an evidence of possible source rock lithologies. Provenance factors include weathering processes and the nature of the sediments supplied to any transport agent. These include relief and elevation, climate, and composition of the bedrock (Raymond, 1995). The nature and abundance of the rock types in the source region will limit the materials in the sediment derived from that region. The main detrital minerals used in the provenance study were quartz, feldspar, mica, heavy minerals, and rock fragments (lithics).

#### Quartz

Quartz grains have been considered as a good indicator of origin and maturity of the sandstones. Quartz was classified based on its crystalline nature into monocrystalline and polycrystalline. The ratio of monocrystalline grains to polycrystalline grains can give an idea about the maturity of the source rock and the proportion of igneous versus metamorphic rocks in the source area (Pettijohn *et al*, 1987).

More monocrystalline grains percentage point to more mature source rocks. Similarly, quartz grains have been categorized based on their undulatory character into undulatory quartz and non-undulatory straight quartz. The ratio between these two undulatory phases indicates the origin of the source rock. Metamorphic source rock samples are interpreted to show more undulatory quartz grains, whereas samples with non-undulatory straight trends are representative of igneous source rock (Pettijohn *et al*, 1987).

The vast majority of the samples studied are monocrystalline quartz types and show non-undulatory or straight extinction. Thus, the origin of the sandstones in the Murta Formation is most likely derived from igneous source rocks. However, some samples are of polycrystalline quartz type and show undulatory extinction. This suggests metamorphic or mixed metamorphic and volcanic rocks also occurred in the source area.

### **Feldspar**

Although feldspar detrital grains are easily altered to clays, the fresh unaltered ones were used in identifying provenance and maturity. The most abundant feldspar type noted was potash feldspar and this suggests a possible alkaline plutonic igneous (cratonic) source rock. On the other hand, the low plagioclase content was interpreted to be of possible volcanic origin. Absence of feldspar in some samples infers the weathering was intense.

### **Mica**

In general, mica is largely an indication of metamorphic origin (Pettijohn *et al*, 1987). Muscovite mica was noted to be abundant over biotite mica in all of the samples studied and this suggests a mature origin.

### **Heavy minerals**

A group of heavy minerals (zircon, tourmaline, and rutile) were noted and used to indicate an alkaline igneous origin. However, the rounded nature of these heavy minerals in some samples suggested a recycled sedimentary or metamorphic source.

### **Rock fragments (lithic)**

The sandstones in the Murta Formation contain both sedimentary and metamorphic rock fragments. Volcanic lithics are only of very small abundance. Sedimentary rock fragments include siltstone and shale. On the other hand, metamorphic rock fragments consist mainly of mica phyllite and schist.

Some rock fragments are difficult to identify due to their small size, and nature and degree of alteration which agrees with Martin (1988) findings.

#### **4.5.2 Interpretation**

The high igneous indicators in the samples studied can be summarized as the following:

- The majority of the quartz grains are of monocrystalline and non-undulatory straight extinction type.

- High abundance of potash feldspar grains.
- High concentration of zircon, tourmaline and rutile.

Moderate metamorphic input includes:

- Minor polycrystalline quartz grains.
- High abundance of mica, particularly muscovite.

Low volcanic input includes:

- Very low plagioclase feldspar grains and minor acid volcanic rock fragments.

A modified provenance ternary plot by Dickinson (1985) and Tucker (1995) was used to locate the provenance terranes of the sandstones in the Murta Formation (Fig. 4.14). The majority of the samples were interpreted to be derived from a craton interior. However, just few samples fall on the recycled orogenic part. The ternary plot explains the well rounded nature of some samples and suggests a possible recycled sedimentary or metamorphic origin. Still, using Dickinson's (1985) ternary plot is limited as most of the samples plot in one corner of the diagram. The craton interior origin for the sediments is in keeping with the known history and setting of the Eromanga Basin.

A geographic provenance study was conducted to see if there is any difference between each locality's provenance. It has been concluded that most of the samples are of craton interior source and some minor input from a recycled orogenic source.

Samples from the Patchawarra Trough area are interpreted to be derived from the Adelaide Geosyncline and Gawler Craton of mainly igneous source and slightly of mixed metamorphic and sedimentary sources (N. Lemon, Santos Ltd., pers. comm.) On the other hand, samples from Strzelecki and Dullingari fields (Tenappera Trough) could have been derived from the Broken Hill Block and interpreted to include volcanic and some metamorphic sources. The Jackson-Naccowlah Trend samples are of mixed recycled orogenic and cratonic sources. Ipundu and Talgeberry wells are interpreted to be of mixed recycled orogenic and craton interior origins (N. Lemon, Santos Ltd., pers. comm.) (Fig. 4.15).

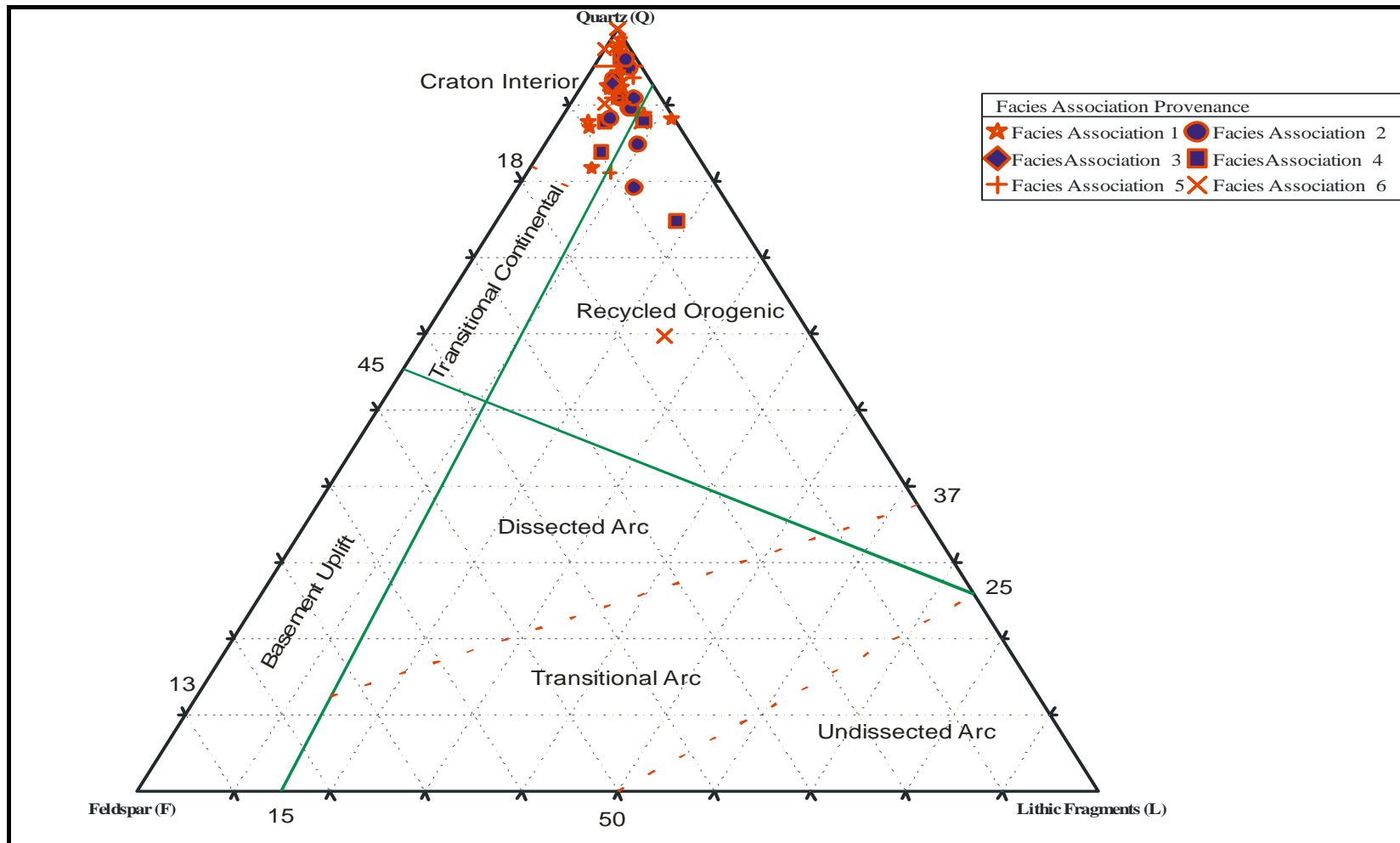


Figure 4.14: Provenance ternary plot of Murta Formation sandstones after Dickinson's ternary plot (1985). Note the craton interior source of most of the samples studied.

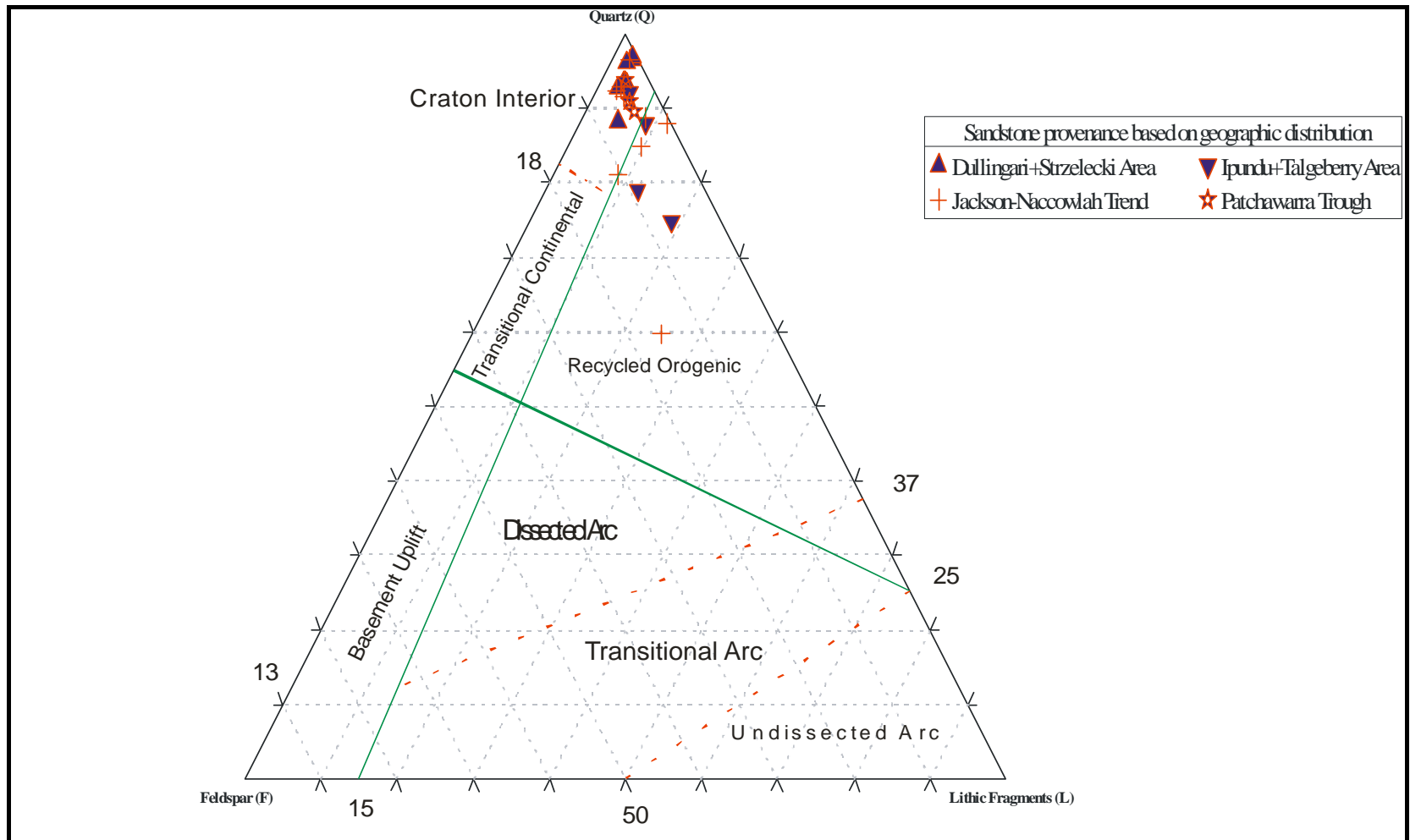


Figure 4.15: Geographic provenance ternary plot, after Dickinson (1985), highlighting the craton interior source of the selected samples.



## Chapter 5 Reservoir Quality and Distribution

### 5.1 Introduction

The main reservoirs in the Murta Formation are quartzarenite. However, a few samples are of sublitharenite and subarkose when plotted on the Folk classification. These reservoirs are moderately to well sorted and fine- to very fine-grained sandstones. Nonetheless, medium to coarse-grained reservoir units are also recognized in the Murta Formation reservoirs. The thin reservoir units in the upper section of the Murta Formation are interpreted to be deposited as lacustrine shoreline associated with delta front deposits (i.e. distributary-mouth bar). Fluvial sand sheets delivered to the lake basin cut through and erode the underlying lacustrine shoreline and associated delta front deposits and mark the top of the unit (Fig.3.6). The McKinlay Member of the Murta Formation is deposited as distributary channels and lacustrine shorelines, particularly in the southwest part of the study area. Generally, the Murta Formation and its McKinlay Member are interpreted to be deposited as prograding fluvial-dominated delta into a lacustrine basin.

Reservoir quality of the Murta Formation is mainly controlled by diagenetic features recognized in core, petrographic study, SEM and XRD analysis. These diagenetic features include quartz overgrowths, carbonate cement, formation of authigenic clays and secondary porosity resulting from grain and cement dissolution. However, the formation of microstylolites and associated mica along the bedding planes has reduced vertical permeability. Porosity and permeability variations in the Murta Formation depend on the grain size only in facies associations 1 and 6. This relationship is due to the influence which original texture of the sediments has had on later diagenetic processes, particularly calcite cementation (Martin, 1987).

Quartz overgrowths were identified in most of the sandstones as widespread cement. Commonly, the presence of clays, mainly kaolinite, will slow down further development of the quartz overgrowths. Facies association 1, as clean and medium- to coarse- grained reservoir sandstones, has more quartz overgrowths cement compared to the very fine-grained sandstones of facies association 6. Quartz overgrowths are best developed in samples with little mica and clay.

Usually, quartz overgrowths completely fills the pore spaces in most samples, but some primary porosity is preserved as a result of incomplete overgrowth development providing some interconnected pores.

Carbonate cement is dispersed through all of the reservoir sandstones as irregular patches. Carbonate content is very high in facies association 6 samples (averages 31.6%), thus, they show very low porosity and permeability readings as a result of fine-grained character and lack of interconnected pores. However, carbonate content of reservoir samples from facies association 1 is low (averages 3.8%). Consequently, they have the highest recorded porosity (averages 9.5%) and permeability (averages 36.8 mD).

Authigenic clays were identified using petrography, SEM and XRD techniques. Kaolinite was recognized as the dominant clay type. Illite, illite-smectite and chlorite were also recorded from few samples within the Murta Formation reservoirs. The average clay abundance in all facies associations is 12.3%. It was noted that the clay abundance increases with increase in mica content. These clays, particularly kaolinite, are disseminated everywhere in all samples with less abundance in facies association 1. However, facies association 3 has the highest clay content.

The porosity types found in the Murta Formation was mainly primary porosity. However, secondary and micro porosities were also recognized to add to the total porosity but in small amounts. Primary porosity is of significant contribution to the permeability in such way that the pore spaces in the primary porosity are interconnected, while in secondary porosity the pore spaces are isolated.

Visual porosity readings and permeability measurements show variation throughout all facies associations. Facies association 1 has the highest average porosity and permeability readings of 9.5% and 36.8 mD respectively. Facies association 6 has the lowest average porosity and permeability readings of 2.5% and 0.26mD respectively. Nonetheless, facies associations 2, 3, 4 and 5 have generally low permeability readings with relatively reasonable porosity readings. From porosity and permeability characteristics of all facies associations, the reservoir sandstones in the Murta Formation can be classified as primary, secondary and non reservoir sandstones.

It is important to mention that, although fluvial sand sheet deposits were identified in facies associations 2 & 3 (shoreline sandstone), facies association 4 (deltaic mouth bar sandstone) and facies association 5 (storm-generated shoreline sandstones (tempestites), they cannot be compared with the fluvial sand in facies association 1 (distributary channels) as facies association 1 is cleaner, coarser, with more angular grains and is highly permeable. The proportions of such sands are higher than any other facies association and this contributes more to the total oil production in the Murta Formation.

Although facies associations 2, 3, 4, and 5 are considered to be of secondary reservoirs, oil stain was documented from these facies associations nominating them as potential reservoir rocks in the Murta Formation. Facies association 6 is not considered of economic value for oil production because of very low porosities and permeabilities.

## **5.2 Variations in reservoir quality**

### **5.2.1 *Non-reservoir sandstones (Facies association 6)***

Facies association 6 encompasses linsen-laminated mudstone with minor siltstone and very fine-grained sandstone. The grain sizes of its sands range from very fine to coarse silt. Bioturbation and soft sediment deformation are described from this facies association. Siderite concretions were recognized in both thin sandy layers and laminated mudstone. It is likely to have been deposited as storm and slope-generated turbidites in an offshore setting.

Most of the very fine-grained samples present in facies association 6 usually show poor sorting because the alteration of feldspar grains to clay can mask the sorting. Facies association 6 has the highest average silt content (54.1%) with the highest average percentage (31.6%) of the carbonate content.

There is a decrease in porosity readings accompanied by a decrease in permeability readings noted from the silt to very fine sand-sized facies association 6. It has the lowest average porosity and permeability readings of (2.6%) and (0.25 mD) respectively.

Due to the presence of extensive microstylolites along with mica in fine-grained samples, vertical permeability are significantly reduced, while horizontal permeability will vary according to porosity variations. Porosity reduction took place as a result of carbonate, grain suturing (microstylolites) and clay (kaolinite) cements. The pore systems in this facies association are not well connected.

This facies association is not considered of economic valuable for oil production because of very low porosities and permeabilities (Fig. 5.1 & 5.2).

### **5.2.2 Secondary reservoir sandstones (Facies associations 2, 3, 4 and 5)**

Facies associations 2, 3, 4 and 5, collectively, are considered to be deposited as shorelines with delta front mouth bars. Sandstones from these facies associations are characterized in general by very fine- to fine-grained sizes. They are characterized by coarsening-upward cycles on wireline logs. Sedimentary structures identified in shoreline and mouth bar sands include wave ripple-laminations and parallel-laminations. Lenticular bedding and clean sand climbing ripples can be seen in facies association 5 of storm-generated shoreline sands. The thickness of these facies associations varies from 5.3 to 8.7 m. Oil stain was recorded from cores of these facies associations suggesting productive reservoirs from this zone.

Facies associations 2, 3, 4 and 5 are generally moderately sorted and of fine-grained character. No clear relationship can be established between average permeability readings and average silt content in facies associations 2, 3, 4 and 5.

These facies associations are characterized by high mica content and clay cement. Facies association 3 has the highest mica content with an average of 3.2% and has been noted to be associated with the highest average clay content (10%) reading in all facies associations. Although these facies associations have generally low carbonate cement, clay content, particularly kaolinite as dominant cement, will not only block the pore spaces, but also extend to the pore throats and block them to prevent the interconnection between the pore network. Therefore, permeability is low in the presence of kaolinite. However, microporosity is expected from the loosely packed kaolinite, but with very

small contribution to the total effective porosity with minor unconnected secondary porosity as a result of the dissolution of isolated feldspar grains (Fig. 5.1 & 5.2).

Siderite, as aggregates of crystals, also will decrease permeability as a result of precipitation in the pore spaces and pore throats. Microstylolites are also noted to inhibit vertical permeability and, in turn, decrease the reservoir quality.

Clays, mainly kaolinite, and siderite are considered to be the major permeability reducing factors in fine-grained samples of these facies associations.

The thin sandy interval (30 cm) at the top of these facies associations is interpreted to be the main reservoir sandstone in these facies associations. Although they have high porosity readings, the problem with these sand sheets is their discontinuous character as they have been delivered to the basin from Namur Sandstone as pulses of fluvial sands. In addition, they are usually cemented with calcite. For that reason, permeability is streaky and unpredictable.

These facies associations, although containing reasonable to good primary porosity (average 7%), have low permeability readings (averages 3.1 mD) due to their fine-grained character and diagenetic features. So, these facies associations are considered of secondary importance for oil production, although they are the main producing units in Queensland and parts of South Australia.

### **5.2.3 Primary reservoir sandstones (Facies association 1)**

Facies association 1 comprises trough cross-bedded (St) and planar-tabular (Sp) well-sorted medium-grained sandstone. Massive (structureless) sandstone was also recorded from this facies association. It shows fining-upward profiles from logs. Its thickness ranges from 1.2 to 3 m. The thickness of each fluvial sand sheet in this facies association is about 10 cm. The trough cross and planar-bedded sandstone is best featured in the distributary channels of the McKinlay Member of the Murta Formation, deposited across the lake shoreline.

Sorting, as a good indicator for reservoir quality, is identified to be the best in facies association 1. Facies association 1 was identified to have almost zero silt content with high average permeability readings. Generally, permeability readings are high in the cleaner sand samples and they increase with an increase in grain size. This facies association has the lowest carbonate and mica content (average 3.8%) and (1%) respectively, because of the medium to coarse grain sizes. The low mica content associated with the lowest clay content (6.7%) was recorded is in facies association 1.

Quartz overgrowths and calcite cement are the dominant cements in this facies association. Although quartz overgrowths completely filled the pore spaces in most samples, some primary porosity preserved as a result of incomplete overgrowth development provides some interconnected pores. Calcite cement, in some samples is not that extensive to restrain the development of quartz overgrowths. Furthermore, kaolinite also was identified in facies association 1 as pore filling.

An increase in permeability was noticed with an increase in porosity in this facies association (Fig. 5.1 & 5.2). Facies association 1 has medium grain size with the highest average porosity reading of 9.5% and a well-connected pores system. The highest average permeability readings (36.8 mD) were recorded from facies association 1. Secondary porosity was developed from the dissolution of framework grains and cements and this adds to the total porosity of the rock.

This facies association was recorded from core description to have oil stain and in addition it has the highest porosity and permeability readings (Fig. 5.1 & 5.2).



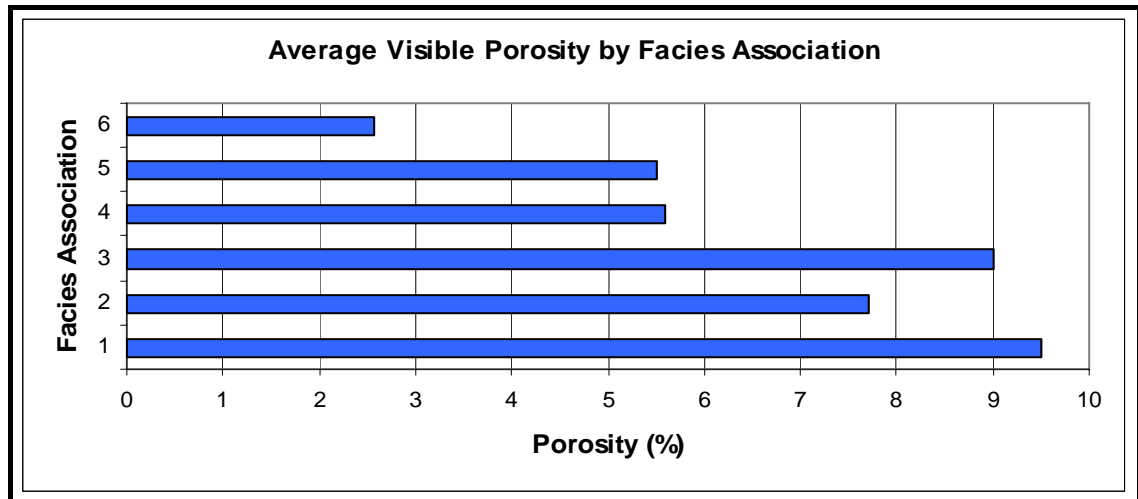


Figure 5.1: Summary histograms of average visual porosity readings from all facies associations.

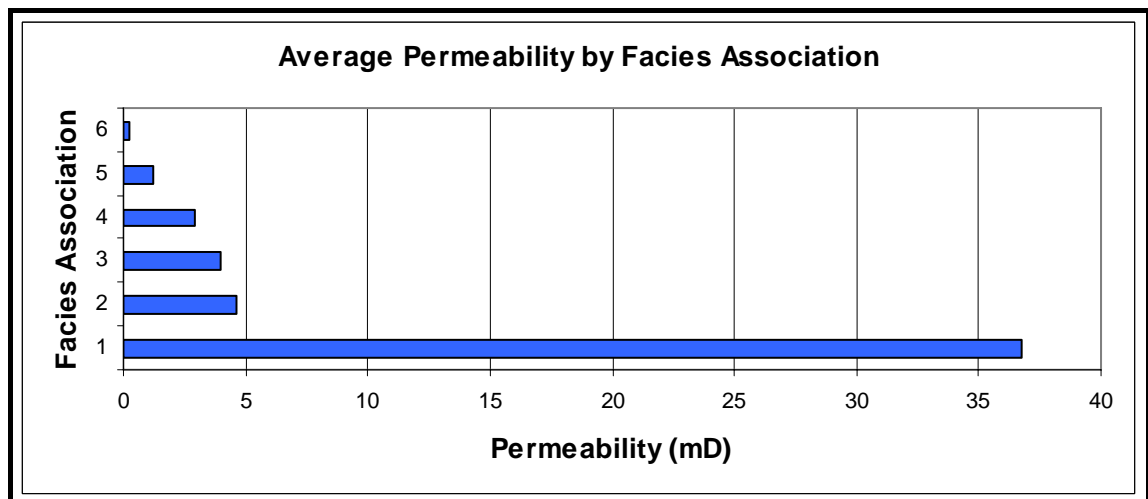


Figure 5.2: Summary histograms of average permeability readings from all facies associations.

Note that although facies associations 2, 3, 4 and 5 have infrequent fluvial sand sheets deposits which will add up to the porosity, they were recognized to be secondary target reservoirs because of their general fine-grained nature and more diagenetic affects compared to facies association 1 which has coarser grain sizes and less diagenetic affects.

### **5.3 Stratigraphic position of key reservoirs**

Porosity and permeability readings in the studied intervals do not show any significant trends with depth apart from those associated with depositional facies associations.

#### **5.3.1 *Non-reservoir sandstones (Facies association 6)***

Facies association 6 was deposited close to or at the two Maximum Flooding Surfaces identified in the Murta Formation (DC50 & DC30) of units 4 and 6 (4910-4950' and 4827-4855' respectively) (Fig.3.6). Furthermore, it is present at the top of the Murta Formation (Unit 1) (4770-4779') close to the contact with the Cadna-owie Formation. Its average thickness is between 15 and 18 m. These rocks are interpreted to be good seals and possible source rocks for the Murta Formation sandstone reservoirs. Low porosity and permeability readings were noted from this facies association.

#### **5.3.2 *Secondary reservoir sandstones (Facies associations 2, 3, 4 and 5)***

The deposition of these facies associations marks the shallowing events (coarsening-upward cycles) in the upper stratigraphic section of the Murta Formation in units 2, 3, and 5 (4855-4910', 4803-4827' and 4779-4803' respectively) (Fig.3.6). They dominantly deposited in a shallow lake setting after the first Maximum Flooding Surface in the Murta Formation. The average thickness of these facies associations is between 10-16 m. These facies associations have relatively good porosity readings, but permeability readings have been reduced by the formation of microstylolites in association with mica.

#### **5.3.3 *Primary reservoir sandstones (Facies association 1)***

The McKinlay Member is located in the lower portion of the Murta Formation (Unit 7 in figure 3.6). The thickness of Unit 7 varies from 9-24 m, while its thickness at its type section is 15 m. The depth of the reservoir sandstones from the McKinlay Member ranges from 4683-4702' in Strzelecki-4 well (its type section defined by Gravestock, 1995). Occasionally, the McKinlay Member contains shoreline deposits in conjunction with the distributary channel deposits. High porosity and permeability readings were noted at depths associated with medium-coarse grain sizes of this facies association.

## **5.4 Variations in reservoir quality with geographic location**

### **5.4.1 *Non-reservoir sandstones (Facies association 6)***

The non-reservoir sands of facies association 6 are deposited mainly in the central basin of Lake Murta during increases in the base level (Fig. 3.23, 3.21-A, 3.19-A, 3.15-B, 3.15-A, 3.11). Very minor, poor quality sands were delivered to the basin as turbidites with dominant muddy lithologies. Tenaperra Trough, Murteree Ridge, Nappamerri Trough and Patchawarra Trough contain the highest concentration of these muddy lithologies, mainly in the South Australian part of the study area (Fig.1.8 & 5.3).

### **5.4.2 *Secondary reservoir sandstones (Facies associations 2, 3, 4 and 5)***

Facies associations 2, 3, 4 and 5 of shoreline, deltaic mouth bar and tempestite sandstones respectively, have contributed to the oil production in most of the study area wells, specifically in Queensland. This includes the Jackson-Naccowlah Trend, Tenaperra Trough and Harkaway Fault area close to the eastern wells with main sand input coming from a northeast direction (Fig.1.8 & 5.3). These facies associations are quite easy to recognize from logs because of their regional extent as coarsening-upward cycles capped by very thin sand sheets. However, the challenge in the reservoir sandstones of these facies associations rises from the very thin sand sheet character of its top (main reservoir sandstones from this secondary reservoir). They are discontinuous, unpredictable and usually cemented with calcite.

The main oil producing reservoir sandstones are from facies association 2, 3 and 4 close to the sand input in Queensland, while facies association 5 is interpreted to be closer to the basin centre as tempestite deposits with low recovery factors (Fig. 3.21-B, 3.19-B & 3.13).

### **5.4.3 Primary reservoir sandstones (*Facies association 1*)**

The McKinlay Member oil bearing sands of facies association 1 and occasionally 2 are concentrated in the southwestern part of the study area in South Australia, particularly in Murteree Ridge, Tenappera Trough, Nappamerri Trough, Patchawarra Trough and GMI Ridge (Fig.1.8 & 5.3). This implies that the main sand input for the McKinlay Member and its facies association 1 came from the southwest direction of the study area (Fig. 3.9 A&B).

This facies association, as well as other facies associations are hard to identify in areas close to the main sand input in Queensland because of steady sand lithologies in that area (east of Jackson-Naccowlah Trend). However, other sand input directions to the basin were suggested by many local studies to contribute to the oil reservoir sandstones (Zoellner, 1988; Gorter, 1994; Theologou, 1995; Hill, 1999).

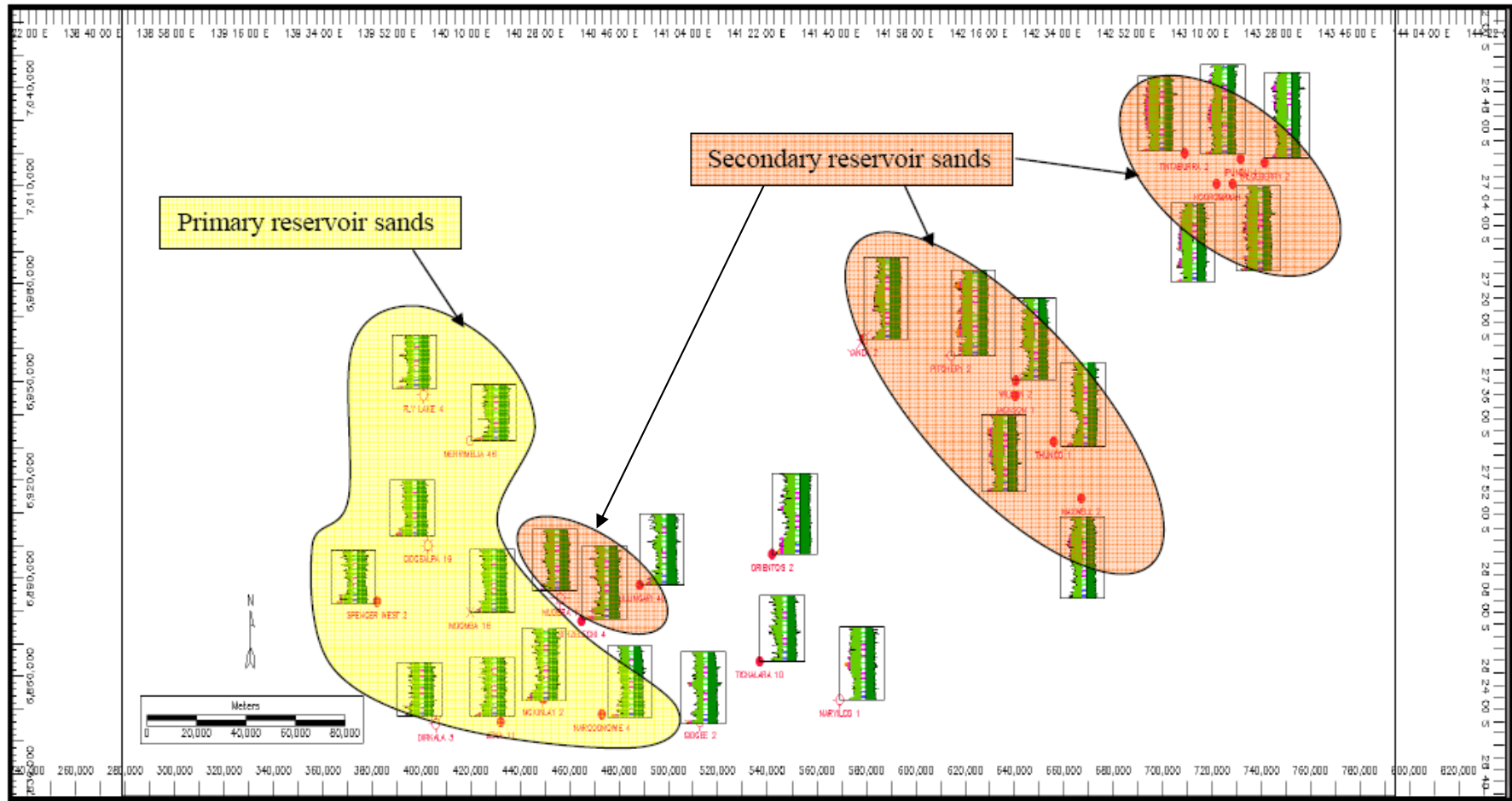


Figure 5.3: Location map of the primary and secondary reservoir sandstones of the Murta Formation across the Eromanga Basin in South Australia and Queensland. Non-reservoir sandstones are concentrated mainly in the central basin.

## Chapter 6 Discussion and Conclusions

This study highlights the effects of the diagenetic features and original texture on the reservoir quality of the Murta Formation and its basal McKinlay Member. Application of sedimentology, sequence stratigraphy and petrography techniques to the reservoirs of the Murta Formation have led to a number of conclusions on the factors dominating reservoir quality, continuity and prospectivity of the reservoir sandstones.

The textural factors of grain size, sorting, and mineralogy of the framework grains are the main controls on reservoir quality. The best reservoir quality throughout the Murta Formation was noted in facies association 1 with moderately-well sorted, medium to coarse-grained sandstones. On the other hand, facies association 6 is considered to be the lowest reservoir quality with very fine grain sizes and poor sorting. Other facies associations (2, 3, 4, and 5) have generally fine grain sizes and are moderately sorted. The high abundance of monocrystalline quartz grains shows development of rhombohedral quartz overgrowths which, in turn, will not block the whole pore spaces, but will leave some primary porosity between quartz grain crystal faces. In the case of polycrystalline quartz grains, the development of microstylolites (pressure solution) led to degrading of reservoir quality by inhibiting vertical permeability. The alteration of feldspar grains to clays will result in low reservoir quality in such a way that these clays will fill the pore spaces and block the pore throats.

The main diagenetic factors affecting the reservoir quality of the Murta Formation are quartz overgrowths, carbonate cement, formation of authigenic clays, formation of microstylolites and the dissolution of the framework grains.

Quartz overgrowths cemented the quartz grains in rhombohedral shape leaving behind some primary good pore spaces between its crystal faces. Occasionally, in very few samples, this cement was extensive and able to block the whole pore spaces. Quartz overgrowths were noticed mainly in facies association 1 and partially in facies association 2, 3, 4, and 5.



Carbonate cement also contributed to the loss of porosity in the reservoirs of the Murta Formation. They form either as disseminated patches of calcite or as aggregates of siderite crystals filling the pore spaces. Calcite patches were noted to be associated with coarser grained samples, while siderite was abundant in fine-grained samples.

Authigenic clays, particularly kaolinite, contain microporosity which may add to the total porosity. Generally, clays form from the alteration of feldspar and/or mica. They degrade the reservoir quality by blocking the pore spaces and throats.

The dissolution of framework grains and cements may also add to the total porosity, but minor spots have been identified to be connected. The formation of the microstylolites (pressure solution) in association with mica parallel to the bedding planes will inhibit the vertical permeability and therefore lower the chances of having good reservoir quality.

The recognition of the diagenetic influence on reservoir quality led to subdividing the reservoirs into three reservoir types: non-reservoir, secondary reservoir and primary reservoir.

Average thin-section porosity estimates and permeability measurements suggest that the most prospective facies association in the Murta Formation is facies association 1. This contains coarse-grain sizes deposited as distributary channels of the McKinlay Member with limited diagenetic affects.

Although facies associations 2, 3, 4, and 5 are considered to be good oil targets in the upper section of the Murta Formation, their fine-grained nature, the formation of microstylolites in the lower part of the formation, the discontinuity of the upper thin sand sheets and diagenetic influences have decreased their prospectivity.

The lowest porosity estimates and permeability readings are recorded in facies association 6. Being the least prospective, diagenetic affects are related to the formation of microstylolites in association with mica that, in turn, will inhibit the vertical permeability. In addition, the horizontal permeability will depend on porosity of the adjacent sediments which is also affected by other diagenetic features, likely clays and carbonate cements. As a result, the porosity in most of the facies associations is fair

enough, but permeability is highly reduced by diagenetic features, formation of microstylolites with mica and grain sizes finer than facies association 1.

By applying the sequence stratigraphy concept and constructing series of paleogeographic maps, the following conclusions have been made for better reservoir exploration in the study area.

Unit 7, with its distributary channel and mouthbar origin, represents the transgressive systems tracts of the McKinlay Member that is considered to be the best target for reservoir development. It has relatively high pay medium to coarse-grained sands with minimal diagenetic affects. Therefore, it has been classified to contain primary reservoir sands. The main localities for these distribuatry channel sands can be predicted in the western and southwestern part of the study area, namely in Murteree Ridge, Tenappera Trough, Patchawarra Trough and GMI Ridge. This indicates that the main sand input for the McKinlay Member and its facies association 1 came from the western and southwestern part of the study area. As a result, the best drilling sites for the McKinlay Member development can be predicted in the Murteree Ridge, southwestern Tenappera Trough, Patchawarra Trough and GMI Ridge, specifically in the Murteree Ridge and southwestern Tenappera Trough in South Australia.

High stand systems tract units 2, 3 and 5 of shoreline, deltaic mouth bar and tempestites origin are considered to be secondary reservoir targets because of diagenetic effects and their fine-grained character. The sedimentological description of these units matches the classification of facies associations 2, 3, 4 and 5. These units and facies associations have contributed to the oil production in most of the study area wells, specifically in Queensland. This includes the Jackson-Naccowlah Trend, northeastern Tenappera Trough and Harkaway fault area close to the eastern wells with main sand input coming from a northeast direction. The sands of these units and facies associations are easy to pick from logs because of their regional coarsening-upward cycles capped by thin sand sheets which, in turn, are discontinuous, unpredictable and usually cemented with calcite.

In Queensland, where these units and facies associations are well developed, oil production can be predicted from units 2 and 3 (facies associations 2, 3, and 4) in areas close to the sand input (i.e. Harkaway fault area and the eastern wells). On the other hand, oil production from middle unit 5 (facies association 5) can be predicted to be away from the main sand input in Queensland close to the central basin (eastern Nappamerri Trough) with low recovery factors.

Units 1, 4 and 6 are not considered of economic value for oil production because of their extremely low reservoir quality and muddy lithologies. They have been interpreted as turbidites and deposited mainly in the central basin of the study area. Facies association 6 sediments which have been described from these units are severely degraded by diagenetic effects. Northeastern Tenaperra Trough, northeastern Murteree Ridge, and eastern Nappamerri Trough are the best candidates for predicting where to find these units and facies association.

## References

- ALEXANDER, E.M., & SANSOME, A., 1996. Lithostratigraphy and environments of deposition. *In: Alexander, E.M. & Hibburt, J.E. (eds.), 1996. The petroleum geology of South Australia. vol.2: Eromanga Basin. South Australia. Department of Mines and Energy. Report Book, 96/20:125-140. p. 49-100.*
- ALLEN, G., LANG, S., MUSAKTI, O., & CHIRINOS, A., 1996. Application of sequence stratigraphy to continental successions: Implications for Mesozoic cratonic interior basins of Eastern Australia. *In: Mesozoic Geology of the Eastern Australia Plate Conference, Geological Society of Australia Inc. Extended Abstracts No. 43, p. 22-26.*
- ALLEN, J.R.L., 1984. *Sedimentary structures, their character and physical Basis - First Edition.* Developments in Sedimentology, vol. 30. Elsevier Publications, Amsterdam. 663p.
- ALLEN, P.A., & COLLINSON, J.D., 1986. Lakes *In: Reading, H.G., (ed.), 1986. Sedimentary Environments and Facies - Second Edition.* Blackwell Scientific Publications, Oxford, p. 63-94.
- AMBROSE, G., SUTTILL, R. & LAVERING, I., 1982. A review of the Early Cretaceous Murta Member in the Southern Eromanga Basin. *In: Moore, P.S. & Mount T.J. (eds.), 1982. Eromanga Basin Symposium, Summary Papers, Geological Society of Australia & Petroleum Exploration Society of Australia. p. 92-109.*
- AMBROSE, G., SUTTILL, R., & LAVERING, I., 1986. The geology and hydrocarbon potential of the Murta Member (Mooga Formation) in the Southern Eromanga Basin. *In: Gravestock D.I., Moore P.S. & Pitt G.M. (eds.), 1986. Contributions to the geology and hydrocarbon potential of the Eromanga Basin. GSA, Special Publication No. 12, p. 71-84.*
- BOGGS, S., 1995. *Principles of Sedimentology and Stratigraphy - Second Edition.* Prentice-Hall, Upper Saddle River, New Jersey. 727p.
- BOHACS, K.M., & CARROLL, A.R., NEAL, J.E., & MANKIEWICZ, P.J., 2002. Lake-basin type, source potential, and hydrocarbon character: an integrated sequence-stratigraphic-geochemical framework. *In: Continental Sequence Stratigraphy workshop notes, presented to Esso Australia/PESA, selected topics, p. 3-33.*

- CATUNEANU, O., 2006. *Principles of Sequence Stratigraphy – First Edition*. Elsevier Publications, Massachusetts. 375p.
- COE, A.L., & CHURCH, K.D., 2003. Sequence stratigraphy and sea-level change *In*: COE, A.L., (ed.), 2003. *The Sedimentary Record of Sea-Level Change - First Edition*. Cambridge University Press. p. 57-98.
- COLEMAN, J.M., & PRIOR, D.B., 1982. Deltaic sand bodies. *The American Association of Petroleum Geologists Education course note series* No.15. Tulsa. p. 75.
- DICKINSON, W.R., 1985. Interpreting provenance relations from detrital modes of sandstones. *In*: Zuffa, G.G. (ed.), 1985. *Provenance of Arenites*. Reidel. Dordrecht. p. 333-361.
- ELLIOT, T., 1986a. Deltas. *In*: Reading, H.G., (ed.), 1986. *Sedimentary Environments and Facies*. Blackwell Publications, Oxford. p. 113-154.
- EUGSTER, H.P., & KELTS, K., 1983. Lacustrine chemical sediments. *In*: Goudie, A.S., & Pye, K., (eds.), 1983. *Chemical Sediments and Geomorphology*. Academic Press, London. p. 321-368.
- FOLK, R.L., 1980. *Petrology of Sedimentary Rocks – Second Edition*. Hemphill Publishing Company, Austin. p. 127.
- FOUCH, T.D., & DEAN, W.E., 1982. Lacustrine environments. *In*: Scholle, P.A., & Spearing, D., (eds.), 1982. *Sandstone Depositional Environments. The American Association of Petroleum Geologists Memoire* No. 31. p. 87-114.
- FRAKES, L.A., BURGER, D., APHORPE, M., WISEMAN, J., DETTMANN, M., ALLEY, N., FLINT, R., GRAVESTOCK, D., LUDBROOK, N., BACKHOUSE, J., SKWARKO, S., SCHEIBNEROVA, V., McMINN, A., MOORE, P.S., BOLTON, B.R., DOUGLAS, J.G., CHRIST, R., WADE, M., MOLNAR, R.E., MCGOWRAN, B., BLAME, B.E., & DAY, R.A., 1987. Australian Cretaceous shorelines, stage by stage. *Palaeogeography, Palaeoclimatology, Palaeoecology*, vol. 59, p. 31-48.
- FRAKES, L.A., & FRANCIS, J.E., 1988. A guide to Phanerozoic cold polar climates from high-latitude ice-rafting in the Cretaceous. *Nature* No. 333, p. 547-549.
- FRIEDMAN, G.M., & SANDERS, J.E., 1978. *Principles of Sedimentology*. John Wiley & Sons, New York. 792p.
- GIERLOWSKI-KORDESCH, E., & KELTS, K., 1994. Introduction *In*: Gierlowski-Kordesch E., & Kelts, K., 1994. *Global geological record of lake basins*, vol. 1, Cambridge University Press, Cambridge. p. 2-9.

- GORTER, J.D., 1994. Sequence stratigraphy and the depositional history of the Murta Member (Upper Hooray Sandstone), Southeastern Eromanga Basin, Australia: Implications for the development of source and reservoir facies. *APEA Journal*, vol. 34 (2), p. 644-673.
- GRAVESTOCK, D.I., 1982. Jurassic to Lower Cretaceous stratigraphy of the Eromanga Basin. South Australia – problems and progress in subsurface correlation. In: Moore, P.S., and Mount, T.J. (compilers), 1982. *Eromanga Basin Symposium, Summary papers, Adelaide. Petroleum Exploration Society of Australia, Geological Society of Australia (SA Branches)*, p. 79-91.
- GRAVESTOCK, D.I., CALLEN, R.A., ALEXANDER, E.M., & HILL, A.J., 1995. Strzelecki, South Australia, sheet SH54-2. *South Australia Geological Survey. 1:250 000 Series – Explanatory Notes*.
- HALYBURTON, R.V., & ROBERTSON, A.L., 1984. Geology of the Jackson oilfield. *APEA Journal*, vol. 24 (1), p. 259-265.
- HILL, A.J., 1999. Reservoir sedimentology and sequence stratigraphy of the Early Cretaceous Murta Member, Maxwell oilfield, Southwest Queensland. Honours thesis, Queensland University of Technology. (Unpublished). 145p.
- KRAPF, C.B.E., & LANG, S.C., 2005. 2<sup>nd</sup> Dryland fluvial reservoir workshop, Lake Eyre Basin, Central Australia: Workshop field guide & progress report. p. 3-18.
- KRIEG, G.W., ALEXANDER, E.M., & ROGERS, P.A., 1995. Eromanga Basin In: Drexel, J.F., and Preiss, W.V., (eds), 1995. The geology of South Australia. vol. 2, The Phanerozoic. *South Australia Geological Survey Bulliten*, No. 54, p.101-112.
- LANG, S.C., GRECH, P., ROOT, R., & HILL, A., 2001. The application of sequence stratigraphy to exploration and reservoir development in the Cooper-Eromanga-Bowen-Surat Basin system. *APEA Journal*, vol. 41 (1), p. 223-249.
- LEGARRETA, L., ULIANA, M.A., LAROTONDA, C.A., & MECONI, G.R., 1993. Approaches to non-marine sequence stratigraphy- theoretical models and examples from Argentine basins. In: Eschrd, R. & Doliez, B. (eds), 1993. Subsurface Reservoir Characterization from Outcrop Observations, *Editions Techip, Paris Collection, Colloques et Seimairies*, No. 51, p. 125-145.



- MARTIN, K.R., 1983. Petrology of the Murta Member, Westbourne Formation and Hutton Sandstone in the Jackson 1 and Jackson South 1, Eromanga Basin, Southwest Queensland. Report to Delhi Petroleum Pty. Ltd. (Unpublished). 25p.
- MARTIN, K.R., 1984. Petrology and reservoir quality of the Murta Member and the Namur Sandstone Member in Sigma 1, Eromanga Basin, Southwestern Queensland. Report to Delhi Petroleum Pty. Ltd. (Unpublished). 22p.
- MARTIN, K.R., 1987. Petrology and reservoir quality of the Murta Member in the Dullingari oilfield, Cooper-Eromanga Basin, South Australia. Report to Delhi Petroleum Pty. Ltd. (Unpublished). 20p.
- MARTIN, K.R., 1988. Petrology and diagenesis of reservoir rocks from the Murta M4 subunit, Dullingari Field, Cooper-Eromanga Basin, South Australia. Report to Santos Ltd. (Unpublished). 15p.
- MIALL, A.D., 1978. Fluvial Sedimentology, *Canadian Society of Petroleum Geologists, Memoir No. 5*. 859p.
- MOORE, P.S., & CASTRO, C., 1984. Petroleum exploration in fluvio-lacustrine sequences, with examples from the Cooper and Eromanga Basins, Central Australia. In: JONES, B.G., & HUTTON, A.C., (eds.), 1984. Fluvio-deltaic systems - facies analysis in exploration. *Australasian Sedimentologists Specialists Group, Wollongong*. p. 307-339.
- MOUNT, T.J., 1981. Dullingari North 1, an oil discovery in the Murta Member of the Eromanga Basin. *APEA Journal*, vol. 21 (1), p. 71-77.
- MOUNT, T.J., 1982. Geology of the Dullingari Murta oilfield. In: Moore P.S. & Mount T.J. (eds.), 1982. *Eromanga Basin Symposium. Summary Papers. GSA and PESA, Adelaide. Australian Sedimentologists Special Group, Wollongong*. p. 307-337.
- OVIATT, C.G., McCOY, W.D., & NASH W.P., 1994. Sequence stratigraphy of lacustrine deposits: A Quaternary example from the Bonneville Basin, Utah. *Geological Society of America Bulletin*, No. 106, p. 133-144.
- PETTIJOHN, F.J., POTTER, P.E., & SIEVER, R., 1987. *Sand and Sandstone - Second Edition*. Springer-Verlag, New York. 553p.
- POONAWALA, M.A., 2006. Controls on polygonal faulting in the Eromanga Basin, Central Australia. Honours thesis, University of Adelaide. (Unpublished). 76p.

- POSAMENTIER, H.W., & ALLEN, G.P., 1999. Siliciclastic sequence stratigraphy: concepts and applications. *SEPM Concepts in Sedimentology and Palaeontology*, No. 7. 210p.
- PRIMARY INDUSTRIES AND RESOURCES OF SOUTH AUSTRALIA (PIRSA), 2006. Cooper and Eromanga Basins consolidated data package. *Primary Industries and Resources SA*.
- RAYMOND, L.A., 1995. *Petrology, The study of Igneous, Sedimentary and Metamorphic Rocks - First Edition*. WCB Communications, Boston. 741p.
- READING, H.G., 1986. *Sedimentary Environments and Facies - Second Edition*. Blackwell Scientific Publications, Oxford. 615p.
- REINECK, H.-E., SINGH, I.B., 1980. *Depositional Sedimentary Environments – Second Edition*. Springer-Verlag Publications, Berlin. 549p.
- REZAEI, M.R., LEMON, N., & SEGGIE, R., 1997. Tectonic fingerprints in siderite cement, Tirrawara Sandstone, Southern Cooper Basin, South Australia. *Geological Magazine*, vol. 134, p. 99-112.
- RIORDAN, S., PAYENBERG, T., LANG, S.C., 2006. Atlas of reservoir analogues. Project to Australian School of Petroleum (ASP), University of Adelaide. (Unpublished).
- ROBINSON, P.A., & BUTLER, G.F., 1989. Development of the Dullingari Murta oilfield. *The Cooper and Eromanga Basins, PESA Publication*, p. 113-119.
- SANTOS Ltd., 2003. Structural elements of the Cooper Basin. (Unpublished).
- SCHULZ-ROJAHN, J.P., 1993. Calcite cemented zones in the Eromanga Basin: Clues to petroleum migration and entrapment? *APEA Journal*, vol. 33 (1), p. 63-76.
- SELLY, R.C., 1985. *Ancient Sedimentary Environments*. Chapman and Hall, London. 317p.
- SHANLEY K.W. & McCABE P.J. 1994. Perspectives on the sequence stratigraphy of continental strata. *The American Association of Petroleum Geologists Bulletin* 78, No. 4, p. 544-568.
- SLY, P.G., 1978. Sedimentary processes in lakes. In: Lerman, A., (ed.), 1978. *Lakes: Chemistry, Geology, Physics*. Springer-Verlag Publications, Berlin. p. 65-89.
- STAUGHTON, D.B., 1985. The diagenetic history and reservoir quality evolution of the Strzelecki hydrocarbon field, Cooper/Eromanga Basins, South Australia, Department of Earth sciences, Monash University. (Unpublished).

- STRUCKMEYER, H.I., & TOTTERDELL, J., 1990. Australia – Evolution of a continent. *Bureau of Mineral Resources, Australia*. p. 71-75.
- STURM, M., & MATTER, A., 1978. Turbidites and varves in Lake Brienz (Switzerland): deposition of clastic detritus by density currents. *In: Matter, A. & Tucker, M.E., (eds.), 1978. Modern and Ancient Lake Sediments. International Association of Sedimentologists. Special Publication No.2.* p. 147-168.
- THEOLOGOU, P., 1995. Murta Formation/McKinlay Member of the Murteree Ridge Nappacoongee-Murteree Block-Improved oil recovery project. PhD thesis, University of South Australia. (Unpublished). 147p.
- TUCKER, M.E., 1995. *Sedimentary petrology, an introduction to the origin of sedimentary rocks. Second Edition.* Blackwell Scientific Publications, Oxford. 260p.
- VAN DIJK, D.E., HOBDAV, D.K., & TANKARD, A.J., 1978. Permo-Triassic lacustrine deposits in the Eastern Karoo Basin, Natal, South Africa. *In: Matter, A., & Tucker, M.E., (eds.), 1978. Modern and Ancient Lake Sediments. International Association of Sedimentologists. Special Publication No.2.* p. 225-239.
- VAN WAGONER, J.C., MITCHUM, R.M., CAMPION, K.M., & RAHMANIAN, V.D., 1990. Siliciclastic sequence stratigraphy in well logs, cores, and outcrops: Concepts for high-resolution correlation of time and facies. *The American Association of Petroleum Geologists Methods in Exploration Series, No 7.* p. 9.
- WALKER, R.G., 1984. Shelf and shallow marine sands *In: WALKER, R.G., (ed.), 1984. Facies models - Second Edition. Geoscience Canada Reprint Series 1.* Ontario. p.141-170.
- WALKER, R.G., 1982. Hummocky and swaley cross stratification. *In: Walker, R. G., (ed.), 1982. Clastic units of the Front Ranges, Foothills and Plains in the area between Field, B.C. and Drumheller, Alberta, Canada. International Association of Sedimentologists, 11<sup>th</sup> International Congress on Sedimentology. Guided book to Excursion 21A,* p. 22-30.
- WECKER, H.R., 1989. The Eromanga Basin. *APEA Journal*, vol. 29 (1), p. 379-396.

- WILSON, M.D., & STANTON, P.T., 1994. Diagenetic mechanisms of porosity and permeability reduction and enhancement. *In: Wilson M.D. (ed.), 1994. Reservoir Quality Assessment and Prediction in Clastic Rocks. SEPM Short Course No. 30. p. 59-118.*
- WRIGHT, L.D., 1977. Sediment transport and deposition at river mouths: a synthesis. *Geological Society of America Bulliten*, 88. p. 857-868.
- ZOELLNER, E., 1988. Geology of the Early Cretaceous Murta Member, Mooga Formation, in the Cooper Basin area, South Australia and Queensland. PhD thesis, Flinders University. (Unpublished). 123p.